Optimal fast-charging strategies for long-distance trips on the highway with all-electric vehicles

Anastasia Popiolek

université PARIS-SACLAY

Stratégies optimales de recharge rapide sur autoroute pour des trajets longue distance en véhicule électrique

Optimal fast-charging strategies for long-distance trips on the highway with electric vehicles

Thèse de doctorat de l'université Paris-Saclay

École doctorale n° 575, Electrical, Optical, Bio-physics and Engineering EOBE
Spécialité de doctorat: Génie électrique
Graduate School : Sciences de l'ingénierie et des systèmes. Référent : CentraleSupélec

Thèse préparée dans l'unité de recherche GeePs (Université Paris-Saclay, CentraleSupélec, CNRS), sous la direction de **Philippe DESSANTE**, professeur des universités, la co-direction de **Marc PETIT**, professeur des universités et la co-supervision de **Zlatina DIMITROVA**, professeure des universités (Stellantis).

Thèse soutenue à Paris-Saclay, le 01 décembre 2023, par

Anastasia POPIOLEK

Composition du jury

Membres du jury avec voix délibérative

Florence OSSART Professeure des Universités, GEEPS, Sorbonne Université	Présidente
Jean-Christophe OLIVIER Maitre de Conférences HDR, IREENA, Université de Nantes	Rapporteur & Examinateur
Benoît ROBYNS Professeur des Universités, L2EP, Junia	Rapporteur & Examinateur
Fabrice LOCMENT Professeur des Universités, AVENUES, Université de technologie de Compiègne	Examinateur
Assaad ZOUGHAIB Professeur des Universités, CES, Mines-Paris, PSL	Examinateur

THESE DE DOCTORAT

NNT : 2023UPAST206

université PARIS-SACLAY

ÉCOLE DOCTORALE
Physique et ingénierie : Electrons, Photons, Sciences du vivant (EOBE)

Titre: Stratégies optimales de recharge rapide sur autoroute pour des trajets longue distance en véhicule électrique

Mots clés: véhicule électrique, trajet longue distance, recharge rapide, communication, optimisation multi-objectif

Résumé: Le secteur des transports routiers représente 12% des émissions de gaz à effet de serre (GES) dans le monde et dans l'optique de réduire ces émissions, les constructeurs automobiles accélèrent la transition vers les véhicules électriques (VEs). Malgré une augmentation rapide des ventes ces dernières années, certains freins à l'adoption du véhicule électrique persistent, parmi eux, une autonomie encore limitée pour la plupart des modèles et des pauses allongées (par rapport à un véhicule thermique) pour recharger lors des trajets longue-distance. Dans ce contexte, l'objective de cette thèse est d'étudier différents aspects de la recharge rapide sur autoroute et de proposer des stratégies de recharge optimales afin d'améliorer l'expérience des conducteurs de véhicule électriques lors de trajets longue-distances. Le premier aspect étudié concerne la gestion intelligente de la charge d'une flotte de véhicule électrique. Une stratégie de communication en temps réel entre les véhicules et les stations est proposée en ce sens. Pour cette communication, nous avons établi deux possibles règles de priorité en stations, une règle de premier-arrivé premier-servi (PAPS) et une règle de réservation, que nous avons comparées. Il apparaît que la communication avec une règle de PAPS est plus performante que la réservation. Nous avons ensuite évalué l'intérêt de cette stratégie de communication dans le dimensionnement de l'infrastructure en proposant une optimisation double niveau visant à minimiser le coût de l'infrastructure sachant que les véhicules optimisent leur plan de charge en utilisant la stratégie de communication. Enfin, nous avons étudié l'impact de la puissance de charge des véhicules électriques sur le coût de l'infrastructure ainsi que sur le temps passé en station. En effet, augmenter la puissance de charge permet de réduire les temps de charge mais les chargeurs haute puissance sont plus onéreux. Cependant, si le développement de l'infrastructure est optimisé, on constate que plus le taux de pénétration de véhicules permettant la charge ultra-rapide est grand et plus le temps passé en station est réduit sans augmentation du coût de l'infrastructure.

Title: Optimal fast-charging strategies for long-distance trips on the highway with electric vehicles
Keywords: electric vehicle, long-distance trip, fast charge, communication, multi-objective optimisation

Abstract: The road transport sector accounts for 12% of global greenhouse gas emissions (GHGs), and to reduce these emissions, automakers are accelerating the transition to electric vehicles (EVs). Despite a rapid increase in sales in recent years, some barriers to adopting electric vehicles persist, including limited range for most models and extended breaks (compared to traditional vehicles) for recharging during long-distance journeys. Therefore, this thesis aims to study various aspects of highway charging to enhance the experience of electric vehicle drivers on long-distance trips. To investigate these aspects, we developed a multi-agent simulation environment that models the interactions between vehicles and charging stations. The first level of improvement involves more intelligent management of charging for a fleet of EVs, relying on regular communication between vehicles and stations: vehicles optimise their charging plan and share it in real-time with stations, which, in turn, assess future waiting times and communicate them to EVs. We compared two strategies using real-time communication: one follows the first-come-first-served (FCFS) rule at the station, while the other allows advance reservation of charging slots. It appears that communication associated with the FCFS rule represents the optimal strategy. The second level of improvement aims to size the charging infrastructure to be developed when the previously described communication strategy is used. The problem was solved using a Grey Wolf Optimizer that minimises the cost of the infrastructure while limiting waiting time at the station. By comparing optimal infrastructures to develop when EVs communicate and when they do not, it is evident that communication reduces infrastructure costs by up to 26%. Finally, we also studied the influence of the charging power of vehicles on the time spent at the station and the cost of the infrastructure to be developed. Increasing the charging power reduces charging time, but the infrastructure must be equipped with higher-power chargers, which are more expensive. The results show that, even without communication, increasing the charging power of vehicles reduces by more than 50% the time spent at the station without incurring additional costs for the infrastructure. Thus, implementing a real-time communication charging strategy enables more efficient use of the infrastructure and reduces the need for infrastructure. If this strategy is coupled with increased charging power, it will, without additional cost, enhance the experience of electric vehicle drivers by reducing time spent at the station.

À Mamé

Résumé

Le secteur des transports routiers représente 12% des émissions de gaz à effet de serre (GES) dans le monde et dans l'optique de réduire ces émissions, les constructeurs automobiles accélèrent la transition vers les véhicules électriques (VEs). Cependant, malgré une augmentation rapide des ventes ces dernières années, certains freins à l'adoption du véhicule électrique persistent, parmi eux, une autonomie encore limitée pour la plupart des modèles et des pauses allongées (par rapport à un véhicule thermique) pour recharger lors des trajets longue-distance. Une des solutions serait de diminuer les besoins en recharge en proposant des véhicules avec de plus grosses batteries mais ce type de véhicule est coûteux et à un impact environnemental important. En effet, même si un véhicule électrique n'émet pas de GES lorsqu'il roule, il n'en va pas de même lors de sa construction : la production de la batterie constitue une part non négligeable des émissions de GES sur sa durée de vie. D'autant plus que les circuits de recyclage des batteries ne sont pas encore déployés à large échelle. Limiter la taille des batteries est donc une solution plus viable mais il faut en contre-parti proposer un service de recharge adapté pour les trajets longue distance afin de favoriser plus facilement l'adoption des véhicules électriques et proposer une mobilité électrique propre et abordable.

Par conséquent, l'objectif de cette thèse est d'étudier différents aspects de la recharge sur autoroute afin d'améliorer l'expérience des conducteurs de véhicule électrique lors de trajets longue distance. Le premier aspect concerne le contrôle du plan de charge des VEs grâce à une communication en temps réel entre les VEs et les stations, le second est orienté sur l'optimisation de l'infrastructure sous contrôle de la charge et le dernier cherche à évaluer l'impact de la puissance de recharge sur le coût de l'infrastructure et le temps passé en station. L'ensemble des éléments présenté précédemment font l'objet du chapitre d'introduction, le **Chapitre 1**.

Une revue de littérature concernant les stratégies de contrôle de la recharge ainsi que du dimensionnement de l'infrastructure est conduite dans le **Chapitre 2**. On trouve de nombreuses méthodes adaptées au milieu urbain alors que celles-ci sont moins présentes pour les cas de recharge lors des trajets longue-distance. Parmi les méthodes adaptées aux trajets inter-cités, on retrouve notamment des méthodes de contrôle de la recharge qui cherche à utiliser le plus efficacement possible l'infrastructure déjà existante. Ces méthodes de contrôle vont jouer sur un ou plusieurs aspects de la charge pendant un trajet longue distance pour améliorer la satisfaction des conducteurs : où et quand le véhicule doit s'arrêter pour recharger, combien d'énergie doit-il recharger en station... Certaines des strategies sont basées sur une communication entre les véhicules directe ou indirecte pour éviter les stations à fortes affluences pour la prochaine charge alors que d'autres tentent d'optimiser le plan de charge complet des VEs avec ou sans communication pour prendre en compte le temps d'attente en station.

Pour le dimensionnement de l'infrastructure de charge sur autoroute, les méthodes présentées dans l'état de l'art visent pour certaines à maximiser le nombre de trajets origine-départ en véhicules électriques qui peuvent être réalisé grâce à l'infrastructure installée alors que d'autres cherchent plutôt à réduire le temps passé en station pour les véhicules. Nous relevons également dans cette revue de littérature les différents processus utilisés pour établir le trafic sur les voies étudiées afin d'élaborer des méthodes d'optimisation adaptées aux besoins réels de charge. L'enjeu de ces méthodes est de dimensionner les stations de charge (localisation et taille des stations) afin de capturer le plus efficacement le flot de véhicules électrique et d'anticiper les futurs besoins en recharge.

Après avoir identifié les points scientifiques non traités dans la littérature concernant les stratégies de recharge, nous présentons dans le **Chapitre 3** l'environnement de simulation

multi-agents que nous avons développé afin de tester les interactions entre les véhicules et les stations suivant les aspects de la recharge étudiés. Un agent représente un véhicule électrique et l'autoroute avec ses stations de recharge constituent l'environnement. Dans l'environnement de simulation, chaque agent peut être paramétré au niveau de ses caractéristiques intrinsèques (capacité batterie, puissance de recharge, etc.) mais aussi du trajet qu'il va réaliser sur l'autoroute (entrée/sortie d'autoroute, heure d'entrée, niveau de charge en entrée...). Pour générer des trajets les plus réalistes possibles, nous avons utilisé des données issues d'open-data mais nous avons également travailler sur des données remontées par les véhicules électriques connectés de Stellantis. Pendant une simulation, chaque véhicule suit une stratégie de recharge qui vise à minimiser le facteur d'insatisfaction du conducteur (compromis entre le temps de trajet et le coût de la recharge) en sélectionnant où il s'arrête, combien il recharge en station, etc.

Nous effectuons dans ce même chapitre une comparaison de plusieurs méthodes d'optimisation de plan de recharge pour minimiser le temps de trajet en prenant en compte les prédictions de temps d'attente communiquées par les stations. Ces méthodes d'optimisation du plan de recharge sont au nombre de trois : la première est une méthode exhaustive listant les plans de charge possibles pour sélectionner le meilleur, la seconde s'appuie sur un algorithme génétique et la troisième utilise la programmation dynamique. La dernière méthode que nous avons développée apparaît comme la méthode de résolution la plus adaptée pour des cas d'application concrets car, contrairement à la méthode exhaustive, elle n'a pas un temps d'exécution exponentiel par rapport au nombre d'arrêts nécessaire pour la recharge ni par rapport au nombre de stations le long de l'autoroute. En effet, la méthode exhaustive devant lister les possibles plans de charge, son temps de calcul est exponentiel car correspond à un problème combinatoire. Cependant, comme nous avons développée la méthode avec programmation dynamique en dernière année de thèse, c'est la méthode exhaustive qui a été utilisée dans l'ensemble du manuscrit pour les études de cas.

Comme vu dans la partie revue de littérature, un premier niveau d'amélioration de l'expérience des conducteurs lors des trajets longue distance repose sur une gestion plus intelligente de la recharge d'une flotte de VEs s'appuyant sur une communication régulière entre les véhicules et les stations : les véhicules optimisent individuellement leur plan de charge et le partagent en temps réel aux stations qui en échange, évaluent les temps d'attente futurs et les communiquent aux VEs. Dans le **Chapitre 4**, nous avons comparé deux stratégies utilisant la communication en temps réel : l'une respecte la règle de premier arrivé, premier servi (PAPS ou FCFS en anglais) en station alors que l'autre permet la réservation en avance de créneaux de charge. Nous avons également comparé ces deux stratégies de communication à une troisième stratégie ne permettant pas la communication mais où les VEs optimisent leur plan de charge pour minimiser leur temps de trajet.

Plusieurs niveaux de saturation de l'infrastructure de charge ont été étudiés pour cerner au mieux les performances de chaque stratégie de contrôle (100, 180 et 300 VEs). Des critères de qualité ont été définis pour comparer les stratégies entre elles et ainsi déterminée la ou les stratégies les plus pertinentes :

1. concernant la longueur des files d'attente, le nombre de véhicules attendant ne doit pas dépasser deux fois le nombre de chargeurs en station ;
2. le temps d'attente avant une charge ne doit pas dépasser 30 minutes.

Il apparaît que la communication associée à une règle de PAPS représente toujours la meilleure stratégie. Ceci est dû au fait que la communication PAPS permet une meilleure répartition des véhicules dans les stations par rapport à la stratégie sans communication grâce au partage d'in-

formation en temps réel concernant les temps d'attente. La stratégie communication PAPS valide les deux critères dans les cas où 100 et 180 VEs parcourent l'autoroute pendant la journée. Dans le cas de la réservation, le critère de file d'attente est respecté pour 100 et 180 VEs dans la flotte grâce au partage d'information mais le temps d'attente lui peut dépasser une heure pour certains véhicules. Ceci est dû au fait que la réservation est possible pour l'ensemble de la flotte et les créneaux de charge deviennent de plus en plus morcelés au fur et à mesure que les réservations augmentent.

Pour le cas où il y a 300 VEs dans la flotte, aucune stratégie ne valide les critères car la saturation de l'infrastructure est trop importante pour être corrigé par une stratégie de contrôle et il faut considérer l'ajout de nouveaux chargeurs pour améliorer l'expérience de recharge.

Dans ce même chapitre, nous avons mesuré la robustesse de la stratégie de communication lorsque des véhicules non communiquant sont injectés dans la flotte de véhicule. Les performances de la communication sont lentement dégradées au fur et à mesure que la proportion de VEs non communiquant augmente car les informations échangées sont de moins en moins nombreuses. Cependant, la communication permet de réduire le temps de trajet moyen non seulement pour les véhicules communiquants mais aussi pour l'ensemble de la flotte. Les conducteurs de véhicule ont donc tout intérêt à communiquer s'ils veulent avoir plus de chance de réduire de façon conséquente leur temps de trajet. Néanmoins, il faudra s'attendre à ce que, lors de la mise en place de la stratégie de communication, peu de véhicules l'utiliseront et donc il faudra trouver un moyen d'améliorer la robustesse de la stratégie de communication ou bien il faudra permettre en premier lieu la réservation pour le petit nombre de véhicule utilisant le partage d'information en temps réel. Pour la suite des chapitres, nous supposons que 100% de la flotte utilise la stratégie de communication PAPS.

Le **Chapitre 5** détaille le second niveau d'amélioration que nous avons étudié, à savoir le dimensionnement de l'infrastructure de recharge à développer lorsque la stratégie de communication décrite précédemment est utilisée. Pour permettre une mobilité propre et abordable, nous avons dimensionné l'infrastructure pour des VEs d'autonomie limitée (60kWh). Ce chapitre vise à évaluer les bénéfices qu'apporte la stratégie de communication dans la réduction du coût du réseau de charge en comparant les infrastructures optimales à développer quand les VEs communiquent et quand ils ne communiquent pas. L'optimisation de l'infrastructure est mené pour minimiser le coût annuel équivalent journalier de l'infrastructure tout en garantissant un temps d'attente limite en station qui ne doit pas être dépassé. Afin de vérifier la contrainte de temps d'attente en station en fonction du nombre de chargeurs dans chaque station de charge, nous utilisons l'environnement de simulation présenté dans le chapitre 3 afin de tester une ou plusieurs flottes de VEs sur l'infrastructure proposée. La taille des flottes étudiées pour ce dimensionnement est de 500 VEs et correspond à une saturation de l'autoroute française A6 pendant 10h. Le temps de simulation étant long lorsque les véhicules utilisent la communication (environ 30 minutes par infrastructure), nous avons limité à 5 le nombre de flottes testées simultanément.

Le problème a été résolu grâce à l'algorithme Grey Wolf Optimiser (GWO) qui minimise le coût de l'infrastructure tout en limitant le temps d'attente en station. Le GWO est un algorithme évolutionnaire basé sur la tactique de chasse des loups gris et a été choisi pour sa plus rapide convergence. Nous avons réalisé plusieurs optimisations en jouant sur les paramètres de simulation tels que le temps d'attente maximal autorisé (20 ou 30 minutes), les niveaux de puissance disponibles en station (50 et/ou 175 kW) ou encore la valeur du temps des conducteurs (20€/h ou 50€/h). On constate que la communication permet de réduire de façon notable (jusqu'à 26 %) le coût de l'infrastructure par rapport à une situation où aucun VE ne communique.

Enfin, nous avons étudié l'influence de la puissance de charge des véhicules sur le temps

passé en station ainsi que sur le coût de l'infrastructure à développer dans le **Chapitre 6**. En effet, augmenter la puissance de charge permet de diminuer le temps de charge et par conséquent le temps d'attente mais cela signifie que l'infrastructure doit s'équiper en chargeurs de puissance plus élevée qui sont plus coûteux. L'objectif premier de l'optimisation est de minimiser le temps passé en station pour les conducteurs et le second objectif est de minimiser le coût de l'infrastructure. Comme dans le chapitre 5, le problème est soumis à une contrainte sur le temps d'attente avec un temps maximal accepté de 15 minutes et de la même façon, l'environnement de simulation a été utilisé pour évaluer les temps d'attente en station et vérifier le respect ou non de la contrainte mais il a aussi été utilisé pour calculer le premier objectif de l'optimisation, à savoir le temps moyen passé en station .

Pour cette optimisation multi-objectifs, les véhicules ne suivent pas de stratégie de communication mais une stratégie plus simple visant à s'arrêter à la dernière station atteignable sans optimiser la recharge. Le temps de simulation pour cette stratégie étant moins important que pour la stratégie de communication, nous avons testé simultanément 100 flottes de 50 VEs pour vérifier la contrainte et calculer le temps moyen passé en station. Un algorithme différentiel avec une convergence utilisant le même principe que l'algorithme NSGA-II a été utilisé pour résoudre le problème d'optimisation.

Nous avons tracé les fronts de Pareto pour plusieurs proportions (1%, 5% et 100%) de véhicules à recharge ultra rapide (puissance de recharge $\approx$ 350 kW) dans la flotte. Les résultats obtenus montrent qu'augmenter la puissance de charge des véhicules permet, même sans communication, de diminuer de plus de 50% le temps passé en station sans engendrer de coût supplémentaire pour l'infrastructure. En effet, même si les véhicules qui rechargent ultra rapidement nécessitent des chargeurs beaucoup plus coûteux car délivrant plus de puissance, le nombre de chargeurs à installer en station pour réduire la file d'attente est faible car, les VEs se rechargeant plus vite, la file d'attente est beaucoup moins importante. De plus, on peut observer que entre une infrastructures correspondant à une situation avec 1% de véhicules pouvant se recharger ultra-rapidement et une correspondant à une situation avec 100% de véhicule à charge ultra-rapide, la puissance a installée augmente de seulement 27% alors que le temps moyen en station est diminué de 55%. Ces résultats sont cependant à prendre avec précaution car pour l'instant aucun VE avec une aussi grande puissance de charge n'existe et la charge ultra-rapide pourrait endommager la batterie et accélérer son vieillissement.

En conclusion, l'environnement de simulation ainsi que les méthodes que nous avons développé et intégrée à l'environnement nous permettent d'évaluer la pertinence des différentes stratégies de charge permettant de favoriser l'adoption des VEs. En particulier, nous avons pu observer que la mise en place d'une stratégie de charge avec communication en temps réel permet d'utiliser plus efficacement une infrastructure donnée et par conséquent de réduire le besoin en infrastructure. Si cette stratégie est couplée à une augmentation de la puissance de charge, elle permettra sans surcoût d'améliorer l'expérience des conducteurs de véhicule électrique en réduisant le temps passé en station.

Les perspectives de ces travaux de thèse sont nombreuses et visent notamment l'adaptation de la stratégie de communication à tout type de perturbation (véhicules non communiquant, ralentissement, déviation dû à un accident). Il conviendrait aussi de considérer lors de l'optimisation du plan de charge, d'autres objectifs qui pourraient impacter la satisfaction du conducteur (nombre d'arrêts, taux de CO_2 de l'électricité rechargée...). Concernant le dimensionnement de l'infrastructure, il serait intéressant d'évaluer l'évolution des besoins en infrastructure en fonction de l'augmentation des véhicules électriques sur les routes au lieu de dimensionner seulement pour une taille de flotte. Enfin, l'environnement de simulation ainsi que les méthodes développées pour ces travaux de thèse pourront être utilisé pour étudier des dé-

fis liés à d’autres types de transport (bus ou camions électriques…) ou d’autres types de trajets (trajets en ville).

Remerciements

J'aimerais tout d'abord remercier mon directeur de thèse, Philippe Dessante, pour ses conseils éclairés et sa bienveillance. Merci Philippe de m'avoir fait confiance sur ce sujet et de m'avoir aidée à mener à bien ces trois années de thèse.

Je remercie également les deux autres membres de mon encadrement, Marc Petit et Zlatina Dimitrova. Merci Marc pour les suggestions de pistes à étudier et pour les remarques constructives sur mes travaux, merci aussi de m'avoir proposé des heures de TDs pour pouvoir vivre pleinement l'expérience doctorale. Merci à toi Zlatina pour tes encouragements, tes conseils en méthode et ton dynamisme incroyable qui m'ont beaucoup motivée ; merci aussi d'avoir validé ma candidature en thèse et de m'avoir ainsi permis de vivre une expérience enrichissante à Stellantis.

Je souhaiterais par la suite remercier les membres de mon jury de thèse, Fabrice Locment, Jean-Christophe Olivier, Florence Ossart, Benoît Robyns et Assaad Zoughaib pour leurs retours sur mon manuscrit et pour les échanges très intéressants que nous avons pu avoir lors de la soutenance. Merci plus particulièrement à Florence qui m'a permis, avec l'aide de Salvy Bourguet, à cibler plus finement mes axes de travail lors du comité de suivi de thèse.

Je remercie chaleureusement mes collègues du laboratoire GeePs, permanents et doctorants, pour l'entraide et les discussions lors des pauses-café salutaires. Merci Vincent Reinbold de m'avoir aidée à résoudre un des problèmes épineux de ma thèse (vive la programmation dynamique !). Merci Anatole Desreveaux pour nos échanges instructifs sur la mobilité électrique. Merci Alexandre Bach pour ton aide lors des TDs ESTP. Merci Pierre Dumont pour tes explications très claires sur les marchés de l'énergie et les aller-retours au Guichet en Peugeot e-208. Merci à toi aussi Gustavo Henn pour ta bonne humeur, tes conseils et tes encouragements.

Mention spéciale à la team goûter : merci Amaury Ajasse, Louise Petit et Ange Sahuquet pour votre jovialité à toute épreuve. Merci à toi Célia Masternak pour ton aide avant, pendant et après la soutenance mais surtout pour nos séances de psy, je suis très heureuse de t'avoir rencontrer au laboratoire il y a trois ans. Bien sûr ces remerciements ne seraient pas complets si je ne remerciais pas Frédéric Reymond-Laruina : merci de m'avoir supportée pendant ces trois années dans notre bureau aquarium avec Jeannette et d'avoir rendu l'expérience ardue de la thèse un peu plus facile.

Un grand merci également à mes collègues de Stellantis qui m'ont accueillie pour ces trois années de thèse. Merci à toute la communauté des doctorants et à mes collègues de la SCEP. Un grand merci à Jamila Leite-Costa et à Sandrine Loze pour votre dynamisme dans l'animation de la communauté PhD et pour votre soutien sans faille. Merci Guillaume Mermaz-Rollet pour le partage de tes connaissances concernant myHPC, cela a littéralement accéléré ma thèse. Merci Sébastien Houillé, David Gaudrie et Wissam Nader pour vos retours constructifs sur mes travaux de thèse et pour vos encouragements, c'était un plaisir de discuter avec vous. Merci à Antoine Simon et à Alfredo Wulf pour votre aide notamment sur les problématiques de recharge. Merci Alain Goussian pour tes retours utilisateurs de véhicule électrique et pour l'intérêt que tu as porté à mon sujet de thèse, ça m'a redonné du courage pour continuer sur ma lancée et finir ma thèse. Merci aussi Soline Corre pour nos discussions animées lors des petit-dejeuners et pour ta présence solaire pendant tes quelques mois de stage.

Toujours à Stellantis, je voudrais remercier Albane Donal pour avoir initié une fructueuse collaboration sur le monde de la data. Merci Albane de m'avoir amenée à considérer mon sujet sous un autre angle et de m'avoir permis d'aller encore plus loin. Merci aussi à Mouhcine Waraq pour son aide précieuse sur le traitement des données de véhicules connectés. Enfin je remercie

Stéphane Mésaric pour son soutien et ses conseils avisés lors de la répétition de soutenance.

Merci à tous mes amis qui m'ont soutenue de près ou de loin lors de cette longue épopée. Merci à tous ceux qui ont pu assister à la soutenance sur place ou en distanciel : votre présence bienveillante et vos encouragements m'ont donné la force de présenter et de tenir jusqu'à la dernière question du jury. Vous étiez nombreux, aussi vous m'excuserez de ne pas vous citer ici mais sachez que je vous remercie tous un à un.

J'aimerais remercier ma famille qui m'a toujours supportée lors des moments difficiles mais qui se réjouit aussi de ma réussite. Merci Maman de m'avoir donné goût à la recherche et de m'avoir encouragée à faire une thèse, tu avais raison, je ne regrette pas du tout d'avoir vécu cette aventure. Merci Papa de m'avoir, comme Maman, donné confiance en moi pour continuer des études d'ingénieur et de me soutenir dans mes choix. Merci aussi à mon frère d'être venu m'écouter lors de ma soutenance, ça m'a beaucoup touché. Merci à ma soeur de s'intéresser autant à la science, j'espère que plus tard on aura un troisième docteur dans la famille. Merci également à mes grands parents de toujours m'encourager et d'être fier de mon nouveau statut de docteur.

Enfin, je voudrais te remercier Alexandre Vigny pour ton soutien, ta gentillesse et ton amour qui m'ont permis de tenir jusqu'au bout de ces trois ans. Merci d'être à mes côtés et de toujours croire en moi.

Contents

List of Figures

List of Tables

1 - General introduction: techno-economic aspects of fast charging for long-distance trips

The paramount environmental need to decrease Greenhouse Gas (GHG) emissions to reach Carbon Net Zero by 2050 has led automotive makers (Original Equipment Manufacturers - OEMs) to accelerate the electrification of their fleet. At the same time, electric vehicle (EV) sales have exploded during the past three years, and the number of EVs on the road continues to grow rapidly. There were more than 10 million EVs on the world road in 2020 (1% of the total cars registered worldwide) [28], and now, there are more than 26 million. According to the IRENA (International Renewable Agency), EVs are expected to be 157 million in 2030 and more than 1 billion in 2050 (Figure 1.1) [1]. In France, the cumulative number of plug-in EVs on the roads was by the end of 2022 above 1 million [29]. This noticeable increase can be explained by public incentives to buy electric cars and a more responsible collective awareness of the climate emergency.

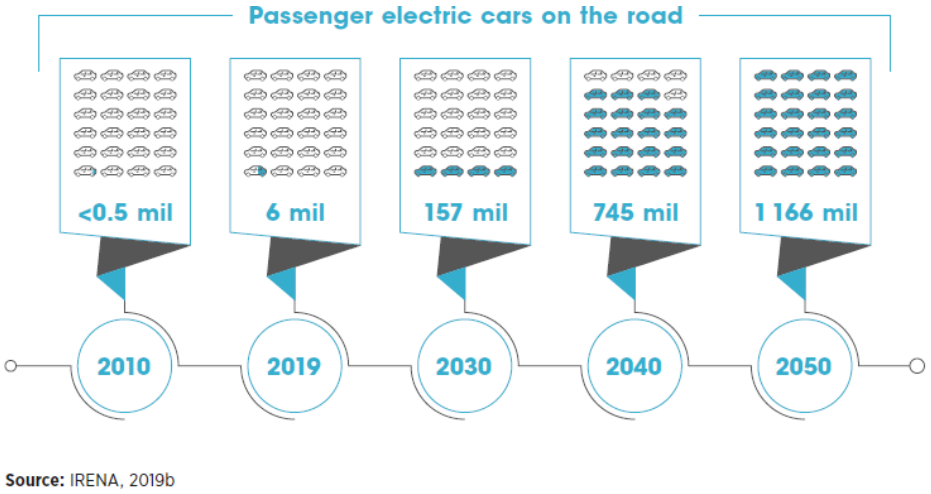

Figure 1.1: Passenger electric cars on the world roads [1]

However, even if the number of EVs is rapidly growing, most EV models' limited range (300 km on average) still disincentives to EVs' acceptability, especially for long-distance trips. Indeed, a gas-powered car has an average of 650 km, which is twice the average range for an EV. Though some EV models can reach the same range as average intern-combustion engine (ICE) vehicles (for example, Tesla Model S and future Peugeot e3008), they need bigger batteries that increase their price (approx. 100 €/kWh) and their environmental footprint.

Due to this limited range, long-distance trips are only possible if EV drivers rely on a public fast-charging infrastructure (≥ 50 kW DC), enabling rapid energy recovery (less than 30 minutes to charge 80% of the battery capacity). At the beginning of this present thesis in 2021, the public fast-charging infrastructure was relatively sparse in France (only 140 out of 440 highway service areas proposed at least one fast-charging point [30]). It was discouraging EV purchases due to range anxiety. Now, thanks in part to the Government subvention of 100 million euros, almost all the service areas propose a fast-charging station (FCS) [9], making the charging network dense enough to reduce range anxiety (on average, one station every 50 km). Nevertheless, this current charging infrastructure is unlikely to support the growing number of EVs, and solutions should be foreseen to address this problem and avoid the upcoming infrastructure saturation.

Moreover, even if some EV model can charge in less than 15 minutes from 10% to 80% of their battery capacity, this is not the case for most EVs (approx. 30 minutes), and this is still three times the refuelling time for a conventional gas-powered vehicle. The extended charging times can cause longer waiting times in stations if the use of the infrastructure is not optimised and if the infrastructure itself is not adapted to the EV fleet. However, as installing public fast-charging stations is costly (up to 120,000€ for a 350-kW charger), the planning of the infrastructure to uptake the EV drivers' expectations should be optimised too.

Thesis objectives

Therefore, the objectives of this thesis are:

- Propose and evaluate the performance of a control strategy based on real-time communication to optimise the charging plan of EVs going on a long-distance trip and stopping in fast-charging stations to recover energy.
- Quantify the benefit of that control strategy when it comes to optimising the fast-charging infrastructure itself since the control strategy is supposed to use more efficiently the available charging network.
- Establish the trade-off between the reduction of infrastructure cost and the reduction of the time spent in stations according to EV charging powers.

Yet, optimising the fast-charging service on the highway for long-distance trips imposes knowing the technical aspects of an electric vehicle and the fast-charging service itself and understanding the economic and environmental problems raised by such a service. After presenting the general context of this thesis work in Section 1.1, we analyse the technical and economic aspects in Sections 1.2 and 1.3 before concluding in Section 1.4 and giving the structure of this manuscript.

1.1 . Climate change context

To limit the global warming of the planet to 1.5°C and avoid difficult living conditions due to climate change, the IPCC [1] has set a target of net zero CO_2 emissions by 2050 (Figure 1.3) called the Carbon Net Zero 2050 target. A reduction in all GHG emissions must accompany this substantial reduction of CO_2 emissions.

The road transport sector is responsible for 12% of the worldwide GHG emissions, so the transition of this sector to low-carbon fuels is essential. In Europe, the European Parliament has set the emission targets for the sales of new passenger cars to an average of 43 gCO_2/km by 2030 (-55% compared with the target of 95 gCO_2/km set for 2021) and 0 gCO_2/km by 2035 [31]. The first objective for 2030 forces the automotive industry to focus on the development of electric vehicles (EVs), particularly plug-in electric vehicles, which can be plugged and charged. The second target imposes that even new plug-in hybrid electric vehicles (PHEV) must not be sold by 2035. Thus, the battery-electric vehicle (BEV) will be the major plug-in EVs on the roads. Today, the BEV part in the EV fleet is two-thirds, and the PHEV part is one-third.

Stellantis has set a more restrictive objective concerning the emission targets: reaching Carbon Net Zero by 2038 instead of 2050 across Scope 1, 2 and 3 (Figure 1.4).

However, the electrification of the transport sector and the energy sector to decarbonise them will lead to a shortage of some raw materials that are not for now rare but that can become

[1] Intergovernmental Panel on Climate Change

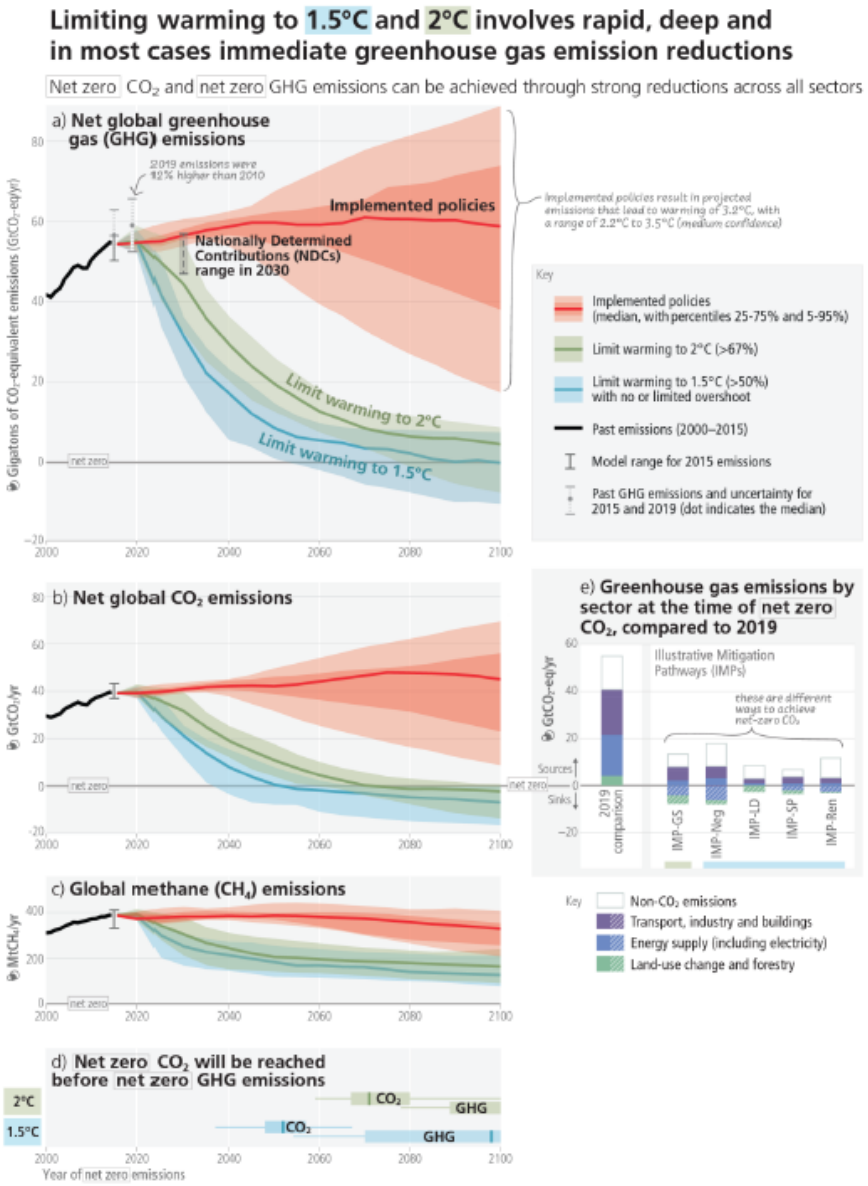

Figure 1.2: Worldwide emissions pathways consistent with implemented policies and mitigation strategies to limit the global warming to 1.5°C and 2°C [2]

critical in the future years (lithium, copper, rare earth metals $\cdots$) [32]. Thus, regarding those supply risks, we can wonder if BEVs should be the only low-carbon technology to be developed and automotive makers also focus on other alternative fuels such as bio-fuels and hydrogen. This matter will not be discussed in this present thesis but is a crucial subject to bear in mind.

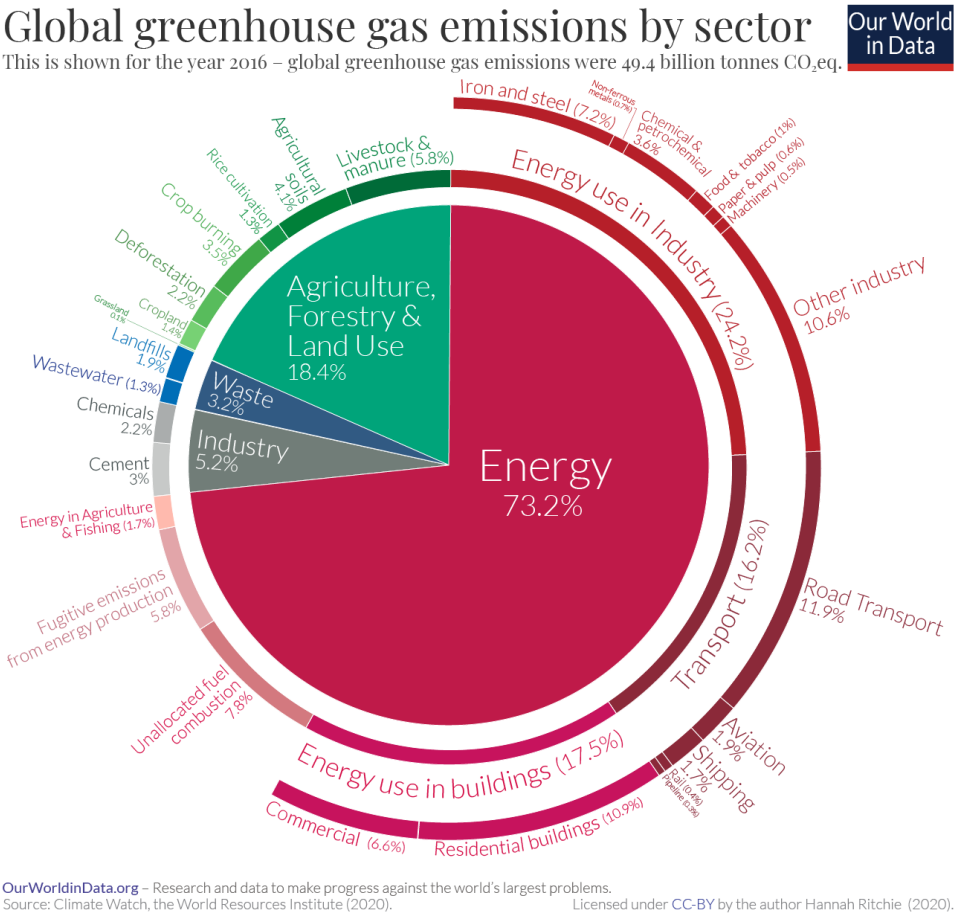

Figure 1.3: Global GHG emissions per sector in 2016 [3]

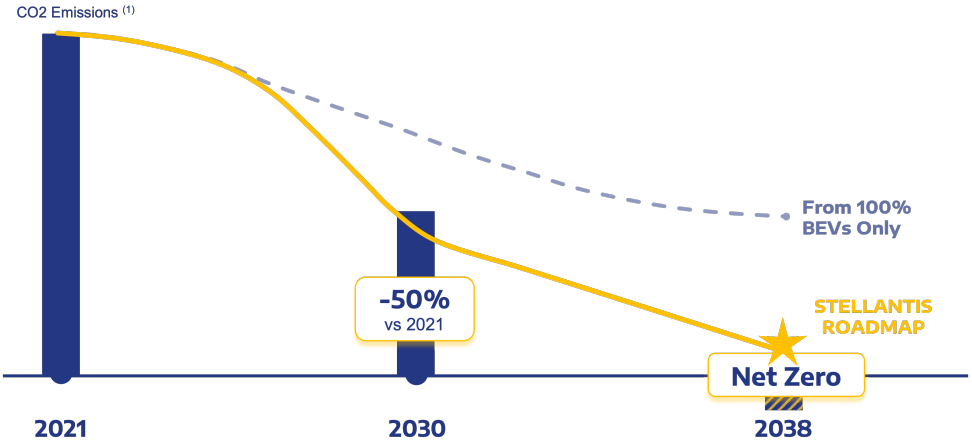

Figure 1.4: Target CO_2 emissions for all Stellantis Scopes (legend: (1) Includes Scopes 1 and 2 (-75% in absolute emissions – ton of CO_2 equivalent) and Scope 3 (-50% in emission intensity – ton of CO_2 equivalents per vehicle) [4]

1.2 . Technological aspects

To understand the stakes of the thesis subject, we should first define a long-distance trip and then focus on the technological aspects of the electric vehicle, the battery and the fast charging infrastructure.

1.2.1 . Long distance trips

Nowadays, most EVs can drive more than 200 km on the highway without charging. Still, according to different mobility surveys, a long-distance trip is defined as a journey of more than 100 km [33], so, in our case studies, we define trips that are in the range $[100, 600]$ km. Moreover, in [33], a long-distance trip or journey accounts for one round trip, but in the present manuscript, we consider only one way of the journey as a long-distance trip.

Long-distance trip with an all-electric vehicle

A **long-distance trip** is a journey over 100 km (80 km by air) needing at least one fast charge on the highway (speed limit $>$ 100 km/h).

1.2.2 . Electric vehicles

1.2.2.1 . Low emission vehicles

There are two different types of electric vehicles: the all-electric vehicles without internal combustion engine (ICE)/gasoline engine and the hybrid vehicles that combine an electric motor with a conventional ICE (see Figure 1.5). The **all-electric vehicles** include the **battery electric vehicles (BEV)** with a battery alimenting the motor and the **fuel-cell vehicles** with a fuel cell converting the hydrogen in electric current to power the vehicle. Hybrid vehicles can either be plugged in to charge their battery (PHEV) or can only regenerate their energy by braking (HEV). The HEVs are not considered low emission vehicles (LEV) since they emit more than 50 CO_2/km. This thesis does not study fuel-cell vehicles as the technology is less mature (less energy efficiency, complex hydrogen management ...) than the plug-in electric vehicle for passenger cars.

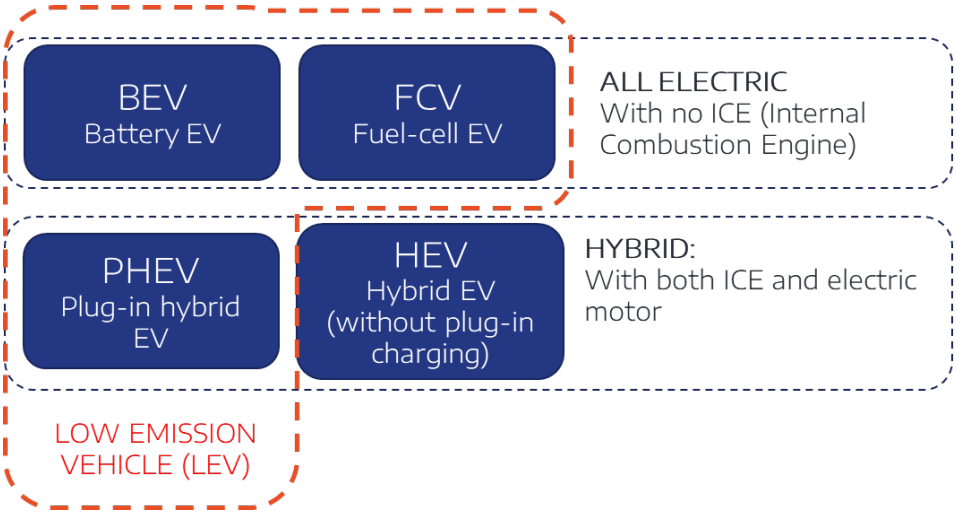

Figure 1.5: Electric vehicle categories

In this study, we will not consider the PHEVs since the models have, on average, only 50 km of range and use the fuel tank instead of the battery on the highway for long-distance mobility. Thus, **this work only focuses on BEVs**.

1.2.3 . Batteries

For BEV, the **battery range** is a factor that must be considered when optimising the charging service for long-distance electric mobility since it will partly influence the behaviour of the driver (range anxiety for example). Traction batteries are a reversible means to transform chemical energy into electrical energy thanks to an oxidation-reduction reaction. Two electrochemical

battery technologies exist: the lithium-ion battery (the most common) and the solid-state battery. **The first technology is heavier and capable of fast charging; the second has a higher energy density but experiences accelerated ageing when fast charged**.

The **lithium-ion battery** is, for now, the major energy storage used for EVs and is the most mature technology. The battery comprises an anode made from carbon or lithium titanate, a cathode generally made with Lithium Cobalt Oxide ($LiCoO_2$) and a liquid electrolyte.

Even if the electric motor conversion efficiency is 95% far better than the one of a powered gas engine (30% in the ideal case for the Carnot cycle), the energy density of a lithium-ion battery is very low (100-265 Wh/kg or 250-670 Wh/L) compared with a fossil fuel (approx. 10 kWh/kg or 10 kWh/L). It is the central aspect responsible for EVs' short range (see Figure 1.6). According to Figure 1.6, fossil fuels have good energy density, and hydrogen is the most energised fuel with the higher specific mass density. Yet, for the hydrogen gas at 700 bar, the energy density of the total fuel storage (gas + tank) is 7 MJ/kg instead of 140 MJ/kg since the tank represents 95% of the storage mass and the H2, 5%. Moreover, the efficiency of the total hydrogen cycle (electrolysis to convert water into hydrogen and then fuel cell to perform the reverse transformation) to power a fuel-cell vehicle is, for now, not as efficient as a Li-ion battery pack.

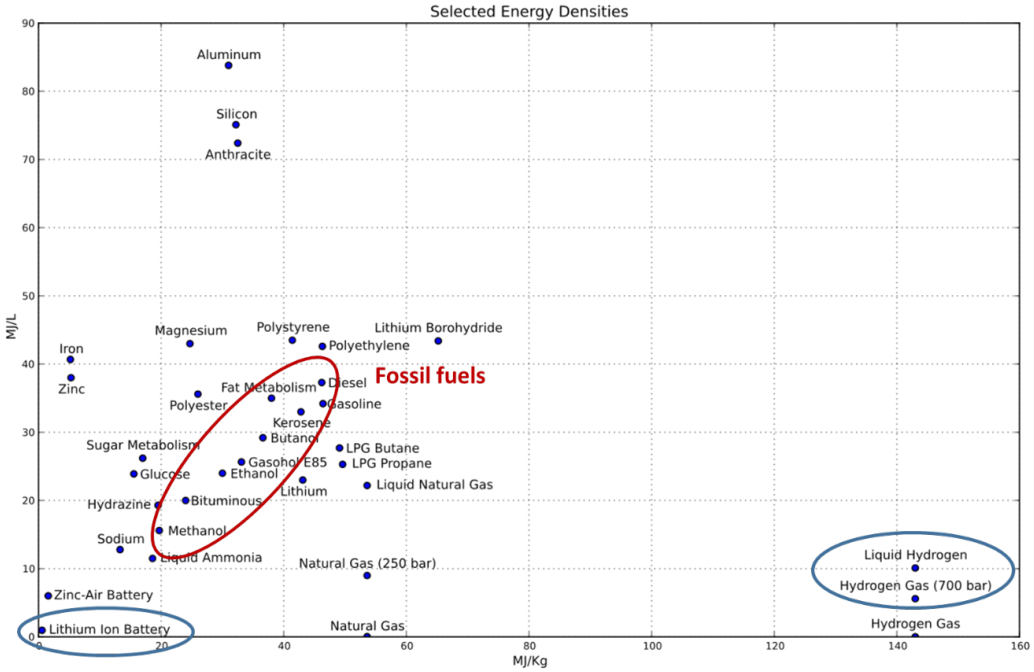

Figure 1.6: Selected energy densities of different components [5]

The **range of the battery** for an electric vehicle is given according to the test made with a WLTP cycle (Worldwide Harmonised Light Vehicles Test Procedure), but in fact, the **accurate range** is most of the time lower and **can be downgraded with a higher consumption rate in case of cold weather or higher speed**. Typically, the highway's consumption rate is twice as much as in urban areas except for some car models with a better aerodynamic shape (*e.g.*, sedan EVs). Indeed, the WLTP cycle is designed for urban areas where the EV will be able to regenerate energy and will drive at slower pace compared to highway.

Solid-state batteries propose an alternative to lithium-ion batteries. They are usually made with lithium metal electrodes (LMB = lithium metal battery) and solid electrolyte. Since the electrolyte is solid and not liquid as in the Li-ion batteries, the specific energy density of the cell is increased and the safety is improved with no possible leakage or inflammation of the electrolyte.

This represents an opportunity to reduce the weight and clutter imposed by Lithium-ion battery and thus, reduce the specific cost (€/ kWh) thanks to the downsizing and the compactness of the technology (packaging opportunity, less materials use and manufacturing) [7]. Reducing the weight of the battery also reduces the vehicle consumption and the downsizing reduces its environmental footprint.

However, fast charging provokes an accelerated aging of solid-state cells by exacerbating the growth of nodules and dendrites on the lithium metal anode, which degrade the battery efficiency. Hence, solid-state batteries cannot be fast-charged. According to [34], as it is more cost-effective to develop batteries that can fast-charge than higher density batteries that cannot fast charge, the lithium-ion battery is for now the best solution for long-distance mobility. J.-Y. Hwang *et al.* [35] have found a promising way to impede the ageing of solid-state battery due to fast charging, but for now, solid-state battery technology is not mature enough to be commercialised as storage for EV applications [7].

1.2.3.1 . EV environmental impact

If we only consider the tank-to-wheel impact, the battery electric vehicle is a zero-emission vehicle while in use, but in fact, the reality is more complex. Indeed, BEVs would be 100% zero-emission vehicles if the electricity they use comes from not emitting energy sources (renewable energies or nuclear). In France, we can say that BEVs are low-emission vehicles thanks to the nuclear energy part of the electric mix, but we cannot say so for other countries (*e.g.*, Germany and Poland).

Moreover, the construction of the battery is responsible for high CO_2 emission (50 kg CO_2 per kWh from the mine to the export point) leading to manufacturing of EVs more energy intensive than conventional gasoline-powered vehicles (see the EV "carbon debt" in Figure 1.7) [6]. The EV should drive a certain amount of km to compensate for the extra CO_2 emissions of the battery construction. Therefore, a life-cycle assessment of the battery cell should be led to exhaustively evaluate the EV technology's environmental impact (Figure 1.8).

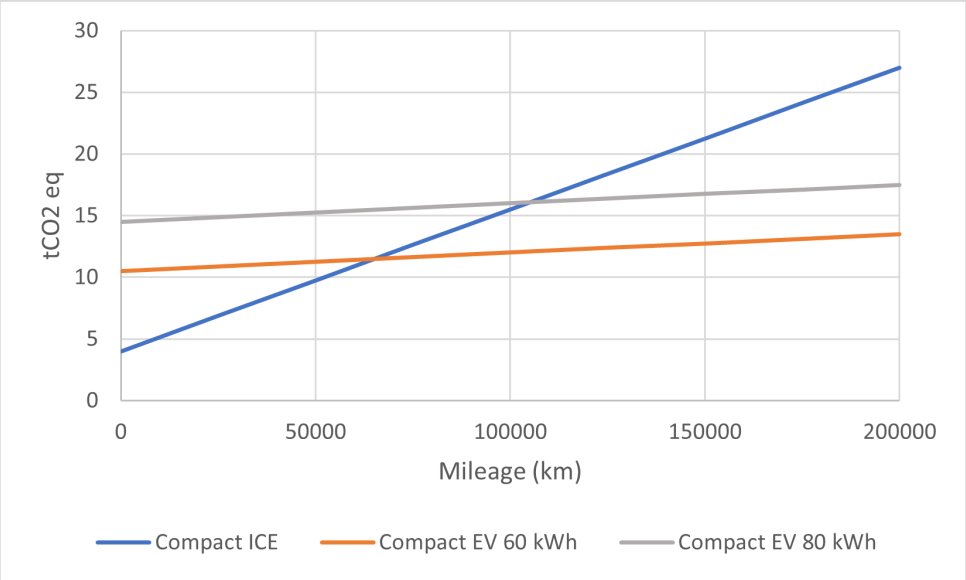

Figure 1.7: Carbon debt of an EV driving in France according to the size of the battery capacity [6]

To reduce the environmental impact of EV batteries, the European Commission has planned to set mandatory minimum levels of recycled content for 2030 and 2035. Ageing batteries can

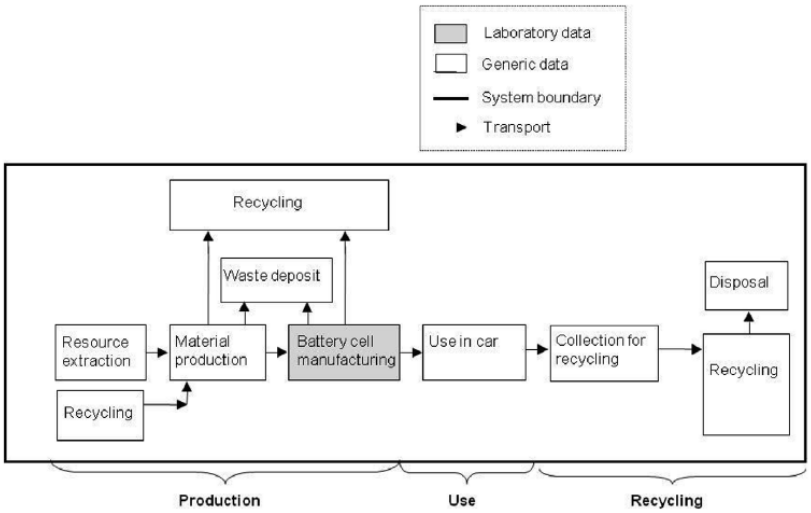

Fig. 1. System boundaries for the LCA of the present study.

Figure 1.8: System boundaries for the LCA of the EV battery [7]

be re-purposed to support the electric grid and store energy generated by intermittent renewable energies (wind power, PV $\cdots$) [36].

Conclusion on the battery technologies and environment challenges

Promising battery technologies (solid state batteries) are emerging to reduce EV weight and environmental impact with less raw materials needed, but they are not mature yet. Therefore, for now, with Li-ion batteries, we should plan to keep limited-range vehicles and develop the fast-charging infrastructure instead of adding raw materials for higher-range battery packs.

1.2.4 . Fast-charging infrastructure

1.2.4.1 . Charging types

An EV can charge using AC or DC charging points [37]. The onboard charging unit of the EV manages the AC-charging to a power usually up to 7 kW (single phase) because the AC-DC converter needed for this power can be placed onboard. However, the charging time for this kind of power is very long (approx. 7 hours) and not feasible for long-distance trips. To reduce the charging time for long-distance trips, the charging power should be increased ($\geq$ 50 kW), but the needed AC-DC converter becomes too large to be placed on board, so it is directly located in the charging point. This is called "DC charging" or charging level 3 [38] and it enables to recover 80% of the battery capacity in less than 30 minutes (fast charging). For this current thesis, as we focus on long-distance trips, we consider only the **DC charging level**.

For DC fast charging, there are different types of charging plugs and vehicle communication standards: the CCS [2] used in the US and Europe, the CHAdeMO used in Japan and finally, the GB/T used in the People's Republic of China [39]. In France, the CHAdeMo, the CCS and the AC Type 2 (43 kW) used to be compulsory on a charging point, but since 2021, the CHAdeMo is no longer mandatory with the adoption of the CCS standard by most of the OEMs (Figure 1.11).

1.2.4.2 . DC charging

[2] Combined Charging System

Table 1.1: DC charging characteristics

Power (kW DC)	Current intensity (A)	Voltage (V)
50 - 350	125 (50 kW) - 500 (350 kW)	400 - 1000

The charging time of an EV is linked to the charging power of the battery pack that depends on the SoC of the EV [19, 40]. The representation of the power according to the SoC is also called the "charging curve". Figure 1.9 shows that there are as many charging curves as EV models. However, those curves can be classified according to the six main categories of charging methods [41]: Constant Current-Constant Voltage (CC-CV - the most used), Constant Power-Constant Voltage (CP-CV), Multistage Constant Current - Constant Voltage (MCC-CV), Pulse Charging, Boostcharging with CC-CV-CC-CV scheme and Variable Current Profile [42].

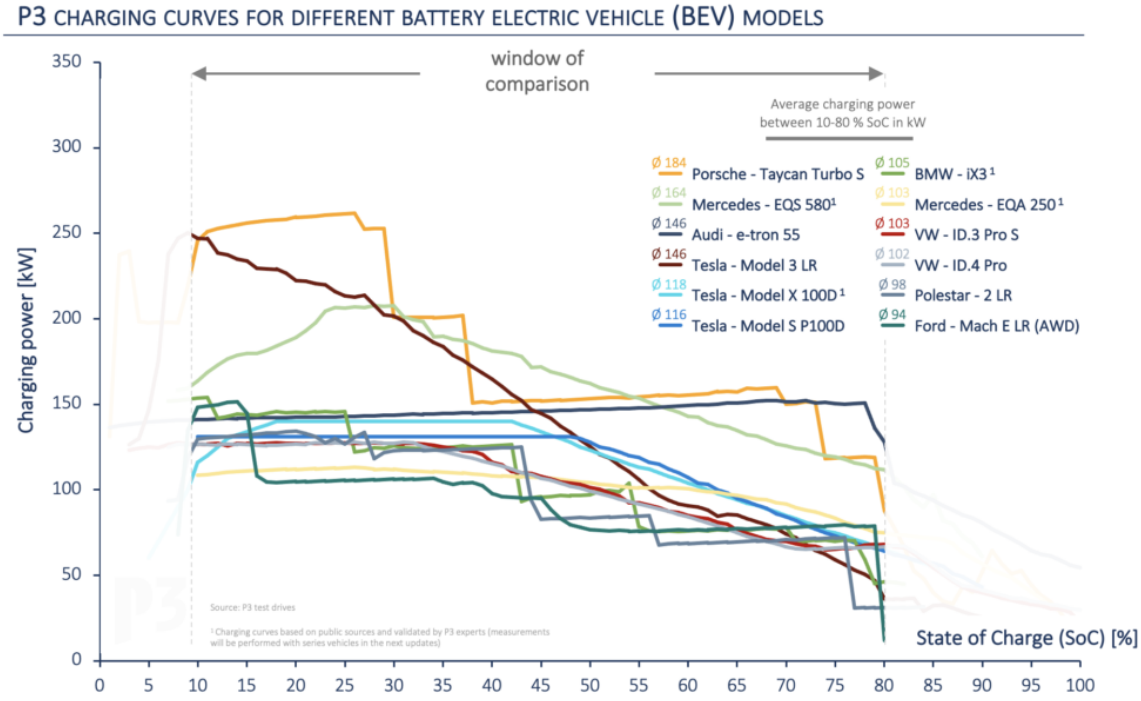

Figure 1.9: Charging curves of different EV models on a charger > 100 kW [8]

To understand the charging process, we study here the most simplified model for the battery cell: the association of an intern resistance R in series with an open-circuit voltage source V_{OC} (Figure 1.10a). The open-circuit voltage V_{OC} evolves with the SoC of the EV. To avoid damaging the battery, the current should be limited at high SoC to keep the voltage cell, V_{cell}, under its maximum value [41]. This is why the Battery Management System gradually decreases the current after a certain time, and we observe the charging power drops for high SoC in Figure 1.9. Often, the charge is limited to 80% of SoC to avoid the longer charging times beyond that SoC. As an example, we represent in Figure 1.10b the evolution of the current i_c in the cell and the voltage cell V_{cell} according to the time in the CC-CV mode: during the Constant Current phase, V_{cell} is increasing and then when V_{cell} is near its maximum value, the current is decreased to keep a constant voltage cell (Constant Voltage phase).

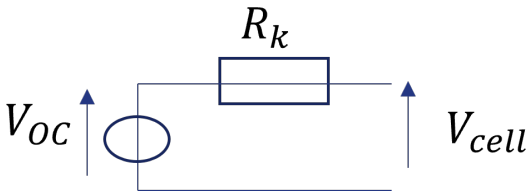

(a) Simplified model of a battery cell

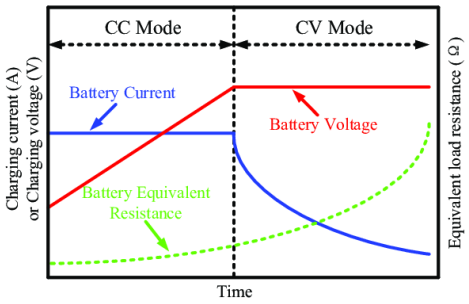

(b) CC-CV charging profile

Figure 1.10: Battery model (a) and charging process (b)

In addition, the real charging power during a charging session is limited by either the charging power of the EV (see Figure 1.9) or by the charging power the charger can deliver.

Even with fast charging, recovering energy during long-distance trips takes time (on average, 20 minutes to charge from 10% to 80% of SoC) and increases the trip time, especially if the infrastructure is insufficient and generates waiting queues in stations.

Therefore, it is essential to develop the charging network to avoid long waiting queues and a significant increase in the trip time.

1.2.4.3 . Charging network

A charging network is a network of charging stations (CSs). Concerning the management of the charging service, a distinction is to be made between the **charging point operators** like Ionity, Total Energies (Figure 1.11a), Fastned (Figure 1.11b), Izivia ... and the **e-mobility operators** like Chargemap (Figure 1.12), Freshmile, Plugsurfing ... [43].

Charging point and mobility operators

A **charging point operator** (CPO) installs and manages the charging stations of a charging network.
An **e-mobility operator** or **E-mobility Service Provider** (EMSP) manages charging access to several charging networks and payments with a pass or a mobile application. Usually, an EV driver pays a subscription to one or more EMSPs to access charging points from multiple partner networks. The EMSP often provides some tools like a charging planner or interactive charging maps listing the charging stations' positions and details.

At the beginning of this thesis (in 2021), the public charging infrastructure on the highway in France was insufficient to support the charging demand for long-distance trips, especially with charging stations spaced too far apart. Indeed, in May 2021, 140 out of 440 highway service areas proposed at least one fast-charging point for long-distance trips. To downplay this lack of infrastructure, the French program ADVENIR (see the section about stakeholders in Section 1.3.1) was aiming to equip all the service areas with a minimum of two ultra-rapid chargers (150 kW) before the end of 2022. Nowadays, the objective is almost reached with 99% of the service areas equipped (Figure 1.13).

The price at a station depends on the operator (**Ionity – 0.79 €/kWh** [44], **Fastned – 0.59 €/kWh** ...) but the offers change. In any case, charging at a public fast charging point is more expensive than at home, except for some parking lots that offer free charging but at a lower power.

1.2.4.4 . Connection to the grid

(a) Total Energies charging station

(b) Fastned charging point

Figure 1.11: Charging points in a charging station

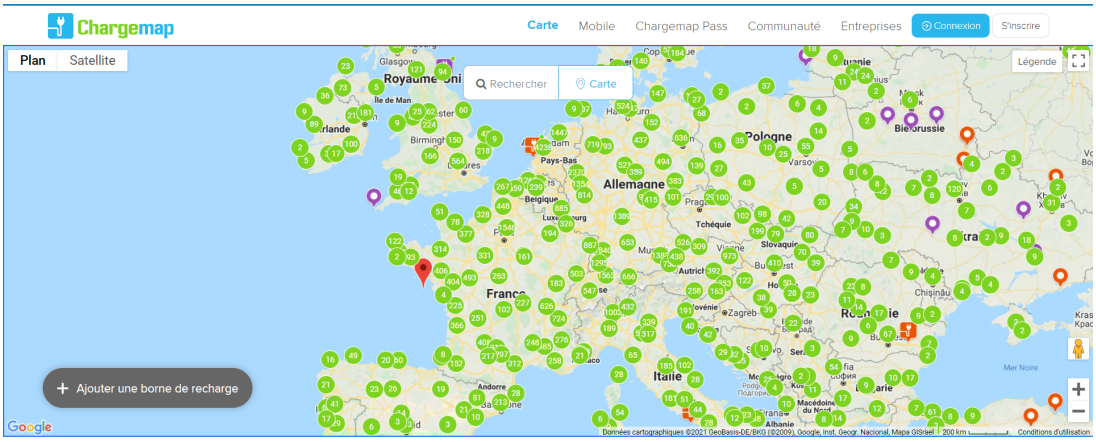

Figure 1.12: Position of charging points from the application Chargemap (not only on highway service areas)

According to the CRE [3], the connection to the grid of fast charging points (≥ 150 kW) on highway service areas would be done on the medium-voltage distribution grid (HTA in France).

In the literature, a lot of papers deal with smart charging to balance the grid power, ensure grid safety and limit charging impact on the grid [25, 45–48]. Those studies are generally about grid balance in cities or microgrids where the charging is localised in the same area and is competitive with the evening peak load. On the contrary, fast charging spreads during the day and is less competitive with the evening peak load. However, according to a study conducted for highways in Texas [25], the fast-charging demand needs high peak powers that could lead to congestion on the grid if the electric network is not reinforced. In France, a report [13] by Enedis and Rte, French operators respectively of the distribution and transmission networks, gives in 2021 an insight on the development of the fast-charging infrastructure on French highways and the impact of the charging network on both the distribution and transmission grids. Like in [25], the report concludes that the grid should be reinforced but with relatively low expenses for both French operators compared with their annual investment in the grid.

Indeed, the report establishes that by 2035, the charging infrastructure will need an installed

[3] Commission de Régulation de l'Energie

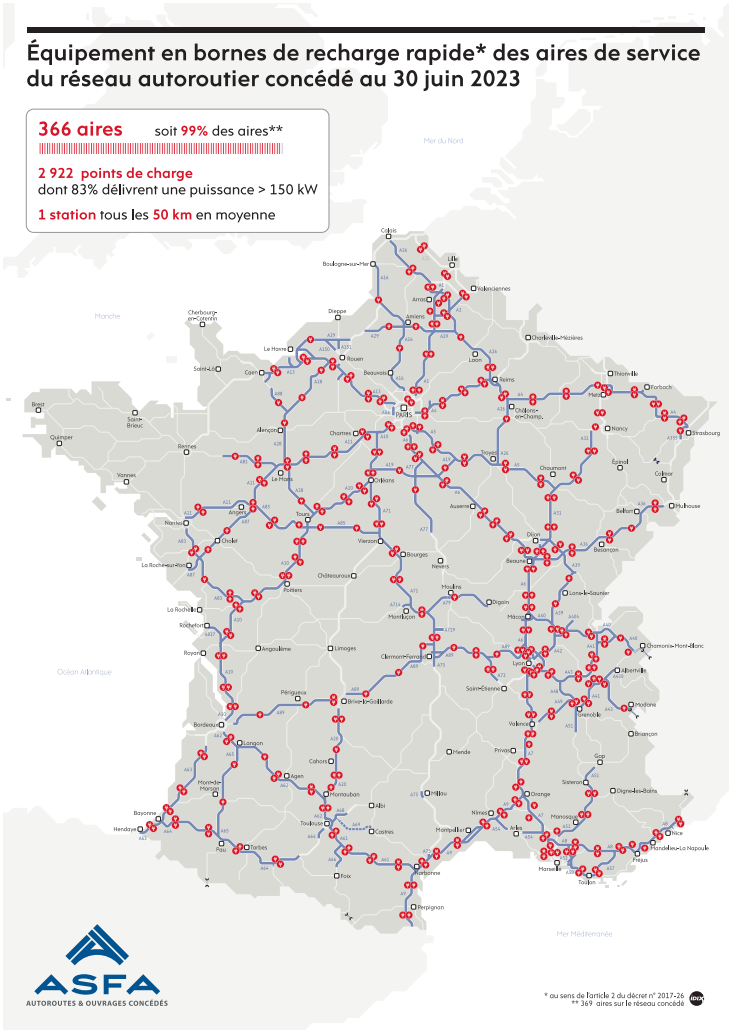

Figure 1.13: Equipment level of the 440 highway service areas in France in June 2023 [9]

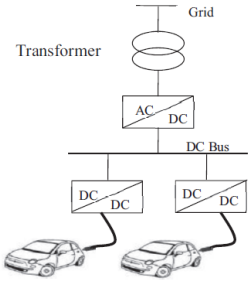

(a)

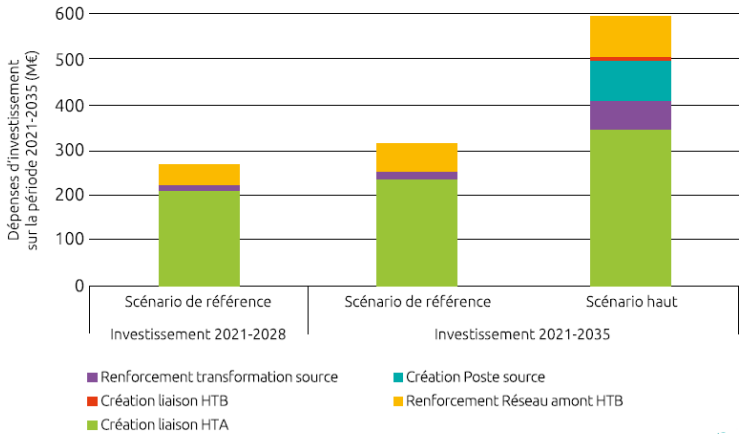

(b)

Figure 1.14: (a) Fast-charging station connection to the grid [10]; (b) Cumulative investment costs in the electric grids (transmission and distribution) during the period 2021-2028 and 2021-2035 for the connection of the charging stations on highway needed for the light long-distance mobility

power **from 2 GW** (reference scenario) to **5 GW** (high variant scenario), which corresponds to 4 MW and 12 MW in average per area. **The total cost of developing the grid** (distribution and transmission) to support the power supply of the fast charging infrastructure on the highway by **2035** is estimated to **300 M€** for the reference scenario and **600 M€** for the high variant scenario. Figure 1.14b details the costs of the different expenditure items; we notice that most are dedicated to creating new distribution lines (HTA lines). Those costs represent respectively only 0.3% and 0.6% of the investment planned by the grid operators. More specifically, for the 15 years from 2020 to 2035, the transmission network (HTB) expects to invest from 60 to 90 M€ (according to the scenario) in the punctual reinforcements of the 63 kV/90 kV grid needed for the fast charging.

The relatively low costs of the connections and the reinforcements of the grid needed to ensure the power supply of the fast-charging infrastructure are encouraging for the development of light electric mobility over long distances. We can add that the connection and reinforcement of the grid do not present technical difficulties, and the fast charging on the highway will have a limited impact on the balance of the grid.

However, the connection to the grid takes time and installing a new charging station can last several years from the project start to the charging point effectively running. Therefore, **the installation of charging points must be anticipated, or solutions to manage the charging for long-distance trips should be implemented**.

Vehicle-to-grid is also an interesting aspect of EV technology to support the electrical grid [49]. However, as the subject of this thesis is linked to long-distance trips, the vehicle will have no interest in giving energy back to the grid (or to other users) because it will need all its available energy to reach its destination, except if the battery of the EV is big enough to charge other cars during trip stops. Consequently, we will not work on vehicle-to-grid (more generally, V2X) problematics in the context of this thesis.

1.2.4.5 . Alternative ways for charging

Other ways of charging EVs exist, such as battery swapping, inductive charging and redox flow battery use.

The **battery swapping** consists of changing the discharged battery with a fully charged one. The time to swap one battery can compete with the time needed for refuelling at the gas station for a conventional thermal vehicle. However, this method is very costly. Drivers can also consider **loaning an additional battery** when they go on long-distance trips to avoid transporting an oversized battery when commuting (short-distance trips).

Inductive charging lanes are portions of the road with coils underneath that establish a magnetic field thanks to an electric current circulating in the coils. This magnetic field enables the creation of an electric current in another coil entering the magnetic field. This second current is used to charge the battery of an EV as it is driving on the road. This technology will not be studied in this thesis but represents another exciting alternative to fast-charging infrastructure for long-distance trips. A cost-efficiency comparison is led in [50] between the fast-charging infrastructure and inductive lanes and concludes that the fast-charging infrastructure development is more cost-effective than installing inductive lanes.

A **redox flow battery** is an electrochemical cell battery where the two chemical components of the reaction are dissolved in liquids from two different tanks. A membrane separates the tanks. The battery works as a fuel cell (we can replace the liquids with new ones like for fossil fuels or hydrogen) or as a rechargeable battery. Thus, the flow battery can reduce the charging time thanks to tank refuelling, but this kind of battery is less powerful and requires more complex electronics.

1.3 . Economic and societal aspects

After summarising the technological aspects of the subject, we develop in this section the economic perspectives of the fast-charging service from drivers' and investors' points of view.

1.3.1 . Stakeholders

The development of the fast charging infrastructure and services linked to electric mobility over long distances involves many stakeholders (Figure 1.15). The **automotive makers** (Stellantis, Tesla, Renault…) need to comply with European environmental objectives and have interest in the development of such an infrastructure that can improve **EV drivers' satisfaction** and so increase EV purchases. **Highway operators** have to consider the layout of service areas to build new charging sockets. **Electric grid operators** should consider new loads in the electric network management with new transformers for the fast charging points. Public institutions (*e.g.*, European Union) set the directives to follow and the penalties for the automotive makers who do not reach the targets (€95 per sold car per gram of CO_2 above the targets). **Governments** use public incentives to accelerate the transition to electric vehicles: the French government dedicated **€100 million** to help build fast charging points on the 440 highway service areas. By the end of 2022, the objective was that each service area had at least four charging points with 2 of more than 150 kW. **Governments** can also grant a bonus for purchasing an electric car (up to €6,000 in France), but that incentive will soon be over.

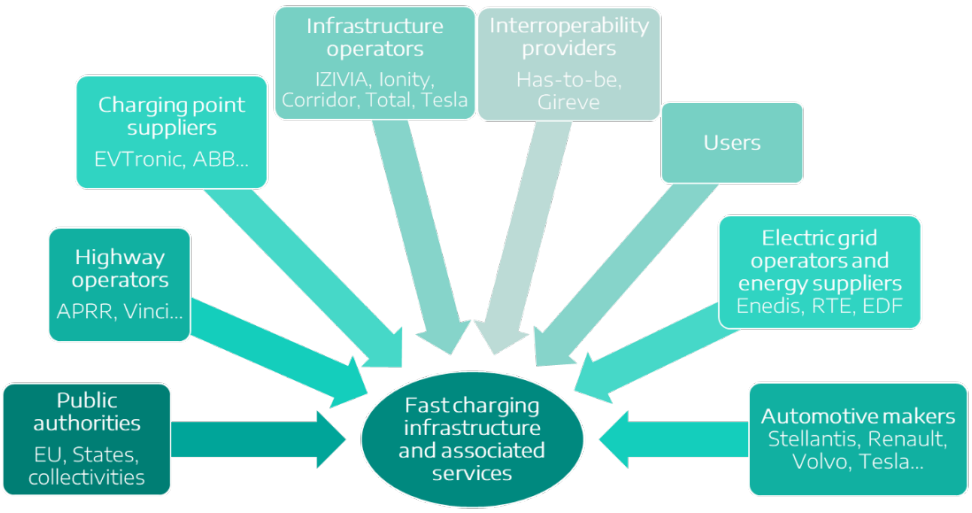

Figure 1.15: Stakeholders of the fast charging infrastructure development

AVERE is the European Association for Electromobility and gathers actors in electric mobility from collectivities, associations, and industries. AVERE-France is one of the ADVENIR program project managers that aims to fund the development of private or public charging points with energy efficiency certificate (CEE in French) [51]. Through this program ADVENIR, the French government planned to invest 100-million-euro incentives in the purchase and installation (electric connection downstream the delivery point) of more than 45,000 new charging points by the end of 2023.

In France, there is no partnership between automotive makers and the government to develop charging infrastructure. Still, for instance, in Germany, automotive makers (BMW,

Daimler…) have participated in the private/public partnership at the origin of the fast-charging network Ionity. The automotive maker Tesla had first developed its own infrastructure network only for Tesla drivers, but now the Tesla superchargers are open to all the other brands.

The strategies differ from one stakeholder to another. Still, their diversity should be considered to see how electric mobility over long distances will be improved thanks to the development of a high-power charging network. The elaboration of an economic model and the calculation of the CAPEX and OPEX depend on the projection scenarios and the stakeholders considered. We present the e-mobility on long distances from the point of view of an EV driver (section 2.1.2) before dealing with the infrastructure operator/investor's point of view (section 2.1.3).

1.3.2 . Social aspect: driver's point of view

The section on the technology aspects (Section 1.2) sheds light on the different challenges electric mobility faces, especially when we compare the performance of the conventional ICE vehicle with one of the electric vehicles. Indeed, as consumers are used to the performance of ICE cars, the transition to an electric car is uneasy. We can identify from Figure 1.16 that the two main drawbacks to EV adoption are range anxiety and long charging times that deter using an EV for long-distance trips.

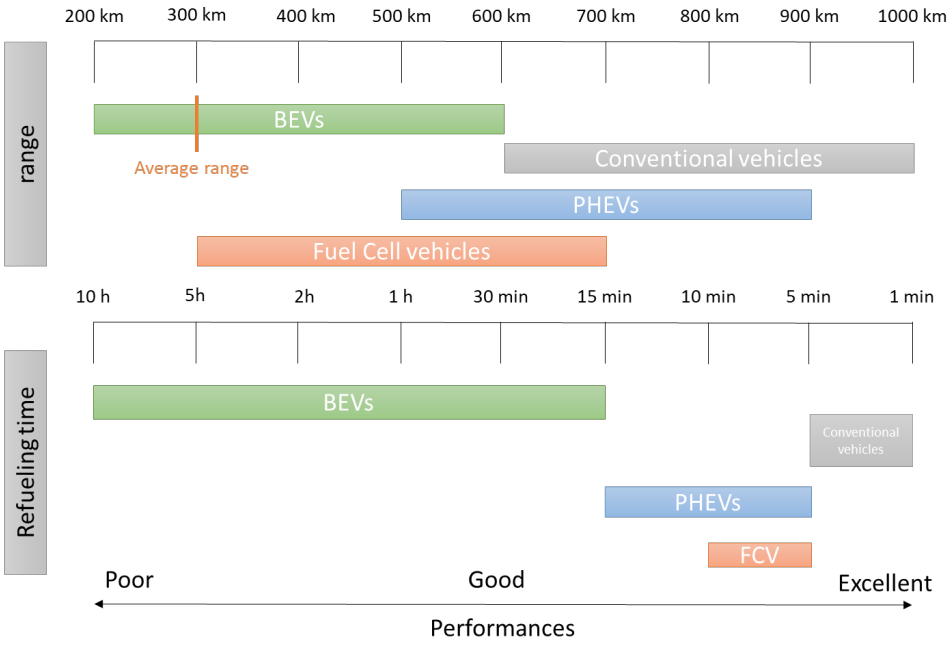

Figure 1.16: Comparison of the range and refuelling time performances of the different vehicle propulsion systems

According to Faizal *et al.* [52], range anxiety is the first drawback to EV adoption. This aspect is closely connected to the feeling that the public charging network is not dense enough and that acquiring a higher battery range is costly (second drawback according to [52]). Therefore, two solutions exist to mitigate range anxiety:

1. The driver buys an EV with higher battery capacity, but the cost of owning is increased (approx. 100 €/kWh) as well as the environmental footprint of the EV (see Section 1.2.3.1).
2. CPOs install a denser charging network with a maximum distance between two charging stations.

For the spacing of the charging stations, G. Napoli *et al.* [53] set the **maximum distance between two charging stations** to $0.8 \cdot r_{min}$, with r_{min} the minimum range in the EV fleet on the highway. Indeed, the drivers seem to perceive they are safe if they use only 80% of their battery capacity [54]. In the study, r_{min} is 133 km, so the maximum distance should be approximately **100 km**. S. Funke *et al.* [55] establish the same maximum value (100 km between two charging stations). In France, the government expects a denser network with a charging station in every service area on the highway, so on average, a charging station every 50 km.

Concerning **long charging times**, when an EV owner needs their car for commuting, they can usually wait the whole night or the whole day to charge (the charging can last 7 hours on a level 1 charging point). However, for long-distance trips, the EV driver aims to charge as fast as possible, so they need public fast-charging infrastructure with DC power ($\geq$ 50 kW). Faster charging also reduces station waiting time (see Section 1.2.4.2). Nevertheless, even with high charging rates, the charge is still longer than refuelling.

Moreover, the higher the SoC of the EV is, the lower the charging power is due to technical constraints and the management of the charging to avoid damaging the battery (see Section 1.2.4.2). Therefore, optimising the charging stops and the energy recovered in stations to charge the battery in the best SoC range (when the power is the highest) is beneficial to gain as much time as possible for long-distance trips.

A report from ACOZE France [56] defines the quality criteria the charging service should observe to improve the EV driver's experience on the highway: the waiting time should not exceed 30 minutes per charging session, and the length of the waiting queue length should be limited to 2 or 3 times the number of chargers in stations. ACOZE suggests building parking spots dedicated to waiting for EVs to avoid congestion in the charging parking lot.

Regarding the technical challenges and the EV drivers' expectations, the solutions to mitigate extended trip times due to long charging times are:

1. Increasing the power rate in stations
2. Increasing the number of station charging points to avoid long waiting times.
3. Planning the charging of the EV to benefit from SoC ranges for which the charging rate is the highest.

Concerning the first solution, the charging cost for a driver is usually higher for higher charging rates. Thus, to evaluate the performances of the different fast-charging strategies we study in this present thesis, we should take into account the **charging cost** in addition to the **trip time** to **model the discontent of an EV driver using the charging service**. Moreover, to benefit from high charging rates, the drivers must possess an EV capable of ultra-fast charging. Therefore, **we develop in this thesis an analysis of the trade-off between the time gain in stations compared with the cost of the infrastructure to develop according to the charging power of the EV fleet.**

Highlights on the EV owner's point of view

The charging service for the EV should propose:

- A charging network dense enough to mitigate range anxiety according to the EV range.
- A sufficient number of charging sockets and adequate station charging rates to limit waiting time.
- A planning of the charging to get lower charging times.

1.3.3 . Charging point operator's point of view

According to the EV drivers' expectations and solutions that need to be implemented to mitigate charging service challenges, the development of fast-charging stations is vital. In the white paper by M. Nicholas and D. Hale from ICCT[4] [38], the relationship between the deployment of fast-charging infrastructure and the number of EVs on the road seems to be more complex than a simple proportional evolution. Indeed, in the beginning, a necessary minimal number of fast-charging stations should be built for geographical cover (limited range) to incite the purchase of EVs. Then, as long as stations are not highly saturated, the installed charging points can support more EVs. S. Funke *et al.* [55] also underline that the number of charging stations can be relatively low from a technical point of view. Still, to deal with range anxiety, we need to add more charging stations to reduce the distance between them and reassure drivers.

Moreover, fast-charging points are costly (up to 120,000 € [26]) so, CPOs or investors must establish a business model to size the infrastructure as close as possible to charging demand. They first need to evaluate the charging needs and then compute the investment and operating costs of the infrastructure according to the stakeholders considered in the model. To evaluate the future charging needs, the investors have to quantify the future number of EVs on the roads that will use the highway charging services. However, this task is uneasy as traffic flow data is not always open. When the CPOs manage to define the traffic flow, they can choose to size the infrastructure according to an average traffic flow or according to high-traffic situations. The first consideration is limiting the infrastructure cost and ensuring good profitability of the infrastructure. Still, the risk is that long waiting times increase drivers' dissatisfaction during occasional high traffic flow. For the second consideration, the investor ensures that the waiting time is limited, but the infrastructure is oversized. Therefore, to avoid long waiting times and oversizing, **a charging strategy must be found to use more efficiently the charging infrastructure when it is saturated.**

Once the charging needs are evaluated, the calculation of the CAPEX and OPEX depends on the projection scenarios and the stakeholders considered.

Highlights on the CPOs' point of view

Fast-charging infrastructure is essential to mitigate the charging service drawbacks, but as a DC-charging point is costly, developing the fast-charging infrastructure is costly, especially for ultra-rapid charging rates (350 kW). Therefore, such infrastructure development should be optimised to limit its costs while improving EV drivers' experience on long-distance trips. A solution should be implemented to use the charging infrastructure more efficiently.

1.4 . Conclusion and presentation of the manuscript structure

The purpose of this PhD thesis is mainly to help automotive manufacturers such as Stellantis abide by the environmental objectives defined by the European Standards and the Carbon Net Zero 2050 strategy. To reach those objectives, the acceptance of EVs must be improved to pursue the development of the technology. For this thesis work, we choose to focus on the long-distance perspective of electric mobility as it is a significant issue for battery electric vehicles and because the literature already proposes many works about urban electric mobility but a few about long-distance electric mobility [20].

[4] International Council of Clean Transportation

In this general introduction, we have analysed the technical, economic and social aspects of the fast-charging service that would enable electric mobility over long distances. This overview points out the complexity of this subject where different aspects affect the charging service (vehicle characteristics, user needs, charging infrastructure characteristics and weather conditions [57]) with different interconnected networks (highway network, power grid and fast-charging infrastructure network) [58] and where trade-offs have to be made between the objectives of the different stakeholders (EV drivers' satisfaction, infrastructure cost minimisation $\cdots$).

Consequently, the **fast-charging infrastructure should be optimised, and new charging strategies should be implemented to control the EV fleet charging** and help limit the infrastructure cost while improving EV drivers' satisfaction.

To address this issue, we first present in **Chapter 2** the various optimisation methods and parameters already considered in the state of the art and the research activities led on the subject to extract the research gaps that drive this PhD thesis.

Then, we present in **Chapter 3** the simulation framework we use to experiment and test the different charging strategies we study during this thesis. The framework was first implemented by J. Hassler *et al.* [21] and enables to dynamically simulate a flow of EVs during a day on a highway with charging stations. The first strategy tested, thanks to the framework, is a strategy of **fleet control** based on communication between EVs and charging stations to limit waiting time in stations. The strategy is called the *First-Come First-Served communication* since the priority in stations is based on the First-come-first-served rule. The previous study of the strategy has shown that the EV drivers' experience can be improved by the use of the *FCFS communication strategy* with, for instance, a reduction of the travelling time thanks to a better use of the charging infrastructure [21].

To go further in the performance evaluation of the *FCFS communication strategy*, we implement another control strategy, the *reservation strategy*, where the EVs communicate their charging plans but also book charging time slots. The comparison of both charging strategies is led in **Chapter 4** to determine which control strategy most benefits the EV drivers.

Concerning the optimisation of the charging infrastructure, we show in **Chapter 5** the benefit of the *FCFS communication strategy* in the reduction of the infrastructure costs by computing thanks to a Grey Wolf optimiser the optimal infrastructure when the fleet uses the *FCFS communication strategy*. The EV drivers' expectations are modelled as a maximum waiting time guarantee by the optimal infrastructure.

Finally, as increasing the charging rate would positively impact the trip time but is costly, we analyse in **Chapter 6** the trade-off between the infrastructure cost and the time spent in stations according to the share of ultra-fast-charging EVs (EVs charging at $\approx$ 350 kW) in the fleet. We optimise the infrastructure to be developed thanks to a multi-objective optimiser: a differential algorithm with NSGA-II convergence.

2 - Literature review on charging strategy optimisation

Considering its technological, economic and societal aspects, the electric mobility on long-distance proves to be a complex problem that should be solved thanks to multi-level and multi-criteria optimisation. Section 2.1 presents the different aspects of the charging service that can be optimised. Then, we focus on the optimisation methods from the literature that are applied to the specific subject of this thesis: development of an optimal EV charging control to reduce charging and waiting time and optimisation of the charging infrastructure. As explained in Section 1.3.3, to propose an efficient charging service that improves EV drivers' satisfaction, we need to evaluate the future charging needs for long-distance trips. Thus, we first determine in Section 2.2 the different methods that are used in the state of the art to estimate the future charging volume and establish charging demand scenarios. Then, in Section 2.3, we depicts the charging control strategies evoked in the literature before presenting the different methods used to optimise the infrastructure (Section 2.4).

Contents

2.1 . How can we optimise the charging service?

2.1.1 . Charging service optimisation: a multi-objectives problem

The aim of this thesis is to improve EV's acceptance by drivers but also to take into account the point of view of other stakeholders such as investors, grid operators and charging infrastructure operators through an optimised development and operation of the fast charging infrastructure on highway.

According to **S. Jawad and J. Liu** [58], the development and the use of the fast charging infrastructure leads to an interdependence of multiple networks: electric power networks, transportation networks and charging service network scheduling. To efficiently plan each network, a cooperative coordination of those interdependent networks is paramount and should mix the forecasting for EV charging, transportation traffic and load on the power system. Concerning the impact of the long distance mobility on the electric power network in France, we have seen in Section 1.2.4.4 that the impact will be limited according to French operators of the grid and will require little grid reinforcements compared to their annual investment forecast on the grid. Consequently, the impact on the grid is not studied in the thesis.

In addition, with the power grid and the traffic fluency constraints, we should above all consider in the study EV driver's satisfaction by **reducing range anxiety and travelling time** while minimising the cost of the charging infrastructure.

The **travelling time** can be divided in three parts: **the driving time, the waiting time and the charging time**. The **driving time** does not differ from the one of a conventional ICE car except when the EV drivers slow down to preserve their range. Indeed, the driving style highly affect the consumption of the EV [19, 59], especially high speeds that significantly increase the consumption. However, as the driving style depends on the driver behaviour, we consider the **speed as an exogenous variable** of the problem and we do not include the speed as a variable in our work. The **waiting time** depends on the availability of the charging infrastructure and can be reduced by a denser network and/or a more efficient use of the infrastructure. The **charging time** is limited by either the power of charge of the EVs or the power of the station: the higher the minimum charging power of charge is, the quicker is the charge. The EV driver can also optimise it charging plan by choosing the strategic level of SoC to charge.

Therefore, to improve the charging service, the optimisation should take into account the battery capacity to find the optimised number and location of the charging stations and find the optimised sizing (number of charging points) and power of the charging stations to avoid waiting time and reduce charging time. The control of the charging represents also an important lever for action by using more efficiently the infrastructure and the EV state. We differentiate in the

rest of the chapter two categories of charging strategies that are using multi-objective methods: the control strategies 2.1.3.3 and the sizing strategies 2.1.3.4.

2.1.2 . Social cost for the EV drivers

As explained in Section 2.1.2, an EV driver expects to find a certain level of charging service quality when going on long-distance trip to be satisfied. Each drawback to EV adoption can be associated to a social cost that the charging service aim to minimise or at least reduce to improve EV drivers' satisfaction and mitigate the challenge. This social cost is used in cost-efficiency analysis of different solutions to mitigate a problem or in optimisation problem as an objective to minimise. We present in Section 2.1.2.1 a cost efficiency analysis where the social cost for the driver is the cost of ownership. In Section 2.1.2.2, the social cost is associated with the trip time.

2.1.2.1 . Cost of ownership

As presented in Section 2.1.2, the two solutions to mitigate range anxiety are: increase the battery or develop the charging infrastructure. To evaluate the cost-efficiency of the first solution, S. Funke *et al.* [55] compute the infrastructure cost (see Section 2.1.3) and the cost of ownership of an EV according to its battery capacity and consider in the calculation the rent of an ICE vehicle if the range is not sufficient to realise a long distance trip with at most two charging stops. The cost of ownership in [55] is evaluated as the difference of equivalent annual cost, ΔEAC, between an EV and a conventional ICE vehicle (2.1). The Equivalent Annual Cost (EAC) corresponds to the annuity whose net present value is equal to the net present value of the investment. The CAPEX difference between an EV and an ICE vehicle corresponds mainly to the battery purchase price (100 to 350 €/kWh in the study). The OPEX includes operation and maintenance costs, annual cost for renting a conventional ICE car for long distance trips if the battery capacity is not enough and the charging/refuelling cost proportionate to the fuel consumption and the annual travelled kilometers.

$$\Delta EAC = (OPEX_{EV} - OPEX_{ICE}) + (CAPEX_{EV} - CAPEX_{ICE}) \times \frac{r(1+r)^L}{(1+r)^L - 1} \tag{2.1}$$

With L the number of periods (the car life time) and r is the discount rate.

According to [55], **investing in fast-charging infrastructure is always more cost-efficient than investing in high battery range**. The result of the study is logical: longer battery range induces more individual cost than the public development of the fast charging infrastructure. Developing the fast-charging infrastructure instead of increasing battery range might also have a more beneficial ecological impact since more range currently means more battery materials use so more ecological impact. However, studies should be led to justify that the infrastructure would not need in that case more materials than the whole longer-range battery packs would have.

2.1.2.2 . Trip time cost

Another drawback we identified in Section 2.1.2 is the long charging time that extends the trip time. Thus, the social cost can be defined as a trip time cost. **T. Oda *et al.*** [15] perform a cost-benefit analysis on the addition of a charging point in a station according to the number of EVs entering a station per day and determines that a charging point should be added every **10 ± 3 EVs per day** to limit the **waiting time to 10 minutes for 90% of the fleet**. In this study, the social cost is the waiting time. In [55], to estimate the number of charging points needed in stations, S.Funke *et al.* add a charging point when **the average waiting time in stations exceed**

five minutes. We see later in Sections 2.3 and 2.4 that multiple papers from the literature use the waiting time or the trip time as a social cost to be minimised.

2.1.3 . Economic model for the charging infrastructure

As already mentioned in Section 1.3.3, a CPO needs to evaluate the future charging demand (Section 2.1.3.1) before computing the investment and operating costs of the infrastructure according to the stakeholders considered in the model.

2.1.3.1 . Evaluation of the charging needs

To evaluate the future charging needs, the investors have to quantify the future number of EVs on the roads that will use the highway charging services. The way the number of EVs on the highway is forecast varies from a study to another: the evaluation of the charging infrastructure needs can be static with a constant number of EVs on the road [60, 61] or more precise with a dynamic evolution of the number of EVs on the roads [11,50]. In addition, some studies focus on evaluating the charging needs according to average traffic flow [53] while other prefer to size the infrastructure based on peak traffic flow [13, 50] during holidays departure for instance. The first consideration limit the infrastructure cost but the risk is to have during occasional high traffic flow, very long waiting time. For the second consideration, we ensure that the waiting time is limited but the infrastructure is oversized.

After evaluating the future volume of EVs on the highway, the charging demand should be evaluated according to long-distance trips statistics. As it is uneasy to find public detailed trip data listing origin and destination of the trip as well as location of charging stops, the papers in the literature usually feed their model with public available traffic data on road sections [55, 62, 63] or with trip details [64] to determine the location of the future charging stops. We detail in Section 2.2 the various means used in the literature review to define the charging needs.

2.1.3.2 . CAPEX and OPEX for the infrastructure

Once the charging needs are evaluated, the calculation of the CAPEX and OPEX depends on the projection scenarios and on the stakeholder considered. For future works on the calculation of the infrastructure costs in this thesis, the CAPEX and OPEX calculation for the charging infrastructure mix the expressions given in the literature.

J. Serradilla *et al.* [11] presented in 2017 the business model of the charging network with the different elements that should be considered when evaluating the **CAPEX** and **OPEX** of the fast charging infrastructure. This article aims to enlighten the future investments and policy decisions in the Rapid Charge Network project (RCN) in the UK. The Figure 2.1 summarises all the sources of costs and revenues for a FCI. The identified **stakeholders** were the **site owners, the infrastructure service suppliers and the charging service operator**.

E. Suomalainen and F. Colet [50] propose a cost-efficiency comparison of the fast-charging infrastructure and the charging lane in France. **W. Kong *et al.*** [45] aim to plan the charging stations sitting that minimise the fast-charging infrastructure cost and satisfy the constraints linked to the drivers, the traffic flow and the power grid. In [61], the authors optimise the location and the size of the charging stations.

According to the previous studies, we can deduce a general expression of the infrastructure cost as the following Net Present Value (NPV):

$$NPV = -I_{CP} - C_{instal.} + \sum_{k=1}^{L} \frac{-I_{CP,k} - C_{instal.,k} - C_{O\&M} + E_{sold} \cdot (p_{client} - p_{elec.})}{(1+r)^k} \tag{2.2}$$

With I_{CP} and $C_{instal.}$ respectively the cost of the chargers installed during year 0 of the investment and their installation cost. The terms $I_{CP,k}$ and $C_{instal.,k}$ represent the same costs

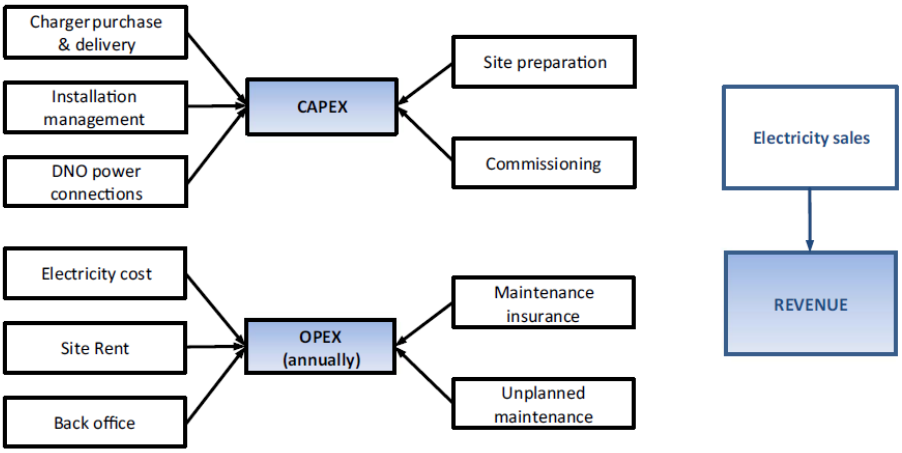

Figure 2.1: Sources of costs and revenues from the operation of a recharging service [11]

during year k if the infrastructure is dynamically built. $C_{O\&M}$ stands for the operation cost and maintenance. The energy sold during a year is E_{sold}, the price paid by the client using the charger is p_{client} and p_{elec} the electricity price paid by the charging operator.

According to a paper from **Lux Research** (2017) [12], the cost of the building and operating of a 120 kW charging point is evaluated to $27,000 (€23,000) and the cost is doubled for a 350 kW charging point 2.2. Those costs seem to be less than the other costs mentioned in other papers cited in this section (for instance, 70,000 € for a 150-kW charging point in a 8-port station in [55] or 120,000 € for a 350-kW chargers in [65].

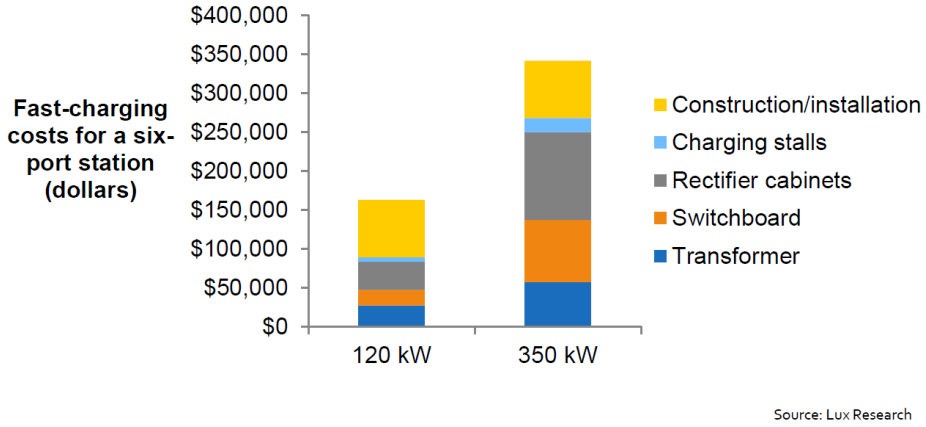

Figure 2.2: Resulting cost per charging station of 6 ports for 120 kW and 350 kW fast charging, segmented by charging station component [12]

As the parameters to compute the NPV vary from a study to another, we choose to consider in our thesis work the cost information listed in the data source of the paper **E. Suomalainen and F. Colet** [65] that gives more detailed costs. This data source is a working paper published in ICCT in 2019 [26]. The Table 2.1 sums up the estimated cost of one charger hardware.

In the same working paper, the installation costs per charger are also depicted. They include the labor, materials, permit and taxes costs. According to the installation cost presented in the working paper and in [55], it is more interesting to install more than one charger in the same station to reduce the installation cost per charger.

2.1.3.3 . Optimisation in control strategies

Table 2.1: Estimated DC fast charge hardware cost

Level and power	Hardware cost per-charger
DC fast 50 kW	$28,401 (24,000 €)
DC fast 150 kW	$75,000 (63,500 €)
DC fast 350 kW	$140,000 (118,500 €)

One of this thesis objectives is to propose a charging strategy that help driver using more efficiently the infrastructure already installed. This charging strategy relies on the control of the charging and can, according to the literature, optimise different aspects of an EV charging plan: what is the optimal path to the destination, where and when the EV will stop to charge, which amount of energy the EV should recover... Section 2.3 gives references about charging control strategies that inspired the ones we present in this thesis work, the *FCFS communication* and the *reservation strategies*.

2.1.3.4 . Optimisation in sizing strategies

The other objective of this thesis is to size the charging infrastructure to minimise its cost and to satisfy drivers' expectations that is usually be able to reach its destination, reduce its trip time and its charging cost. The planning of the infrastructure can concern only the location of the station (especially for maximum flow coverage) or both station locations and number of charging points per power level in each location. Section 2.4 describes the state of the art of those infrastructure planning methods.

2.2 . Modelling charging demands

From cost-efficiency analysis of the charging service to charging control of the fleet, the authors in the literature propose different methods to generate charging demand scenarios. Depending on the study, authors can use only historical charging data to evaluate the waiting time in station and deduce the needed infrastructure to mitigate it or use traffic flow information on the road (highway or not) (Section 2.2.1) to deduce the charging demand in stations (Section 2.2.2).

2.2.1 . Modelling the traffic flow

The traffic flow can be determined according to different methods and its use depends on the objectives of the charging strategy or the service quality criteria observed. To test the efficiency of control strategies for EV charging, the papers use either complete trip generations such as in [20, 24, 66] or traffic flow on section roads (for instance in [67]). When the cost-efficiency analysis or the optimisation deals with the charging station location and sizing, the authors propose also to either based their charging demand estimation on complete trips or on traffic flow between nodes of the transportation network. Usually, when the objective is the maximisation of the share of covered trip (Section 2.4.1), the traffic flow is represented as complete Origin-Destination (O-D) trips [22, 68]. On the contrary, when the objective is more oriented on reducing the social cost (for instance the waiting time), the evaluation of traffic flow on road sections is more used to deduce the charging demand in stations [53, 61].

2.2.1.1 . Share of EVs in the fleet

Before evaluating the traffic flow, the share of EVs on the road has to be defined. Indeed, the existing data concern usually traffic flow mixing ICE vehicles and EVs. Moreover, for long-distance trips, EV owners do not necessary use their EV since the EV was initially an urban technology due to its limited range and was not designed for long distance trips [50]. According to a survey by Enedis [69], approximately 50% of EV owners use their EV for long-distance travels.

2.2.1.2 . Trips from data source

The easiest way to generate complete trips is to use data from real trips databases such as in [64], [13] and [70]. The trips are sampled from complete Origin-Destination trips database that give more or less details on the vehicle journeys. For instance, in [64] or in [70], complete itineraries of vehicle are used to estimate where an EV would stop to charge whereas in [22], the database only gives O-D pairs and a shortest-path between the origin and destination is found to create the routing of the vehicle.

2.2.1.3 . Trips from entry/exit probability

When we do not have O-D trips from real world dataset, we can create trips on the highway according to arbitrary or real-world based entry and exit probabilities on an highway in addition to the time of entrance. For instance in [71], the arrival rate on the highway follow a Poisson law and the O-D pair are randomly selected. In [24], the time of entrance is selected according to hourly entrance flow on the French highway A6 that is deduced from opendata source.

2.2.1.4 . Traffic on road sections

Other papers evaluate the charging needs only according to traffic on road sections near a station and do not consider complete trips. In [55] and in [61], the charging demand per hour in each potential charging station location is statistically estimated from traffic volumes near the station that is reconstituted from German traffic data. In [50], the traffic volume on the whole highway corridor is considered without differentiating the traffic on smaller sections.

2.2.2 . Modelling the charging demand in stations

Once the traffic flow is estimated, the effective charging demand in stations or on specific road sections is evaluated. The demand in a station can be directly deduced from traffic volume, battery range and charging frequency but it can also be evaluated with more complex models of EV charging process such as queueing theory and charging distribution depending on the EV charging strategy.

2.2.2.1 . No strategy when choosing the charging stop

E. Suomalainen and F. Colet [50] evaluate the cost of the charging infrastructure to be developed on the French highway A6 according to the peak charging demand on the highway. This power peak is simply computed with:

$$P_t^{peak\ per\ station} = e \times d \times EV_t^{highway,peak} \tag{2.3}$$

With e the consumption rate of the EV, d the distance between stations and $EV_t^{highway,peak}$ the traffic peak on the highway A6 in year t (this traffic peak is established to 9600 vehicles per hour). A similar method is used in [53] to determine the number of charging points according to the traffic flow near the charging station and in [63], the demand for a charging station is the peak traffic volume times the estimated energy consumption between the station and the next station (flow-capturing approach).

In [13] and in [64], the position where the EV stops to charge is evaluated from O-D trips (with starting time) and the battery capacity of the EVs and then, the power needed per hour is

evaluated to deduce the sizing of the charging stations. In [13], the number of charging points is set such as there is no waiting time during the 30th busiest hour of the year (Figure 2.3).

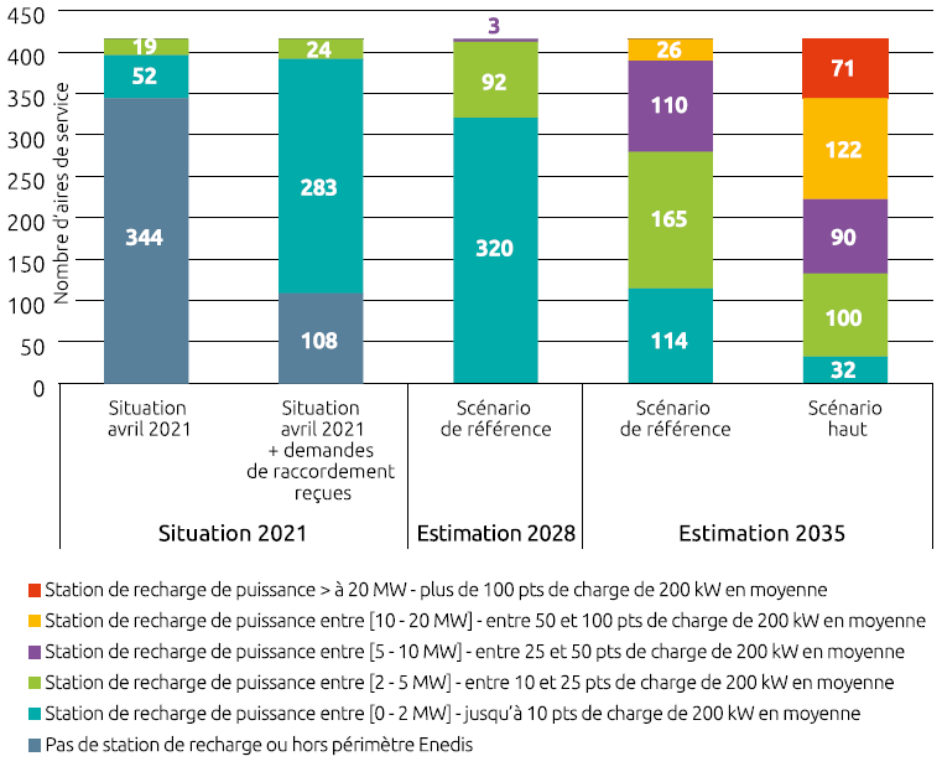

Figure 2.3: Number of service areas equipped with high power charging points [13]

2.2.2.2 . Charging stops depending on the EV strategy

The charging demand in a station can also depend on the EV strategy that choose the station to charge.

Some of the papers use game theory to determine where the EVs are going to charge. Game theory is the use of mathematical models to analyse the strategy of several rational decision-makers dealing with a competitive situation where the outcome of a participant's choice of action depends critically on the actions of other participants. This theory can be useful to understand and model the uncertain behaviour of decision makers for example in case of price variations. As we will see later in the chapter, game theory is used in [72] where a game problem is solved by finding one of the Nash Equilibrium of this game if one exists. The Nash equilibrium is the situation where no player can improve its outcome by being the one to change his or her strategy. In Nash equilibrium, the outcome is optimal for each player considering the decision of others.

Other papers will determine where the EV charge thanks to simulation of complete trips where the EVs optimise their charging stops [20, 24].

2.2.2.3 . Queuing theory

After determining where the EVs are going to stop, the model of the charging process can go further. For control strategy based on waiting time information-sharing [73] or for sizing strategies linked to waiting time reduction, the waiting time can be estimated according to queuing theory [15, 55, 60, 61].

In the **queuing theory**, the waiting system is defined with a flow of "clients" whose arrival spread over time and who ask for a service. One random variable A rules the arrival process of the client and another random variable S represents the service time distribution. The simplified Kendal notation $A/S/s$ gives the first letter of the process followed by each random variable (A and S) and "s" informs on the number of "servers" that can perform the service. For instance, the $M/G/s$ queuing model corresponds to a queue model where the arrivals are Markovian (M), the service durations have a General distribution (G) and there are s servers. Markovian stands for an evolution of the arrivals during a time period following a Poisson process of rate λ or an exponential process.

Markov chain uses a chain of states and a matrix of probability to describe the probability to be in a certain state at the next iteration considering the previous state. As found in the literature [14,55,60], the queuing evolution at a station is often modelled by a $M/M/s/N$ model with its Markov chain following a birth-and-death process (see Figure 2.4):

- The arrival time follows a Poisson process with an arrival rate λ (birth rate).
- The charging duration follows an exponential distribution with an average duration of $1/\mu$ (μ is the death rate).
- There are s charging points and $N - s$ waiting places.
- There is only one charging queue for all the charging points.

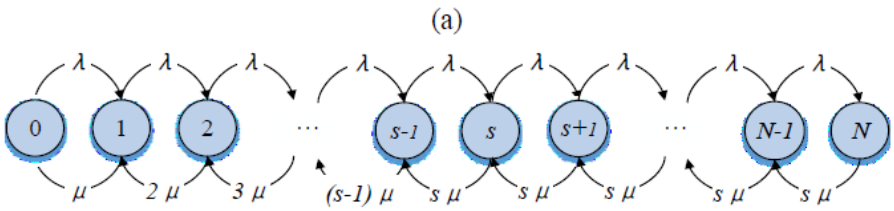

Figure 2.4: Markov chain describing a flow of EVs in a charging station with s charging points and $N - s$ waiting places [14]

Shabbar *et al.* [60] introduce a probability α that characterises the choice of an EV to stop and wait at a full station (all the charging points are busy) or to continue its trip (see the resulting Markov chain and probability expression in the paper). The arrival rate can differ from a station to another to take into account the local charging demand and dimension more adequately every charging station [55]. The arrival rate at a given station is deduced from the traffic situation on the highway segment near the station or according to the charging selection strategy of the EVs. The average waiting time in stations given in [60] is:

$$W_q = L_q/\lambda_a \tag{2.4}$$

Where L_q represents the average amount of time the EVs spend in the queue and λ_a is the real arrival rate in stations.

The average waiting time is often used to scale the fast charging station by adding an average waiting time criterion. For instance, Funke *et al.* [55] set the average waiting time criterion to 5 minutes: **if W_q exceeds 5 minutes, another charging point should be added to the station**.

In [72], a birth-death process is used for the $M/M/s/c$ **queue model** associated to the charging queue at stations. The arrival rate at a station is derived from the EV strategies. In [15], the

arrival rate in the station is not deduced from traffic flow but according to a real-world charging dataset. In this paper, a cost efficiency analysis is done using queuing theory to determine for how many charges per day in a station, a charging point should be added (Figure 2.5): a new fast-charging unit should be added if the number of EV per day per charging station is equal to 10 ± 3 to guarantee a 10-minutes maximum waiting time.

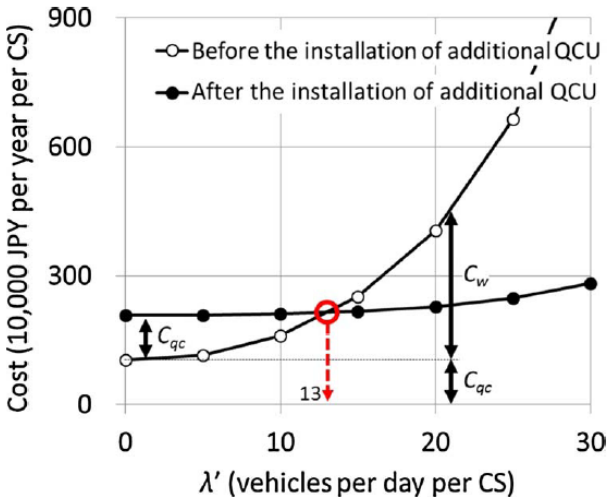

Figure 2.5: Cost-benefit analysis for installing an additional charging point (QCU = quick charging unit) [15]

2.3 . Control strategies of the charging in the literature

A strategy improving the charging experience of EV drivers, before adding new charging points, proposes charging services based on the control of the charging to deal with a sparse charging infrastructure before developing the charging infrastructure itself.

The objectives of those strategies are numerous such as minimising the variation of the grid load or minimising the travelling time of each EV. The way the control of the charging schedule is done depends on the studies. Most of the time, real-time information-sharing between stations and EVs such as pricing feedback (Section 2.3.1) or congestion feedback on the road or in stations (Section 2.3.2) in stations enable to manage the charging schedule of the EVs [58]. The EVs can plan the optimal next station where they should stop but, in case of multiple needed charging stops, they should also consider planning their whole charging schedule (Section 2.3.3). We describe in Section 2.3.4 the paper dealing with both congestion in stations thanks to real-time information-sharing and whole charging stops planning.

2.3.1 . Dynamic pricing to control EV charging

The price variation of the electricity during the day is a classic lever to delay the electric demand to off-peak periods. The same mechanism can be used to control the charging schedule (when) or location (where) of the EVs. **Amin *et al.*** [16] reviews the different dynamic pricing schemes that a station operator can adopt to influence and coordinate EVs' charging plans and reduce the impact of the charging infrastructure on the electric grid. Depending on the cited papers in the review, the dynamic pricing can be used to minimise the power loss on the grid, minimise the peak demand, maximise renewable energy sources contribution in the EV charging or simply minimise energy cost.

In addition to the review of dynamic pricing schemes that are given in the literature to control EV charging, **Amin *et al.*** first arbitrate between a centralised (the decision is made by the aggregator) and a distributed (the decision is made by the driver) framework to manage the charging process strategy of EVs. The aggregator is the interface between drivers and network operators. The **distributed framework** is more acknowledged in a context of EV charging control because it is more flexible and more scalable with less computational complexity. Then, the paper aims to determine which dynamic pricing policies should be preferred among Real Time Pricing (RTP), Time of Use (TOU), Critical Peak Pricing (CPP) or Peak time Rebates (PTR) (see Figure 2.6 for the definitions). It appears that the RTP scheme is the most encouraging solution since it is fairer and enables higher economic efficiency than the other schemes. However, RTP presents higher billing instability since the price is varying every hour.

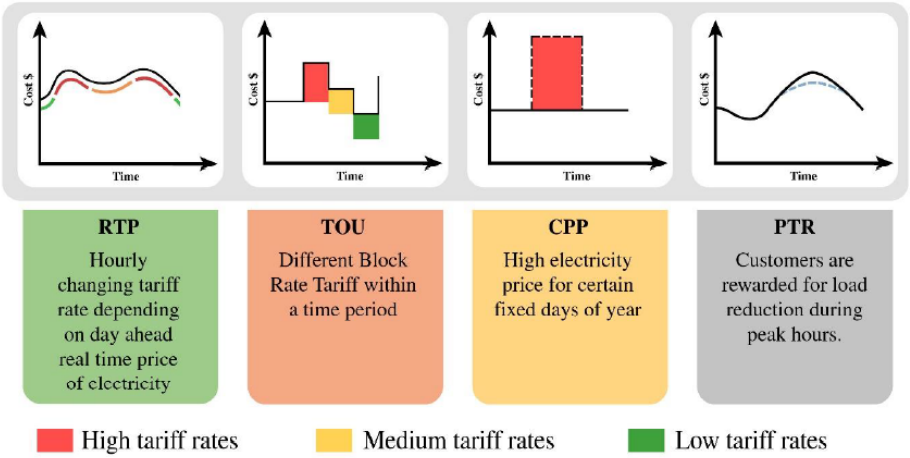

Figure 2.6: Dynamic charging pricing schemes [16]

Other papers present dynamic pricing method and model the interaction between the different stakeholders of the system thanks to the game theory. For instance, **Tan & Wang** [72] describe a two-level **hierarchical game** approach (game theory) to model the pricing strategy of fast charging stations in **urban area** as a non-cooperative game and that simulates the choice of charging stations by EVs thanks to multiple evolutionary game formulations. The **upper level** is associated to the **fast charging stations' pricing strategy** where each station aims to maximise its profit where the electricity price purchase for the CS is based on TOU pricing according to the load on the grid. The Nash equilibrium of the non-cooperative game on this level is computed thanks to Particle Swarm Optimisation (PSO). The **lower level** is designed for **EVs charging navigation strategies** that **depend on the price set by fast charging stations (FCSs)**. This study aims to show the interest of a pricing strategy adopted by FCSs for electric network and EV drivers. Indeed, **the real time evolution of the price makes EVs charge at off-peak hours and reduces in the same time the trip time of EVs** compared with a short-path strategy. This pricing strategy is used in an urban context and not in a long-distance trip situation but, this might be implemented for fast-charging stations on the highway.

Rana *et al.* [49] propose also a two-layer approach with cooperative games where the energy is traded between Evs who want to discharge and others who want to charge. The negotiations of the energy price are done in peer-to-peer mode through a cloud server. However, this system is not applicable in our work since we suppose that no EV will accept to discharge during a long distance trip as it will accentuate the refuelling time problem we are trying to palliate in this thesis. Still, we can imagine an equivalent trading system where the EVs deal charging time

slots by biding for instance the price they are willing to pay according to their state of charge. In another paper, **C. Liu *et al.*** [17] also describes a peer-to-peer trading system using **blockchain** where EVs, solar panels and storages can trade electricity among them to minimise the power grid fluctuations and flatten the power consumption profil (Figure 2.7). Again, the application of this mechanism is implemented for microgrids and not for long-distance travels but this Peer-to-Peer trading system using blockchain could be used to set secured and decentralised reservations of charging time slots in fast charging stations.

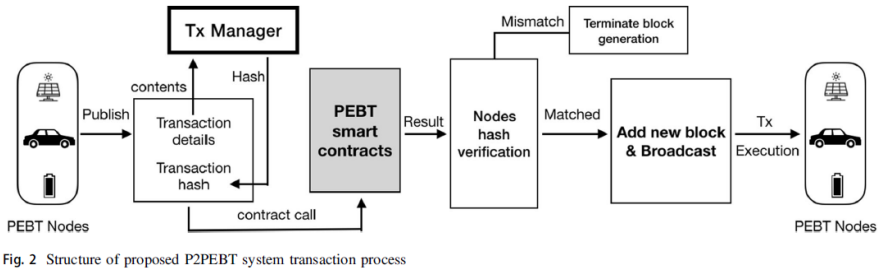

Fig. 2 Structure of proposed P2PEBT system transaction process

Figure 2.7: Structure of the proposed P2PEBT system transaction process [17]

Other papers focus on flattening the load on the power grid thanks to dynamic pricing [48, 74,75]. In [46], a method is implemented to modulate the charging power of idle EVs to minimise divers aspects linked to the grid operation such as load peak and grid loss and minimise the charging cost and time to charge on the EV side in an area mixing residential, industrial and commercial activities. In all those papers, they observe how the EVs are acting according to pricing policies under scheduling constraints but only for EVs that are idle (at home or at work) and not travelling. The different models could be adapted to long distance trips if we see the time of pausing as schedule constraint but the EV might not be enough time idle to delay the charging time.

Yeh and Tsai [47] focus on a dynamic pricing that maximises the parking lot agent revenues in a case of regular charging (as opposed to fast charging). In a case of fast charging, the charging price is not considered and the objective of the charging controller is to minimise the charging time of the EV agents by allocating charging power to EVs thanks to a genetic algorithm.

Finally, **Bernal *et al.*** [76] present the optimal **charging price and reservation fees** a charging station operator should set to maximise its operation revenue from charging service and participation in real time electricity market. The EVs can **reserve in advance** a charging slot specifying its arrival time and expected charging time but according to the reservation fee and the probability to be served without booking, the EV decides if it should book or not a charging session.

Highlights on pricing variation control strategies

All the charging strategies relying on price control we depict in this section (except maybe the latest [76]) are set for urban area where pricing schemes help to shave the peak load on the electric grid and we did not find references about charging price variation strategies for long distance trips. However, some of those pricing mechanism can be adapted to charging on highways, for instance, using smart contracts [17] to influence the choice of fast-charging schedule and location according to the carbon footprint of the electricity. Still, as we do not study the impact of the long-distance charging on the electric power grid, those considerations are perspectives of this thesis work.

2.3.2 . Reducing the travelling time with information-sharing

Other papers more oriented toward selection of the next optimal charging station during trips, set the minimisation of the travelling time or the waiting time as the primary objective instead of playing on the charging price modulation to redirect the EVs to less crowded stations. According to [71], EV coordination on-the-move should be **decentralised** to reduce the computation time and be adequate for real-time scheduling.

The literature on **decentralised charging strategies** using **communication between EVs and stations** to **reduce waiting time** by selecting the optimal station to charge is rich. **Qin *et al.*** [71] propose a coordination scheme where EVs can communicate with the nearest charging station and select the station with the minimum waiting time for their next charging session. The waiting time is estimated thanks to **EVs' communication of charging intentions**. The method given by **Yang *et al.*** in [77] also selects the next charging stop with the minimum waiting time. However, there, the waiting time is estimated according to the current waiting queue at the station rather than on waiting time prediction.

A reliable reservation process called REBECA is depicted in [73, 78] to guarantee the efficiency of the charging service and thus reduce charging delays at stations. The EVs are allocated with the charging time slots that will minimise the latency time of the EV (the time before the EV will be charged including travelling time to the station and the estimated waiting time there) and maximise the power use in stations by balancing EVs between stations. This last objective is meant to increase the average use rate of the stations and might help reducing the charging point needed in stations if we want to minimise the charging infrastructure cost.

Yudovina *et al.* [79] demonstrate how decentralised policies to assign EVs to near charging stations can reduce waiting time. **Gusrialdi *et al.*** [67] goes further with a mathematical demonstration proving the benefit of a decentralised charging strategy based on a **consensus among EVs** approaching the same charging station. The EVs agree on which EVs will charge at that station and which EVs will stop at the next station to distribute the EVs in stations evenly and reduce waiting time. The method relies on **V2V communication and vehicle to station communication**.

Y. Luo *et al.* [80] propose a method based on **weighting the road links** between nodes of the transportation network to solve a **multi-objective optimisation with a Dijkstra algorithm**. The weights of the road are modified in real-time according to the updates from the transportation system and the grid system to **minimise the travelling time** and **the traffic congestion near charging station** and **to maximise the grid safety performance**. The method determines the optimal charging station for each EV thanks to a shortest-path research using the weights.

A. Viziteu *et al.* [18] use reinforcement learning to optimise the selection of the next charging station and the charging time interval to avoid long waiting queues according to the length of the trip, the current battery charging state and the reservations made in each station on the road. As it is uneasy to create a dataset with all the optimal solution for every potential road situations, supervised learning is not possible to address this problem and reinforcement learning should be used instead. The authors choose a Deep Q-Network (DQN) to learn the optimal strategy: where to stop and which time interval should be booked in stations. The steps of the optimisation using the trained DQN model are shown in Figure 2.9. Due to a lack of real-world trip data, the authors have trained their model with multi-agent simulations to reproduce real-world cases. This method represents an interesting perspective of our thesis work as it can be adapted to our problem and trained using the multi-agent simulation framework to improve the control strategies we propose in this manuscript.

However, all those previously mentioned papers only focus on reducing the waiting time

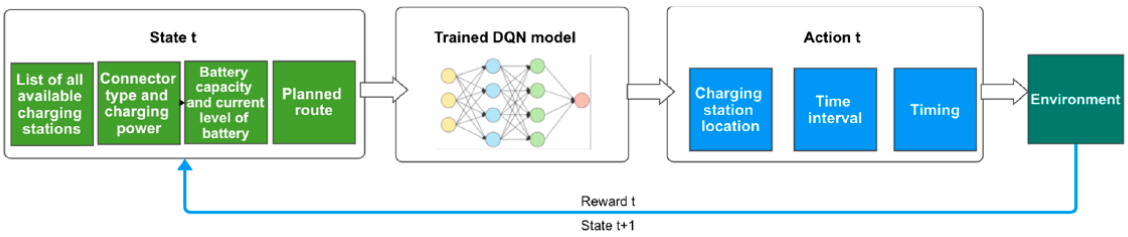

Figure 2.8: Charging station and charging time interval selection with a trained DQN model [18]

or the travelling time for **the next charging stop** and do not seek to optimise the whole charging plan of EVs during their trip that might need several charging stops. The charging plan represents the energy charged at each station along the way.

2.3.3 . Complete charging plan optimisation

Some papers propose centralised strategies to optimise the charging schedule of all EVs. In [81] , the authors propose a genetic algorithm to optimise EVs routing and charging according to multiple objectives, including the minimisation of the travelling time. However, the proposed centralised method is tested on a fleet with only 6 EVs whereas we need to find solutions for fleets with at least 100 EVs to represent future flows of EVs on highway. The proposed method seems hardly scalable on a large vehicle flow because of computation time and according to [71], EV coordination should be **decentralised** to reduce the computation time and be adequate for real-time scheduling of large EV fleet charging.

Like in the next three papers, **dynamic programming** is often used to solve the charge planning problem. **Pourazarm *et al.*** in [82] propose a way to minimise the travelling time and the charging time for a large fleet by decomposing the flow of EVs in sub-flows with the same charging strategy. **Wang *et al.*** [83] optimises the routing of one EV to minimise like in [82] the travelling and charging time but [83] includes in addition the charging cost as an objective. None of the two previously cited papers considers the waiting time in the routing optimisation contrary to **Souley *et al.*** [19] that integrates a fixed waiting time at stations. Still, this waiting time is not updated according to the real affluence at the station.

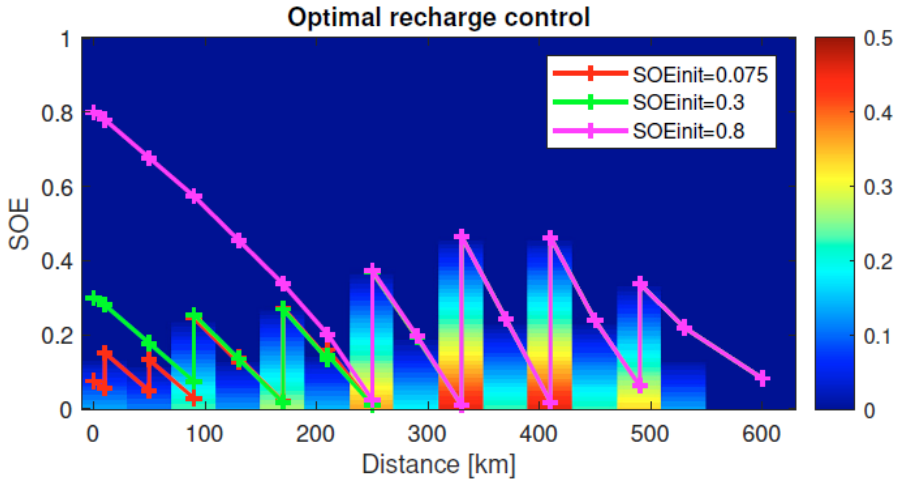

Figure 2.9: Optimal energy profile results for a long distance trip on the highway for several initial State of Energy (SOE) presented in [19]

In the paper by **F.He *et al.*** [84], the objective is to minimise the trip time of the BEV considering the travelling time and the charging time based on the level of drivers' range anxiety. The problem is formulated as different network equilibrium problems that are solved iteratively with CPLX to find the equilibrium flow pattern (which route and where to charge) an EV should follow from the origin of its trip to its destination. In this paper, the waiting time is not considered.

Highlights on complete charging plan strategies

In this section, all the papers optimise the complete charging plan of the EVs to reduce travelling time and/or charging time. However, the waiting time is not considered during the optimisation [81–84] or is supposed to be constant during the day [19] whereas it can have an important weight in the trip duration and highly variates according to the time of day.

2.3.4 . Complete charging plan optimisation with information-sharing

To take into account the real-time affluence in stations when optimising the whole charging plan, **Del Razo *et al.*** [20] proposes a decentralised strategy where EVs can dynamically send booking requests for their whole trip according to the optimal charging schedule found by an improved **A* shortest-path search** algorithm. The problem is formulated as a graph of states (see Figure 2.10) and the shortest path is the path that minimises the trip time for each EV, including the waiting time. The waiting time is deduced from the reservation made by the EVs.

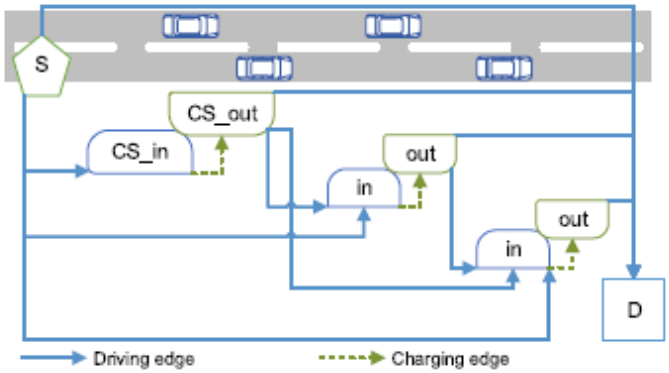

Figure 2.10: Graph of states for one EV [20]

The trip characteristic generated for the simulation are data-driven. The performances of this smart charging scheduler are compared to the situation where EVs charge to the last station they can reach (LiR: last in range) and the results showed that the scheduler improves EVs situation by reducing the queue lengths and enables to predict on a short term the power needs for charging.

However, the authors in [20] do not optimise the charging plan but the charging schedule since they do not consider the energy amount charged at a station as an optimisation variable. In contrast, it is a critical parameter when minimising the total travelling time. Indeed, the arrival time at one station, and consequently the waiting time, depends on the charging time at the previous stations and thus depends on the quantity of energy charged there. Therefore, most strategies we depict in this thesis use the optimal control of the energy quantity charged at each stop for the whole trip instead of only optimising the charging stop schedule.

J. Hassler *et al.* [21] propose a service of communication that aim to optimise both the charging time and the waiting time dynamically. Through this communication service, the EVs can share they intention of charge to charging stations to reduce their travelling time and charging cost. The implemented framework simulates off-line a flow of EVs during one day on a highway. As in [20], the charging stations compute the estimated waiting time at station according to the intention of charge the EVs have previously sent and each EV establishes the charging plan that minimises the individual objective function C:

$$C = (1 - X).T_{trip} + X.C_{trip} \tag{2.5}$$

Where T_{trip} is the total trip time the EV will spend on the highway (including charging and waiting time), C_{trip} is the energy cost of the trip and X reflects the driver preferences in term of cost or time savings ($0 \leq X \leq 1$). No reservation of charging time slot are made so the rule at a station is on a first-come-first-served basis. The article compares the performance of the service of communication to the situation where the EVs do not communicate (without communication scenario) and another of global optimisation where the flow of vehicle is not simulated but the optimal charging planning for each EV is calculated thanks to a **differential evolution algorithm**. The Pareto curves of the different scenarios are shown in Figure 2.11. According to the figure, the communication scenario gives similar results than the global optimisation and can be executed dynamically while the EVs are driving (contrary to the differential evolution algorithm) which is encouraging.

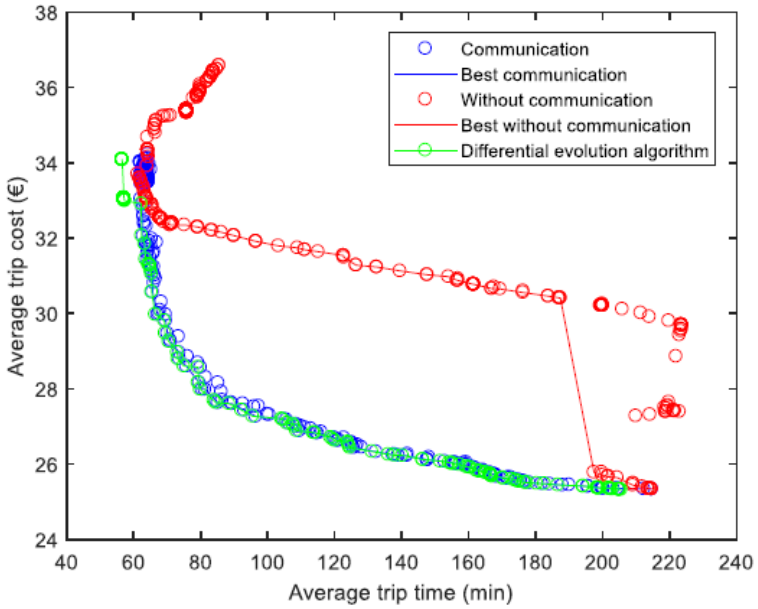

Figure 2.11: Cost- trip time Pareto curve [21]

Control strategy selection

The communication service proposed in papers [21,24] is the *FCFS communication strategy* that we study in this thesis and that we describe in Section 3.1.4.

2.3.5 . Introducing priority level among EV drivers

Most control strategies presented in the previous sections rely on the **priority rule for charging based on the time of arrival in stations without pre-emption**. This **priority rule** means

that the **first-arrived EV in station will be served first (FCFS)** and the **non-pre-emption** signifies that if EV_v is already charging, it cannot stop its charging to let another EV with higher priority charge. Other control strategies are based on sorting the Evs according to their priority level and depending on the method, the higher prioritised EVs can pre-empt or not the charging session of lower prioritised EVs (see [85] for the definition of pre-emptible queues in advance reservation systems). The priority level can be set according to the role of the EV (for instance military or police vehicles) [86] or according to the time of the reservation, in other words, the firsts EVs to book are the first to be served. Note that when a paper speaks about reservation request or booking, the priority is not always based on the first who made the reservation but can be based on the first arriving in station [20, 73].

Y. Cao *et al.* [86] aim to optimise the selection of the charging station to minimise charging waiting time (elapsed time before being charged) by proposing a **centralised strategy** where EVs can make reservation and according to their level of priority, they can pre-empt the charging of an EV with lower priority. The reservations enable the charging station to estimate future waiting times. The article concludes that reservation with pre-emption and different levels of priority reduce more efficiently the average waiting time in stations for both High and Low-prioritised EVs compared with only reservation system without pre-emption and a First-Come-First-Served (FCFS) rule in station. The **FCFS reservation strategy** described here is somehow similar to the *FCFS communication strategy* we develop in this thesis work, this is why we compare in Chapter 4 the *FCFS communication strategy* to another strategy with a different priority rule in stations.

As we do not want to set high-priority categories of EVs and we do not want to allow pre-emption in the charging service to avoid user discontent, we review in next paragraph the strategies based on strict reservation of charging time slot to define a new priority rule.

R. Flocea *et al.* [87] propose a priority level based on **advanced reservation** to avoid waiting queue in stations without overlapping charging sessions. The driver can book charging sessions several days in advance before a long-distance trip to guarantee **no other EV will be able to charge during that reserved time interval**. The driver has to precise the starting and ending times of the charging session. This reservation model is the one called **planned reservation** by **Basmadjian *et al.*** in [88]. Basmadjian *et al.* oppose the planned reservation to the **ad-hoc reservation**. With the ad-hoc reservation, the EV books a charging session for a given duration prior arriving in station (for instance 20 minutes before arriving) and the charging point appears as occupied to other EVs as soon as the EV confirms the reservation. According to **Basmadjian *et al.***, the planned reservation is better at reducing trip time than the ad-hoc reservation. **B.Vaidya and H.Mouftah** [89] describe the same planned (or advanced) reservation system as the two previous papers [87, 88] and propose in addition a method to optimise the slot allocation in the charging point by minimising the discontent factor of the EVs. The discontent factor of the user depends on different aspects such as the waiting time, the reservation duration and the received energy. The charging sessions are non-pre-emptive so a charging session cannot be stopped and then resume later.

In [66], **I. García-Magariño *et al.*** evaluate the benefit of charging time slot booking in the reduction of the average trip time and waiting time in the stations of a city. For this purpose, the paper implements a multi-agent framework to compare the reservation strategy with other charging policies. In the reservation strategy described here, each EV has to charge once on its way and aims to minimise its trip time. The EV select its station according to the charging time-slot available in the station to reduce its waiting time there and its detour time to the station. Upon selecting the charging station, the EV books the available charging session that is the closest to its estimated arrival time in the station. After running the multi-agent simulation,

the reservation strategy proves to reduce significantly the average trip and waiting times of the whole fleet compared with a strategy without communication and reservation.

Highlight on reservation strategies

The *reservation strategy* we compare in Chapter 4 to the *FCFS communication strategy* is inspired by the **planned reservation** described in the previously mentioned papers [66, 87–89], especially [66]. Indeed, we do not wish to consider pre-emption possible in the reservation process to reduce EV driver discontent. To compare the *planned reservation strategy* to the *FCFS communication strategy*, we develop a similar multi-agent framework to the one presented in [66].

2.4 . Fast-charging infrastructure planning

We have seen in Section 2.3 the possible control strategies of the charging to improve the use of the charging infrastructure but another way to enhance the charging service is to develop the charging network itself. As the development of fast-charging stations is costly (see Section2.1.3) but is necessary for the adoption of EVs, the location and sizing of the infrastructure should be optimised. The optimal location and sizing depend on the traffic flow on the different sections of the highway, the range of the EV, the load distribution on the power network, etc. Generally, the optimal locations of the charging stations are selected among the existing highway service/rest areas, which reduces the possibilities but the problem is still complex. The variables we want to maximise or minimise by selecting the best location and sizing are various and influence the method used to solve the problem.

2.4.1 . Maximise the share of long distance trips covered

As explained in Section 2.1.1, the infrastructure should be developed to favour EV adoption, especially to reduce range anxiety and effectively cover long-distance trip demands. In the literature, the planning of the infrastructure to maximise the share of long distance trips covered is done by optimising the location of the charging station.

The paper [22] uses a fuel-refuelling location model [90] to maximise the share of long-distance trip (>50 miles = 80 km) completed in the USA in function of the number of charging stations the budget can afford (constraint). The studied network consists in nodes and links of the highway network in the USA (846 nodes as potential station locations) and the demand for each link is also considered. As explained in Section 2.2.1, the demand is modelled from a reduced dataset of Origin-Destination trips in the US. The number of stations varies from 50 to 250 stations and different battery range scenarios are tested (from 60 miles to 300 miles). The problem is solved with a **branch-and-bound algorithm**. The article concludes that **batteries of more than 250 miles (400 km) of range do not benefit much the drivers since all the trips are already covered with a 250-mile battery and 150 stations** (Figure 2.12). With only 100 stations placed strategically, 93% of the trips are covered for a battery of 200 miles (320 km) and with 150 stations, almost 99% of the trips are served for the same battery range. Therefore, it is more efficient to strategically place the charging stations instead of increasing the battery range. Yet, a range of at least 100-miles appears to be necessary in order to complete more than 85% of the trip with the maximum count of station (250) because for 60-mile range, the share of covered trips drops to 65% with 250 stations. A 200-mile battery with 150 stations seems to be a good compromise in terms of cost and trips covered with 98.79% of the trips covered.

H. Gao *et al.* [91] use a two-level model to find the **fast charging station location** that

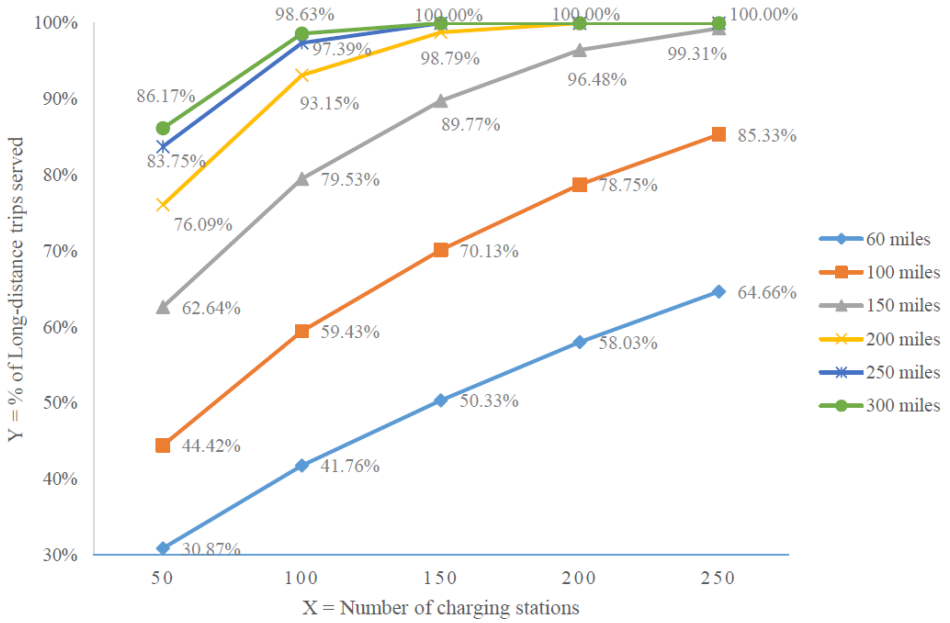

Figure 2.12: Share of long distance trip covered according to the range and the number of station [22]

also maximise the coverage flow under **elastic demand** (demand heavily affected by price). The paper takes into account the presence of gasoline-powered vehicle to model the traffic and determine the relationship between the location of the CSs and the traffic flow distribution. The model is implemented in **two levels**. On the **upper level**, a **maximum-flow covering model** positions the charging stations on links with higher demands. On the **lower level**, the SUE-ED model (stochastic user equilibrium model under elastic demands) distributes the EVs on the different paths and computes the travel cost for the user using a **mixed-integer non-linear problem** formulation solved by a **heuristic algorithm**.

Napoli *et al.* [92] optimise the position and the number of charging points in stations to circumvent range anxiety and propose the minimum number of charging stations and charging points on the highway network. The authors model the highway network as a graph and consider the minimum range among the commercialised EVs to determine the maximum distance between stations. The sizing of the charging stations is determined according to traffic flow on each link of the graph (see Section 2.2.1 for the method). The charging stations are iteratively added on each link by starting from primary nodes (cities or towns considered to have charging stations) to respect the maximum distance between stations. This method is tested on the Italian highway network with average hourly trend for weekday traffic flow representing the highest average traffic situation.

In [68], **Y. Wang *et al.*** go further by optimising both the location and the sizing of the charging station to maximise the share of charged plug-in EV flows in the network under budget constraint. A plug-in EV flow is a flow of EVs on the same Origin-Destination trip and this flow is considered as charged when all the EVs in the flow can be charged in the stations they have selected according to their utility function. The charge of the whole flow is possible only if the stations are correctly spaced and if the capacity of the charging stations (number of EV that can be charged per day) is sufficient. The problem is formulated with an extended version of the flow refuelling location model used in [22] and solved with three different algorithm: a genetic algorithm, a heuristic algorithm implemented by the authors and an algorithm mixing a genetic algorithm and the heuristic.

2.4.2 . Reduce social cost with infrastructure development

Other optimisations aim in reducing the social cost of the drivers. The social cost can include the travelling time, the charging cost, the EV cost or only the waiting time. To reduce the social cost, the infrastructure can be planned with either an objective directly representing this social cost while the cost of the infrastructure is reduced or the optimisation can only have the infrastructure cost minimisation as objective while the social cost is represented as a constraint.

2.4.2.1 . Social cost reduction as a constraint

Q. Yang *et al.* [14] focuses on the **optimal sizing** (number of charging points and waiting space) of the charging stations in an urban area to maximise the profit of CS operators. The profit of an operator includes the profit from charging service but also the penalty costs of waiting and rejection (when an EV cannot wait because there is no waiting place left) as well as the maintenance cost. The charging demand is determined thanks to a temporal analysis of EV's SoC based on a Monte Carlo simulation and an iterative evolution (every 30 min) of each EV state. The iterative evolution is ruled by a Markov transition probability matrix that determines the probability for an EV to go from a certain state to another. The temporal state of a PEV can be driving, charging at a station or parking. The arrival at station is model by a Poisson process and the arrival rate λ is deduced from the previously determined statistical evolution of the states (number of EVs in a certain state at a given hour) and a charging time in average of $1/\mu$ (30 min in the article). The results gives that the **maximum profit of $859.43** in a day can be achieved with **11 charging sockets** and **7 waiting spaces** at each station. However, **those results concern an urban simulation and should be adapted to long-distance trip.**

W. Kong *et al.* [45] proposes a two-level method to minimise the construction cost of the charging infrastructure by selecting the optimal combination of locations for the charging stations while satisfying the constraints linked to the driver, the traffic fluency and the load on the electricity network.The **first level** of the model computes the combination of CS locations that **minimise the cost of the infrastructure** and then the model runs a simulation on 24-hour traffic to check the **constraints** of the **second level**. If one of the constraints of the second level is not satisfied, the algorithm removes the combination from the possible solutions and starts again from the first level. The algorithm goes on until it finds a solution satisfying all the constraints. The constraint linked to the **driver satisfaction** imposes that the charging waiting time for an EV should be less than a giving threshold and the constraint on **traffic efficiency** verifies that the congestion rate of the road after the adding of a CS is still acceptable. The constraint on the MV/LV **transformers** limits the **voltage shift** (deviation of the three-phase power supply voltage compared to the nominal voltage) to **7%**. The paper works on an urban case study and the locations of charging stations are not selected among service areas but among areas of the town which differs from our subject on long-distance trips. However, the two-level optimisation depicted in [45] is interesting as it uses a simulation of a traffic flow to check that the constraint linked to the charging waiting time are met. We use the same method to check the waiting constraint in Chapters 5 and 6.

In [63], **Bräunl *et al.*** propose a strategy to determine the location and size (number of charging points and their power) of DC fast charging limiting the cost of the charging infrastructure needed to be installed on the Western Australia highway networks. This charging infrastructure must ensure a complete coverage of the highway network and limit the waiting time in stations to 60 minutes with the proper power and number of charging points (50, 150 or 350 kW). The charging demand for each site is based on traffic flow capturing and is estimated according to real-world traffic data (see Section 2.2.2). The stations are sized according to charging peak demand during a day that was averaged over a week.

Shabbar *et al.* [60] aim to maximize the net profit of the charging station operators by optimizing the location and sizing of the CSs under budget and routing constraints. A birth-death Markov chain model gives the relationship among the charging demand, the charging station size (number of charging points) and capacity (number of EVs that can charge or wait in the station). The location of CSs are determined using a **Grey Wolf Optimization (GWO) algorithm** [93] (meta-heuristic algorithm) to maximise the net profit of CSs. The net profit is estimated thanks to the **Markov-chain model** at each iteration. The **constraints** deal with **construction cost**, **available routes between CSs, waiting time, and the maximum distance an EV can drive** after a 100% charge. The **study on an urban area** concludes that slow charging stations should be placed in areas with low charging demands and fast charging stations need to be placed on areas with higher demands.

According to [60], genetic algorithm and Particle Swarm Optimization are also meta-heuristic algorithm but the GWO algorithm is the fastest and most efficient meta-heuristic algorithm in this case. This is why, in the development of this manuscript, we consider this optimiser to plan the infrastructure in Chapter 5

In Chapter 5 and 6, we choose also to size the infrastructure with the waiting time as a constraint and not as an objective to focus more on the charging operator point of view by setting the infrastructure cost minimisation as an objective. Still, in Chapter 6, the waiting time is a constraint but the time spent in stations (charging time and waiting time) is an objective of the multi-objective optimisation we perform and we see in Section 2.4.2.2 the existing methods to minimise the social cost (time spent in stations).

2.4.2.2 . Social cost reduction as an objective

In [94], **A. Saldarini *et al.*** detail a method consisting in adding charging stations and charging points in already existing stations of a specific highway to minimise the travelling time of EVs. In the paper, the siting of new charging stations and the sizing of all the charging stations is determined to reduce the waiting time in the worst case scenario. The author use agent-based simulation to determine the waiting time for a given scenario. This waiting time is deduced from the distribution of EV agents in the stations and the amount of energy they are recovering according to their trip characteristic, the model of their car and their consumption. As the consumption depends partially on the weather, the worst scenario is a case of cold weather and high traffic. The optimisation of the infrastructure enable to save a trip time of nineteen hours over all the EVs of the tested fleet.

The paper by **J. Liu *et al.*** [61] goes further and propose a **multi-objective optimisation** to the **location and sizing of the CSs** in order to satisfy charging demand, limit EV drivers waiting cost and reduce the construction cost of the infrastructure. The problem is presented as a **mixed integer nonlinear problem** (MINLP) and is solved thanks to a **genetic algorithm**. The decision variable is a logical vector specifying if a service area on the motorway have charging facilities or not. The optimisation is performed over three scenarios. The first one aims to minimise only the construction cost of the infrastructure. The two other scenarios minimises respectively the **total social cost** (construction cost, waiting cost and inconvenient driving cost) and the charging station operating cost (waiting cost and construction cost).

2.4.3 . Minimise the CO_2 emissions

The reduction of CO_2 emissions (while driving) often stands for PHEVs and might not be a major subject of concern for the development of fast-charging infrastructure on highway. Indeed, the PHEVs will use their fossil fuel tank during long-distance trips. However, in addition with the emissions generated by the use of gasoline with a PHEV, the article [95] also considers

the emissions generated when producing a kWh of electricity for the calculations of the objective function. Thus, the method described in the article might be adapted for a case study with BEVs on a highway instead of PHEVs in urban area. A **Particle Swarm Optimization** method is used to solve the problem and the candidate gasoline stations for the implementation of charging station are selected using taxi GPS tracking data and parking lot events.

2.4.4 . Infrastructure optimisation under information-sharing

Some papers dealing with infrastructure planning consider in addition that the EVs in the fleet optimise their charging strategy according to the waiting time announced in stations in real-time thanks to information-sharing between EVs and the stations. As we have seen it in Section 2.3.2, knowing the waiting time or the affluence in station in real-time help the EVs adapt their charging and use more efficiently the infrastructure. In that condition, the charging infrastructure needs are decreased and the papers in this section propose methods to take into account real-time information sharing between EVs and stations when optimising the infrastructure.

For instance, **C. Vandet and J. Rich** [96] propose to optimise the placement and the sizing of the charging infrastructure when a part of the fleet is using real-time waiting-time information from the stations. The charging demand in space and time is determined thanks to a discrete event simulator that maps trips sampled from a real-world large-scale trip diary and a given charging infrastructure. The waiting times estimated thanks to a G/G/c queueing process and other KPIs are extracted from the simulation and then used in the optimiser that will change the infrastructure and feed it to the event simulator. The same process is repeated until the optimisation converges.

To optimise the infrastructure on the Denmark highway networks under maximum waiting-time guarantee, **J. Rich *et al.*** [97] use an improved version of the information-sharing system presented in [96] for the simulation of the charging demand: the charging stations also share prediction of the waiting time as it is the case in the *FCFS communication strategy* we propose to study in this thesis. J. Rich *et al.* evaluate the infrastructure needs according to different accepted level of waiting time for 99% of the fleet and 100% of the fleet. It appears that sizing the infrastructure to a maximum waiting time for the 99% percentile of the waiting-time distribution saves a significant amount of chargers to be installed (15%) and limiting the waiting time to 10 minutes, only need 250 additional chargers compared with a waiting-time guarantee of 20 minutes.

The previous papers [96, 97] give interesting method to size the infrastructure when the fleet is using information-sharing to estimate the waiting time. However, in those papers, the charging strategy of the EVs seems to be different to an optimisation of the whole charging plan as the charged amount in station is not optimised like in the *FCFS communication strategy*. Moreover, the charging demand is evaluated with probability for an EV to charge at a given station whereas we want to evaluate the precise impact linked to information-sharing and charging plan optimisation on the infrastructure to be developed. Regarding the complexity of our problem, we need to consider the use of other optimisation methods.

A solution closer to our problem is presented in **A. Pan *et al.*** [70]. A. Pan *et al.* optimise the siting and the sizing of charging stations for electric taxis (ETs) to minimise several objectives such as the infrastructure cost, the cost associated to electric grid loss, the passengers electric taxi cost if their demand is not covered and the electric taxi driver cost (time and/or charging cost). They propose a method that first establish the charging demand of the ET by supposing the charging infrastructure already deployed and simulating in the network ET agents and passenger agents thanks to real-world trip data of taxis (see Section 2.2.1). The ET agents can com-

municate with the charging stations and retrieve information about the queuing time or charging price in station to optimise their charging station selection according to their preferences (minimising charging cost and/or trip time. Thanks to those simulations, key sitings of charging station are identified and then a multi-objective optimisation is solved with an improved genetic algorithm to determine which charging station siting should be chosen and which sizing. The evaluation of the multi-objective cost function is done thanks to the agent simulations.

Highlight on the infrastructure optimisation under information-sharing

As we want to see the benefit of a control strategy (the *FCFS communication strategy*) on the reduction of the infrastructure cost in Chapter 5, we need to simulate the interaction between the EVs and the charging stations as it is the case in [70] where the problem is solved with a genetic algorithm. Therefore, unlike [97] that find the use of genetic algorithm or simulated annealing not appropriate to the scale of the problem, we use also an evolutionary based algorithm (Grey Wolf Optimiser) to optimise the charging infrastructure when the fleet use a control strategy based on real-time information-sharing.

2.5 . Conclusion

We review the different control and sizing strategies to optimise or improve the charging service. Regarding the state of the Art and the problematics of our thesis work, we identify that the *FCFS communication strategy* presented in [24] is the most complete control strategy that minimise the total travelling time in real-time thanks to an optimisation of the whole charging plan (stations to stop and energy to be recovered in stations) and information-sharing about waiting time predictions. However, the priority rule in stations is based on the arrival time of EVs in stations (FCFS) and as the EVs are not cooperating with each other, we can wonder if another priority rule would not be more adapted. Therefore, we will test another control strategy where the EVs book charging sessions and the priority is define according to the time of the reservation (the reservation strategy). To compare the different control strategies, we need a multi-agent simulation framework [66] where the EVs are the agents and the charging infrastructure is the environment.

We also aim to show the benefit of a strategy based on communication between EVs and the infrastructure development by optimising the infrastructure when all the EVs of a fleet are using communication. Regarding the complexity of the problem and the literature review, we choose to optimise the infrastructure with an evolutionary solver (Grey Wolf Optimiser) and we define the waiting time as a constraint and not as an objective to emphasise the CPO's point of view. Another objective of this thesis is to evaluate the impact of the EV charging power on the infrastructure cost and the social cost (time spent in stations) and for this purpose, we test an evolutionary optimiser to plan the charging infrastructure with different share of ultra-fast charging EVs in the fleet.

Finally, as the optimisation of the charging strategies should be done to correspond to realistic charging demands, we generate for all the case studies of this manuscript complete long distance trips that are inspired from real-world data statistics on traffic flow, EV long-distance trips from Stellantis-connected vehicles and EV model characteristics from the market. Those trips are then simulated in the framework developed to answer the different problematics of this thesis.

The mind map in Figure 2.13 sums up the implications and links between the different stakeholders and parameters of the multi-objective problem we are facing.

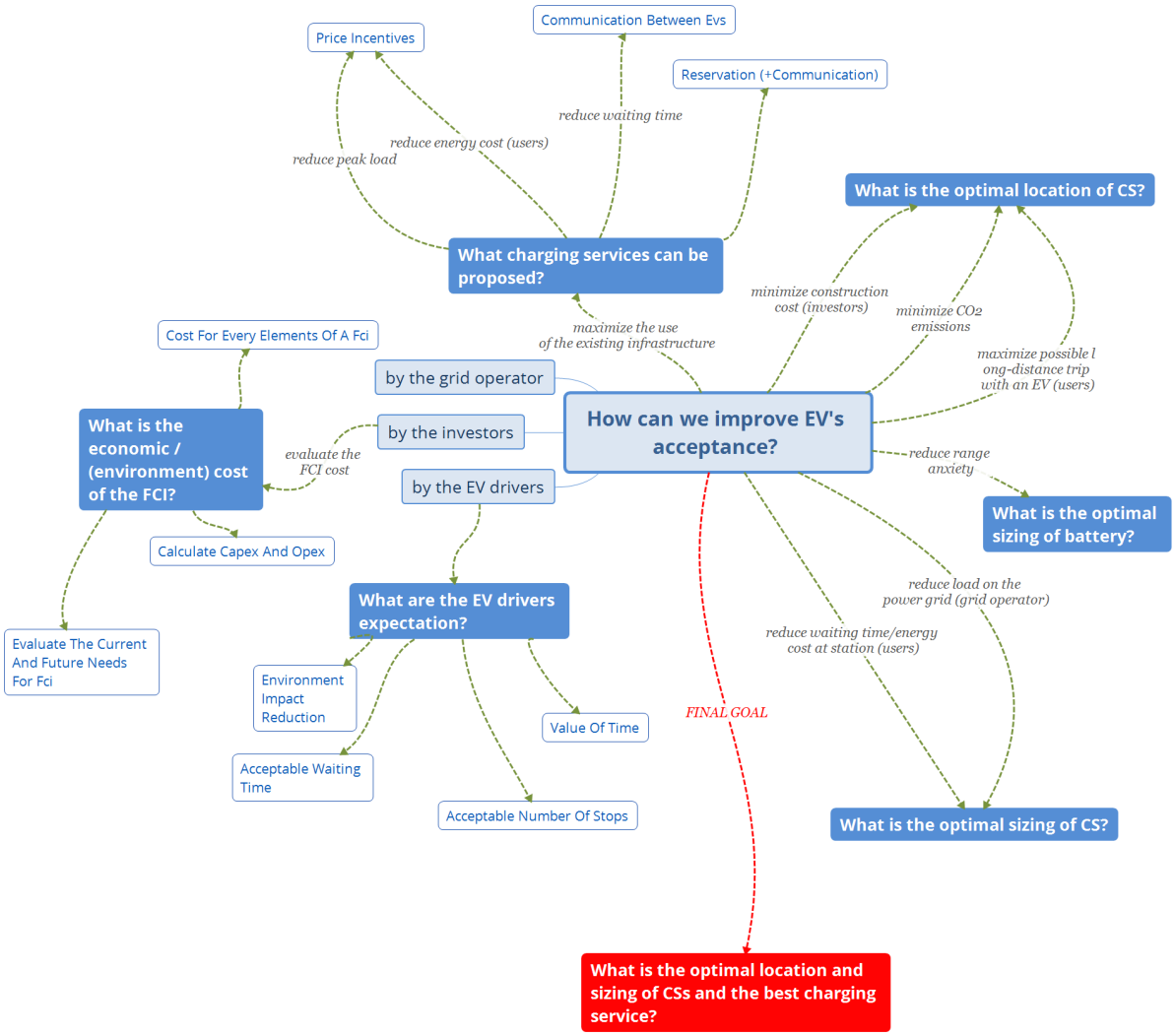

Figure 2.13: Mind map of the thesis subject toward EV's acceptance

3 - Simulation framework and charging strategy with real-time communication

This thesis work is a straight continuation of the PhD thesis by Jean Hassler [98]. This previous work proposes a means to control the charging of an EV fleet going on long-distance highway trips. The control was imagined to be possible thanks to a high-level charging service establishing a communication in real-time between EVs and CSs. The EVs using the service follow the *FCFS communication strategy*, a distributed charging strategy where they evaluate the optimal charging plan minimising their trip time and charging cost. To study the interest of such a charging strategy, a simulation framework was implemented in [98] to run multi-agent simulation modelling the interactions between EVs and CSs. We will give in Section 3.1 the details of the simulation framework and define a charging plan as well as the FCFS communication strategy imagined in [98] before giving in Section 3.2 the improvements we realise on the simulation framework. Then, we will present in Section 3.4 the different methods of charging plan optimisation we inherit or investigate to select the most appropriate method.

Contents

3.1 . Simulation framework

3.1.1 . Framework description

The framework enables the simulation of a daily flow of electric vehicles going on the highway for a long-distance trip (see Figure 3.1). It consists in:

- *A highway* represented by a set of entrances/exits $\mathbb{E}$ and N_{CS} fast-charging stations (CSs) $\mathbb{CS}$. The whole infrastructure has a finite set of charger types, P ($|P| = N_p$), with $p_j \in P$ the power rate of one charger type. One $CS_i \in \mathbb{CS}$, with $i \in \{1, \ldots, N_{CS}\}$, is described by its position on the highway, and its number of sockets per charger type $s_{i,j}$ ($j \in [\![1, N_p]\!]$).
- *A fleet* $\mathbb{F}$ of EVs travelling on the highway. Each $EV_v \in \mathbb{F}$, with v the position of the EV in the order of entrance on the highway, has its intrinsic parameters (battery capacity $E_{batt,v}$, maximum charging power P_v and consumption ρ_v) and trip characteristics (entrance and exit number respectively noted o_v and d_v with $[o_v, d_v] \in \mathbb{E}^2$, entry time $t_{in,v}$ and SoC at entrance $SoC_{start,v}$).
- *A program* simulating an EVs flow on the highway for one day. We use a multi-agent simulation (MAS) to precisely model the interactions between the EVs (the agents) and the highway with its charging infrastructure (the environment). Depending on the strategy of the EVs (described later in Section 3.1.5) and their trip characteristics, the program computes where, when, and for how long the EVs will stop to charge (charging plan) and then the model deduces the waiting time (see Section 3.2.2) for each EV at each stop. With the *FCFS communication strategy*, the day is divided into time steps Δt where EVs communicate their charging plan and adapt to the waiting time announced at the station.

The MAS permits the simulation of complete journeys to consider trip coherence and optimise the whole charging plan instead of modelling affluence in a station with stochastic models from queuing theory [20].

For a given fleet $\mathbb{F}$, each $EV_v \in \mathbb{F}$ has a target SoC, $SoC_{tar,v}$, it should have when reaching its highway target exit d_v to have enough energy to finish its trip. To leave the highway with at least $SoC_{tar,v}$, EV_v will have to charge during its trip a certain amount of energy $E_{total,v}$ that is evaluated by EV_v's computer according to the SoC at entrance $SoC_{start,v}$, the consumption of

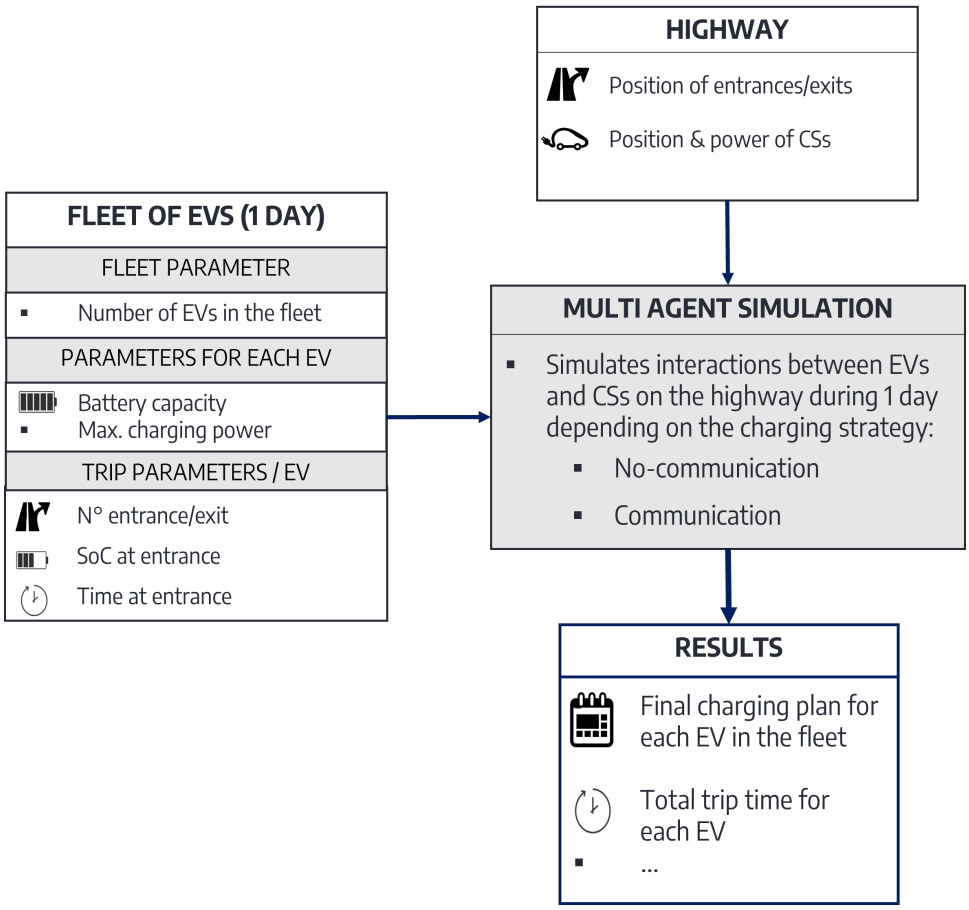

Figure 3.1: Details of the simulation environment with the inputs and the outputs of the MAS

the EV ρ_v considered as a constant, the distance D_v between the entrance o_v and the exit d_v and $SoC_{tar,v}$ (3.1).

$$E_{total_v} = (SoC_{tar,v} - SoC_{start,v}) \times E_{batt_v} + \rho_v \times D_v \tag{3.1}$$

During the simulation, each EV_v will compute its optimal charging plan ω_v^* (see Section 3.1.2 for the definition of a charging plan) to minimise its discontent factor (see Section 3.1.3) and ensure it will leave the highway with enough SoC ($SoC_{tar,v}$) to reach its final destination. The EVs' SoC is also constrained and must always be above a threshold: SoC_{min}.

3.1.2 . Charging plan

We should first define what a **charging plan** is in this thesis report and the difference between a **charging plan** and a **stop plan** or **charging schedule**.

Stop plan and charging plan

Stop plan: lists the stations where the EV plans to stop to charge and possibly the charger type used (level of charging power). In [20], this charging stop plan is referred to as **charging schedule**.
Charging plan: like a stop plan, lists the stations where the EV plans to stop to charge and the power level used but also depicts the amount of energy charged in each station from the stop plan.

The expression of a charging plan ω_v of EV_v is given by (3.2).

$$\omega_v = \begin{pmatrix} x_\omega \\ p_\omega \end{pmatrix} = \begin{pmatrix} x_1 & \cdots & x_{N_{CS}} \\ p_1 & \cdots & p_{N_{CS}} \end{pmatrix} \quad \text{with} \sum_{i=1}^{N_{CS}} x_i = E_{total,v} \tag{3.2}$$

Where x_i is the amount of energy charged at the station CS_i and p_i is the power level of the charging point selected at station CS_i.

Souley *et al.* [19] proposes an optimisation of the EV's speed in addition to the charging plan. Still, we focus only on the charging plan as it is difficult to impose an exact speed on the vehicle even if the EV is autonomous, for instance, with traffic jams. Thus, in this thesis, the driving speed is an exogenous variable of the problem and we consider it constant. Its value equals the speed limit, $speed_v$, that is, either the speed limit authorised on the road section ($speed_{road}$) or the speed ($speed_{driver}$) the EV driver observes to limit its consumption for example when driving an urban type EV with shorter range (3.3).

$$speed_v = min(speed_{driver}, speed_{road}) \tag{3.3}$$

3.1.3 . Charging plan optimisation to minimise user's discontent factor

We define for each EV_v a discontent factor (3.4) that takes into account the charging cost C_{charge} (3.7) and the total travel time T_{trip} (3.5) of the EV driver including the driving time, the waiting time and the charging time. A coefficient $X \in [0\ ,\ 1]$ models the user preferences between the reduction of the travel time and the charging cost in the discontent factor.

$$DF_v(\omega_v) = (1 - X) \cdot T_{trip}(\omega_v) + X \cdot C_{charge}(\omega_v) \tag{3.4}$$

3.1.3.1 . Trip time T_{trip}

The trip time T_{trip} expression is given by (3.5).

$$T_{trip}(\omega_v) = T_{travel} + T_{charge}(\omega_v) + T_{wait}(\omega_v) + T_{other}(\omega_v) \tag{3.5}$$

With:

T_{travel}: time spent on the road driving, we assume that the speed of EV_v is constant and equal to $speed_v$ (3.3).

$T_{charge}(\omega_v)$: time spent charging, depends on the charging powers selected in stations $(\ p_1, \cdots, p_{N_{CS}}\ )$, the charging power limitation of EV_v, P_v, and the amount of energy charged in stations $(\ x_1, \cdots, x_{N_{CS}}\ )$ (see Section 3.2.1).

$T_{wait}(\omega_v)$: time spent waiting for an available charging point (see Section 3.2.2).

$T_{other}(\omega_v)$: aggregated time to stop (deceleration to enter a station), to plug the EV and to accelerate when leaving a station. We suppose that the charging stations can only be located in highway service areas, so we assume that the detour time is short, and we set t_{other} to 5 minutes per stop [20]. t_{other} can also be seen as a time that penalises the action to stop.

We note T_{CS} the total time spent in stations by EV_v during the trip and it corresponds to:

$$T_{CS}(\omega_v) = T_{charge}(\omega_v) + T_{wait}(\omega_v) + T_{other}(\omega_v) \tag{3.6}$$

3.1.3.2 . Charging cost C_{charge}

The total cost of the charge for the whole trip is:

$$C_{charge}(\omega_v) = \sum_{i=1}^{N_{CS}} x_{i,v} \times p_{charge}(p_i) \tag{3.7}$$

$p_{charge}(p_i)$ corresponds to the price of the charge at the power level p_i. We suppose the charging price increases with the power level [44]. In real life, the CPOs propose subscriptions to their customers to reduce the charging price p_{charge} but regarding the wide spectrum of subscription modalities and prices, we focus on the simplest pricing previously described.

3.1.3.3 . Value of time

The parameter X depends on the value of time, noted vot, of a driver. The value of time is the price that travellers are willing to pay to decrease their trip time. According to Hess *et al.* [99], if w_t and w_c are respectively the time and cost weights in the utility function of a travelling option for the user (here one option is one charging plan), the vot is $\frac{w_t}{w_c}$ (see Appendix A.1). The utility function of the driver is the discontent factor DF, so the expression of X according to the vot is:

$$vot = \frac{w_t}{w_c} = \frac{1-X}{X} \Rightarrow X = \frac{1}{1+vot} \tag{3.8}$$

Therefore, when X is not equal to 0 or 1, we have to specify the vot_v of the driver to reflect the driver's preferences.

3.1.3.4 . Objective of the charging plan optimisation

The objective of each EV is to compute the optimal charging plan that minimises its discontent factor DF_v (3.4) while complying with the constraints on the SoC (3.9, 3.10, 3.11, 3.12).

$$Objective : \min_{\omega_v}(\ DF_v(\omega_v)\ ) \tag{3.9}$$

$$s.t.\ SoC_v \geq SoC_{min} \tag{3.10}$$

$$s.t.\ \forall\, x_{i,v} > 0,\ SoC_{out,i,v} \leq 80\% \tag{3.11}$$

$$s.t.\ SoC_{end,v} \geq SoC_{tar,v} \tag{3.12}$$

The constraint (3.10) represents the threshold below which the SoC must not fall. We set this threshold to SoC_{min} = 15% to model range anxiety. Concerning the charging, as the charging rate drops for values of SoC > 80% and charging above this value accelerates the ageing of the battery [100], we constrain the vehicles in the simulation to charge only up to 80% of SoC (3.11). The last constraint (3.11) stands for the final condition on the SoC.

In Section 3.4, we will detail the method used in this thesis to optimise the charging plan and present the other methods we tested.

3.1.4 . Charging strategies

How the EVs interact with the charging infrastructure depends on the charging strategy used by the fleet. We define in the following text box the charging strategy.

Charging strategy

A **charging strategy** describes how an EV determines its charging plan to minimise its discontent factor DF.
A **centralised charging strategy** means that the optimisation of EVs' charging plans is done by a central entity (a mobility operator for example). The objective of the optimisation is for the whole fleet and not for an individual EV.
A **decentralised charging strategy** means that the optimisation of the charging plan is done individually by each EV.

Nowadays, it is possible to plan in advance where and how much we will charge during a long-distance trip, for example, with the application A Better Route Planner [101]. J. Hassler [98]

implemented a charging strategy modelling that charging strategy where the EVs optimise their charging plan ω before going on a trip. EVs do not communicate with the charging infrastructure in real time, so this strategy is named the *no-communication strategy*.

No-communication strategy

The **no-communication strategy** represents the strategy of reference existing nowadays thanks to cloud applications. The EVs do not communicate during the trip and calculate their charging plan to minimise their travelling time, only knowing the position and the charging power of the CSs. They do not know the estimated waiting time at the station. The rule at the station is first come, first served (FCFS).
The objective to minimise for the *no-communication strategy* does not include the waiting time (3.13).

$$Objective : \min_{\omega_v}((1-X) \times \big(T_{travel} + T_{charge}(\omega_v) + T_{other}(\omega_v)\big) + X \times C_{charge}(\omega_v)) \quad (3.13)$$

Another application, Charge Finder enables one to know in real time the number of available charging sockets in the stations on the way. We choose to not include in the *no-communication strategy* the feature of knowing in real time the share of charging sockets currently available since it already implies communication in real time between the EVs and the CSs.

J. Hassler proposed a strategy more elaborated than the one proposed by Charge Finder [98] to use more efficiently the charging resources. This strategy, called the *FCFS communication strategy* enables, like Charge Finder, a communication in real time between the EVs and the CSs, but in the new strategy, the CSs can estimate the future waiting time in stations thanks to a communication by the EVs of their intended charging plan.

FCFS communication strategy

With the **FCFS communication strategy**, the EVs on the road regularly communicate their charging plan to stations and determine their charging plan ω^* to minimise their discontent factor DF in accordance with the estimated waiting times communicated by the stations. The rule at a station is FCFS as for the *no-communication strategy*.
Therefore, the objective includes the waiting time (3.14).

$$Objective : \min_{\omega_v}((1-X)\times\big(T_{travel} + T_{charge}(\omega_v) + T_{wait}(\omega_v) + T_{other}(\omega_v)\big)+X\times C_{charge}(\omega_v)) \quad (3.14)$$

The information exchanges between the EVs and the CSs can be established via the mobile network (3G-4G). It is already done for connected vehicles and most new EV models, so the coordination is technically feasible. By managing the communication, the computation and the choice of the best charging plan, using an automatic planner would avoid the dangerous distraction of the driver, who would only have to follow the instructions of the EV's monitor like a GPS.

In the next section, Section 3.1.5, we see the detailed steps of the multi-agent simulation according to the charging strategy.

3.1.5 . The steps of the Multi-Agent Simulation

3.1.5.1 . No-communication strategy

When the EVs follow the *no-communication strategy*, they compute before travelling the optimal charging plan $\omega^*_{noCom.}$ that will minimise their discontent factor DF without knowing the

waiting time in stations since they do not communicate with the CSs. Once they have determined their charging plan $\omega^*_{noCom.}$, they follow this plan no matter what happens during the trip. As no charging plan changes during the day, the simulation framework only determines the waiting queues and computes each charging session's waiting time (see Section 3.2.2). We retrieve the total trip time $T_{trip}(\omega^*_{noCom,v})$, including the computed waiting time for each EV_v at the end of the simulation.

3.1.5.2 . FCFS Communication strategy

For the *FCFS communication strategy*, as the EVs and the CSs communicate in real time, we need to divide the simulated day into constant time intervals to describe the interaction between the EVs and the CSs during each time interval. A time interval starting at time $t-1$ and ending at time t represents the iteration "t" and lasts Δt minutes (Δt is constant).

Each station CS_i has a charging request table R_i listing the latest charging request sent by each EV identified by id_{EV}. One charging request is associated to the optimal charging plan of an EV and precises the EV's id, estimated arrival time $t_{in,i}(\omega^*)$ and estimated charging time $t_{charge,i}(\omega^*)$.

During the simulation, the steps described in Figure 3.2 are executed at each iteration t (every Δt).

- **Step 1**: EV_v asks the stations in their charging plans about the estimated waiting times.
- **Step 2**: each station CS_i, upon receiving the id, id_v, during step 1, computes the corresponding waiting times according to the information received during the previous iteration $t-1$ ($R_i(t-1)$) from the whole fleet and sends the waiting times back to EV_v. Section 3.2.2 describes how the charging station CS_i computes the waiting times according to the charging request table R_i.
- **Step 3**: EV_v computes the optimal charging plan ω^*_v according to the estimated waiting times.
- **Step 4**: EV_v informs the stations from its optimal charging plan ω^*_v of its estimated arrival time $A.T.$ and estimated charging time $C.T.$ (and charging socket) in station.
- **Step 5**: according to the $A.T.$ and $C.T.$ received, each charging station updates its charging request table R_i that will be used to compute the waiting times during the next iteration.

Each EV_v starts in advance the communication process (execution every Δt of step 1 to step 5) before entering the highway. This anticipation time before entering the highway is noted as $T_{adv.}$ and J. Hassler determined in his thesis [98] that the adequate tuple ($T_{adv.}$, Δt) is equal to (20, 5) minutes. Those values will be used in the rest of the manuscript. When an EV starts the communication process, we say that this EV is "on the road" even if the EV is not effectively driving on the highway.

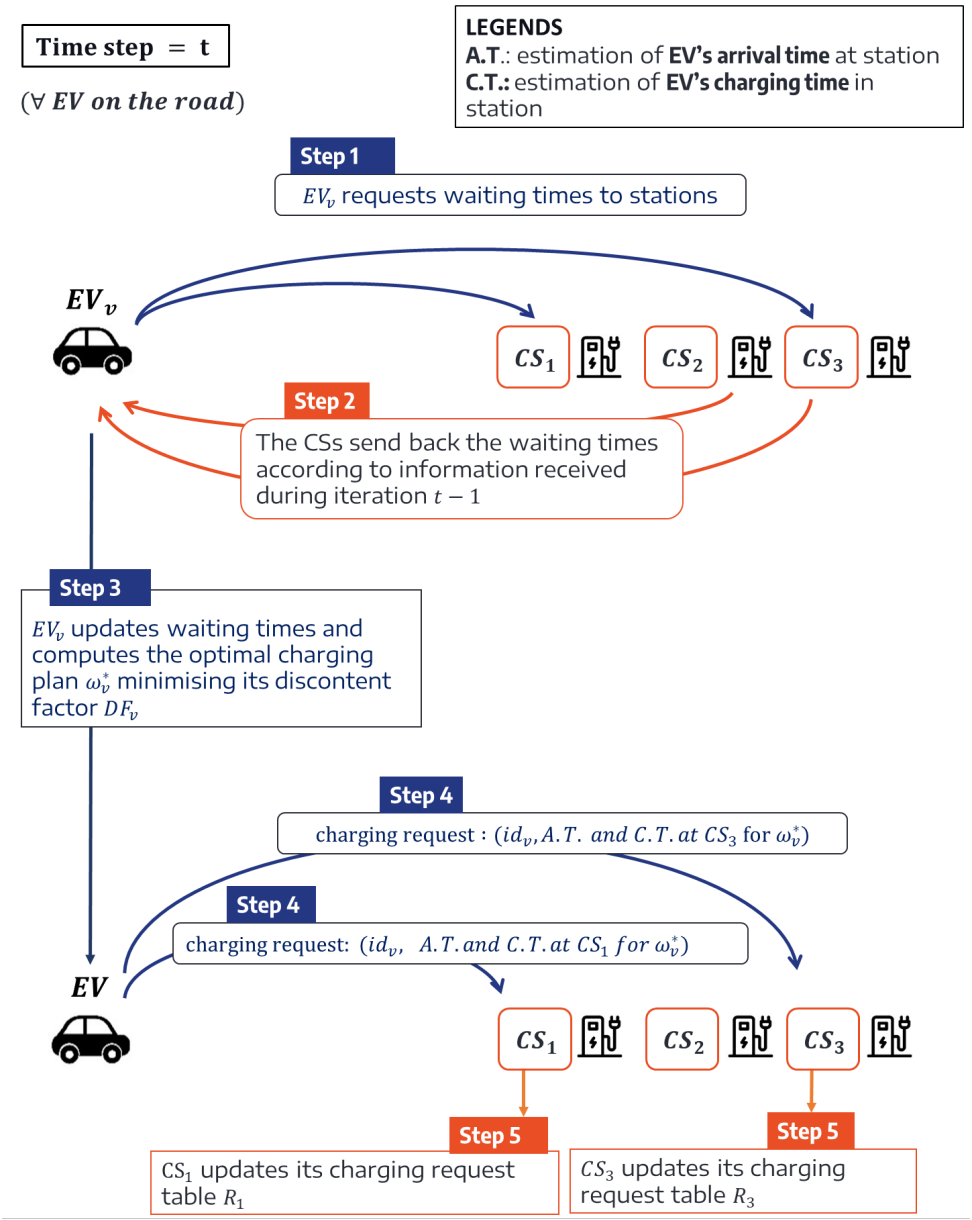

Figure 3.2: Communication scheme in the FCFS communication strategy

3.2 . Major MAS features details

3.2.1 . Charging time calculation

The charging of an EV is a complex process that depends on various parameters, such as the value of open circuit voltage of a battery cell V_{OC} varying with the SoC, the intern resistance R depending on the SoC and the cell temperature T. As those data are confidential (intern resistance $R(SoC, T)$, open-circuit voltage V_{OC} and temperature of the cells evolutions according to the SoC), we choose to simplify the problem and take as models charging curves given by charging operators (like Fastned [102]) or other database listing EV model characteristics (automobile propre [23], insideEV [103]). From those charging curves, we select some points and approximate the curve linearly as it is possible to deduce the charging time from linear approximation, as we will see next.

The charging power curve corresponds to the minimum between the power $p_{i,j}$ delivered

by the socket of type j at station CS_i and the power P_v accepted by EV_v during the charge (3.15).

$$P_{charge,i,j}(SoC) = min(p_{i,j}, P_v(SoC)) \tag{3.15}$$

Thus, the charging curve of the EV is modified according to the power limitation of the charger (in fact, the current limitation of the socket since the battery pack imposes its voltage). We give examples of an EV's charging curves for different power levels of the charger (Figure 3.3).

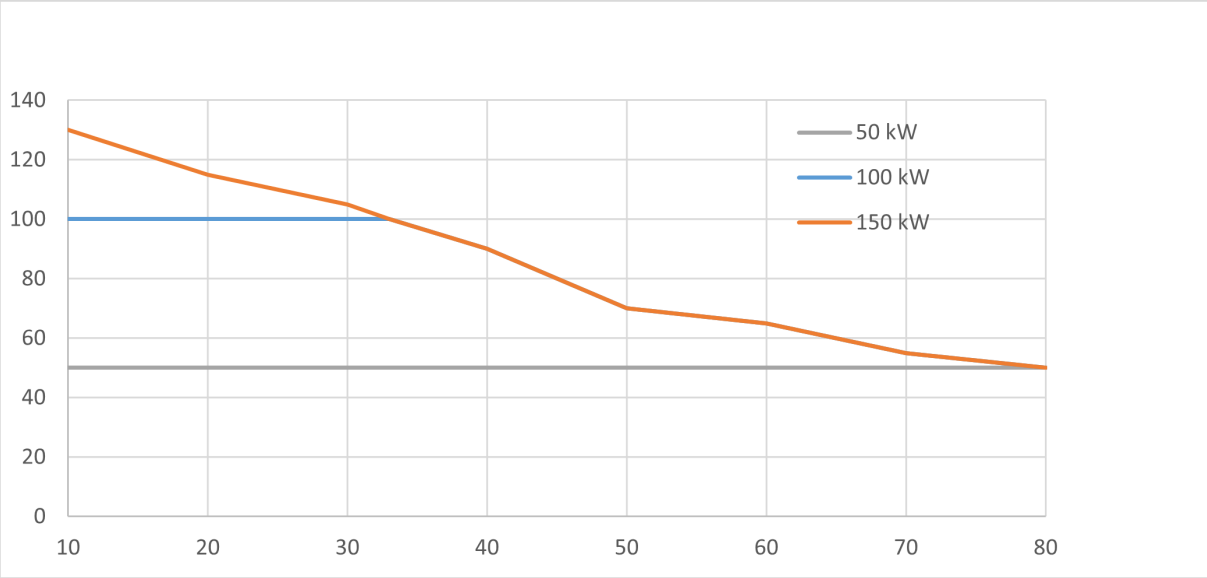

Figure 3.3: Simplified charging curves of a Megane-etech on chargers with different power rates (50, 100, 150 kW) [23]

To compute the charging time, we have to distinguish the part of the charging curve that is constant from the linear ones.

On the interval $[SoC_i, SoC_{i+1}[$, if the function $P(SoC)$ is constant and equal to P_{cst}, the charging time in second on that part between SoC_{start} and SoC_{end} is directly:

$$t_{charge} = \frac{E_{batt}}{3600 \cdot P_{cst}} \cdot (SoC_{end} - SoC_{start}) \tag{3.16}$$

Where E_{batt} is the battery capacity of the EV. We prove this result in Appendix A.3.1.

If the function $P(SoC)$ is linear on the interval $\left[SoC_i, SoC_(i+1)\right[$ (see Figure 3.4), we express $P(SoC)$ as follow :

$$\begin{aligned} P\left(SoC(t)\right) =& a_i, (SoC(t) - SoC_i) + b_i \text{ with } a_i = \frac{P_{i+1} - P_i}{SoC_{i+1} - SoC_i}, \\ P_{i+1} =& P\left(SoC_{i+1}\right), \; P_i = P\left(SoC_i\right) \text{ and } b_i = P_i \end{aligned} \tag{3.17}$$

In this case, the expression of the charging time t_{charge} is given by the equation (3.18).

$$t_{charge} = \frac{E_{batt}}{3600 \cdot a_i} \cdot \log\left(\left(SoC_{end} - SoC_i + \frac{b_i}{a_i}\right) / \left(SoC_{start} - SoC_i + \frac{b_i}{a_i}\right)\right) \tag{3.18}$$

We prove this result in Appendix A.3.2.

In some case studies, we assume, like in [40], that $P_v(SoC)$ is linear on the interval $[15,\ 80]\ \%$ with the slope depending on the charging coefficient c_v and $P_{max,v}$ representing the intersection between the linear curve $P_v(SoC)$ and the axis $x = 0$ (3.19). The $SoC(t)$ is expressed in percentage (%).

$$P\left(SoC(t)\right) = P_{max,v} - \frac{c_v}{100 \cdot E_{batt}} \cdot SoC(t) \tag{3.19}$$

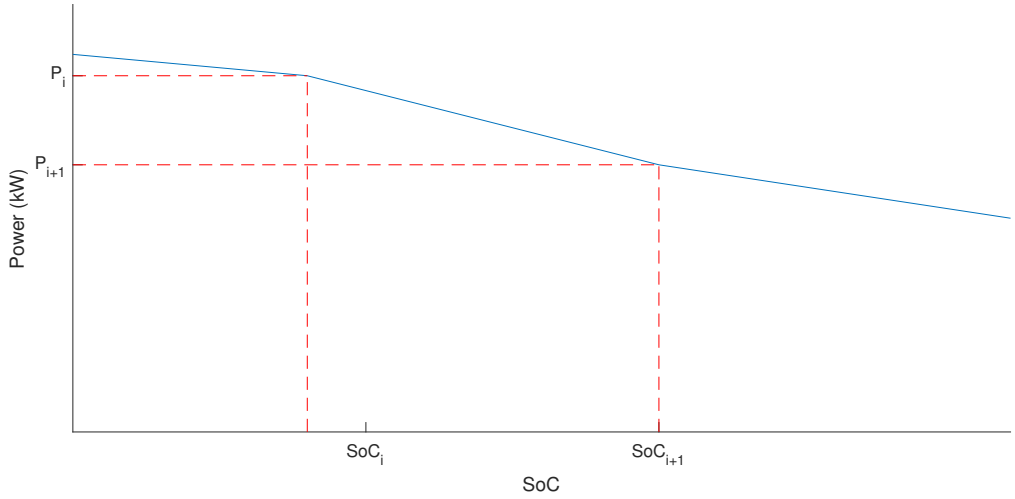

Figure 3.4: Charging power linear according to the SoC on interval $[SoC_i, SoC_{i+1}[$

3.2.2 . Waiting time calculation

3.2.2.1 . Steps of the calculation

Regarding the First-Come-First-Served (FCFS) priority rule in stations, the waiting time depends on the arrival time t_{in} of the EV in the stations. This is why when an EV communicates its optimal charging plan, it should precise its estimated arrival time (see $A.T.$ for step 4 in Figure 3.2).

According to [104], in a queueing system with multiple servers, having one single queue for all the servers instead of one queue per server reduces the average waiting time. However, when the EVs are using the *no-communication* or **FCFS communication strategy**, EVs are optimising the charging power they are going to use so they know when entering a station at which type of socket, j, they will plug. Therefore, two EVs waiting for different socket types do not wait for the same service and should wait in two different lines. This is why we implement one queue per charger type j in each station with multiple charger types.

The waiting queue and the waiting time in the simulation framework are computed thanks to the process described in Figure 3.5.

Firstly, during the **Step 2** described in Figure 3.2, for each possible charging plan $\omega_v \in \Omega_v$ of the EV_v, one $CS \in \mathbb{CS}$ computes the estimated waiting time asked by EV_v given its arrival time $t_{in}(\omega_v)$ at this station for this specific plan ω_v. For this calculation, CS keeps a charging request table R listing the latest charging request sent by each EV identified by id_v (so one EV cannot have more than one request in R). For **Step 2**, the table R is in read-only mode, so it contains requests that are up to date with the previous iteration $(t-1)$. When an EV asks for the estimated waiting time in the station according to its arrival time, CS will determine the position K of this EV in the order of arrival of all the EVs listed in $R(t-1)$. Then, according to the number of charging points s_i at the station, CS deduces the estimated waiting time:

- If $K \leq s$, the EV will not wait.
- If the $(K-s)^{th}$ EV leaving the station leaves before the arrival of the considered EV, the EV will not wait.
- In all other cases, the waiting time equals the difference between the departure hour of the $(K-s)^{th}$ EV leaving the station and the arrival time of the EV.

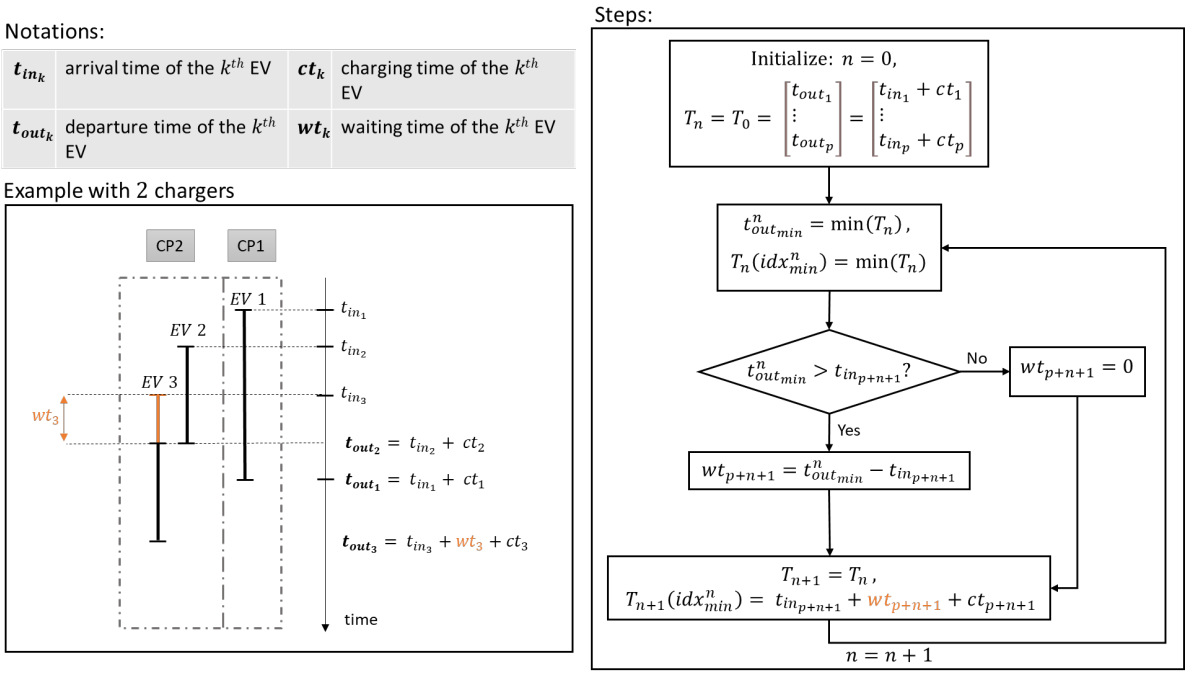

Figure 3.5: Waiting time computation steps for the FCFS communication strategy (on the right) with a schematic example (on the left)

Secondly, during **Step 5** (Figure 3.2), the table R is in write mode and registers the new charging requests the EVs have selected according to the previously estimated waiting time computation. After registration, the CS establishes the current waiting queue at the station to estimate the departing hour of the EVs from the station. The EVs registered in the table R are ordered by arrival time. A vector T is initialised with the departure times (arrival time t_{in_k} + charging time ct_k) of the first s EVs of the table. Then, the algorithm takes the next EV in the ordered table that is not in T and compares the minimum departure time $t_{out_{min}}$ in the vector T with the arrival time $t_{in_{s+1}}$ of the next EV. If $t_{out_{min}} > t_{in_{s+1}}$, the next EV will wait during $t_{out_{min}} - t_{in_{s+1}}$. Else, there is no waiting time. The departure time of the next EV (arrival time + charging time + waiting time) replaces $t_{out_{min}}$ in T and so on (see Figure 3.5).

As the waiting time estimations during Step 2 (Figure 3.2) are based on information from the previous iteration $(t-1)$, the actual waiting time in a station might differ as the EVs can update their charging plan at every iteration. This is why, even if we consider an ideal situation in the simulations (see Section 4.2.2 in Chapter 4), the charging plans change during the simulations with the *FCFS communication strategy*.

I corrected the algorithm to have a more accurate estimation of the waiting time: J. Hassler was estimating the waiting time according to the N^{th} EV leaving the station, whereas this estimation should be done according to the $(N-s)^{th}$. The demonstration is given in Appendix A.2.

3.2.2.2 . The Waiting table WT

In the inherited version of the framework, the EVs asked the waiting time for each ω, generating as many requests as charging plans they have in Ω. To make the communication of waiting times between the stations and the EVs more feasible in real life, we implemented an algorithm that builds only one waiting time table WT depending on the EV requesting waiting time information. Then, sharing this waiting timetable requires only one communication between the charging station and the EV. In addition, using the waiting time table WT enables speeding up

the computation of the waiting time during the simulation since the station needs to perform the calculation only once instead of for each charging plan.

We know that the waiting time in a station is not continuous according to the arrival time but is piecewise linear (see Figure 3.6). Therefore, the waiting table $WT_{i,v}$ of the station CS_i for EV_v

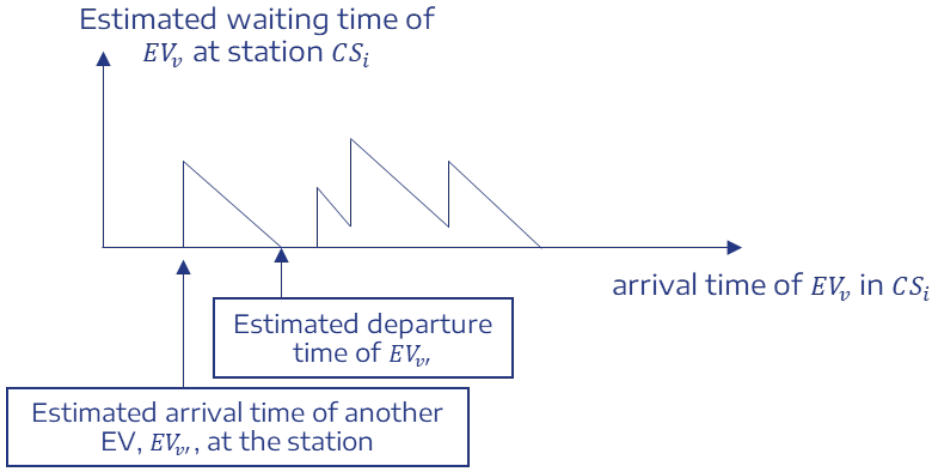

Figure 3.6: Non-continuity of waiting time according to the arrival time of an EV (EV_v) in a station (CS_i).

lists the time interval during which the waiting time is linear according to the arrival time of EV_v (see Figure 3.6). For each time interval, $WT_{i,v}$ gives the lower and upper bounds of the interval (t_{low}, t_{up}) and the constant parameters (a, b) of the straight curve. Thus, for a given arrival time t_{in}, the waiting time t_{wait} can be directly expressed by (3.20).

$$t_{wait}(t_{in}) = a.(t_{in} - t_{low}) + b \text{ with } t_{low} \leq t_{in} < t_{up} \tag{3.20}$$

We use a similar process as in Figure 3.5 to determine a and b.

3.3 . Generation of the case studies

In this manuscript, we present three different case studies:

- **Case study 1**: 3 fleets are generated to represent 3 different traffic situations (100, 180 and 300 EVs). The case study is used in this chapter to test the charging plan optimisation methods (Section 3.4.5) and in Chapter 4 to compare the performance of the control strategies.
- **Case study 2**: 5 fleets are generated to represent 5 different crowded days with 500 EVs going on long-distance trips. The case study is used in Chapter 5 to evaluate the benefit of the *FCFS communication strategy* in reducing the cost of the optimal infrastructure to be developed.
- **Case study 3**: 100 fleets are generated to represent 100 different low traffic days (50 EVs). The case study is used in Chapter 6 to evaluate the trade-off between the infrastructure cost and the time spent in stations according to the share of ultra-fast charging vehicles (charging power = 350 kW) in the fleet.

For all the case studies, we consider the French A6 highway from Paris to Lyon. However, in each case study, the parameters concerning the highway environment change (position of the

entrance/exit, probability for an EV to enter at a given entrance ...). We detail in Section 3.3.1 the disposable data sources we found for long-distance trip generation, and we explain which ones were used to generate the charging scenarios studied in this manuscript. We present in Section 3.3.2 how the entrance time ($t_{start,v}$) is selected for each EV according to the case study and then we summarise the different trip parameters for each case study in Sections 3.3.3, 3.3.4 and 3.3.5.

3.3.1 . Data sources

A multi-agent simulation enables the study of the charging strategy with trip-based simulations instead of queuing theory statistics computed from the traffic per highway section (see Section 2.2). However, retrieving long-distance trip open data is uneasy, and most of the time, the data are incomplete or not detailed enough to be of use in our model. Still, we have found one study [105] realised by the INSEE[1] with long-distance trip data (departing day and hour, town of origin and destination of the trip) but the trips concern the whole France so we did not have enough data to sampled specific trips on one specific highway (as we are focusing on a corridor and not on a network).Still, this data could represent a good trip database for the following studies. Other information concerning long-distance travel in France can be found in [27], and we used data from Opendata.gouv [106] to get the AADT on A6 highway sections and set the entry/exit probabilities.

Nevertheless, as we are dealing with electric vehicles and the previous data only gives information about all vehicles, ICE and electric vehicles, we do not have information concerning the SoC of the EVs and the behaviour of EV drivers, whereas we need to precise the SoC when the EV enter the highway to generate adequate trips (see $SoC_{start,v}$ in Section 3.1.1). This is why we contacted the fablab of Stellantis to work on data collected by Stellantis-connected EVs. Appendix B.2 explains how we exploit the raw data from connected vehicles.

Thanks to work on the connected vehicles data, we identified, for one year, 380 connected EVs that have made at least one long-distance trip, as we defined it in the textbox 1.2.4.3. The selected journeys are the trips with a distance travelled superior to 100 km and where at least one charging session occurred on the highway as defined in Section 1.2.1.

To circumvent the lack of complete trip data, the entrance, o_v, and the exit, d_v, of an EV are selected according to the entry probabilities on the highway, and this probability changes from one study to another. Since we do not have specific data about long-distance travel on Highway A6, we arbitrarily set the entry and exit probabilities to roughly reflect the annual average daily traffic (AADT) on A6 sections with more or less details.

3.3.2 . Entrance time

Each EV's entrance time for all case studies is determined according to the average incoming flow per hour on the French A6 highway in Ile-de-France (Figure 3.7a). The blue curve in Figure 3.7a is the resulting average of the hourly traffic on the road sections leading to the highway A6 in Ile-de-France. The hourly traffic data can be found on the website data.gouv [106] and comes from inductive loop counters that measure the number of vehicles driving past their loop during an hour. We then simplified the blue curve to obtain a vehicle flow between 3:00 a.m. and 11:00 p.m.

The entrance time is consistent with the demand on the highway we found in the literature [25] as the cumulative power on the highway, like the entrance time, is spread during the day without a charging peak as it is the case for residential charging during evening peak (Figure 3.7b). A similar distribution of long-distance trip starting time is used in [94] where the EV agents

[1] French National Institute of Statistics and Economic Studies

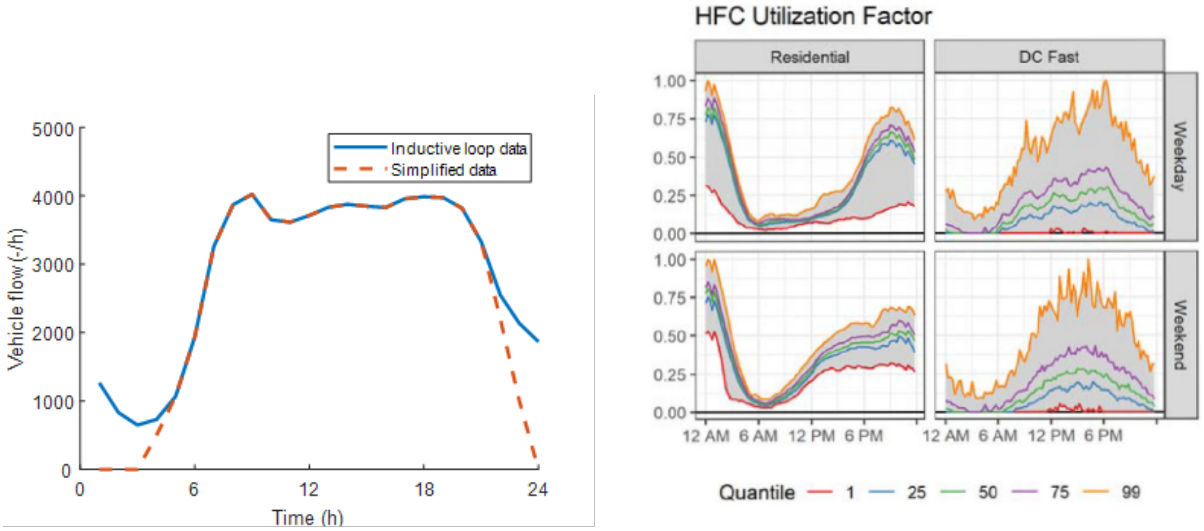

(a) (b)

Figure 3.7: Figure (a): Average incoming vehicle flow per hour of the French highway A6 in Ile-de-France [24]. The blue curve is the resulting average of the A6 highway sections in Ile-de-France traffic flow inductive loop data counting. Figure (b): Cumulative charging power drawn during the day on residential and highway charging stations (HFC stands for Highway fast-charging station) [25]

constituting the tested fleet commence their journey with uniformly distributed times across the day.

The entrance time for one EV is obtained by iso-probabilistic transformation of the cumulative density function of the hourly traffic flow curve in Figure 3.7a. The method is explained in Appendix B.1.

3.3.3 . Case study 1

Use cases: in the comparison of charging plan optimisation methods and in the comparison of the FCFS communication and reservation strategies.

The highway environment for Case study 1 is given by Figure 3.8. This is a simplified version of the French A6 highway with 6 stations and 11 entrances/exits. **Three different traffic situations** are generated with one fleet per traffic situation: low traffic situation (100 EVs), average traffic situation (180 EVs) and high-traffic situation (300 EVs). Each fleet includes **3 different types of EVs** listed in Table 3.1. The entrance, o_v, and the exit, d_v, of each EV is selected according to the entry/exit probabilities depicted in Figure 3.8, and the trip length must be higher than 100 km. The **SoC at entrance** $SoC_{start,v}$ is randomly selected between 50 and 100 % and a SoC when leaving the expressway, SoC_{end}, set to 20%. Table 3.2 summarises the trip generation parameters of Case study 1.

3.3.4 . Case study 2

Use case: in the comparison of optimal infrastructure to be deployed under FCFS communication strategy and under no-communication strategy.

The highway environment of the Case study 2 is depicted in Figure 3.9 and represents the real French A6 highway. The positions of the service areas are the real ones but the number of entrance and exit is simplified (there are around 50 entrances/exits in reality).

The SoC_{start} of each EVs is established according to the density function in Figure 3.10. In

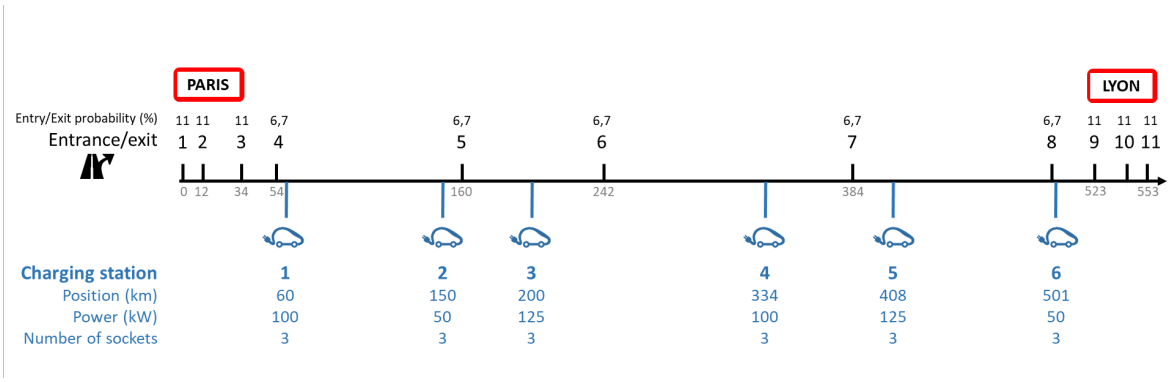

Figure 3.8: Highway description for the comparison of the charging strategies

Table 3.1: Type of EVs considered in the study

EV Type	Battery capacity (kWh)	Maximum charging power $P_{max,v}$ (kW)	c_v	ρ_v	Speed limit (km/h)	Percentage in the fleet
urban	50	50	250	0.15	110	30%
sedan	60	100	500	0.18	130	60%
luxury	95	125	1062	0.18	130	10%

Table 3.2: Parameters of Case study 1

Parameter	**Value**
Strategies	*FCFS communication strategy* and *reservation strategy*
Battery capacity	depends on the EV type (see Table 3.1)
Charging power	see $P_{max,v}$ and c_v in Table 3.1
Number of traffic situation	3 (100, 180 and 300 EVs)
Number of fleet per traffic situation	1
Number of charging point per CS	3
entrance/exit selection	Entry/exit probability in Figure 3.8 and $D > 100$ km
SoC_{start}	$U([50, 100]\%)$
SoC_{end}	20%

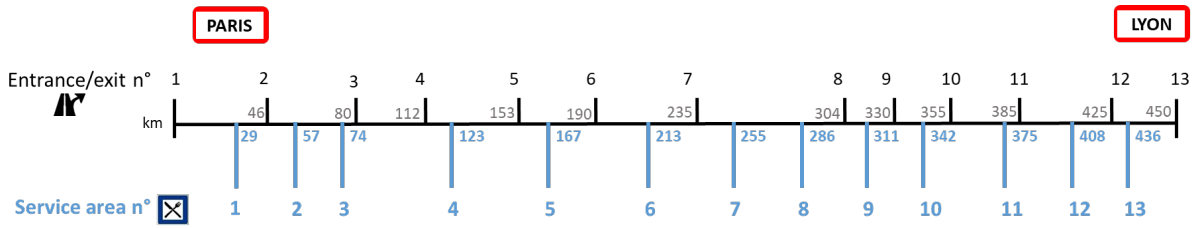

Figure 3.9: French highway A6 with simplified entrances/exits

Case study 1 (see Section 4), we supposed that the SoC when entering the highway was uniformly distributed from 50 % to 100 % because we assumed that a driver prefers charging at home before a long distance trip instead at highway service areas where the charging price is higher. It is surprising to see that, in Figure 3.10, a part of the EVs enters the highway for a long distance trip with less than 50 % of SoC. This might be due to EVs driving in other countries than France where the configuration of highways is different: for instance, in Germany, it is easier to leave the highway to find a fast charger in an urban area near the highway that is cheaper because it is not on a service area. We could not filter those kind of results because of the closeness of the charging station to the highway or other reasons we could not determine from the data.

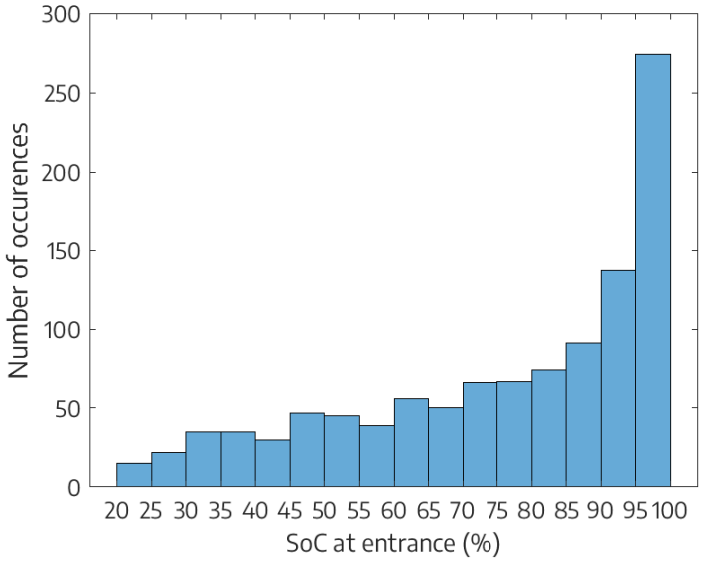

Figure 3.10: SoC at entrance distribution of the long distance trips extracted from the 380 Stellantis connected EVs

As in this case study we optimise the charging infrastructure, we need different fleets to represent different days so we generate 5 fleets of 500 EVs (see Table 3.3). To partially reflect the sensitivity of the charging strategies to the trip parameters, we introduce two different methods explained later in Section 5.3.2 to select the exit d_v of each EV. The method used depends on the fleet.

3.3.5 . Case study 3

[2]SoC distribution given in Figure 3.10.

Table 3.3: Parameters for the trip generation according to the fleet

Fleet i	Exit selection method	$SoC_{start,v}$ selection method	$P_{max,v}$ (kW)	c_v (-)
F_1	see section 5.3.2	SoC distribution[2] truncated (50% - 100 %)	140	6000
F_2	-	SoC distribution truncated (50% - 100 %)	130	6000
F_3	-	SoC distribution truncated (50% - 100 %)	130	6000
F_4	-	SoC distribution	130	5000
F_5	-	SoC distribution	130	5000

Table 3.4: Parameters of Case study 2

Parameters	Value
Strategies	*FCFS communication strategy* and *no-communication strategy*
Number of traffic situation	1 (500 EVs)
Number of fleet per traffic situation	5
Number of charging point per CS	- (optimisation)
Charging power in stations	Depends on the Optimisation ($\{175\}$ or $\{50, 175\}$ kW)
Battery capacity	60 kWh
Charging power	see column $P_{max,v}$ and c_v in Table 3.3
entrance/exit selection	Depends on the fleet (see Section 5.3)
SoC_{start}	see column $SoC_{start,v}$ in 3.3
SoC_{end}	$U([20, 30]\%)$

Use case: in the establishment of the trade-off between time spent in stations and infrastructure cost with different share of ultra-fast-charging EVs

The highway environment for the Case study 1 is given by Figure 3.11 and represents the French highway A6 with all the real entrance/exits. The entrance and exit probabilities are given in Figure 3.13 and Table 3.5 summarises the parameters of the case study.

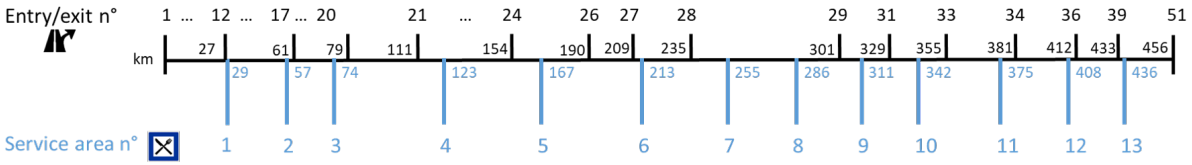

Figure 3.11: French highway A6

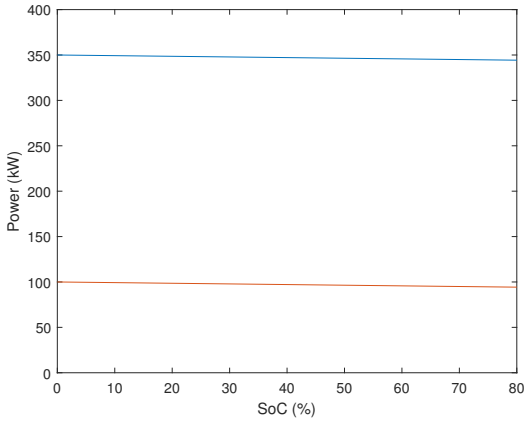

Figure 3.12: Charging curves of the 100kW and 350kW-charging EVs

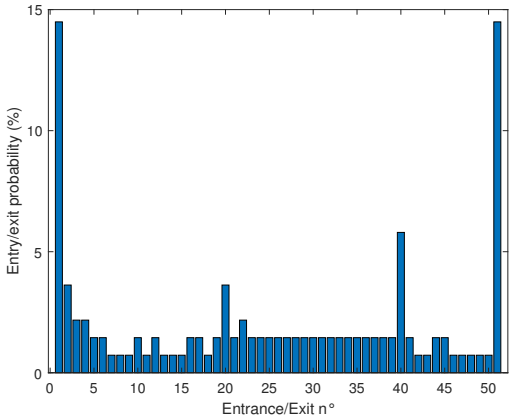

Figure 3.13: Entry and exit probabilities of each entrance/exit of the highway

Table 3.5: Parameters of Case study 3

Parameters	Value
Strategies	*Last station reachable strategy*
Number of traffic situation	1 (50 EVs)
Number of fleet per traffic situation	100
Number of charging point per CS	- (optimisation)
Battery capacity	70 kWh
Charging power	see Figures 3.12
entrance/exit selection	Entry/exit probability from Figure 3.13
SoC_{start}	$N(80\%, 15)$ truncated at 40% and 95%
SoC_{end}	20%

3.4 . Methods for the charging plan optimisations

3.4.1 . Charging plan optimisation challenges

Concerning the charging plan optimisation (3.9), the objective of the optimisation, DF_v, depends on $T_{charge}(\omega_v)$ (3.5). Yet, the charging time with a fast charger is usually not a linear function of the energy charged [40] (see Section 3.2.1). If the charging time dependence on the energy is not linear, neither the trip time optimisation is, so we cannot solve the problem with linear programming.

Moreover, for the *FCFS communication strategy*, the objective of the optimisation includes $T_{wait}(\omega_v)$ (3.5), which is the sum of waiting time at each station where the EV stops to charge ($x_i > 0$). As the waiting time in a station depends on the **arrival time** in this station, we need to compute the optimal charging plan based on the arrival time at each station. This arrival time depends on the amount of energy recovered at the previous stations and the power used to charge that energy (as T_{charge} depends on the charging power). In addition, the waiting time is not continuous according to the arrival time (see Figure 3.6), so we do not have one mathematical expression of the waiting time according to the arrival time. Thus, we need to **discretise the energy charged in stations** to have a list of arrival time values and deduce the waiting time for each value.

To circumvent all those challenges, Jean Hassler implemented an exhaustive method depicted in Section 3.4.2 that list possible discretised charging plans before evaluating them and deducing the optimal one. We improved the exhaustive method during this present thesis, and we ran it for all the case studies presented in this manuscript because of its implementation maturity. However, we explored other charging plan optimisation methods, such as the genetic algorithm described in Section 3.4.3 and the dynamic programming in Section 3.4.4. We will see that the last method, the dynamic programming method, could represent an interesting alternative to the exhaustive method, especially for real-world applications.

We set a case study to test the three optimisation methods and determine the best method in Section 3.4.5.

The discontent factor DF to be minimised also includes the cost of the charge, but as we consider the charging price linear according to the charged energy, the optimisation of DF is not complicated by the charging cost.

3.4.2 . Exhaustive or "brute force" method

The exhaustive method is the method of reference for the charging plan optimisation as it was tested and checked during the previous thesis and this current thesis. It is also simple to check the correctness of its results since all possible solutions are listed.

As a reminder, the exhaustive method for optimising the charging plan lists possible discretised charging plans before computing the objective value for each potential solution to find the optimal one. Since the computation time of the charging plan listing rapidly grows with the number of stops in the charging plans (combinatorial), we need for this method a limited number $N_{limit,\,v}$ of stops in the charging plans to be able to list them in a feasible time. Initially, we will assume that N_{limit} equal to the minimum number of charging stops ($N_{min,v}$) the EV needs to reach its destination with $SoC_{tar,v}$ ($N_{limit} = N_{min}$).

Therefore, before listing the charging plans, EV_v determines the minimum number of charging stops ($N_{min,\,v}$). For this purpose, EV_v establishes the last station on the road it can reach with its initial SoC, $SoC_{start,v}$. Then, it assumes that its battery is charged to 80% at that station and the EV reiterates the process until it virtually reaches the destination. $N_{min,\,v}$ is then the number of time EV_v stops to charge the battery to 80%. The charging plan found with this method is called the "last-reachable charging plan" and is written $\omega_{lr,v}$.

Then, the EV_v lists in Ω_v all the possible charging plans with N_{min} charging pauses it can follow to reach its destination. One charging plan $\omega_v \in \Omega_v$ (Equation 3.2) is a list of N_{min} tuples (i_k, x_{i_k}) where $i_k \in \{1\,,\ldots,\,N_{CS}\}$ identifies a station on the path of EV_v and $x_k > 0$ the amount of energy planned to be stored at station CS_{i_k} (see equation 3.21). For one list of station IDs $(i_1, ..., i_{N_{min}})$ representing one-stop plan (see textbox 3.1.2), we discretise the total energy E_{total_v} and constitute all the possible combination of discretised energies x_{i_k} that we distribute among the stations from the stop plan.

$$\omega_v = \begin{pmatrix} i_1 & \dots & i_{N_{min}} \\ x_{i_1} & \dots & x_{i_{N_{min}}} \end{pmatrix} \text{with} \sum_{k=1}^{N_{min}} x_{i_k} = E_{total_v} \tag{3.21}$$

It is possible to add a charging stop to the $N_{min,\,v}$ stops to offer more charging plans and increase the flexibility of the FCFS communication strategy. However, as the listing of the charging plans is combinatorial, the computation time when listing the charging plans before the beginning of the simulation is exponential with respect to the number of stops, and the calculation time at each iteration also increases according to the number of stops. This is why we are limiting the possibility of adding one charging stop only to the EVs with $N_{min,\,v} \leq 2$. We note $N_{limit,\,v}$, the maximal number of charging stops a charging plan ω_v is allowed to have.

To speed up the calculations, we detail before the simulation for each charging plan the driving time between two stations (with a constant speed $speed_v$), the estimated charging time (see 3.2.1), the estimated SoC when entering each CS of the charging plan and the SoC when leaving them. Those elements are kept in a $data_{charge}$ structure during the simulation. To simplify the simulation, we suppose those elements never change during the simulation, and only the waiting time and the estimated arrival time (depending on the waiting time in the previous stations) are updated at each iteration t. Consequently, there is no difference between the estimated state variables ($SoC_{in,v,i}$, $SoC_{out,v,i}$, $t_{charge,v,i}$, t_{drive}) and the actual state of the EV when it effectively reaches a station during the simulation.

As we are only updating the waiting times for each listed charging plan before determining the minimal value of a list of times during the simulation, using the exhaustive method is fast. Although the computation time increases exponentially with the number of charging stops, this time stays under 1 second. However, suppose we want to consider traffic hazards (difference between estimated driving time and actual ones) or different charging times from the estimated ones. In that case, we have to update the information listed in $data_{charge}$, which can be time-costly.

During the simulation, one step executed at each iteration t consists in updating the EV's optimal charging plan (step 3 on Figure 3.2). As explained in Section 3.4, we use for **all the case studies** in this manuscript the exhaustive method (Section 3.4.2) to optimise the charging plan of the EVs since it was the method implemented by J.Hassler [98] and so, the more mature approach.

However, the performance of the FCFS communication strategy were downgraded due to the way the charging plans were listed for the exhaustive method in the inherited version. We explain in Appendix D.1 the correction we brought to the algorithm.

Even if we improved the way the charging plans were listed to give more flexibility to the EV, the exhaustive method still has a major issue: the optimisation depends on a limited number of charging stops, $N_{limit,\,v}$. As we will see in the following chapters (especially in Section 4.4 and in Section 4.6.1.3), it can be beneficial to add as many charging stops as possible and, so we need to find charging plan optimisations methods that do not depend on the number of charging stops.

3.4.3 . Evolutionary algorithm for the resolution

An evolutionary algorithm is one method that does not need a presetting of the maximum charging stop number and can handle complex problems like ours. We tested the genetic algorithm (GA) [107]. The GA is inspired by the natural selection process and works on a population of individuals representing for each of them a solution to the optimisation problem, here a charging plan (3.2). The i^{th} gene of an individual gives the amount of energy x_i charged at the i^{th} station along the way of the EV, and $x_i > 0$ means that the EV will stop and charge at the

corresponding station CS_i. If the charging stations have several levels of charging power p_i, the gene should also give the power level used per station (see Figure 3.14).

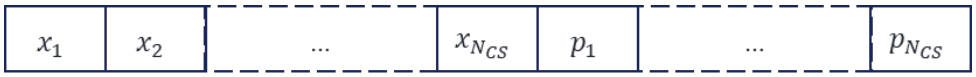

Figure 3.14: Description of a gene representing one charging plan with x_i the amount of energy charged in CS_i and p_i the power of the socket used

We use the genetic algorithm "ga()" by Matlab [108] to perform the optimisation. The constraints on the SoC are linear according to the optimisation variables (the vector of energy charged per station x), so we only need to define the matrix **Aineq** and the vector **bineq** representing the linear constraints of the algorithm (3.22).

$$Aineq.x \leq bineq \tag{3.22}$$

We define next the expression of the constraints according to the charging plan (the optimisation variable). As there is no constraint on the power used in the station, we suppose in the rest of this section that a gene represented by x only describes the x_i and not the p_i.

It is possible to convert the first constraint (3.10) on the SoC threshold SoC_{min} below which EV_v cannot fall into a constraint only on the SoC when EV_v drives past a charging station ($SoC_{in,i,v}$):

$$\forall i \in [\![1;\ N_{CS}]\!], \quad SoC_{in,i,v} \geq SoC_{min} \tag{3.23}$$

However, this constraint (3.23) is non-relevant for $i = 1$ since $SoC_{in,1,v}$ does not depend on the charging plan $(x,\ p)$, only on the initial $SoC_{start,v}$ that is not an optimisation variable. Thus, we focus on $i \in [\![2;\ N_{CS}]\!]$ because $SoC_{in,1,v}$ $(i = 1)$. Moreover, $SoC_{end,v}$ $(i = N_{CS} + 1)$ is also constrained by the SoC_{min} so, if we assume that $i = N_{CS} + 1$ represents the exit d_v, we should apply the constraint for $i \in [\![2;\ N_{CS} + 1]\!]$. Therefore, the constraint (3.23) can be expressed with the variables of the charging plan to be optimised (linear constraint):

$$\forall i \in [\![2;\ N_{CS} + 1]\!], \quad SoC_{in,i,v} = SoC_{start} - \sum_{k=0}^{i-1} cons_{k \to k+1} + \sum_{k=1}^{i-1} x_k \geq SoC_{min} \tag{3.24}$$

with $cons._{k \to k+1}$ the energy consumption (%) between the station CS_k and CS_{k+1}. The indice $k = 0$ corresponds to the entrance o_v so the consumption $cons._{0 \to 1}$ is the consumption between the entrance and the first station CS_1. The constraint (3.24) is represented by matrix $N_{CSCS}\ A_1$ and vector b_1 defined as follow:

$$A_1 = -\frac{1}{E_{batt}} \begin{pmatrix} 1 & 0 & \dots & \dots & 0 \\ 1 & 1 & 0 & \dots & 0 \\ \vdots & \vdots & \vdots & \dots & \vdots \\ 1 & 1 & 1 & \dots & 1 \end{pmatrix}, \quad b_1 = \begin{pmatrix} SoC_{start,v} - \sum_{k=0}^{1} cons_{k \to k+1} - SoC_{min} \\ SoC_{start,v} - \sum_{k=0}^{2} cons_{k \to k+1} - SoC_{min} \\ \vdots \\ SoC_{start,v} - \sum_{k=0}^{N_{CS}} cons_{k \to k+1} - SoC_{min} \end{pmatrix}$$

The constraint (3.11) concerning the final SoC when EV_v charges in a station can be expressed by:

$$\forall i \in [\![1;\ N_{CS}]\!] \text{ such as } x_i > 0, \quad SoC_{out,i,v} = SoC_{start} - \sum_{k=0}^{i-1} cons_{k \to k+1} + \sum_{k=1}^{i} x_k \leq 80\% \tag{3.25}$$

Therefore, the constraint (3.25) is represented by matrix $N_{CS} \times N_{CS}$ A_2 and vector b_2 defined as follow:

$$A_2 = \frac{1}{E_{batt}} \begin{pmatrix} 1 & 0 & \dots & \dots & 0 \\ 1 & 1 & 0 & \dots & 0 \\ \vdots & \vdots & \vdots & \dots & \vdots \\ 1 & 1 & 1 & \dots & 1 \end{pmatrix}, \quad b_2 = \begin{pmatrix} -SoC_{start,v} + cons_{o_v \to 1} + SoC_{max} \\ -SoC_{start,v} + \sum_{k=0}^{1} cons_{k \to k+1} + SoC_{max} \\ \vdots \\ -SoC_{start,v} + \sum_{k=0}^{N_{CS}-1} cons_{k \to k+1} + SoC_{max} \end{pmatrix}$$

In the same way, the final constraint (3.12) on $SoC_{end,v}$ according to the charging plan is represented by matrix $1 \times N_{CS}$ A_3 and scalar b_3 defined as follow:

$$A_3 = -\frac{1}{E_{batt}} \begin{pmatrix} 1 & 1 & 1 & \dots & 1 \end{pmatrix}, \quad b_3 = \left(SoC_{start,v} - \sum_{k=0}^{N_{CS}} cons_{k \to k+1} - SoC_{tar,v} \right) \tag{3.26}$$

Finally, the matrix **Aineq** and the vector **bineq** are given by the equation (3.27).

$$Aineq = \begin{pmatrix} A_1 \\ A_2 \\ A3 \end{pmatrix}, \quad bineq = \begin{pmatrix} b_1 \\ b_2 \\ b_3 \end{pmatrix} \tag{3.27}$$

The GA is a non-deterministic method, meaning we can have different final results with the same input (the initial population). This is why we need to set stopping criteria to end the GA and retrieve the best solution found so far. One of the stopping criteria is the number of iterations without significant changes to the best solution. With the GA from Matlab, we can set a **FunctionTolerance** threshold that made the "algorithm stop if the average relative change in the best fitness function value over **MaxStallGenerations** generations is less than or equal to FunctionTolerance" [108]. To avoid long computation time in case the **FunctionTolerance** threshold is not hit, we set a maximum number of iterations, **MaxGenerations**.

Another parameter of the GA is of importance: to be sure that the constraints on the SoC are taken into account, we notice after several tests that we need a low **ConstraintTolerance** threshold (for example, 1e-10).

3.4.4 . Dynamic programming

The charging plan optimisation problem can be assimilated into an optimal control problem (3.28). The state variable is the SoC of the EV because of the constraints on the SoC in (3.28) and the **control variables** are x_ω (the vector of energies charged in each station, see Section 3.9) and p_ω (the vector of charging power used in each station). The set of charging plans is noted Ω.

$$\begin{aligned} \{ x^*_\omega, p^*_\omega \} = & argmin_{(x_\omega, p_\omega) \in \Omega} DF_v(x_\omega, p_\omega) \\ & s.t.\ SoC_v \geq 15\% \\ & s.t.\ \forall\, x_i > 0, SoC_{out,i,v} \leq 80\% \\ & s.t.\ SoC_{end,v} \geq SoC_{tar,v} \end{aligned} \tag{3.28}$$

One of the usual methods to solve an optimal control problem is dynamic programming (DP) by R. Bellman [109] if the problem is divisible into sub-problems. We will explain in Appendix C how the problem is subdivided and in which order we will implement the forward and backward method of dynamic programming.

The constraint on the $SoC_{end,v}$ and the control variable x force us to keep track of the SoC evolution when the EV leaves a station (SoC_{out}).Thus, we choose to break down the problem into subproblems linked to a station, and we define the SoC when the EV leaves a station, SoC_{out}, as the **state variable**. The subproblem i is the subproblem linked to the station CS_i and returns as result for a given $SoC_{out,i}$:

- the minimum needed time $t_{trip\ min,o_v \to i}\left(SoC_{out,i}\right)$ from the beginning of the trip to have $SoC = SoC_{out,i}$ when leaving the station CS_i.
- the associated partial charging plan $(x_1, \ldots, x_i; p_1, \ldots, p_i)^*$ that enables to reach the SoC target $SoC_{out,i}$ with the minimum trip time $t_{min,o_v \to i}\left(SoC_{out,i}\right)$.

As explained in Section 3.4.1, the energy charged x_i in stations should be discretised, so we need to discretise also the SoC_{out} that depends on x_i. The whole process is depicted in Appendix C with an example.

We need the results of the previous subproblem to solve the current subproblem mostly because of the waiting time that depends on the arrival time in station . Thus, we must start the problem resolution from the beginning of the trip (**forward method**) to record the arrival time at each station according to the time spent in the previous stations.

With this dynamic programming method, the charging plan optimisation is independent of the number of charging stops (see Appendix C). There is no need to list all the possible charging plans before starting the simulation or to update information in $data_{charge}$ (see Section 3.4.2) if a change occurs for an item other than the waiting time because the change will already be updated when initialising the parameters of the optimisation.

3.4.5 . Comparison of the charging plan optimisation methods

In this part, we will only focus on the trip time minimisation in DF ($X = 0$ in (3.4)) because, as mentioned in Section 3.4.1), the charging cost is linear according to the charged energy. We take the highway of Case study 1 described in Section 3.3.3 to compare the three optimisation methods. The highway layout is described by Figure 3.8.

We create an EV_{test} going on this highway for a long-distance trip with the characteristics given in Table 3.6. To simplify the problem, we assume the charging power to be constant according to the SoC and equal to the power level delivered by the station ($P_v = p_i$).

Table 3.6: Characteristics of EV_{test}

Intrinsic parameters		Trip parameters	
Parameter	Value	Parameter	Value
C (kWh)	50	SoC_{start} (%)	85.3
$speed_{driver}$ (km/h)	130	SoC_{tar} (%)	20
ρ (kWh/km)	0.22	o, d ($\in \mathbb{B}$)	1, 9
charging coefficient $c_v()$	250	t_{start}	9:00 am

3.4.5.1 . With no waiting time

We first optimise the charging plan using the three methods without considering the waiting time (for the *no-communication strategy*). As t_{drive} does not depend on the charging plan (the optimisation variable), the fitnesses of the different solutions given in this section are the time spent in station T_{CS} ($T_{CS} = T_{charge} + T_{wait} + T_{other}$) instead of the whole trip time T_{trip}.

3.4.5.1.1 Exhaustive method

The exhaustive method gives the following charging plan with $N_{limit} = N_{min}$ and the energy discretisation step equals to 0.25 kWh: The fitness of this optimal charging plan without the

Table 3.7: Charging plan $\omega_{Ex.}$ computed with the exhaustive method and $\Delta E = 0.25$ kWh

charging station i	energy charged x_i (kWh)	$t_{in,i}$	$t_{wait,i}$ (s)	$t_{charge,i}$ (s)	$SoC_{in,i}$ (%)	$SoC_{out,i}$ (%)	p_i (kW)
1	9	09:27:42	0	624	58.9	76.9	100
3	32.25	10:42:42	0	1228.8	15.3	79.3	125
4	13.5	12:05:02	0	786	20.84	47.84	100
5	27.66	12:52:17	0	1096.61	15.28	70.6	125

driving time t_{drive} is T_{CS} = **62.26 minutes** with four stops ($N_{min} = 4$). The computation time of the optimisation part was in average 1.55 seconds, but the initialisation of $data_{charge}$ lasted 832 seconds.

As the initialisation of $data_{charge}$ is quite long, we run the same optimisation with a step equal to 0.5 kWh to reduce the computation time and summarise the results in Table 3.8.

Table 3.8: Charging plan $\omega_{Ex.}$ computed with the exhaustive method and $\Delta E = 0.5$ kWh

charging station i	energy charged x_i (kWh)	$t_{in,i}$	$t_{wait,i}$ (s)	$t_{charge,i}$ (s)	$SoC_{in,i}$ (%)	$SoC_{out,i}$ (%)	p_i (kW)
1	9	09:27:42	0	624	58.9	76.9	100
3	32	10:42:42	0	1221.6	15.3	79.3	125
4	14	12:04:55	0	804	20.84	47.84	100
5	27.41	12:52:28	0	1089.41	15.28	70.6	125

The fitness of this optimal charging plan without the driving time t_{drive} is T_{CS} = **62.32 minutes** so the EV only lost 3 seconds in station compared to the case where the energy step is more precise ($\Delta E = 0.25\ kWh$). The EV stops at the same stations as the case with more precise stops. The optimisation part lasted **216 milliseconds** and was 7 times faster than the case with $\Delta E = 0.25\ kWh$. The initialisation of $data_{charge}$ took **71,7 seconds** to complete, which is more than 10 times faster than the other case with more precise energy steps. Therefore, for the exhaustive method, a high precision on ΔE is not necessary since we gain only 3 seconds on the fitness T_{CS} with $\Delta E = 0.25\ kWh$ compared with $\Delta E = 0.5kWh$ for more than 7 times longer calculations when initialising $data_{charge}$ and optimising the charging plan. This is why, for the rest of the manuscript, we use $\Delta E = 0.5kWh$ or higher values.

3.4.5.1.2 Genetic Algorithm

With the GA method, as explained in Section 3.4.3, the result of the GA is non-deterministic contrary to the two other methods we studied in this manuscript, so the result returned by the GA might be a local minimum and not the global minimum of the objective. We have run a first optimisation with MaxGenerations = 6000, FunctionTolerance = 1e-6 and as initial population, the

solution ω_{lr} which value is given in (3.29). The result was returned in 20 seconds but corresponded to a fitness of 70 minutes which is more than the result found by the exhaustive method. We tested another combination of GA options summarised in Table 3.9. The MaxGenerations equals 6000 for all the tests.

$$\omega_{lr} = \begin{pmatrix} 0 & 9.83 & 29.94 & 31.06 & 11.58 & 0 \end{pmatrix} \tag{3.29}$$

Table 3.9: GA options, initial population and results obtained according to the optimisation parameters

Result	Function tolerance	Initial population	T_{CS} (min)	Computation time (s)	nb. iterations
1	1e-6	ω_{lr}	47.98	50.6	100
2	1e-10	ω_{lr}	70.07	20	1985
3	0	ω_{lr}	69.5	120	6000
4	0	-	62.77	116	6000
5	1e-10	-	62.6	32	985
6	0	$\omega_{Ex.}$	62.3	17	805

Table 3.10: Detailed charging plans computed with the GA method according to the GA options described in Table 3.9

Result	ω^* (kWh)
1	$\begin{pmatrix} 0 & 9.6 & 28.8 & 30.2 & 13.9 & 0 \end{pmatrix}$
2	$\begin{pmatrix} 0 & 8.9 & 31.9 & 17.1 & 24.6 & 0 \end{pmatrix}$
3	$\begin{pmatrix} 0 & 8.9 & 29.5 & 29.8 & 14.2 & 0 \end{pmatrix}$
4	$\begin{pmatrix} 10.5 & 0 & 27.8 & 16.2 & 27.8 & 0 \end{pmatrix}$
5	$\begin{pmatrix} 10.1 & 0 & 29.0 & 15.5 & 27.8 & 0 \end{pmatrix}$
6	$\begin{pmatrix} 8.9 & 0 & 32.3 & 13.5 & 27.7 & 0 \end{pmatrix}$

When the FunctionTolerance is set to 0, the algorithm only stops when the maximum number of iteration (MaxGeneration) is reached, so after 6000 iterations (approximately 120 seconds of computation). If we want to reduce the number of iteration, and so the computation times, we should set the FunctionTolerance to a non null value (for instance 1.e-10). Several results enable to have a solution after less than 50 seconds with FunctionTolerance = 1e-10.

We notice that the initial population is important too since when we initialise with ω_{lr} (results 1 to 3), the algorithm converges to solutions with high values of fitness (68, 69.5 and 70.7 minutes) and when we do not initialise the population (results 4 to 5), the algorithm finds solutions with a fitness approaching the fitness given by the exhaustive method (62.31 minutes).

The results 1 to 3 seem to have fall into a local minimum. When we give as initial population the charging plan found by the exhaustive method $\omega_{Ex.}$ (result 6), the algorithm converges to a better solution with a fitness equal to 62.25. However, this last result supposes we already know the result of the exhaustive method which is not the aim here if we want to replace the exhaustive method.

The results are very different from a running of the GA to another and the time to compute the best solution varies from 17 to 120 seconds so the GA seems to be inappropriate for the optimisation of a charging plan. Yet, this algorithm is interesting if we want to compute the best solution and to compare it with the result given by the exhaustive method.

3.4.5.1.3 Dynamic programming

We use a discretisation step of 0.5 % of SoC for the dynamic programming method. This corresponds to a SoC of 0.25 kWh ($\Delta E = 0.25\ kWh$). The charging plan given by the Dynamic method is shown in Table 3.11.

Table 3.11: Charging plan computed with dynamic programming

charging station i	energy charged x_i (kWh)	$t_{in,i}$	$t_{wait,i}$ (s)	$t_{charge,i}$ (s)	$SoC_{in,i}$ (%)	$SoC_{out,i}$ (%)	p_i (kW)
1	9.25	09:27:42	0	633	58.5	77	100
3	32.5	10:42:51	0	1236	15	80	125
4	13.5	12:05:18	0	786	21	48	100
5	28	46353.46	0	1106.4	15	71	125

The fitness of the optimal charging plan found by DP is **62.69 seconds** and the computation time is **0.26 seconds**

3.4.5.1.4 Comparison of the results

The charging plan given by the three methods are similar with the EV stopping in the same stations to charge ($CS1,\ 3,\ 4$ and 5). The energy charged in each station differs by only 0.25 kWh from one method to another. The total amount of energy charged is higher for the DP method, 83.25 kWh, against 82.41 kWh for the exhaustive method since we overestimate the consumption in the DP method for computation purposes.

Table 3.12 sums up the computation time of the different optimisation methods, the energy charged, and the time spent in station T_{CS} per solution.

We have seen in Section 3.4.5.1.1 the exhaustive method with $\Delta E = 0.5\ kWh$ is more interesting than the same method with $\Delta E = 0.25\ kWh$. In addition, the exhaustive method with $\Delta E = 0.5kWh$ gives a better fitness $T_{CS}(\omega_v^*)$ than dynamic programming with $\Delta E = 0.25\ kWh$ (62.32 seconds against 62.69 seconds). The performance of the dynamic programming is slightly outperformed by the exhaustive method because we need to round the SoC from a subproblem to another in dynamic programming and we choose to overestimate the consumption between stations, leading to a higher amount of energy to charge, E_{total}, with DP (see Table 3.12).

Moreover, the exhaustive method with $\Delta E = 0.5\ kWh$ is the fastest method to optimise the charging plan (see column "Time to optimise ω_v") even if DP method is almost as fast (0.26

Table 3.12: Comparison of the optimisation methods without waiting time

Method	Time to initialise $data_{charge}$ (s)	Time to optimise ω_v (s)	$E_{total}(\omega_v^*)$ (kWh)	$T_{CS}(\omega_v^*)$ (min)
Exhaustive ($\Delta E = 0.25\ kWh$)	832	1.55	82.41	62.26
Exhaustive ($\Delta E = 0.5 kWh$)	71.7	0.216	82.41	62.32
GA	-	17 – 116	82.4	62.25 – 70.07
DP ($\Delta E = 0.25\ kWh$)	-	0.26	83.25	62.69

seconds against 0.216 seconds). The exhaustive method is faster because the charging plan data are already listed in $data_{charge}$, and the algorithm only needs to update the waiting time and find the minimum in a list of values. However, if $\Delta E = 0.25\ kWh$, the optimisation takes longer times (1.55 seconds) since the number of waiting times to update is higher and we can assume the optimisation would be slowed down also if $\Delta E = 0.5\ kWh$ but the number of stations on the road is increased, since the number of listed charging plans would be increased too.

The time to list the data in $data_{charge}$ for the exhaustive method with $\Delta E = 0.5\ kWh$ is still quite long (71.7 seconds) even if it is feasible before going on a long-distance trip and far less than for the case with $\Delta E = 0.25\ kWh$. The use of this method is not recommended for a situation where the $data_{charge}$ has to be updated entirely regularly (for instance, in case of a traffic jam and real-life variation of SoC). For this situation, the DP Method is more advisable since it does not need the initialisation phase with the building of $data_{charge}$. Still, for the majority of the studies in this manuscript, the traffic situation is ideal, so $data_{charge}$ do not need to be updated during the simulation and, as we are optimising the charging plan of hundreds of EVs at the same time in the framework, we aim to use the method with the fastest optimisation part.

We should also mentioned that the EV we tested in this Section needs to perform at least four stops ($N_{min} = 4$) which leads to high computation time. For others EVs with $N_{min} < 4$, the computation times with the exhaustive method is significantly reduced whereas the computation time for the dynamic programming will be the same as it depends on the number of stations on the road and not on the number of stops. Consequently and as the exhaustive method is the most mature method of charging plan optimisation in our framework, we used this method for the majority of the studies even if the DP method is promising.

The Genetic Algorithm appears to be the less interesting method since it is not regular on the results returned and is slower than the two other methods in the best case (17 seconds). Even if the GA enables to find the charging plan with the best fitness among the three method (62.25 seconds), this result is obtained when initialising the GA population with the result of the exhaustive method $\omega_{Ex.}$ so this means longer computing times.

3.4.5.2 . With waiting time

Now, we test the exhaustive and the dynamic programming methods with waiting times to evaluate if the dynamic programming gives similar results compared to the exhaustive method, which is the reference method for the charging plan optimisation (see Section 3.4.2). The GA

was not tested with waiting time since we have shown in the previous section, Section 3.4.5.1.4, that the GA is outperformed by the two other methods.

The waiting time tables WTs were computed from the reservation tables R obtained for the simulation of Case study 1 with 180 EVs and FCFS communication strategy.

The result returned by the exhaustive method is detailled in Table 3.13.

Table 3.13: Charging plan computed with the exhaustive method ($\Delta E = 0.5\ kWh$) with waiting times

charging station i	energy charged x_i(kWh)	$t_{in,i}$	$t_{wait,i}$ (s)	$t_{charge,i}$ (s)	$SoC_{in,i}$ (%)	$SoC_{out,i}$ (%)	p_i (kW)
1	9	09:27:42	0	624	58.9	76.9	100
3	29.5	10:42:42	0	1149.6	15.3	74.3	125
4	32	12:03:43	0	1452	15.34	79.34	100
5	11.91	13:02:04	269.11	643.01	46.78	70.6	125

We performed the optimisation with dynamic programming and detailed the results in Table 3.14.

Table 3.14: Charging plan computed with dynamic programming (= $0.25\ kWh$)

charging station i	energy charged x_i(kWh)	$t_{in,i}$	$t_{wait,i}$ (s)	$t_{charge,i}$ (s)	$SoC_{in,i}$ (%)	$SoC_{out,i}$ (%)	p_i (kW)
1	9.25	09:27:42	0	633	58.5	77	100
3	32.5	10:42:51	0	1236	15	80	125
4	29.5	12:05:18	0	786	21	80	100
5	12	13:02:09	263.71	1106.4	47	71	125

Both methods return very similar results: the charging plans change in the same way compared with the case without waiting times (Sections 3.4.5.1.1 and 3.4.5.1.3) by charging more at station 4 (32 kWh and 29.5 kWh respectively for the exhaustive method and the dynamic programming). The waiting time in station 5 is nearly the same (269 and 263 seconds). The fitness of the exhaustive method is still slightly less than the fitness of the dynamic programming (68.96 minutes against 69 minutes). Therefore, the dynamic programming represents a correct alternative to the exhaustive method.

Highlights for the comparison of the three charging plan optimisation methods

The dynamic programming method represents a promising option for the computation of the charging plan as it does not depends on the number of stops of the charging plan and gives similar results as the exhaustive method in a feasible time (less than 1 second). Even if the optimal charging plan returned by the dynamic programming increases the trip time compared with the exhaustive method, the difference is insignificant (less than

1 minutes). For real-life application, the dynamic programming appears to be the best solution as it does not need an initialisation of the charging plan (as it is the case for the exhaustive method) and therefore can adapt more quickly to a change in the Ev's state or in the traffic.
The genetic algorithm is not adapted for both ideal cases and real-life applications.

3.5 . Conclusion

We presented in this chapter the simulation framework and the *FCFS communication strategy* we inherited from the previous thesis by J.Hassler [98]. The simulation framework is a tool to evaluate the interest of the *FCFS communication strategy*, and we will compare in the next chapter, Chapter 4, the *communication strategy* with another charging strategy, the *reservation strategy*. We also proposed some improvements to the simulation framework, such as another method for the optimisation of the charging plan with dynamic programming (Section 3.4.4) or a correction and a speeding up of the waiting time calculation (Section 3.2.2.2). We will see in the following chapters how we use the simulation framework to answer the scientific objectives of the thesis.

4 - Control of the electric vehicle fleet charging: FCFS communication or reservation strategy

In Chapter 3, we described the charging strategy controlling the charging of EVs thanks to real-time communication between EVs and charging stations. The rule at the station is set to first-come-first-served (FCFS) for this strategy. Contrary to [67], the coordination of the EV for the *FCFS communication strategy* does not rely on a consensus between EVs to choose which EVs will charge at the near station and which EVs are going to charge at the next station. The *FCFS communication strategy* is based on a non-cooperative game since each EV optimises its charging plan individually, only knowing the waiting time estimation given by the stations. The non-cooperation combined with an FCFS rule at the station does not ensure that one EV will effectively charge during the time window that minimises its trip time. Let's consider EV_1 entering the highway first and minimising its trip time if it charges in station CS_i during the time window τ. It is possible that another EV, EV_2, arrives before EV_1 in CS_i and goes past EV_1 to charge during the time interval τ. Given all those considerations, we study another strategy in this chapter, the *reservation strategy*, that enables the EVs to book time slots in advance, minimising their trip time. We will detail the steps of the *reservation strategy* before comparing that strategy to the *FCFS communication strategy* to evaluate which priority rule at stations, FCFS or reservation, will enhance the charging service the most.

Results similar to the first part of this chapter are presented in an article published in the journal Transportation Research Part D: Transport and Environment: Comparison of decentralised fast-charging strategies for long-distance trips with electric vehicles, Anastasia Popiolek, Zlatina Dimitrova, Marc Petit, Philippe Dessante [110].

In the second part, we will perform the robustness study of the best charging strategy and propose solutions to improve it if necessary.

Contents

4.1 . Changing the priority rule: the reservation strategy

4.1.1 . *Reservation strategy* description

4.1.1.1 . Priority rule

We found in the literature many references about the *reservation strategy* [20, 67, 73, 76, 87–89].

The reservation system described by [20] and in [67], if we disregard the way the optimisation of the charging plan is realised (see Section 3.1.4 in Chapter 3), looks like the *FCFS communication strategy* (Section 3.1.4) with the same priority rule in stations (FCFS). The stations do not impede the EVs from charging if they do not reserve a charging point, and the bookings evoked in those papers are, in fact, notifications sent by EVs that the stations keep in memory to estimate waiting times. J. Rezgui and D.Said [73] evoke a "pre-reservation" of charging time slots, but even if the way they describe their reservation request looks like a booking of charging time slot, the priority rules in the station seem to be based on FCFS. Indeed, the EVs are served "upon arrival" and "without delay" if a socket is available, no matter if another EV requests a charging session starting shortly after.

The reservation system described by **B. Vaidya *et al.*** in [89] enables the EVs to book ahead of-time charging sessions in stations with a priority rule set according to the order of reservation and not according to the arrival time in the station. **Bernal *et al.*** [76] consider a charging strategy based on advanced reservation, and the servers are allocated in a first-reserved-first-allocated manner. **R. Basmadjian *et al.*** [88] also focuses on strategies that rely on reservation as a priority rule.

As we want to evaluate the impact of the priority rule in stations, we choose to consider a *reservation strategy* inspired by the ones presented in [88] and detailed in [89]. R. Basmadjian *et al.* [88] defines two types of reservation systems: the **ad-hoc reservation** and the **planned reservation** (see the text box 4.1.1.1).

The different reservation strategies (priority rule)

Ad-hoc reservation: The EV v near a station books a charging session starting when the station receives the reservation. Then, v has a certain delay (for example, 20 min) to reach the station and start a charging session. During that delay, no other EV can charge at the socket booked by EV_v. After EV_v arrives, it can start its session and charge without specifying when the charging session will stop.
Planned reservation: The EV v sends in advance a reservation notification to each station i in its charging plan ω_v with its estimated arrival time $t_{arr,v,i}$ and the estimated charging time $t_{charge,v,i}$ so that each station makes a strict reservation starting from $t_{arr,v,i}$ modulo a certain waiting time and lasting $t_{charge,v,i}$. During that booked time interval, no other EV can charge on the charger blocked by the station for v.

According to R. Basmadjian *et al.* [88], the **planned reservation** is more efficient than the **ad-hoc reservation**. Moreover, the solution proposed by [89] can be assimilated to a planned reservation, so we choose to implement a *reservation strategy* with a priority rule based on **planned reservation**.

4.1.1.2 . Planned reservation

The *reservation strategy* relies on the same principles as the *FCFS communication strategy* (see Figure 4.1) except that the EVs following the *reservation strategy* can book charging time slots in advance as we have seen previously (Section 4.1.1.1). This is a decentralised strategy where each EV v individually computes the charging plan ω_v (3.2) that minimises its discontent factor DF_v (3.4) knowing the estimated waiting time according to a given arrival time in the station. The reservation order determines the priority in the station and not according to the order of arrival in the station (FCFS). That priority rule induces a different method to compute the **estimated waiting time** in the station described in Section 4.1.2.

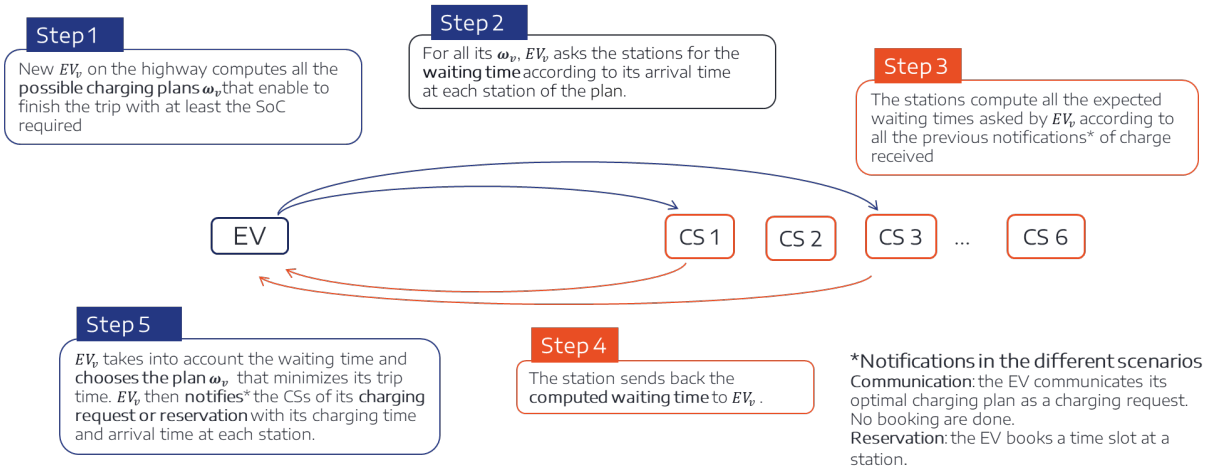

Figure 4.1: Communication scheme in the *FCFS communication and reservation strategies*

Here, we define the time notions we will use to explain the reservation steps.

Def. : Time slot and time interval for charging session (see Figure 4.2)

Time slot: noted δt is a unit of time delimited by the estimated timestamp of two events that will occur in the station. An event can be either the arrival or the departure of an EV. Thus, a time slot can be delimited by two arrival times, two departure times or one

arrival time and one departure time.
Time interval: noted τ is an accumulation of adjacent time slots δt that can be booked ahead of time for a charging session.

At every step of time t during the simulation, each $EV_v \in \mathbb{F}$ in the fleet computes the total travelling time $T_{trip}(\omega_v)$ for each possible charging plan ω_v like for the *FCFS communication strategy* (Figure 4.1). Then, the EV_v deduces the charging plan ω_v^* with the minimal discontent factor DF_v (3.4) and makes a reservation at the stations corresponding to the charging sessions listed in ω_v^* with the estimated arrival time $t_{arr,v}$ and the duration of the charging sessions $t_{charge,v}$. Then, each station that has received a notification reserves a strictly delimited time interval τ_v corresponding to the demand.

4.1.2 . Waiting queue construction and waiting time estimation

We describe in this section how the waiting queue is built and how the waiting times are estimated for the *reservation strategy*.

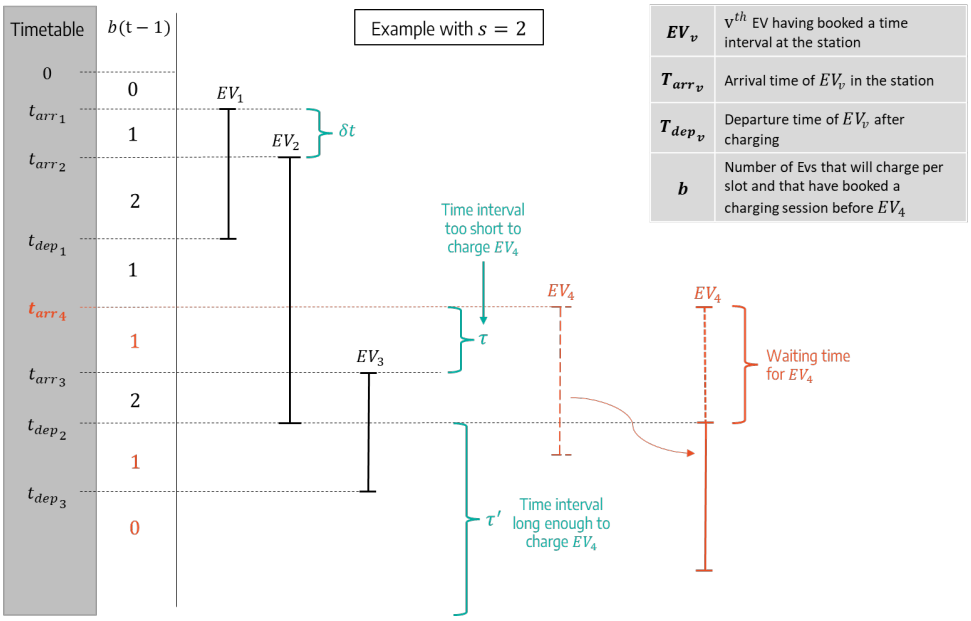

Figure 4.2: Waiting time computation schematic example for the reservation strategy

With the *reservation strategy*, when EV v is about to enter the highway (with an anticipation period lasting $T_{adv.}$), it computes its optimal charging plan ω_v^* according to the time intervals already reserved by other EVs. It sends reservation requests to the charging stations in ω_v^*, and each CS_i will book a charger for the adequate time interval $\tau_{i,v}$. For example, in Figure 4.2 representing the reservation table of CS_i, EV_4 is the 4$^{\text{th}}$ EV to enter the highway. EV_4 will enter the highway in less than $T_{adv.}$ minutes, and we are at the iteration t. EV_1, EV_2 and EV_3 have already booked a charging session at CS_i (EV_k is the k^{th} EV entering the highway). The EV_4 is the next one to make its reservation. It will reach the charging station before EV_3, so a charging socket would be free at that time ($s_i = 2$ and EV_2 will be the only one charging), but the time interval τ free before the arrival of EV_3 will not be enough to charge EV_4: EV_4 will have to book a time interval τ' at the end of EV_2's charging session.

Formally, for each possible charging plan $\omega_v \in \Omega_v$, the EV v will ask the estimated waiting time at each station. For this calculation, the station $CS_i \in \mathbb{CS}$:

- Builds a timetable listing by crescent order the arrival and departure times of each EV that has booked a charging session.
- Computes the number of bookings b in each time slot δt.
- Finds, according to the arrival time $t_{arr,v,i}$ of v, the nearest time interval τ such that for each time slot δt of that time interval, $b_{\delta t} < s_i$, and lasting enough for the EV_v to charge. If τ contains the arrival time of the EV v, $t_{arr,v,i}$, there will be no waiting time. EV v will have to wait until τ starts.

When EV_v selects the charging plan ω_v^*, the CS will similarly update all the estimated waiting times.

In an ideal situation with no traffic jams or longer charging sessions than predicted, the EVs do not change their booking during the simulation. In fact, in this situation, the first reservation made by the EVs when they enter the highway corresponds to the best charging plan they can follow, given the bookings of the other EVs on the road. Thus, all the EVs will keep their first reservations for their whole trip before entering the highway, and no EV will change its bookings. In this chapter, we hypothesise that traffic is ideal when comparing the *FCFS communication and reservation strategies*.

4.2 . Methodology of the charging strategies comparison

4.2.1 . Comparison method

We want to evaluate which real-time information-sharing charging strategy proposes the best service quality concerning the EVs' discontent factor DF minimisation (see Section 3.1.3). As in [84], we choose to consider for this case study to simplify the problem only considering the travelling time T_{trip} (3.5) in the minimisation of DF. However, we will see in Section 5.2.3.2 that the reason given in [84] to justify the consideration of only the travelling time in the objective of EV is debatable when the charging price is more than doubled on the highway (in [84] the charging cost is 0.12 $/kWh whereas on highways in Europe, it starts at 0.3 $/kWh). We also add two quality criteria described in subsection 4.2.2 to evaluate the performance of each real-time information-sharing strategy.

In addition to the comparison of the two real-time information-sharing strategies, we compare those dynamic charging strategies with the *no-communication strategy*, which represents the current charging strategy an EV can follow thanks to existing charge planning applications (A better route planner [101], Chargemap, ...). The last strategy is a reference to assess how a dynamic strategy with real-time information-sharing such as the *FCFS communication* or the *reservation strategy* can improve the current charging service proposed to EV drivers on long-distance trips.

As explained previously, we consider only the travelling time in the discontent factor for this comparison, so the aim of each EV v following either the *no-communication, the FCFS communication* or the *reservation strategies* is to minimise the travelling time (3.5) by choosing the optimal charging plan ω_v according to the processes explained in Sections 3.1.5 and 4.1.1. We use the **exhaustive method** to compute the optimal charging plan (Section 3.4.2) with only the minimum number of charging stops possible ($N_{limit} = N_{\min}$) for the first comparison (Section 4.3) and then we permit the addition of another charging stop ($N_{limit} = N_{\min} + 1$)) for the second comparison (Section 4.4.2).

The difference between the *no-communication strategy* and the two other strategies is that the EVs do not know the waiting time in the station. So we remind that for the *no-communication*

strategy, $\forall\, \omega_v \in \Omega_v$, $T_{wait}(\omega_v) = 0$. The *reservation strategy* differs from the *no-communication* and the *FCFS communication strategies* in the priority rule at stations: we have a reservation priority and an FCFS rule, respectively (see Figure 4.3).

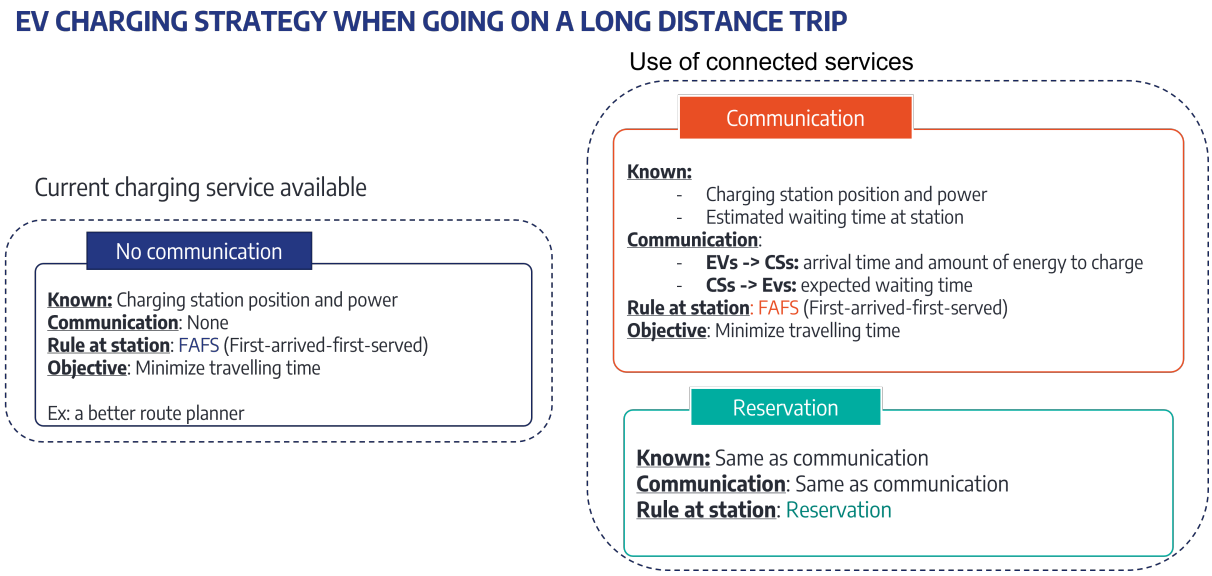

Figure 4.3: Information shared and priority rule in station according to the strategy

We use the MAS framework described in Chapter 3 to simulate the behaviour of the EVs in the fleet according to the charging strategy.

Insurance companies and the government advise drivers to stop 15 minutes every 2 hours to avoid accidents due to fatigue [111] and T_{charge} and T_{wait} represent means to satisfy the recommended pausing. This is why, to evaluate the real impact of longer charging times on the total travelling time, we compare the trip time $T_{trip,v}$ of EV v to the trip time $T_{trip_{conv,v}}$ of a conventional vehicle (ICE - internal combustion engine) making the same trip and stopping 15 minutes every 2 hours as recommended (4.1).

$$T_{trip_{conv,v}} = T_{travel,v} + T_{pause,v} + T_{other_{conv,v}} \tag{4.1}$$

$T_{pause,v}$: time equivalent to all the 15-minute stops every 2 hours.

$T_{other_{conv,v}}$: time during which the vehicle is not driving at its maximum speed, so this includes the time to stop (deceleration to enter the service area), to look for a parking lot and to accelerate when leaving the service area. We consider that if a conventional vehicle needs to refuel on the highway, as a refuelling lasts at most 5 minutes and a conventional vehicle needs to refuel less often than an EV, the time the conventional vehicle takes to wait, refuel and pay will not exceed the cumulated pausing time $T_{pause,v}$. As we include the time to start a refuelling session in $T_{pause,v}$, we set $T_{other_{conv,v}}$ to 2 minutes per stop (deceleration, acceleration and movement to a parking place).

$T_{travel,v}$ is equal for the electric and the conventional vehicle, so we technically compare $T_{charge,v} + T_{wait,v} + T_{other,v}$ with $T_{pause,v} + T_{other_{conv,v}}$.

We introduce the time loss ratio to measure the adequate time lost compared with a conventional vehicle due to longer charging and waiting times for EVs (4.2).

$$TL_{\%,v} = -\frac{T_{trip_{conv,v}} - T_{trip,v}}{T_{trip_{conv,v}}} \tag{4.2}$$

In a case the charging and waiting times together last less than the recommended breaking time $T_{pause,v}$, the result of Eq. (4.2) will be negative. To avoid that, we consider that the EV driver will stay longer in the station (by moving to a parking place during $T_{pause_{ext.,v}}$ minutes) to respect the minimum pausing time $T_{pause,v}$.

$$T_{trip,v} = T_{travel,v} + T_{charge,v} + T_{wait,v} + T_{other,v} + T_{pause_{ext.,v}} \tag{4.3}$$

With $T_{pause_{ext.,v}} = \max(T_{pause,v} - (T_{charge,v} + T_{wait,v} + T_{other,v}), 0)$

4.2.2 . Quality criteria and hypotheses

A charging strategy will be beneficial if all the quality criteria explained next are validated. The quality criteria used in this study were mentioned in a report by ACOZE France [56]. They can be formulated as follows:

Quality criteria

1. Queue length in a station should be at most twice the number of charging points.
2. Waiting time for each charging session $\leq$ 30 minutes.

The report establishes that EV drivers would rather wait in a dedicated parking place than in an informal queue, and the number of dedicated places should be at least two per charging point. As we want to set the most restrictive criterion, we consider that the number of dedicated places is equal to the minimum required, so they should be two. Concerning the charging sessions, we suppose, like in [89], they are non-pre-emptive, meaning they cannot be interrupted and started later.

We hypothesise that the EV drivers follow the indications given by the model and charge the exact amount of energy as required by the planner. No EV stays in charge more than necessary. In real life, the driver might not strictly respect the instructions and stay longer. However, introducing T_{other} when calculating the total trip time should consider this delay for other users. We also assume that once an EV starts to slow down to enter the station i in its charging plan (at $t_{in,i,v}$), it cannot change its charging plan concerning the station i and will stay in the station to charge even if the waiting queue is longer than expected. Furthermore, we suppose that the traffic is fluent with no traffic jams delaying the arrival of some EVs at a station.

We also assume that, whatever the strategy an EV follows, once an EV slows down to enter a station, it will stay in the station and charge the exact amount of energy in its charging plan even if the waiting queue is longer than expected.

4.2.3 . Case study

We consider for the comparison of the strategies (see Figure 4.4) the case study 1. The highway has six charging stations with three charging outlets each ($s_i = 3$ for CS_i) of the same power level p_i. However, the power level p_i can differ from one station to another. The charging power level can be 50, 100 or 125 kW. With a number $s = 3$ per station, the waiting queue length should not exceed $3 \times 2 = 6$ EVs as stated by the first quality criterion (see Section 4.2.2).

To test the strategies over different traffic situations, we generate three fleets, each with a different number of EVs. One fleet with **180 EVs** models the daily EV traffic on highways in France in 2021. The number of 180 EVs was calculated according to the total number of vehicles and EVs registered in France and the annual average daily traffic (AADT) on motorways in France. Argus estimated the number of all-electric passenger cars and utility vans to be 248,000 [112], and AVERE France counted 338,000 [113]. We took the average of both estimations, corresponding

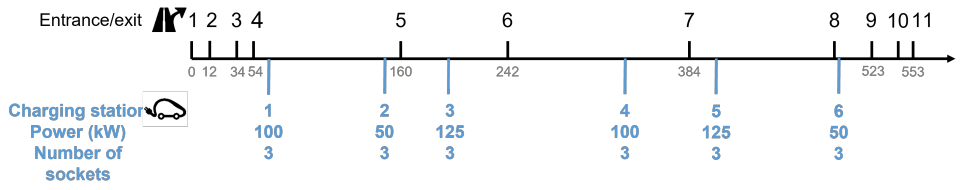

Figure 4.4: Highway description for the comparison of the charging strategies

to an all-electric vehicle share of 0.72% with 40.8 million cars licensed in France. The AADT of light-duty vehicles on French motorways was approximately 24,600 in 2017 [114], and we suppose it remains constant until 2021. We obtain a current daily traffic of $\frac{0.72}{100} \times 24,600 \approx 180$ EVs. We also generate a fleet of **100 EVs** and another with **300 EVs**.

Since we are comparing three charging strategies over three traffic situations, we have to simulate nine scenarios: one per traffic situation and a charging strategy. For one scenario, all the EVs in the fleet use the same charging strategy. We will simulate in Section 4.6 the case where EVs of the same fleet can have different strategies. We will see in Section 4.3 that, on the one hand, the scenarios with 100 EVs lead to a low saturation of the infrastructure with few EVs waiting in stations and, on the other hand, the scenarios with 300 EVs induce a heavy saturation.

The three fleets are generated in the same way. Each EV has a SoC at the entrance of the highway SoC_{start} randomly selected between 50 and 100 % and a SoC when leaving the expressway, SoC_{end}, set to 20% as in [83]. The EV time of entrance on the highway, t_{in}, is chosen according to the method explained in Appendix B.1.

Each fleet includes three types of EV to represent the diversity of EV models on the road in 2021 (see Table 4.1).

Table 4.1: Type of EVs considered in the study

EV Type	Battery capacity (kWh)	Maximum charging power $P_{max,\,v}$ (kW)	c_v	ρ_v	Speed limit (km/h)	Percentage in the fleet
urban	50	50	250	0.15	110	30%
sedan	60	100	500	0.18	130	60%
luxury	95	125	1062	0.18	130	10%

4.3 . Results of the comparison

We first compare the time loss ratio for all the scenarios in Section 4.3.1 before presenting the quality evaluation of each charging strategy in Section 4.3.2.

4.3.1 . Time loss ratio comparison

Figure 4.5 depicts the distribution in quartiles of the time loss ratio $TL_{\%}$ (4.2) for the nine scenarios studied in this chapter.

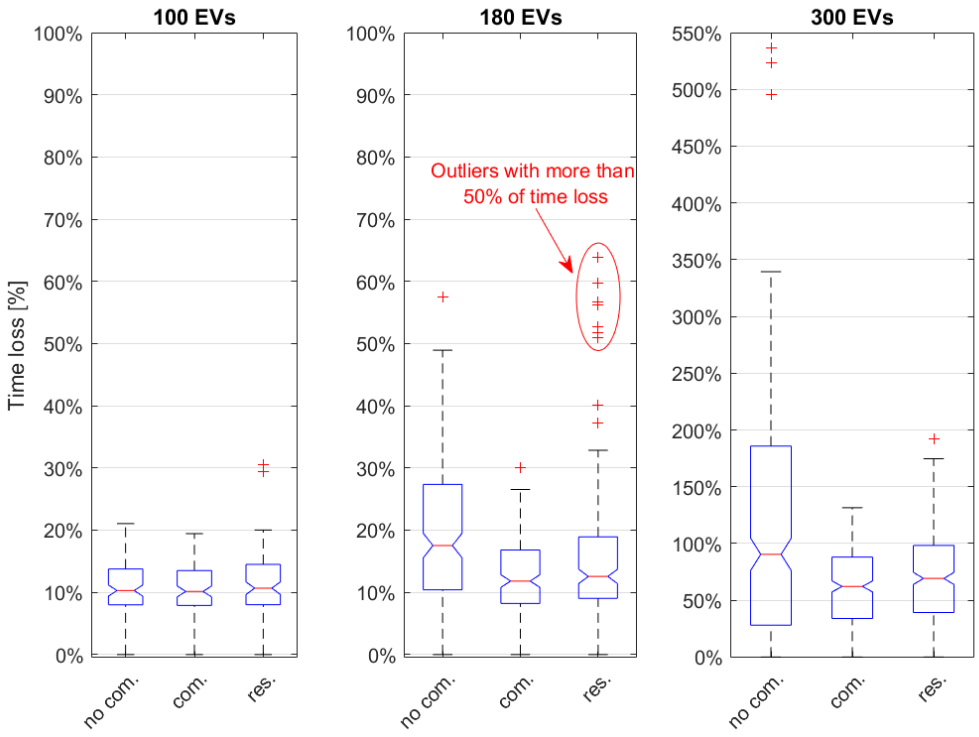

Figure 4.5: Time loss ratios $TL_{\%}$ for each strategy (no com.: no-communication, com.: FCFS communication, res.: reservation) in the different situations of traffic (**100 EVs, 180 EVs, 300 EVs**) regarding the time $T_{trip_{conv}}$ a conventional ICE vehicle would spend making the same trip. The graph corresponding to the 300-EV scenarios has a different scale for the y-axis.

The red segment on each boxplot corresponds to the median of the data set, and the red crosses point out the outliers[1] (see Figure 4.5).

Table 4.2: Average trip length and trip time T_{trip} per EV

scenario	Average trip length (km)	Average T_{trip} (h)			
		Conventional vehicle	No-communication	FCFS communication	Reservation
100 EVs	465	4h09	4h35	4h35	4h35
180 EVs	479	4h17	5h05	4h46	4h55
300 EVs	469	4h10	8h41	6h43	7h02

In the case of a 100-EV fleet, the three strategies (*no communication, FCFS communication* and *reservation strategies*) have the same median value, approximately 10.5% of time lost compared with the trip time of a conventional vehicle (Equation 4.1). This percentage is equivalent to a time loss of 26 minutes. We get the same time loss on average, which means that to make a trip of 465 km (average trip length in the 100-EV fleet), an ICE vehicle pausing as recommended ($T_{pause_{conv}}$) will take 4h 09 whereas an EV will on average spend 26 minutes more on the road

[1] An outlier is a value that is 1.5 interquartile ranges above the upper quartile (75 %) or below the lower quartile (25 %) of the distribution [115]

for the same trip length. We can wonder if those 26 minutes are reducible or not. Let's consider the average waiting time for the three strategies: it does not exceed 2 minutes for the 100-EV traffic situation (Table 4.3). Thus, this traffic situation corresponds to a light saturation of the infrastructure, and there is not much room for manoeuvre to reduce the time loss by playing on the waiting time. The time loss is primarily due to the charging time T_{charge} and T_{other} induced by the charging stops that are not compressible since the EVs need to charge to reach their destination. We evaluate the minimum charging time the fleet can have on average with the results of the scenario with *no-communication strategy*. This strategy should have the minimum average charging time compared to the other strategies since the EVs following the *no-communication strategy* minimise only the charging time and do not consider the waiting time. We have, on average per EV, the sum of T_{charge} and T_{other} equals 48 minutes (Table 4.4) with two charging stops which means that, on average, $T_{charge} = 48 - 2 \times T_{other} = 38$ minutes, a result similar to average charging time for long-distance trip in France evaluated to 30 minutes by the study in [116].

Two outliers for the scenario 100 EVs/ *reservation strategy* lose more than 30% of $T_{trip_{conv}}$ (Figure 4.5), and we will decide in Section 4.3.2.1 if those two outliers can be accepted in the performance evaluation of the *reservation strategy*.

Table 4.3: Average waiting time per EV (min)

Scenario	No-communication	FCFS communication	Reservation
100 EVs	0.97	0.63	2
180 EVs	24.53	6.34	12.83
300 EVs	245.8	124.4	143.8

Concerning the situation with **180 EVs**, the dynamic strategies (FCFS communication and reservation) enable a decrease in the time loss median compared with the *no-communication strategy*, but the more noticeable improvement is reached by the *FCFS communication strategy* with an apparent reduction of the maximum time loss from 58% to 30% compared with the *no-communication strategy* (see Figure 4.5). The *FCFS communication strategy* enables keeping the average waiting time under 4 minutes, which is four times less than for the *reservation strategy* and eight times less than for the *no-communication strategy* (Table 4.3). The *FCFS communication strategy* also proves to be efficient in reducing the trip time when we look at the average trip time. For an average trip of 479 km lasting 4h17 with an ICE vehicle, the average trip time is 4h46 for the FCFS communication, while it lasts 4h55 with reservation and 5h06 without communication. Although the *reservation strategy* reduces the median time losses and average trip

Table 4.4: Average $T_{charge} + T_{other}$ per EV (min)

Scenario	No-communication	FCFS communication	Reservation
100 EVs	47.97	47.99	48
180 EVs	48.16	48.81	49.3
300 EVs	47.73	50.21	50.64

time compared with the no-communication strategy, multiple outliers see their $TL_{\%}$ increase to more than 50% for this strategy (Figure 4.5), which is worse than for the scenario of reference without real-time information-sharing.

For the scenarios with the **300-EV fleet**, the infrastructure is highly saturated with an exploding time loss for all the strategies (Figure 4.5). However, real-time information-sharing strategies drastically reduce median and average time losses (Table 4.2). FCFS communication saves on average 43.5% of time losses compared with reference strategy, and reservation saves 36.5% (Table 4.2). Again, the *FCFS communication strategy* has the best performance and also guarantees a maximum time loss of 150% (Figure 4.5) contrary to the *reservation strategy* that reaches almost 200%.

4.3.2 . Quality evaluation

4.3.2.1 . Light saturation (100 EVs)

According to the results presented in Section 4.3.1, the traffic with **100 EVs** results in a low saturation of the charging infrastructure. We can come to the same conclusion when we look at the queue length for the *no-communication strategy* on Figure 4.6: at most, two EVs wait concurrently when there is no communication. Therefore, as the EVs hardly wait and are not coordinated (no-communication strategy), the charging infrastructure is adapted to a traffic flow of 100 EVs daily.

From Figure 4.6, all the charging strategies validate the **first criterion** (Section 4.2.2) since for each of them, the queue is never exceeding the queue length threshold of 6 EVs waiting simultaneously in the same station.

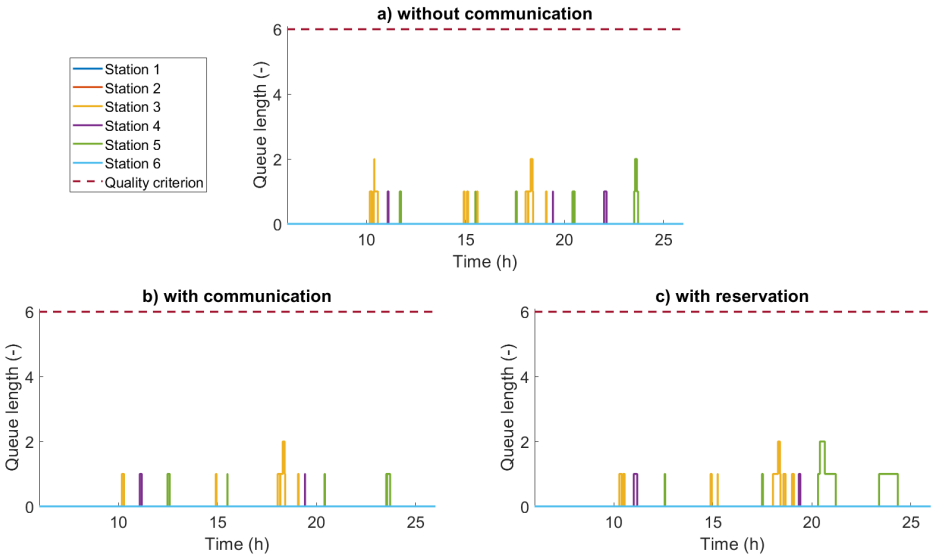

Figure 4.6: Length of the waiting queue in each station throughout the day for the 100-EV fleet according to the strategy. The dashed curve illustrates the first quality criterion.

The **second criterion** can be verified thanks to Figure 4.7 depicting for each strategy the cumulative waiting time distribution of the fleet. The y-axis gives the share of EVs in the fleet waiting less than the x-amount of time in a station. The **second criterion** is validated if the curve stays on the left side of the dashed curve representing the quality threshold of 30 minutes since this case means that the share of EVs waiting more than 30 minutes before charging is null. In the scenario with *no-communication strategy*, the **second criterion** is validated (Figure 4.7a), whereas the EVs are not coordinated. Although the *FCFS communication strategy* enables

some EVs to save a few minutes and fulfils the **second criterion** (Figure 4.7b), this strategy is of little use in this situation of light saturation because the *no-communication strategy* is already enough to fulfil the second quality criterion. However, the *reservation strategy* makes 2 EVs wait for nearly twice as much as the waiting time threshold in station 5 (Figure 4.7c), whereas the charging infrastructure is very lightly saturated. Those 2 EVs correspond to the outliers we have seen in Section 4.3.1 and, because of the high waiting times experienced by those vehicles, we choose to consider that the *reservation strategy* invalidates the **second criterion**.

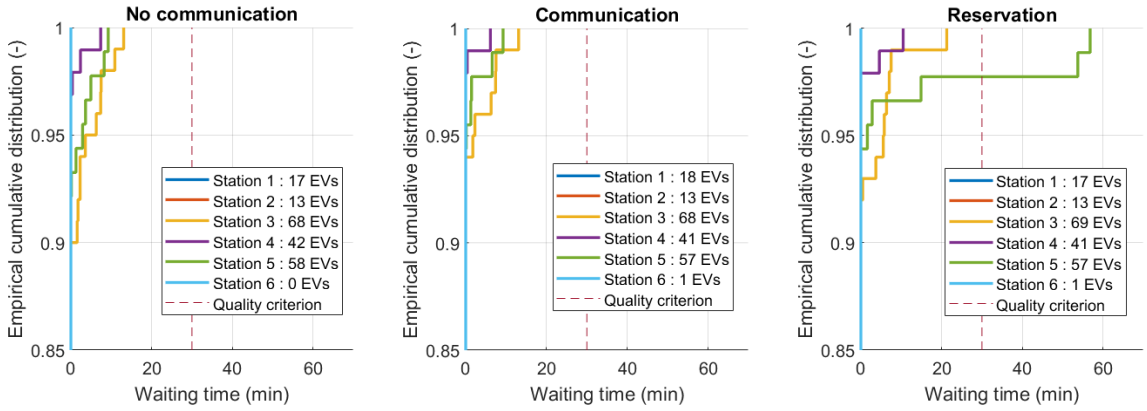

(a) without communication (b) with FCFS communication (c) with reservation

Figure 4.7: Cumulative distribution of waiting time in each station for the 100-EV fleet. The dashed line illustrates the second quality criterion.

Highlights for the light traffic situation

As an intermediate conclusion, using the *FCFS communication strategy* is unnecessary for this light saturation situation since the strategy of reference without communication validates all the quality criteria. The *reservation strategy* penalises some EVs with high waiting time and consequently does not fit with the performances we defined for the service quality.

4.3.2.2 . Average traffic (180 EVs)

We now compare the strategies over a situation corresponding to the average EV daily traffic in 2021 (**180 EVs**). With the *no-communication strategy*, station n°3 saturates at some hours (Figure 4.8a) with more than 6 EVs in the queue between 3:00 pm and 8:00 pm. The third station saturates mostly because it has the highest available power (125 kW), so the EVs select this station to charge faster and supposedly reduce their travelling time. This station is also in the middle of the highway, so it is more likely to be on the path of EVs, contrary to stations at the ends of the highway. The other stations do not experience much saturation, with queue length staying under 4 EVs during the day. The *strategy of FCFS communication* reduces by three the maximum queue length in station 3 and keeps the queue under 6 EVs for all the stations (Figure 4.8b). The *FCFS communication strategy* validates the first quality criterion. With the *reservation strategy*, the first quality criterion is also validated, the waiting queue being always under six EVs (Figure 4.8c), but the performance of the FCFS communication model is slightly better with fewer EVs waiting in the queue. For this **first criterion**, we can see the advantages enabled by a dynamic charging strategy in the case of moderate saturation of the charging infrastructure.

Concerning the second quality criterion, we have represented each station's cumulative distribution of waiting time (Figure 4.9). For the *FCFS communication strategy*, 2 EVs are waiting

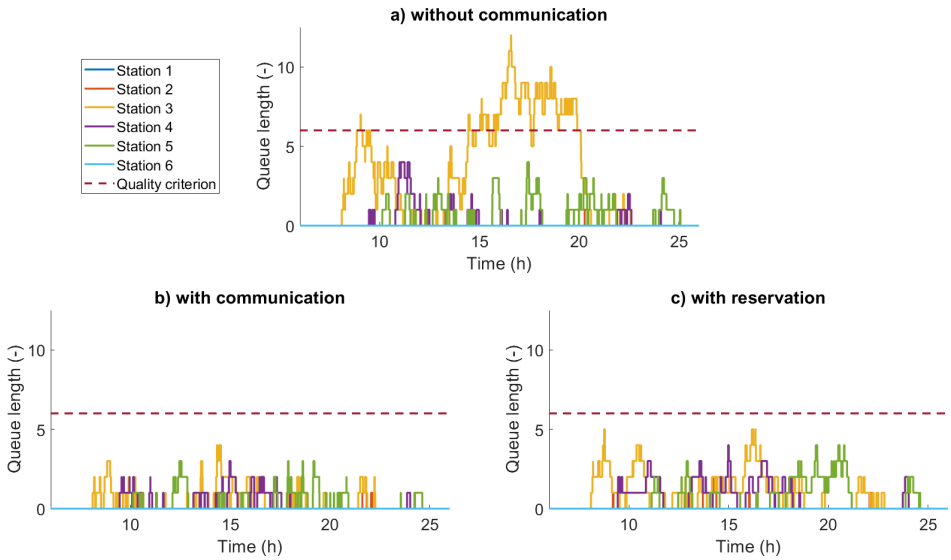

Figure 4.8: Length of the waiting queue in each station throughout the day for the **180-EV fleet** according to the strategy. The dashed curve illustrates the first quality criterion

longer than the accepted time limit of 30 minutes (Figure 4.9b), but since the waiting time is only a few minutes longer (respectively 2 and 5 minutes) than the threshold, we choose to consider that the *FCFS communication strategy* validates this criterion. We will see in Section 4.4.2 that this choice is relevant. On the contrary, when reservations are made possible (Figure 4.9c), 15% of the fleet waits more than 30 minutes before charging, with some EVs experiencing two to almost four times the maximum acceptable waiting time. The *reservation strategy* does not validate the **second criterion**. We will explain in Section 4.4 the reason for those long waiting times and give propositions to improve the performance of the *reservation strategy*.

However, we notice that the *reservation strategy* is beneficial for the EVs entering the highway first since they can secure charging sessions by booking time intervals before other EVs reach the station and take the slots as it can happen with the *FCFS communication strategy* (first-come-first-served basis). In fact, contrary to the *strategy with FCFS communication*, EVs never change their charging plan during the trip because if no perturbation occurs on the road, their first reservations correspond to the combination of time slots that best minimise their travelling time, knowing all the reservations already done. Nevertheless, with that strategy, the later an EV enters the highway, the higher the risk is for this EV to experience waiting time as the number of available best-suited time intervals is going down.

According to Figure 4.9, *FCFS communication* and *reservation* better balance the vehicle flow over the stations with fewer EVs charging at the most saturated station, station 3 (130 EVs without communication and less than 110 EVs with FCFS communication or reservation). We can point out that station 6 is used in the *FCFS communication* and *reservation strategies* while no EV stops there with no communication. Both dynamic strategies increase the use rate of the whole infrastructure. However, the *FCFS communication strategy* is more interesting since it reduces the maximum waiting time in each station, contrary to the *reservation strategy*.

Highlights for the average traffic situation

Thus, as the *reservation strategy* does not validate the second quality criterion with higher time losses for some outlier EVs (see Figure 4.5), the *FCFS communication strategy* represents the best choice for this traffic situation.

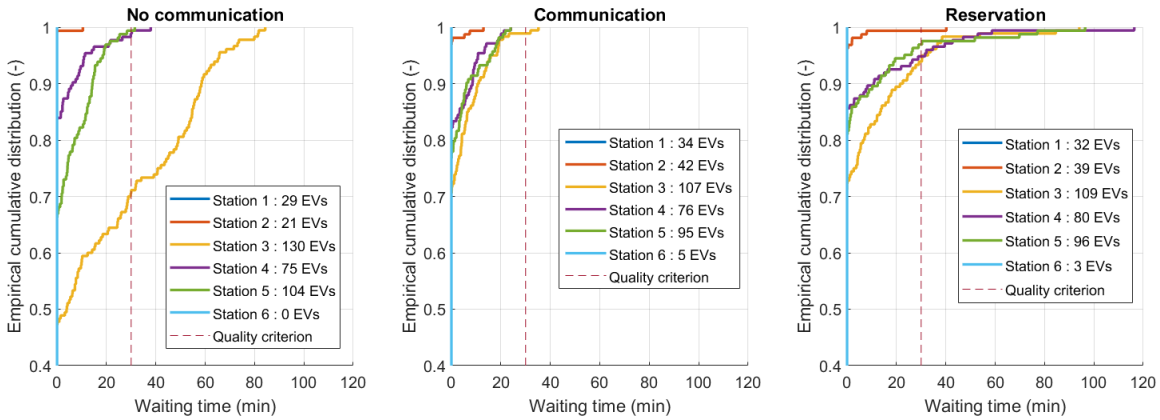

(a) without communication (b) with FCFS communication (c) with reservation

Figure 4.9: Cumulative distribution of waiting time in each station for the fleet of **180 EVs**. The dashed line illustrates the second quality criterion.

4.3.2.3 . Heavy saturation (300 EVs)

Suppose we raise the number of EVs during a day to 300. In that case, we already observe a significant saturation of the charging infrastructure (see Figure 4.10), whereas the number of EVs is not even doubled compared with the previous traffic case. *FCFS communication and reservation strategies* highly improve the situation for the EV drivers, dividing by almost three the queue length in station 3 compared with the *no-communication strategy*. Still, the queue length for both dynamic strategies reaches high values (25 EVs > 6 EVs) throughout most of the day, invalidating the first quality criterion.

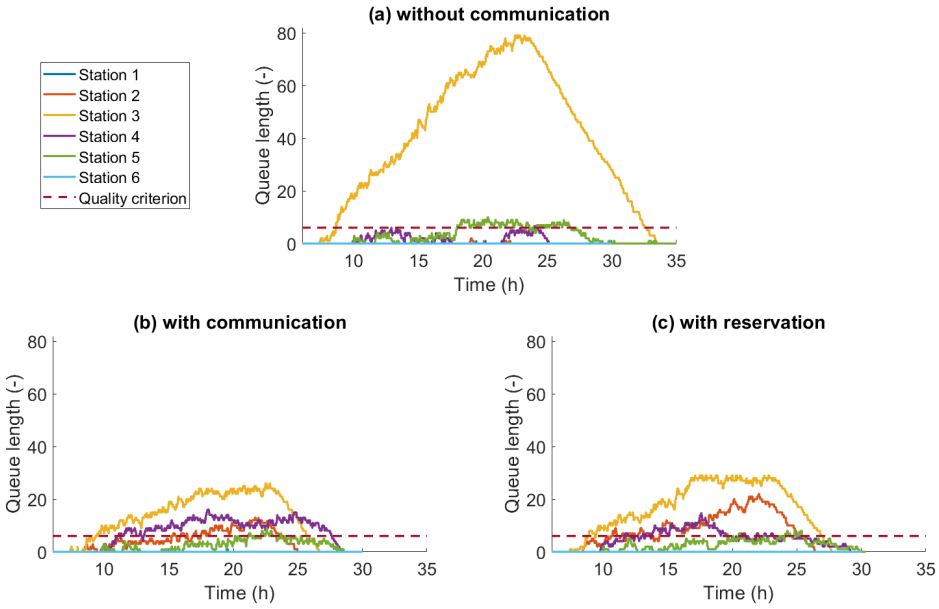

Figure 4.10: Length of the waiting queue in each station throughout the day for the 300-EV fleet according to the strategy. The dashed curve illustrates the first quality criterion

The second quality criterion is also not fulfilled with either *FCFS communication* or *reservation strategy* (see Figure 4.10b & 4.10c) even if the studied dynamic strategies enable to reduce the waiting time in station 3 drastically (Table 4.3). This reduction in trip time is made possible by better allocating the EV fleet to the whole infrastructure instead of overloading station 3. In

fact, with *FCFS communication* and *reservation strategies*, one-third of the fleet is dispatched from stations 3 and 5 to the other stations. In return, the waiting time in stations 2 and 4 is far more significant than for the *no-communication strategy*.

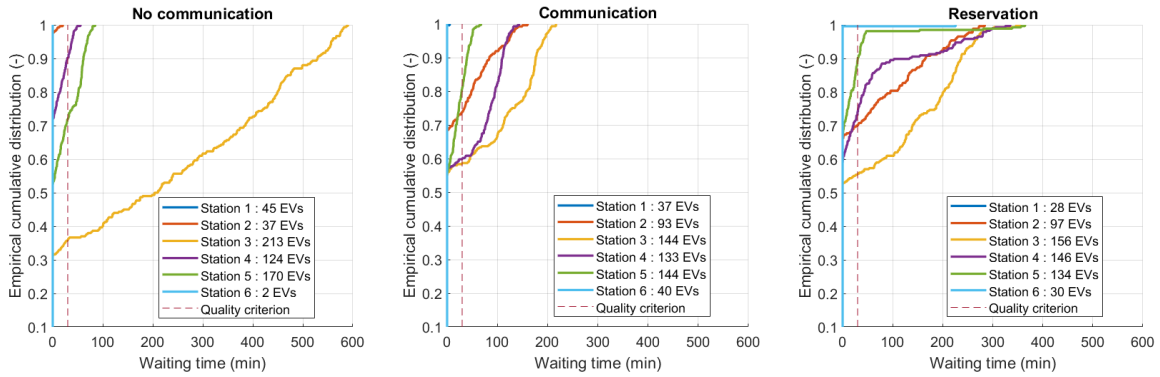

(a) without communication (b) with FCFS communication (c) with reservation

Figure 4.11: Cumulative distribution of waiting time in each station for a fleet of 300 EVs

Still, even if the *FCFS communication strategy* (and to a minor extent the *reservation strategy*) helps reduce the trip time and better allocate the EVs to the whole infrastructure, the highway service areas will probably not be able to handle the maximum queue length of 25 EVs (Figure 4.10b & 4.10c).

Highlights for the heavy traffic situation

Thus, the enhancement of the charging service with either FCFS communication or reservation is limited. We must find other solutions to complete those dynamic charging strategies, such as adding new charging points (at station 3, for example) to satisfy the quality criteria in this heavy traffic situation. We will see in Chapter 5 how we can optimise the infrastructure when the EVs use the *FCFS communication strategy* to plan their trip.

4.3.3 . Highlights on the comparison of the different strategies with $N_{limit} = N_{min}$

Table 4.5 sums up the performance results of each strategy considering the traffic situation.

With poor saturation of the charging stations (**100 EVs**), the *FCFS communication* and the *reservation strategies* hardly enhanced the situation for EVs because the quality criteria asked by the drivers are already fulfilled with a *strategy of no communication*. The charging infrastructure is adapted for this traffic flow, so users already experience very few waiting times when they do not use any coordination. The *reservation strategy* invalidated the quality criterion based on station waiting time, leading to a worse situation than a *strategy with no communication*. Consequently, both dynamic strategies appeared to be of little use with low saturation of the charging infrastructure.

If we consider a moderate infrastructure saturation, like in the second situation with daily average traffic flow (**180 EVs**), FCFS communication between EVs and stations validates both waiting queue length and waiting time quality criteria. The *FCFS communication strategy* improves EVs' charging experience by fairly balancing the fleet over the whole charging infrastructure. On the contrary, the *reservation strategy* shows less attractive performances by invalidating the waiting time criterion with EVs waiting more than one hour and a half, which is worse than when EV drivers do not communicate. Yet, the results obtained for the *reservation strategy* should be considered carefully as the framework imposes some limits that penalise this strategy and that

Table 4.5: Performance results of each charging strategy (no communication, FCFS communication and reservation) for the three traffic situations. A check mark means that the strategy for the described saturation validates the quality criterion; conversely, a cross means the criterion is not validated.

		No communication		FCFS communication		Reservation	
		1st criterion	2nd criterion	1st criterion	2e criterion	1st criterion	2e criterion
Low saturation 100 EVs	Time loss	+30 min		+30 min		+30 min	
	Quality criteria	✓	✓	✓	✓	✓	✗
Medium saturation 180 EVs	Time loss	+50 min		+35 min		+40 min	
	Quality criteria	✗	✗	✓	✓	✓	✗
High saturation 300 EVs	Time loss	+4h35 min		+2h35 min		+2h55 min	
	Quality criteria	✗	✗	✗	✗	✗	✗

we will expose in Section 4.4.1. However, with the current framework, the *FCFS communication strategy* is the best solution to reduce travelling time and increase EVs' acceptability without building new charging sockets.

With a high saturation level for the charging infrastructure (**300 EVs**), *FCFS communication and reservation* improve the situation for EV drivers compared with the *no-communication strategy*. Indeed, the trip time is reduced on average by 42% with the *reservation strategy* and 52% with the *FCFS communication strategy*. However, those dynamic strategies need to be revised to fulfil the quality criteria set by the drivers. We should consider installing new charging points besides developing one of the dynamic charging strategies to meet them (see Chapter 5).

4.4 . Limitations of the *reservation strategy*

4.4.1 . Reasons why the reservation does not validate the waiting criterion

We pointed out in the previous subsections (of the Section 4.3) that, for the *reservation strategy*, some EVs were experiencing high waiting times compared to the rest of the fleet, which led to the invalidation of the **second criterion** for this strategy. Those significant waiting times can be explained either by the conditions of the EV when entering the highway or by the model's limits in the framework. For instance, EVs with a low SoC (around 50%) when entering the highway must stop at the first station they are passing by, even if there is a long waiting time. Indeed, their SoC will go under 15% if they try to reach another station, and the simulation model does not allow this (see the first constraint in Equation 3.9). Concerning the limit of the model, we use the exhaustive method (Section 3.4.2) to optimise the charging plans with several charging sessions restrained to the minimum ($N_{limit} = N_{min}$) so the adaptability of EVs charging plans is reduced by removing interesting charging combinations with more stops than the minimum required. The absence of these possible solutions means that some EVs wait longer than they would if they could spread the energy required for charging over a larger number of stations. We could have added the possibility for EVs to book in the same station time slots that are not adjacent to avoid EVs waiting in front of free sockets because their charging time $t_{charge,v}$ does not fit into the time interval during which the socket is free. However, adding this possibility would have made some EVs have very fragmented charging sessions, with multiple going and comings between the chargers and the free parking places to let other EVs that have booked earlier charge.

Thus, we should consider in the model the possibility of having charging plans in Ω_v with more charging stops than the minimum required ($N_{limit} \geq N_{min}$) to see if the performances of the *reservation strategy* can approach the ones of the *FCFS communication strategy*, but this would mean that some EVs will have to stop more often than necessary and risk having a highly fragmented trip with many stops. Moreover, if we authorise more charging stops for the *reservation strategy*, we should also authorise it for the *FCFS communication strategy*. Consequently, the performances of the *FCFS communication strategy* might also outperform the ones of the *reservation strategy*. In addition, the *reservation strategy* will unlikely reach the lowest waiting time average for the fleet contrary to the *FCFS communication strategy* because the first EVs to reserve charging time slots do not take into account the attendance in the station since the reservation will guarantee no waiting time for them. With the *FCFS communication strategy*, all EVs are compelled to consider the waiting time in stations since the priority in the stations is FCFS: they will fan out more evenly by themselves among stations to avoid long waiting files. To have more precise ideas on that possibility, we will test in the next section, Section 4.4.2, the effect on charging strategies of having the possibility to add one charging stop to the charging plan.

4.4.2 . Comparison of the strategies with a possible additional stop, $N_{limit} = N_{min} + 1$

In this subsection, we enable the EVs with $N_{min} \leq 2$ to have in their charging plan an additional charging stop so, for those EVs, $N_{limit} = N_{min} + 1$ (see Section 3.4.2). To evaluate the effect on the trip time of authorising one additional charging stop, we verify the **second criterion** for all the charging strategies in the scenario with 180 EVs in the fleet. The case study is the same, except EVs can have an extra stop in their charging plan.

We obtain Figure 4.12 after the simulations. We notice that the *reservation strategy* still leads some EVs to wait for more than the waiting time threshold even if the waiting time for those EVs is reduced compared to the situation with $N_{limit} = N_{min}$ (see Figure 4.9). The maximum waiting time peak is reduced by almost 30%, and the average waiting time is decreased from nearly 13 minutes to less than 7 minutes (see Figures 4.9c and 4.12c). However, this is not enough to validate the **second criterion**.

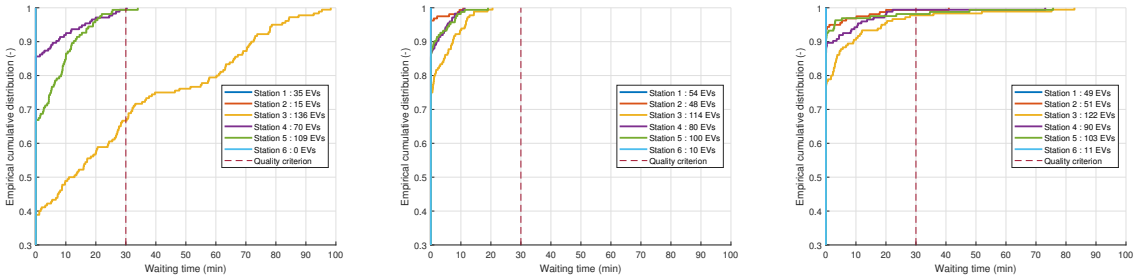

(a) without communication (b) with FCFS communication (c) with reservation

Figure 4.12: Cumulative distribution of waiting time in each station for the fleet of 180 EVs. The dashed line illustrates the second quality criterion.

As foreseen in Section 4.4.1, the *FCFS communication strategy* still performs best compared to the other strategies with an even lower waiting time maximum: it decreases from 35 to 22 minutes. However, as we test the effect of adding a charging stop in only one situation, we cannot conclude that adding a stop in the charging plan is always beneficial for the whole fleet. Still, we can state that the number of stops allowed influences the global performances of a real-time information-sharing strategy.

However, although the performances of the *FCFS communication and reservation strategies* are improved with the possibility of an additional charging point, the *no-communication strategy* does not benefit from that possibility. The proportion of EVs waiting in station 3 is increased: 60% of the EVs charging at station 3 are waiting compared with 50% in the case "$N_{limit} = N_{\text{min}}$" (Figures 4.9a and 4.12a). Moreover, the waiting time maximum rises by 25% from 80 minutes to 100 minutes. This might be due to the higher number of charging sessions in station 3 (6 EVs in addition compared with the case "$N_{limit} = N_{min}$).

Highlights on the strategies comparison with an additional charging stop (N_{limit}=N_{min}+1)

The possibility to add a stop to the minimal number of required charging stops improves the performances of the *FCFS communication and reservation strategies* concerning the waiting time. However, those improvements are insufficient for the *reservation strategy* that still invalidates the second quality criterion.

4.5 . Overall highlights on the comparison of the FCFS communic-

ation strategy and the reservation strategy

In this chapter, we studied the interest of two charging strategies relying on real-time information-sharing between EVs and charging stations and decentralised charging plan optimisation. Both strategies, *FCFS communication* and *reservation strategies*, appear to be a way to reduce, **on average**, the total travelling time for EV drivers on a long-distance trip without adding new charging points. They lead to more efficient use of the charging infrastructure.

We have studied the strategies' performance over three different traffic flow situations thanks to a MAS framework to evaluate the limits of the *FCFS communication* and *reservation strategies*. For each traffic flow situation, we have compared the performances of the real-time information-sharing strategies regarding a strategy of reference (no-communication) when EVs cannot communicate their charging plan or book charging time slots.

When the infrastructure was lightly saturated (**100 EVs**), the quality criteria were already fulfilled by the reference strategy without communication, so the dynamic strategies such as the FCFS communication and reservation strategies are unnecessary. The *reservation strategy* even made the situation worse for 1% of the fleet compared with the *no-communication strategy*.

For daily average traffic (**180 EVs**), the *FCFS communication strategy* validated all the quality criteria and proved to be efficient in the improvement of EV drivers' travelling experience as the strategy of reference did not validate any of the criteria in this situation. The *reservation strategy* effectively reduced the waiting queue throughout the day but had bad performances concerning the second criterion, with EVs waiting far more than 30 minutes before charging.

The last situation with **300 EVs** on the highway represented a day with a high saturation of the charging infrastructure. Even though the FCFS communication and reservation strategies fanned out the fleet more evenly over the highway's different charging stations, none validated a quality criterion. This situation pointed out the limit of the real-time information-sharing strategies studied in this chapter, and we will see in Chapter 5 other solutions to complement and support the use of a real-time information-sharing strategy.

As the *reservation strategy* never validates the quality criterion based on the waiting time, we proposed to add a charging stop in the EVs' charging plan to improve the *reservation service* quality. To compare the strategies with the same hypothesis, we tested the three strategies when EVs can stop at an additional charging station. This possibility reduces the waiting time maximum and average for the *FCFS communication and reservation strategies*, but this was not enough for the *reservation strategy*, which still invalidates the second quality criterion. **The *FCFS communication strategy* appears to be the best charging strategy with a priority rule based on FCFS**. Moreover, according to ACOZE [56], the possibility to reserve a charging session should not be considered as it brings more complexity and reduces the use rate of the infrastructure (as we have seen in the Section 4.3). The reservation could also create conflict and frustration.

Consequently, we choose to use as optimal control of the fleet the *FCFS communication strategy* for the next chapters.

The results obtained for this study show that the *FCFS communication strategy* enables to improve the global situation of EV drivers going on long-distance trips. Yet, we made the hypothesis that the traffic is fluent, and we did not take into account traffic incidents in the simulation, such as traffic jams, that can delay the arrival of some EVs in a station. However, as the *FCFS communication strategy* is based on dynamic scheduling, we expect EVs to adapt to traffic changes by updating their charging plans. We will test the robustness of the *FCFS communication*

strategy in the next section, Section 4.6.

4.6 . Robustness study of the fleet control

We have seen in the previous sections that the rule of the first-arrived-first-served (FCFS) is better than the reservation when the EVs communicate. Now, we want to evaluate the robustness of the FCFS communication strategy. We will see how the EVs following the *FCFS communication strategy* react to the introduction of disturbers in the fleet that do not communicate (following the *no-communication strategy*).

4.6.1 . Introduction of disturbers in the fleet

4.6.1.1 . Disturbers definition

The disturbers are EVs going on long-distance trips and using the charging infrastructure but not communicating with the charging stations. They follow the *no-communication strategy* and may disturb the real-time coordination of other EVs that share information with the infrastructure. We want to evaluate the impact of different percentages of disturbers in a fleet.

Disturber definition

Disturber: An EV following the *no-communication strategy* whereas other EVs in the fleet follow the *FCFS communication strategy*

When entering a charging station, we hypothesise that the disturbers indicate to the station the time they will spend charging: this is a strong hypothesis but feasible in reality. We assume that once an EV (whether a disturber or not) slows down to enter a station, it will stay in the station and charge the exact amount of energy in its charging plan, even if the waiting queue is longer than expected.

4.6.1.2 . Case study and notations

The case study is based on a medium saturation (180 EVs) from Section 4.3.2.2 with the same fleet. We run 100 simulations with the simulation framework for each percentage of disturbers $x_{dist.}$. For one simulation, the disturbers are selected randomly among the 180 Evs of the fleet according to the percentage of disturbers $x_{dist.}$: for instance, if $x_{dist.} = 10\%$, we randomly select 18 EVs in the fleet and run a simulation with those 18 EVs as disturbers and the other EVs using the FCFS communication strategy. The EV's characteristics remain unchanged (same intrinsic and trip characteristics). Since the addition of a charging stop to the minimum number of stops ($N_{limit} = N_{min}$) improves the quality of the FCFS communication strategy (see Section 4.4.2), we keep this parameter for the simulations in this section.

We note $F_{x,f}$ the f^{th} fleet tested with $x\%$ of disturbers. $T_{CS}(v_{x,f})$ is the total time spent in stations (charging + waiting time + T_{other}) by EV_v in the situation described by the fleet $F_{x,f}$. Similarly, $T_{CS}(v_0)$ is the total time spent in stations by this same EV_v in the situation without disturbers ($x = 0\%$). The **relative additional time spent in stations by EV_v in the fleet $F_{x,f}$ (or time loss)** compared with the FCFS communication scenario ($x = 0$) corresponds to:

$$\Delta T_{CS}(v_{x,f}) = \frac{T_{CS}\left(v_{x,f}\right) - T_{CS}\left(v_0\right)}{T_{CS}\left(v_0\right)} \tag{4.4}$$

We note $\Delta T_{CS}\left(F_{x,f}\right)$ the **average relative additional time spent in stations by the EVs**

of the fleet $F_{x,f}$ (4.5).

$$\Delta T_{CS}(F_{x,f}) = \frac{1}{N_{EV}} \cdot \sum_{v_{x,f} \in F_{x,f}} \Delta T_{CS}\left(v_{x,f}\right) \tag{4.5}$$

As we want to assess the robustness of the FCFS communication strategy to the introduction of disturbers, we also look at the **average ΔT_{CS} of the FCFS communication users** for the situation given by the fleet $F_{x_{dist.},f}$. We note this relative additional time $\Delta T_{CS}(F_{x_{dist.},f,com.})$ (4.10) with $F_{x_{dist.},f,com.}$ the part of the fleet $F_{x_{dist.},f}$ containing only the communicating EVs.

$$\Delta T_{CS}(F_{x_{dist.},f,com.}) = \frac{1}{(1 - x/100) \cdot N_{EV}} \cdot \sum_{EV_v \in F_{x_{dist.},f,com.}} \Delta T_{CS}\left(v_{x_{dist.},f}\right) \tag{4.6}$$

In addition, we compute the average relative additional time spent in stations by an EV when it communicates and when it is a disturber according to the percentage of disturbers: $\Delta T_{CS,com.}(v_x)$ (4.7) and $\Delta T_{CS,no\ com.}(v_{x_{dist.}})$ (4.8).

$$\Delta T_{CS,com.}(v_{x_{dist.}}) = \frac{1}{\sum_{f=1}^{100} card\left(F_{x_{dist.},f,com.}\right)} \cdot \sum_{f \in [\![1,100]\!] | EV_v \in F_{x_{dist.},f,com.}} \Delta T_{CS}\left(v_{x_{dist.},f}\right) \tag{4.7}$$

$$\Delta T_{CS,no\ com.}(v_{x_{dist.}}) = \frac{1}{\sum_{f=1}^{100} card\left(F_{x,f,no\ com.}\right)} \cdot \sum_{f \in [\![1,100]\!] | EV_v \in F_{x_{dist.},f,no\ com.}} \Delta T_{CS}\left(v_{x_{dist.},f}\right) \tag{4.8}$$

Finally, we note $\overline{\Delta T}_{CS,x}$ the average relative additional time spent in stations per EV according to the percentage of disturbers, $\overline{\Delta T}_{CS,x,com.}$, the average relative additional time spent in stations per EV when they communicate according to the percentage of disturbers and $\overline{\Delta T}_{CS,x,no\ com.}$, the average relative additional time spent in stations per EV when they are disturbers according to the percentage of disturbers (4.11).

$$\overline{\Delta T}_{CS,x_{dist.},com.} = \frac{1}{N_{EV}} \cdot \sum_{v=1}^{N_{EV}} \Delta T_{CS,com.}\left(v_{x_{dist.}}\right) \tag{4.9}$$

$$\overline{\Delta T}_{CS,x_{dist.},no\ com.} = \frac{1}{N_{EV}} \cdot \sum_{v=1}^{N_{EV}} \Delta T_{CS,no\ com.}\left(v_x\right) \tag{4.10}$$

$$\overline{\Delta T}_{CS,x_{dist.}} = \frac{1}{100} \cdot \sum_{f=1}^{100} \Delta T_{CS}\left(F_{x_{dist.},f}\right) \tag{4.11}$$

$$\tag{4.12}$$

Note that the average of $\Delta T_{CS}(F_{x_{dist.},f})$ (4.5) for a share of disturbers $x_{dist.}$ is $\overline{\Delta T}_{CS,x_{dist.}}$ (4.11) and the average of $\Delta T_{CS}(F_{x_{dist.},f,com.})$ (4.10) is $\overline{\Delta T}_{CS,x_{dist.},com.}$ (4.11).

4.6.1.3 . Results

Figure 4.13a depicts the distribution of the average relative additional time spent by the users of the FCFS communication strategy in the station, $\Delta T_{CS}(F_{x_{dist.},f,com.})$, compared with the situation without disturbers (4.10). The time spent in stations we take as a reference for the situation without disturbers (0%) is given in Section 4.4.2 when all the EVs communicate (FCFS communication strategy) and $N_{limit} = N_{min} + 1$ if $N_{min} \leq 2$. We also plot the distribution of $\Delta T_{CS}\left(F_{x_{dist.},f}\right)$ corresponding to the average relative additional time spent in stations by all the EVs in the situation described by the fleet $F_{x_{dist.},f}$ (see Figure 4.13b).

According to Figure 4.13a, the average relative additional time spent in stations per EV communicating, $\overline{\Delta T}_{CS,x_{dist.},com.}$, over all the simulations, is linear according to the disturber percentage. Hence, the performances of the FCFS communication strategy are slowly downgraded

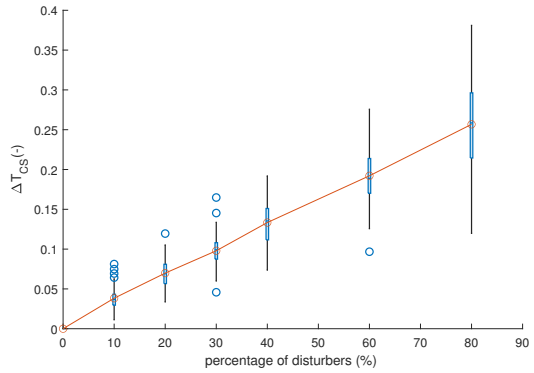

(a) Distribution of $\Delta T_{CS}(F_{x_{dist.},f,com.})$ and average of $\Delta T_{CS}\left(F_{x_{dist.},f,com.}\right)$ $(\overline{\Delta T}_{CS,x_{dist.},com.})$

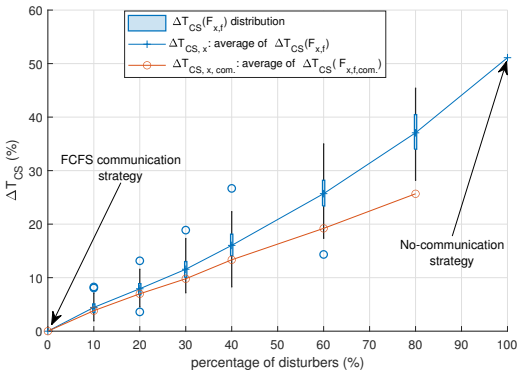

(b) Distribution of $\Delta T_{CS}\left(F_{x_{dist.},f}\right)$, average of $\Delta T_{CS}\left(F_{x_{dist.},f}\right)$ $(\overline{\Delta T}_{CS,x_{dist.}})$ and average of $\Delta T_{CS}\left(F_{x_{dist.},f,com.}\right)$ $(\overline{\Delta T}_{CS,x_{dist.},com.})$

Figure 4.13: Distribution of $\Delta T_{CS}(F_{x_{dist.}f,com.})$ and $\Delta T_{CS}(F_{x_{dist.},f})$ with the averages of those distributions according to the percentage $x_{dist.}$ of disturbers in the fleet.

when we introduce disturbers not communicating, even if we suppose the disturbers indicate their charging time when entering stations (strong hypothesis). In fact, the FCFS communication is sometimes not enough when, for instance, a communicating EV realises too late that a disturber is ahead of them in the waiting queue and cannot change their plan. Indeed, suppose a disturber EV_v stops at $t_{in,i,v}$ in the station CS_i during iteration t and a communicating EV, $EV_{v'}$, plans also to stop during iteration t but $t_{in,i,v'} > t_{in,i,v}$, and there are no other free chargers: $EV_{v'}$ will be aware too late of the presence of the disturber and will not be able to change its plan to avoid waiting time. If now we assume $EV_{v'}$ stops during the iteration $t+1$ and not during the iteration t, $EV_{v'}$ will be able to change its plan only if it has enough range to reach CS_{i+1} or if they did not already pass the station CS_{i-1} and can still stop there to charge. In the other cases, $EV_{v'}$ will have to wait for a charging socket to be free in station CS_i.

Nevertheless, the FCFS communication increases the probability for an EV to reduce its relative time loss compared with the situation where all the EVs communicate: the average relative time loss, $\overline{\Delta T}_{CS,x_{dist.},com.}$, for the communicating EVs stays always under $\overline{\Delta T}_{CS,x_{dist.},no\ com.}$, the average relative time loss for the disturbers (Figure 4.14).

Therefore, the more the EVs are communicating, the less the ones communicating are losing time, but also the whole fleet sees its relative time loss decreased compared with the situation with 100 % of disturbers ($\overline{\Delta T}_{CS,100,no\ com.} = 51\%$). The *FCFS communication strategy* might not be robust, but it enables to limit the average time loss for communicating EVs, $\overline{\Delta T}_{CS,x_{dist.},com.}$, to 10% when the percentage of disturbers is under 30 % of the fleet. For higher disturbers percentages, as the information quality decreases logically with fewer EVs communicating, the FCFS communication is insufficient to avoid long waiting times. Thus, we should think of an additional means to back up the FCFS communication strategy in evaluating the waiting time estimation when there are more than 30 % disturbers. This additional feature will also be of use when there are no disturbers in the fleet since even with 100% of real-time information sharing; the received information depends on the charging plan selected during the previous iteration and not the current iteration (see Section 3.2.2).

4.6.1.4 . Suggested improvements of the FCFS communication strategy

With or without disturbers, using an event handler to update the charging plans as soon as an event happens and not at every constant timestep represents a solution. Still, the risk of

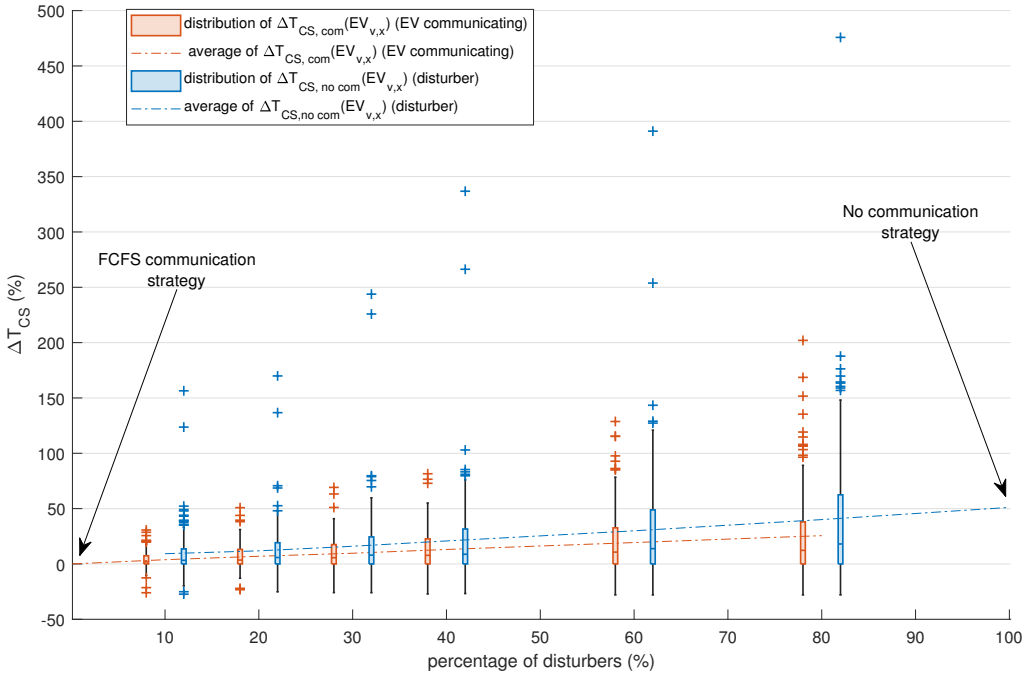

Figure 4.14: Distribution of the relative average additional time spent in stations by a) an EV communicating ($\Delta T_{CS,com.}(v_x)$) and b) a disturber ($\Delta T_{CS,no\ com.}(v_{x_{dist.}})$) according to the percentage of disturbers in the fleet. The plus signs '+' represent the outliers of the distributions.

this solution is that we fall into an infinite loop when some EVs compete for the same charging session. Each of them oscillates between two or more charging plans when one changes its charging plan: we need to set a limit of changes made after an event associated with a charging plan update.

Another solution would be to determine, thanks to statistics or reinforcement learning, the waiting time profile considering the previous intentions of charge sent by the EVs during the whole day and even during other crowded days instead of considering only the charging request sent at the previous iteration ($t-1$). The paper [71] proposes a solution with the same idea that might be adaptable to the *FCFS communication strategy* presented in this manuscript.

For high shares of disturbers in the fleet, the solution may be to use the *reservation strategy* for the communicating EVs instead of the *FCFS communication strategy*. Still, the efficiency of this solution remains to be proven and the percentage threshold of disturbers above which the *reservation strategy* performs better than the *FCFS communication strategy* has to be determined. Moreover, the *reservation strategy* might worsen the situation for the disturbers since the preemption is not possible in the simulation (the reason why is given in Section 4.4.1) and the reservation of charging session will induce more significant delays for the charging of non-communicating EVs compared with the FCFS communication. In fact, communication without reservation (FCFS communication) is beneficial for the whole fleet as it reduces the average time in stations per EV and not only for the communicating EVs (see the distribution $\Delta T_{CS}\left(F_{x_{dist.},f}\right)$ in Figure 4.13b).

4.7 . Conclusion

Firstly, we have compared two communication strategies with different station rules: the FCFS communication and the reservation strategies. Both strategies, *FCFS communication* and *reservation strategies*, are a way to reduce the waiting queue length in stations and the average travelling time for EV drivers on a long-distance trip without adding new charging points. They lead to more efficient use of the charging infrastructure on average, but the *communication strategy* is the charging strategy with the best performance. The underperformance of the reservation is due to the non-preemption that sometimes forces the non-utilisation of free chargers if an EV with higher priority arrives and the remaining time to charge is insufficient to start and finish a charging session. The preemption could improve the performance of the *reservation strategy*, but it will introduce other inconveniences the drivers will likely not accept. This is why the *FCFS communication strategy* remains the best strategy in comparison.

From a certain level of saturation (300-EV scenario in this case study), even if the *FCFS communication* (and to a lesser extent the *reservation*) enables to reduce by 52% the average trip time compared with the *no-communication strategy*, the real-time communication is not sufficient to meet the quality criteria so we need to add more charging points to improve drivers' satisfaction. In the next chapter, Chapter 5, we will see how we can optimise the infrastructure size to be developed when the fleet is using the *FCFS communication strategy*.

Secondly, we have quantified the time loss experienced by the EVs when one part of the fleet is not communicating and the other is using the *FCFS communication strategy*. The best charging strategy with the presence of disturbers not communicating is not performing as well as with 100% of communicating EVs, but still, the *FCFS communication strategy* enables to reduce the average time spent in stations compared to the situation when no EV is communicating (situation of *no-communication*). The *FCFS communication strategy* can be improved with means to anticipate more accurately the waiting time by crossing the information retrieved from an iteration to another (statistics, reinforcement learning...).

For the rest of the manuscript, we will keep the **FCFS communication strategy** as the best control strategy of the fleet charging, and we will assume there are no disturbers in the fleet.

5 - The benefits of communication in reducing infrastructure costs with limited-range electric vehicles

We have seen in Chapter 4 the benefit of the *FCFS communication strategy* for a given infrastructure layout that is subject to medium saturation. For higher saturation, we have seen that strategy is not sufficient to reduce the waiting time so we need to efficiently add charging points. In this chapter, we will prove the value of considering the communication strategy when sizing the charging infrastructure, especially if the range of the EVs is limited. With this in mind, we propose a multi-level optimisation where the lower level is dedicated to the optimisation of the charging plan for the EVs on the highway thanks to the communication strategy and the upper level aims to optimise the infrastructure itself (location and sizing of the charging stations). Firstly, we present in Section 5.1 the challenges raised by the sizing of the charging infrastructure on the highway if we want to reduce the size of the EV's battery pack. Secondly, we introduce in Section 5.2 the optimisation problem of the charging stations' planning to minimise the cost of the infrastructure while guaranteeing a minimum level of service. Then, in Section 5.3, we detail the different scenarios we studied with each time a comparison of the optimal infrastructure layout obtained for the *communication strategy* and the one obtained for the *no-communication strategy* representing the situation of reference. Section 5.4 sums up the results for the different scenarios.

A part of this chapter results has been published and presented during the 2023 IEEE Transportation Electrification Conference: A. Popiolek, P. Dessante, M. Petit, Z. Dimitrova, et M. Waraq, "Highway charging infrastructure costs reduction for limited-range electric vehicles with real-time communication", in *2023 IEEE Transportation Electrification Conference Expo (ITEC)*, june 2023, p. 1-8. doi: 10.1109/ITEC55900.2023.10186939. [117]

Contents

5.1 . Fast-charging infrastructure development challenges with limited-range batteries

5.1.1 . Short range and infrastructure needs

As we have seen in Section 2.1.2, the shorter range of most EVs compared to traditional internal-combustion-engine (ICE) vehicles discourages their use for long-distance trips or leads to the purchase of high-range models with larger batteries. However, larger batteries increase the environmental impact of an EV due to high CO_2 emissions during battery production, resulting in higher total emissions for EV production than for conventional ICE vehicles (see Section 1.2.3.1). To reduce the number of mileages needed to repay the manufacturing emissions "debt", the battery capacity should be limited (≤60 kWh), according to the French Environment and Energy Management Agency (ADEME) [6].

As a shortened battery range induces more charging events, the charging point operators (CPOs) must densify the fast-charging network and add new charging points to enable long-distance trips and limit the waiting time in stations [55]. To hasten the charging process, the charging power must be high (≥ 50 kW) but fast-charging points are costly (approximately €60.000 per 150-kW charging point [26]), so the charging network deployment must be optimized (see Section 2.4).

5.1.2 . Infrastructure optimisation with FCFS communication strategy

Most of the optimisation methods listed in Section 2.4 passively capture the existing charging demand for long-distance trips. Suppose the infrastructure is dimensioned to fit the average demand during the year. In that case, the waiting time will explode during traffic peaks (e.g. holiday departures) and discourage long-distance trips with an EV. On the contrary, if the

stations are scaled to avoid long waiting times during those occasional crowded days, the infrastructure will be oversized compared with the demand for the rest of the year when the number of long-distance trips drops, creating an important difference between the revenues and the investments. Thus, CPOs need a way to control the charging demand to circumvent the infrastructure oversizing and to support the occasional charging demand peaks. We have seen in Chapter 4 that the communication strategy increases the infrastructure's rate of use and represents an interesting control strategy of the fleet to tackle this problem.

Vandet and Rich [96] show the benefit of information-sharing when sizing the charging infrastructure for the Greater Copenhagen Area, and Rich *et al.* [97] take the same model to optimise the charging infrastructure this time for long trips on Denmark state roads. Those papers propose a method to minimise the infrastructure cost while guaranteeing a limitation of the waiting time under various thresholds. In this present chapter, we aim also to measure the infrastructure cost gains provided by the *FCFS communication strategy* (see description in Section 3.1.4) compared to an infrastructure developed in case of *no-communication*.

To guarantee a good level of charging service, we chose, like in [97] to constrain the waiting time of each charging session under a given threshold. Yet, contrary to [97], we want to guarantee this level of service during traffic peaks [50] for holiday period and not only for average traffic during the year, so we generate fleets that represent a typical day of holiday departure. In this chapter, we base our scenario on the French highway A6 with the real positions of the actual service areas where the charging stations are or will be installed. We approximate the size of the fleets we study to **500 EVs** which corresponds to 10 hours of saturation ($t_{sat.} = 10$ h) of the highway lanes (2 lanes on average on A6, $n_{lane} = 2$) and a future share of 3% of EVs on the French roads ($n_{EV,\%} = 3\%$) with only 50% of EV owners taking their EV to go on long-distance trips ($n_{trip,\%} = 50\%$) [69]. The saturation of the highway is modelled by the lane capacity l_{limit} (1730 vehicles/h [118]) so we can approximate the fleet size to:

$$t_{sat.} \cdot n_{lane} \cdot l_{limit} n_{EV,\%} \cdot n_{trip,\%} = 519 \approx 500 \tag{5.1}$$

For a given infrastructure layout, when the *FCFS communication strategy* is used, we need to compute with the multi-agent simulation the interaction between the EVs from the generated fleets and the stations to retrieve the real waiting time the EVs experience during a simulated day and compare those times to the threshold. However, a multi-agent simulation is time-costly (a few tens of minutes for a large fleet of 500 EVs) so testing all the combinations of infrastructure layout with an exhaustive method is possible but not recommended for such a complex problem. Thus, we use a meta-heuristic algorithm evolutionary-based, the Grey Wolf Optimiser (Section 5.2), to optimise the infrastructure layout under the waiting time constraints.

5.2 . Method: infrastructure optimisation with Grey Wolf Optimiser (GWO)

5.2.1 . Problem formulation: upper-level optimisation

We note N_f the number of fleets (so the number of crowded days) that are tested at the same time to check the waiting time constraint. Indeed, as we are using MAS and regarding the high number of parameters that influence the fleet's characteristics (see Section 3.1.1), we have to verify the waiting time guarantee on several fleets to get closer to the infrastructure proposing the highest quality service. However, since we did not have time to perform the optimisation on a high number of fleets, we only study five fleets with the method and leave the optimisation of the infrastructure for a larger number of fleets to industrials.

Concerning the cost reduction, the objective of the optimisation problem is the minimisation of the **daily equivalent annual cost** of the fast-charging infrastructure $DEAC_{FCI}$ (5.2) (see Section 5.2.2). As the French government plans to equip all the service areas with charging stations in the near future, we add the constraint that all service areas have at least one charging point (5.4). We hypothesise that the charging stations can only be located in service areas and that an unique CPO operates the whole infrastructure. The number of service areas is noted N_{area}

The whole optimisation problem is given by Equation 5.2.

$$Objective : \min_{s} \ DEAC_{FCI}(s) \tag{5.2}$$

$$s.t. \forall EV_v, \ \forall \ CS_i \in \mathbb{CS}, \ t_{wait,v,i} \leq T_{thres.} \tag{5.3}$$

$$\forall i \in [\![\ 1; \ N_{area}]\!] \ \exists j \in [\![\ 1; \ N_p]\!] \ s_{i,j} \geq 1 \tag{5.4}$$

The vector s lists the number of chargers (or sockets) per station according to their rate, so with N_p different charging rates possible in the infrastructure, we have:

for $i \in [\![\ 1; \ N_{area}]\!]$,

$$\begin{cases} s[N_p.i] = s_{i,N_p} \ : \text{ number of charger with the highest-rate type } p_{N_p} \text{ in } CS_i, \\ s[N_p.i-1] = s_{i,N_p-1} \ : \text{ number of chargers with a charging rate } p_{N_p-1} \text{ in } CS_i, \\ \dots \\ s[N_p.i-(N_p-1)] = s_{i,1} \ : \text{ number of lowest-rate } p_1 \text{ chargers in } CS_i. \end{cases}$$

In Chapter 4, the maximum charging power in the case study was 125 kW as only few EV models were able to charge above that power at the beginning of this thesis, but now, regarding the current charging power installed in stations [44, 119], the maximum power in this chapter is 350 kW ($p_{N_p} = 350 \ kWh$) and the possible charging rates are $P = \{50, \ 175, \ 350\} \ kW$.

To show the benefit of sharing information in real time on the minimisation of infrastructure cost, for each study presented in this chapter, we evaluate the optimal infrastructure when the EVs use the *FCFS communication strategy* but also when the EVs do not communicate (*no-communication strategy* - see 3.1.4) to represent the infrastructure we should develop in the current situation.

5.2.2 . Charging infrastructure cost $DEAC_{FCI}$

The cost of the charging infrastructure is usually evaluated as the equivalent annual cost of the infrastructure [45, 55, 61]. The equivalent annual cost EAC of the FCI is the equivalent constant annuity whose net present value (NPV) over the lifetime L of the infrastructure is equal to the NPV of the installed FCI itself [55]. The definition of the infrastructure NPV is given by:

$$NPV(FCI) = \sum_{k=1}^{L} \frac{R_k - C_k}{(1+r)^k} - I_0 \tag{5.5}$$

With R_k the revenue of the k^{th} year and C_k the cost during the k^{th} year. I_0 represents the initial investment during the year 0 and r is the discount rate. According to the definition of EAC_{FCI}, we have:

$$NPV(FCI) = NPV\left(EAC_{FCI}\right) \equiv \sum_{k=1}^{L} \frac{-EAC_{FCI}}{(1+r)^k} = -\frac{(1+r)^L - 1}{r.(1+r)^L} \times EAC_{FCI} \tag{5.6}$$

If we suppose the revenues R_k and the costs C_k constant from one year to another and

equal respectively to R and C, we obtain the expression:

$$\begin{aligned} NPV(FCI) &= NPV\left(EAC_{FCI}\right) \\ \Rightarrow \frac{(1+r)^L-1}{r.(1+r)^L} \times (R-C) - I_0 &= -\frac{(1+r)^L-1}{r.(1+r)^L} \times EAC_{FCI} \\ \Rightarrow EAC_{FCI} &= \frac{r \cdot (1+r)^L}{(1+r)^L-1} \times I_0 + C - R \end{aligned}$$

However, this formulation, at least in the way it is used in the previously cited references, implies that the number of chargers in stations is fixed during the lifetime of the infrastructure with all the investment performed the year 0. Yet, the fleet of EVs is currently growing quickly and is not going to reach a steady state soon so the infrastructure should be planned dynamically too [50]. Nevertheless, as the running time of our simulation is high and to simplify the problem, we assume like in the previously cited references that we are planning the infrastructure for a steady state in the evolution of EVs on the road.

As each simulation accounts for a one-day situation, we compute the daily equivalent annual cost to represent the infrastructure cost C_{FCI}. This daily equivalent annual cost is simply the equivalent annual cost of the FCI EAC_{FCI} divided by 365. Precisely, $DEAC_{FCI}$ is the sum of the investment cost at the year 0 (including the hardware cost, $C_{hard.}$, of each charger and their installation cost, $C_{install.}$), and the annual maintenance and operation cost, $C_{O\&M}$, minus the daily average revenue, R_{avg}, during the year (5.7). According to [26], the hardware and the installation costs are both proportional to the charger power since the higher the power is, the higher the furniture and the grid connection will cost (see Table 5.1 for the installation costs). The same relation is observed for the O&M cost since the CPO will have to pay a subscription that increases with the grid connection power.

$$\begin{aligned} DEAC_{FCI}(s) = &\frac{r(1+r)^L}{365((1+r)^L-1)} \cdot \sum_{i=1}^{N_{area}} \sum_{j=1}^{N_p} \left(s_{i,j} \cdot \left[C_{hard.,j} + C_{instal.}(s_{i,j})\right]\right. \\ &+ \frac{1}{365} \cdot C_{O\&M} - R_{avg}(s) \end{aligned} \tag{5.7}$$

We choose a discount rate r rather high for a partnership between private and public stakeholders (r = 10% like in [61]) since the help of public actors in France is now limited to the creation of new charging stations and not to the addition of chargers in existing charging stations.

Concerning the revenue, as the fleets we simulate represent crowded days and not an average traffic day, the real annual average daily revenue perceived by the CPO should be computed according to the average traffic day. In Chapter 4, we evaluate the average daily BEV traffic on the highway to 180 EVs so, as a crowded day is represented by a fleet of 500 EVs in this case study (see Section 5.1), the average daily traffic is one third of a crowded day traffic ($500/180 \approx 1/3$). Therefore, we assume that the annual average daily revenue is one third of a crowded-day revenue. The revenue of one crowded day is the net revenue perceived by the operator during that day and, as we test N_f crowded days (one day per fleet), the daily average revenue R_{avg} is given by:

$$R_{avg} = \frac{1}{3} \cdot \frac{1}{N_f} \cdot \sum_{f=1}^{N_f} \sum_{v \in F_f} \left[C_{charge,v} - E_{total,v} \cdot p_{el}\right] \tag{5.8}$$

The electricity price p_{el} represents the price paid by the CPO per kWh sold and we set it to 0.15 € as we suppose the industrial electricity price given in [55] (0.13 €/kWh) has slightly

increased since 2019. In reality, the real electricity price the charging operator pays depends on the charging power but we use an electricity price independent from the charging power and we assume that the price difference is included in the operation and maintenance costs $C_{O\&M}$ of the chargers (linked to the charger's power). The charging cost for an EV driver, $C_{charge,v}$, is defined in Section 3.1.3.

As we mention it before, the installation cost per charger depends on the level p_j of the charger but also on the number of chargers with the same charging power level $s_{i,j}$ installed in the station [26] (Table 5.1). Table 5.2 gives the values of the different parameters to compute the $DEAC_{FCI}$.

Table 5.1: Charger hardware installation cost according to the level of power. The figures are obtained from [26] by multiplying the installation costs expressed in dollar by the changing rate of 0.88 to convert the costs in euro

	Installation cost per charger depending on the number of chargers to install in the station (k€)			
charger power	1 charger	2	3 - 5	more than 6
50 kW	40	32	24	16
175 kW [1]	42	33.5	25	16.4
350 kW	58	46.2	34.4	22.5

5.2.3 . Waiting time constraint T_{thres} and lower-level optimisation

As previously mentioned in Section 5.1, the constraint on the waiting time is checked thanks to a simulation of one or several fleets representing a crowded day on the highway using the simulation framework described in Chapter 3. This part of the method corresponds to the lower optimisation level with the optimisation of the discontent factor for all EVs. N_f is the number of fleets F tested during the evaluation of one given layout s in the optimisation problem (5.2) and N_{EV} is the number of EVs in each fleet F_f.

5.2.3.1 . Waiting time threshold T_{thres}

Depending on the optimisation (see Section 5.3.3), we evaluated the infrastructure needs for two different waiting time thresholds T_{thres}:

- $T_{thres.}$ = 30 minutes. In Chapter 4, the maximum waiting time accepted was 30 minutes but if we want to size the infrastructure for the near future, as the infrastructure and the new EV models enable more and more ultra-fast charging, the exigence of drivers will be higher in quality of service.

[1] We consider 150 and 175-kW chargers equivalent

[2] prices charged by Fastned [119] for charging at 175kW chargers and by Ionity in France [44] at 50 kW and 350kW chargers.

[3] indicative hardware costs for the 350-charger given by an ABB exhibitor at the Paris Auto Show 2022, the hardware cost for the other power rates correspond to an annual decrease by 3% of the costs given in [26] from 2019 to 2022.

Table 5.2: Values of the parameters used in this chapter

parameter	description	value %
p_{el}	electricity price per kWh for industrials (€)	0.15
$p_{charge,j}$	energy price per kWh for EV drivers (€)	0.35 (50 kW)/ 0.59 (175 kW)/ 0.79 (350 kW) [2]
$C_{hard.,j}$	hardware cost per networked charger (€)	22,000 (50 kW)/ 60,000 (175 kW)/ 90,000 (350 kW) [3]
$C_{O\&M}$	maintenance cost	1% of the investment
r	discount rate	10%
L	lifetime of the chargers	15 years
N_{area}	number of service areas along the highway	13
N_f	number of fleets in the sample	1-5

- $T_{thres.} = 30$ minutes to evaluate the gain on the infrastructure cost and the degradation of the trip time we can expect if we authorise 10 minutes more on the waiting time threshold as it is the case in Chapter 4.

5.2.3.2 . Value of time when $N_p > 1$

When running the MAS (for the communication and the no-communication strategy), each EV optimise its charging plan depending on the trip time and the charging cost (see Section 3.1.3). If there is only one available power level, p, in the infrastructure ($N_p = 1$), as we assume the charging price proportional to the energy charged ($E_{total,\,v}$) (see Section 3.1.3.2), the charging price $C_{charge,\,v}$ is always the same whatever the charging plan is (5.9). Therefore, we do not need to consider the charging cost (and consequently the drivers' value of time) when optimising the charging plan ($X = 0$).

$$C_{charge,\,v}(\omega_v^*) = \sum_{i=1}^{N_{CS}} p_{charge}(p_i^*) \cdot x_i^* = p_{charge}(p) \cdot E_{total,v} \tag{5.9}$$

However, if there are multiple charging rates possible in the infrastructure ($N_p > 1$), we have to take into account the drivers' value of time (included in X) since the charging price depends on the power of the socket used (p_j). In Section 4.2.1, we choose to consider only the trip time in the discontent factor as indicated in [84], but, on European highways, the kWh price is higher than 0.12 $/kWh (prices start at 0.3 €/kWh on fast DC chargers and can go up to 0.8 €/kWh), so the charging cost should be considered in the discontent factor.

The values of time used in this chapter are:

- $vot = 20$ €/hr: this value comes from the paper [64] that evaluates the median personal value of time to 19 €/h that we round up to 20 €/hr. We found a similar value of time, 20 $/hr, for the lowest vot considered in [120].

- $vot = 50$ €/hr: this value is similar to one of the values of time given in [120] (50 $/hr). This value represents the vot for professional trips and for users giving more importance to the reduction of their trip time, especially the ones investing in more expensive cars to have more battery capacity and higher charging rates.

5.2.3.3 . Lower-level optimisation with the *no-communication strategy*

When the strategy used by the EVs is without communication (*no-communication strategy*), as the EVs establish their charging plan before their trip and do not interact with the infrastructure, the charging plan of each EV stays the same during the whole day, and the MAS only serves to emulate the waiting queue and to compute the final waiting time for each charging session. The time cost for those calculations is relatively low compared to when we have to simulate real-time interactions (for *communication strategy*) but still, the number of combination is high so we cannot test all the layout combinations.

In a case where there is only one possible charging rate in the infrastructure ($N_p = 1$), we can simplify the optimisation and compute iteratively the optimal infrastructure. The EVs following the *no-communication strategy* optimise their charging plan only according to the location and the power level in the charging stations. As the station locations are fixed with the constraint of one station at each service area (5.4) and if the power level is the same for all the stations, we only need to simulate once the fleet on the highway with one charging point per station (initial infrastructure) to know where the EVs from the fleet are going to stop. Since the EVs will not change their plan, whatever the number of charging points will be in stations, we can determine the optimal infrastructure iteratively by emulating the infrastructure with the MAS and then adding one charging point in the station with the smallest position on the road where at least one EV waits more than the waiting-time threshold. Therefore, we do not need a GWO to test charging point distribution among the stations when there is only one power level in the infrastructure.

When $N_p > 1$, determining the optimal infrastructure is more complex. We can determine iteratively the sufficient infrastructure for the *no-communication strategy* like for the case $N_p = 1$ with an initial infrastructure with one charger per power level. Again, we add, progressively, station after station, one charging point per power level for which at least one EV waits more than the waiting-time threshold. As we will see in Section 5.4.2.2 and in Section 5.4.3, the value of the vot may lead the whole fleet choosing only on power level across the whole infrastructure. Therefore, in this situation, proposing different power levels per station is useless. However, if the revenue for one charger type is higher but is not chosen by the EVs if they have access to several power levels in a given station, the optimisation will favour the solutions with, in this given station, only one available power level, the one giving the highest revenue, to force the EV to charge at this power level. Therefore, if we authorise a station to have only one charger type but the whole infrastructure can propose different power level, it is not possible to find iteratively the best combination of charging points. Thus, the GWO should be used to optimise the infrastructure

5.2.3.4 . Lower-level optimisation with the *communication strategy*

When the strategy used by the EVs is the *communication strategy*, the MASs have longer running time since we need to detail the interaction between the EVs and the CSs at every iteration t, so we need to use the grey wolf optimiser to determine the optimal infrastructure (see Section 5.2.4 for GWO algorithm). For this strategy, the constraint on the waiting time is expressed as a penalty we add to the cost $C_{CFI}(s)$ of the layout s. The penalty $t_{pen,\,v,\,i}$ is null if no EV in all the tested fleets experiment a waiting time above T_{thres}; it is exponential with respect to the gap between the waiting time above the threshold and T_{thres} for each EV waiting longer than

accepted (5.10). The times are in seconds in the penalty expression with $T_{pen} = 10000\ seconds$ and $T_{gap} = 60\ seconds$. To avoid useless long running time, we stop the MAS for a layout as soon as one EV waits more than twice the threshold T_{thres} and start the next simulation for another layout.

$$t_{pen,\,v,\,i} = T_{pen} \cdot \frac{\exp\left(\max\left(t_{wait,\,v,\,i} - T_{thres}, 0\right) - 1\right)}{\exp\left(T_{gap} - 1\right)} \tag{5.10}$$

The step of the multi-level optimisation realised with a Grey Wolf Optimiser is described in the next section (Section 5.2.4).

5.2.4 . Grey Wolf Optimiser

As explained in Section 5.1, the complexity of the problem (non easily differentiable and similar to a combinatorial problem) and the running cost of the fitness evaluation due to the use of multi-agent simulations to compute the constraints lead us to solve the problem with a meta-heuristic algorithm. We selected an evolutionary algorithm, the Grey Wolf Optimiser (GWO) [93], as it converges fast thanks to the use of the three best solutions at the same time to update the population to be tested at the next iteration of the optimiser [60]. We have tested the Genetic Algorithm from Matlab and a differential evolution algorithm based on NSGA-II for other studies about sizing the infrastructure (see Chapter 6) but the running time was too long to consider those methods when simulating the *FCFS communication strategy*.

This GWO is inspired by grey wolves' hunting tactic to encircle and hunt prey. In this chapter, the position of the prey is the optimal layout s^* of the infrastructure for our problem and at each iteration of the algorithm, the wolves in the pack update their positions (s) to get closer to the prey. As a reminder, the vector s lists the number of charging points at each service area according to the power level and describes the infrastructure layout (Section 5.2). The fitness of one grey wolf (whose position corresponds to one layout s) is the cost function $C_{FCI}(s)$.

In the hierarchy of the grey wolf pack, the alpha (α), beta (β), and delta (δ) wolves lead the rest of the pack to the prey at the position s^*. In our case, we do not know where the prey is since we are looking for its position so we suppose that the leading wolves are the ones with a better knowledge of the prey position. Consequently, at each update of the wolves' position, we place the alpha wolf at the position with the best fitness found so far and we give the second-best and third-best positions respectively to the beta and delta wolves. To model at the same time the hierarchy in the pack, the hunting (exploration), and the encircling (convergence) of the prey, the position $s(k)$ of each wolf at the k^{th} iteration is updated as follow:

$$\overrightarrow{D_\alpha} = |\overrightarrow{B_1}.\overrightarrow{s_\alpha} - \overrightarrow{s}(k)| \qquad \overrightarrow{D_\beta} = |\overrightarrow{B_2}.\overrightarrow{s_\beta} - \overrightarrow{s}(k)| \qquad \overrightarrow{D_\delta} = |\overrightarrow{B_3}.\overrightarrow{s_\delta} - \overrightarrow{s}(k)| \tag{5.11}$$

$$\overrightarrow{s_1} = \overrightarrow{s_\alpha} - \overrightarrow{A_1}.\overrightarrow{D_\alpha} \qquad \overrightarrow{s_2} = \overrightarrow{s_\beta} - \overrightarrow{A_2}.\overrightarrow{D_\beta} \qquad \overrightarrow{s_3} = \overrightarrow{s_\delta} - \overrightarrow{A_3}.\overrightarrow{D_\delta} \tag{5.12}$$

$$\overrightarrow{s}(k+1) = \lfloor \frac{\overrightarrow{s_1} + \overrightarrow{s_2} + \overrightarrow{s_3}}{3} \rfloor \tag{5.13}$$

The coefficient of vectors $\overrightarrow{A_j}$ and $\overrightarrow{B_j}$ are computed as follow:

$$A_{j,m} = 2\,a\,r_1 - a \qquad B_{j,m} = 2\,r_2 \tag{5.14}$$

with r_1 and r_2 random values uniformly distributed between 0 and 1 and a given by:

$$a = 2 - k\,\frac{2}{Max_{iter}} \tag{5.15}$$

Max_{iter} is the maximum number of iterations that can be performed during the optimisation. In Appendix D.2, we detail how we corrected and adapted the 2011 version of the algorithm developed by S. Mirjalili [121] to our problem.

Table 5.3: Parameters of the Grey Wolf Optimiser

Optimisation	Number of grey wolves in the pack	Number of iterations (Max_{iter})
Optimisation 1-3	20	20
Optimisation 4-6	30	20

As presented in Section 5.2.3, the constraint on the waiting time is checked thanks to a simulation of the infrastructure layout that is evaluated (Figure 5.1). We remind here that to avoid long computation time, we stop the MAS as soon as one EV experiences a waiting time twice as much as T_{thres}. In addition, to accelerate the GWO convergence, we introduced a novel possible update to the position of the grey wolves, specifically adding charging points to stations where EVs had previously encountered waiting times that violated the constraints. This modification is described in Appendix D.2.

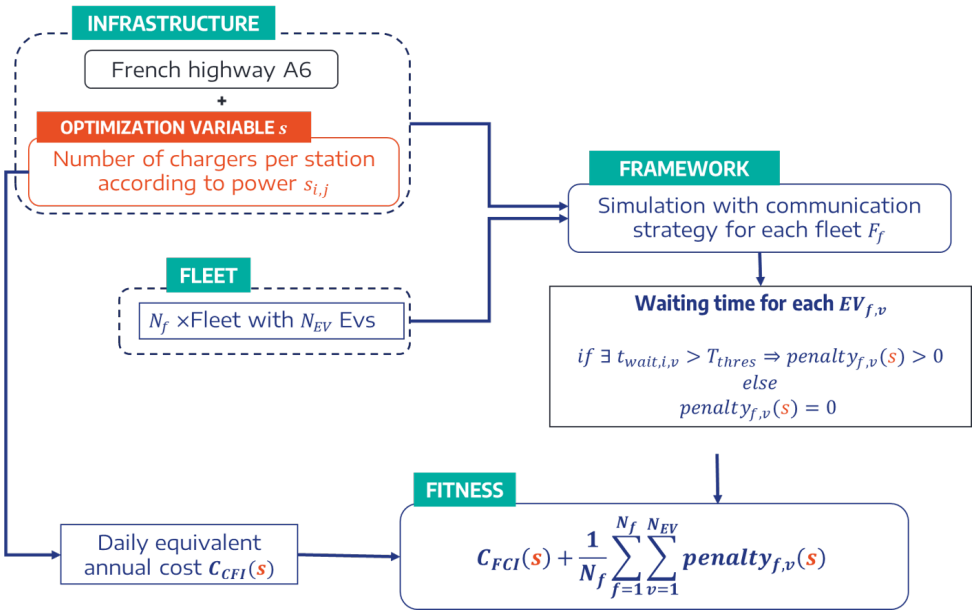

Figure 5.1: Fitness calculation for one wolf

The Grey Wolf Optimiser is stopped after a maximum number of iterations Max_{iter} and the optimal layout corresponds to the wolf's position with the minimal fitness in the pack, so the latest alpha wolf's position.

The choice of the GWO parameters is inspired by the paper [60] that has a population size of 50 grey wolves and 20 iterations. We keep 20 iterations but reduce the population size to 20 as the evaluation of the fitness of one individual takes time (approx. 30 min if need to simulate the whole day).

We run the two-level optimisation by paralleling the calculation on 12 matlab workers. We can use 24 workers but, as the size of the fleets containing EVs' $data_{charge}$ is important, the jobs are slowed down when the fleets' data are copied 24 times instead of 12 times.

5.3 . Case studies

5.3.1 . Highway details

The considered highway in this chapter is a more precise version of the French highway A6 compared with the case study in Chapter 4. Still, we reduce the number of entrances/exits and the probability of entry or exit at each highway exit is arbitrarily set according to a rough approximation of Average Annual Daily Traffic (AADT) on each section of the French highway A6 and to the closeness of large agglomerations such as Paris and Lyon.

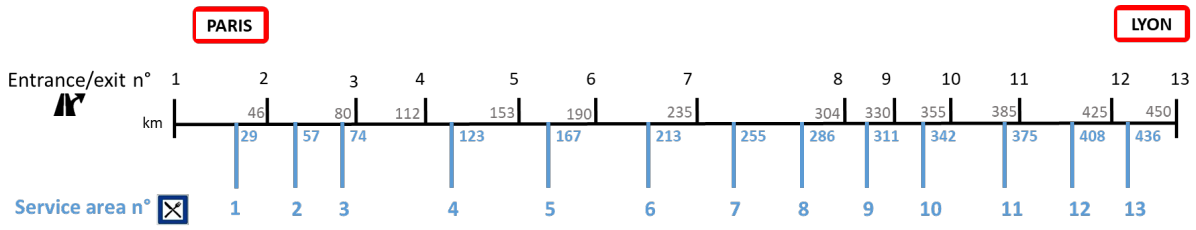

Figure 5.2: French highway A6 with simplified entrances/exits

We keep the same service areas as highway A6 (13 service areas so $N_{area} = 13$) for the case study and those areas are the potential locations of the charging stations (today, almost all service areas of the highway are equipped [122]). Note that the number of charging stations more than doubles compared with Case study 1 from Chapter 4 but the computation of $data_{charge}$ (Section 3.4.2) with $\Delta E = 0.5kWh$ is still feasible in a reasonable running time. However, when $N_p > 1$, the parallelisation of the computation is not possible for $\Delta E = 0.5kWh$ since the size of $data_{charge}$ is too important to be handled by the workers. Therefore, when $N_p > 1$, we use $data_{charge}$ with $\Delta E = 1kWh$ to reduce the size of $data_{charge}$ and make the parallelisation possible.

5.3.2 . Characteristics of EV fleets

As explained in Section 5.2.1, we optimise the infrastructure over five different fleets (F_1 to F_5) and we present in this section, how we generate the trip parameters.

5.3.2.1 . Entrance (o_v) and exit (d_v) choice

Concerning the spatial parameters of each trip, the entrance o_v, where EV_v enters the highway is selected according to the entry probabilities depicted in Table 5.4. Since we do not have specific data about long-distance travel on highway A6, we arbitrarily set the entry and exit probabilities we gave in Table 5.4 to roughly reflect the annual average daily traffic (AADT) on A6 sections.

To partially reflect the sensitivity of the charging strategies to the trip parameters, we introduce two different methods explained later to choose the highway exit point for each EV.

The **first method** selects the EV's exit, d_v, according to the exit probability specified in Table 5.4. **The fleets F_1, F_2 and F_3 are based on that first method**. We obtain fleets where the majority of the generated trips cover the whole length of the highway, as we can see in Figure 5.5, Figure 5.6 and Figure 5.7: the number of EVs in fleet $F1$, $F2$ and $F3$ passing in front of each service area is in average equal to 70% of the fleet size ($N_{EV} = 500$ EVs).

In the **second method**, the exit points selected by the EVs depend on the travelling distance distribution given in [27] and summed up in Table 5.5. **We generate two fleets, F_4 and F_5, with the second method**.

We notice in Section 5.4 (Figure 5.8 and Figure 5.9) a higher number of EVs travelling the first half of the highway (until service area 6) for both fleets F_4 and F_5 compared with the fleets F_1, $F2$ and $F3$.

Table 5.4: Location of entrances/exits and entry/exit probabilities for the different fleets based on simplified A6 AADT

n_{entry}	1	2	3	4	5	6	7
Location (km)	0	46	80	112	153	190	235
Entry probability for all the fleets (%)	45	6	2	2	2	2	2
Exit probability for $F1$, $F2$ and $F3$ (%)	0	0	0	5	5	5	5
n_{entry}	8	9	10	11	12	13	14
Location (km)	264	304	330	355	385	425	450
Entry probability for all the fleets (%)	2	30	5	0	0	0	0
Exit probability for $F1$, $F2$ and $F3$ (%)	5	5	5	5	20	10	30

Table 5.5: Number of long-distance journeys by cars in 2014 according to the distance [27]

Distance (km)	100-300	300-600	600-1000	>1000
Number of journeys (millions)	87	47.1	19.7	2.9

5.3.2.2 . SoC_{start} and SoC_{tar} choice

The SoC of each EV when they enter the highway ($SoC_{start,v}$) is picked according to the SoC distribution extracted from Stellantis connected vehicles data (see Figure 5.3 and Appendix B.2). To have an idea of the impact of the $SoC_{start,v}$ distribution on the sizing of the highway, we truncated the distribution in Figure 5.3 from 50% of SoC for the fleets F_1 to F_3 and we kept the original distribution for the fleets F_4 and F_5.

The target SoC required by the EV when leaving the highway is uniformly distributed in the interval $[20, 30]$ %.

5.3.2.3 . Charging curves

For the EV model with a 60-kWh battery pack, we take as example two models: the Renault Megane e-tech whose charging curve is given in [23] and in [102] and the Nissan Ariya [4] [123]. We approximate both charging curves linearly (see Figures 5.4a and 5.4b).

The fleets F_2 and F_3 have a charging curve associated to the Megane E-Tech and fleets F_4 and F_5 are associated to the Ariya (see $P_{max,v}$ and c_v in Table 5.6). The fleet F_1 is a mix between

[4]The charging curve of the Nissan Ariya 63 kWh is given at 6'14" in the video

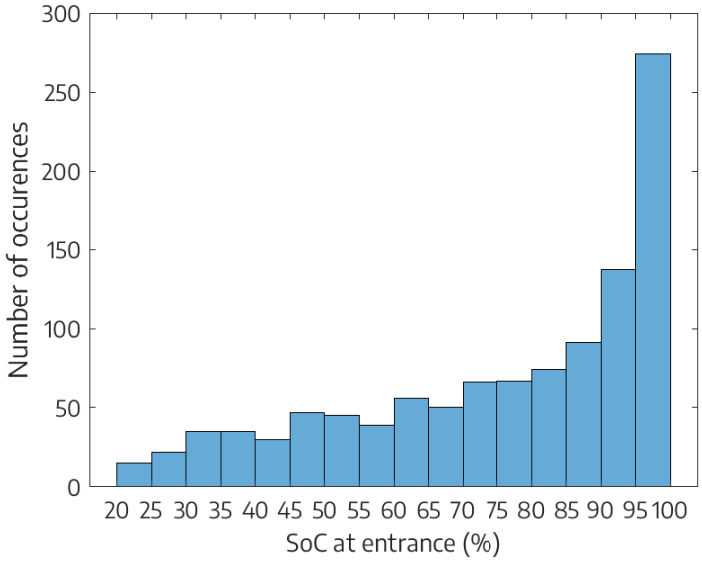

Figure 5.3: SoC at entrance distribution of the long distance trips extracted from the 380 Stellantis connected EVs

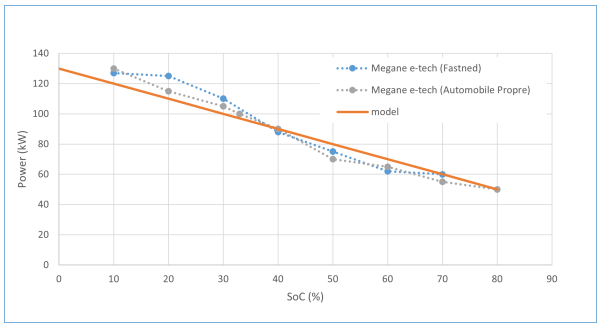

(a) Megane e-tech - $P_{max,\,v} = 130kW$, $c_v = 6000$

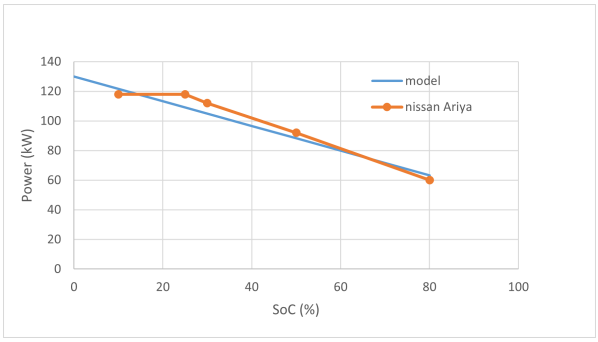

(b) Nissan Ariya 63 kWh - $P_{max,\,v} = 130kW$, $c_v = 5000$

Figure 5.4: Charging curves of the Megane e-tech and the Nissan Ariya. The curve noted 'model' corresponds to the charging curve implemented to compute the charging times in our simulation.

the two charging curve.

Table 5.6 recaps the parameters for the trip generation per fleet.

5.3.3 . Optimisations description

To comply with ADEME recommendation [6], the battery capacity for all the EVs in the fleets is **60 kWh**.

We first optimise the infrastructure for one fleet at the time and with one level of power ($N_p = 1$). For this optimisation (**optimisation 1**), as we consider only one charging rate in stations and as EV models on the roads today with a 60-kWh battery pack have a charging power under 175 kW, the only available power is **175 kW**. We set as waiting time threshold T_{thres} = 20 min. The revenue is not consider when optimising the $DEAC_{FCI}$ for **Optimisation 1** since all the chargers in the infrastructure have the same power ($P = \{175\ kW\}$) so the same char-

[5] SoC distribution given in Figure 5.3.

Table 5.6: Parameters for the trip generation according to the fleet

Fleet i	Exit selection method	$SoC_{start,v}$ selection method	$P_{max,v}$ (kW)	c_v (-)
F_1	simplified AADT	SoC distribution[5] truncated (50% - 100 %)	140	6000
F_2	simplified AADT	SoC distribution truncated (50% - 100 %)	130	6000
F_3	simplified AADT	SoC distribution truncated (50% - 100 %)	130	6000
F_4	distance	SoC distribution	130	5000
F_5	distance	SoC distribution	130	5000

ging price. Consequently, as the charging price is proportional to the energy charged (Section 3.1.3.2), one fleet generates the same income ($p_{charge}(175\ kW) \times \sum_{v \in F} E_{total,v}$) whatever the infrastructure layout is so there is no use in comparing the revenues in the optimisation. However, we precise the revenue generated R_{avg} for each fleet to compute the daily equivalent annual cost $DEAC_{FCI}$ of the optimal layout associated to each fleet.

Then, for the second optimisation (**Optimisation 2**), we plan the optimal infrastructure for the five fleets at the same time as if each fleet represents a crowded day that might occur during the year. There is still only one charging type ($P_2 = \{175\ kW\}$) and the waiting time threshold is equal to 20 minutes (T_{thres} = 30 min). When it comes to the *no-communication strategy*, the optimal infrastructure guaranteeing the waiting time threshold for all the fleets is built iteratively with all the fleets tested at each iteration to progressively determine the optimal number of charger in each station suitable for all the fleets.

In **Optimisation 3**, to assess the influence of the waiting time threshold on the infrastructure development, we perform the same optimisation as Optimisation 2 but with T_{thres} = 30 minutes.

For **Optimisation 4** and **Optimisation 5**, $N_f = 5$ and $N_p > 1$. As the power level choice is $\{50, 175, 350\}$ and a 60-kWh EV can charge only up to 130 kW, we test two charging power levels: 50 and 175 kW. In **Optimisation 4**, the vot of all the EVs is 20 €/h whereas it is equal to 50 €/h in **Optimisation 5**.

Table 5.7: Parameters according to the optimisation

Optimisation	T_{thres}	N_f	N_p	P (kW)	capacity battery (kWh)	vot (€/h)
Optimisation 1	20 min	**1**	1	$\{175\}$	60	-
Optimisation 2	20 min	5	1	$\{175\}$	60	-
Optimisation 3	**30 min**	5	1	$\{175\}$	60	-
Optimisation 4	20 min	5	2	$\{50, 175\}$	60	**20**
Optimisation 5	20 min	5	2	$\{50, 175\}$	60	50

5.4 . Optimisation results

5.4.1 . Optimisation 1: optimisation for each fleet individually ($N_f = 1$)

5.4.1.1 . Optimal infrastructure comparison for the strategies with and without communication

For this optimisation, there is only one charging power level possible (175 kW) and the waiting time threshold T_{thres} is equal to **20 minutes**.

Table 5.8 summarises the costs $DEAC_{FCI}$ and the number of charging points obtained for each fleet and each strategy. We indicate as well the daily equivalent annual expenditure, $DEAE_{FCI}$, that refers to the cost of the FCI $DEAC_{FCI}$ without considering the revenue R_{avg} (5.7). A negative $DEAC_{FCI}$ means that the infrastructure is profitable. We notice that all the infrastructure layouts found for both charging strategies are profitable with the definition of the revenue we considered: one third of the revenue generated during the crowded day represented by the fleet (5.8). The limit of revenue for which the infrastructure layouts obtained for the communication strategy are still all profitable is 13.5% of the revenue generated during a crowded day and for the no-communication strategy, this revenue is 14.5% of this crowded-day revenue.

According to Table 5.8, we can say that the *communication strategy* always permits to decrease both the number of optimal charging points and the infrastructure cost $DEAC_{FCI}$ compared with the *no-communication strategy* (see the line "$DEAC_{FCI}$ reduction" in the Table 5.8) whatever the trip generation probabilities are. The lowest relative reduction concerns the fleet F_2 where the communication decreases the $DEAE_{FCI}$ by 12.2% and the equivalent annual cost $DEAC_{FCI}$ by 8.3% with 6 chargers less than for the reference case without communication. However, for the other fleets, the communication brings more noticeable benefits and even enables a reduction of 15% for fleet F_1. As we use an evolutionary algorithm, the optimal layout we found for F_2 might not be the global minimum, and a better result may exist with an even lower $DEAC_{FCI}$.

The communication enables the fleets to flatten the peak of charging points in the station 5 needed with the strategy without communication (see Figure 5.12a, Figure 5.8b, Figure 5.12b and Figure 5.9b). In fact, the communication spreads more evenly the EVs across the

Table 5.8: Number of charging points per station and daily equivalent annual cost $DEAC_{FCI}$ of the optimal infrastructure according to the fleet and the strategy (T_{thres} = 20 min)

Fleet	F_1	F_2	F_3	F_4	F_5
Total number of CPs w/o communication	38	40	35	41	39
Total number of CPs with communication	28	34	29	32	30
Total number of CPs reduction (%)	26.3	15	17.1	22	23.1
$DEAE_{FCI}$ w/o communication (€/day)	1,202	1,264	1,121	1,285	1,261
$DEAE_{FCI}$ with communication (€/day)	929	1,110	959	1,034	991
$DEAE_{FCI}$ **reduction (%)**	22.7	12.2	14.4	19.5	21.4
Total energy charged by the fleet (kWh)	20,582	21,377	20,868	22,878	22,077
R_{avg} (€/day)	3,019	3,135	2,686	2,944	2,841
$DEAC_{FCI}$ w/o communication (€/day)	−1,817	−1,871	−1,537	−1,659	−1,580
$DEAC_{FCI}$ **with communication (€/day)**	−2,090	−2,025	−1,727	−1,910	−1,850
$DEAC_{FCI}$ reduction (%)	15	8.3	8.4	12.1	13.7
T_{CS} w/o communication (min/EV)	36.8	43.8	40.1	40.6	39.5
T_{CS} with communication (min/EV)	37.7	45.1	41.5	43.7	40.0
T_{CS} reduction (%)	−2.4	−3.1	−3.5	−7.6	−1.3

stations [124] because the EVs adapt their charging stops to the affluence in stations, so the highly crowded stations without communication see their demand decreases with communication.

Nevertheless, concerning fleets F_1, $F2$ and $F3$, even if the strategy of communication decreases the global number of points needed (Table 5.8), some stations have their number of points increased compared to the case without communication, creating new charging points peak instead of flattening them (Figure 5.5b, Figure 5.6b and Figure 5.7b). This is due to the decrease of the installation cost for one charger when the number of points installed in the

same station increases: the optimizer favours the solution with some large stations to make the charger cost go down and where the rest of the stations have only one point to satisfy the second constraint in (5.4).

Moreover, although the number of EVs going past each station is approximately the same for the fleets F_1, F_2 and F_3 (Figure 5.5a, Figure 5.6a and Figure 5.7a), the peaks of charging points are not necessarily located at the same stations. For instance, a peak is located at station 9 (where more EVs move past compared with other stations) for the fleets F_1 and F_2 but the optimal infrastructure for fleet F_3 as a peak at station 8 and 10 and not at station 9. We can conclude that the number of EV passing in front of stations is insufficient to forecast the optimal infrastructure: it also depends on the time when the EVs move past the station, the SoC of the EVs at that time and the information previously shared by the EVs. This complexity corroborates the need for a meta-heuristic algorithm to test randomly different layouts of the infrastructure and approach the optimal charging network.

Finally, concerning the average time spent in stations (T_{CS}), its value is always slightly higher for the *communication strategy* compared with the *no-communication strategy*. This result is certainly due to the fact that the communicating EVs spent more time charging than the non-communicating EVs because, when optimising their charging plan, they do not focus on minimising only their charging time, contrary to the non-communicating EVs.

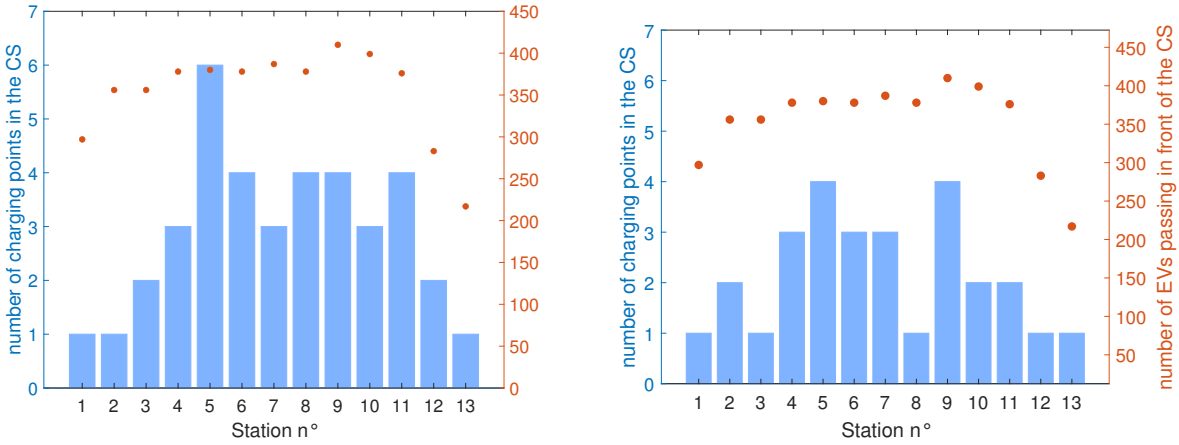

(a) with *no-communication strategy* (b) with *communication strategy*

Figure 5.5: Optimal infrastructure (left axis) and number of EVs passing in front of each station (right axis) for F_1

5.4.1.2 . Highlights and limit of the optimisation on one fleet at a time

The optimal infrastructure with the communication strategy is always better than the one with the *no-communication strategy* (on average 18.1 % of $DEAE_{FCI}$ and 11.5 % of $DEAC_{FCI}$ reduction). In addition, the optimal infrastructure found in this study for the communication might not be the best one since we use a non-deterministic algorithm (GWO) whereas the optimal infrastructure computed for the no-communication is the infrastructure with the global minimum for the $DEAC_{FCI}$ (see Section 5.2.3.3). Thus, the gain in infrastructure cost we found between both strategies is likely to be even bigger.

We studied the interest of the *communication strategy* on only five fleets. Still, as the cost reduction is similar for each case, whereas the trip generation method was different, we can state that the communication always enables the infrastructure cost reduction. Nevertheless, we have seen that the resulting optimal infrastructure differs from one fleet to another (see

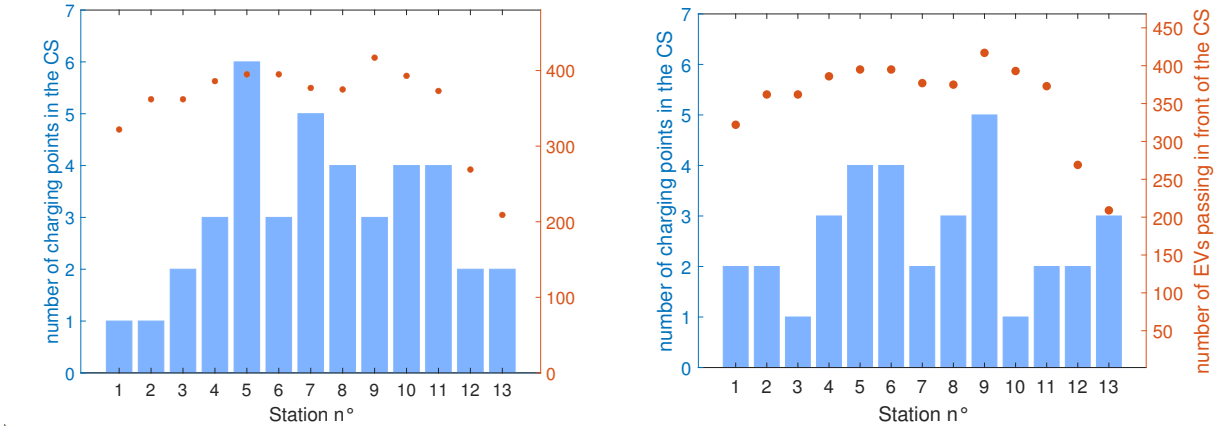

(a) with *no-communication strategy* (b) with *communication strategy*

Figure 5.6: Optimal infrastructure (left axis) and number of EVs passing in front of each station (right axis) for F_2

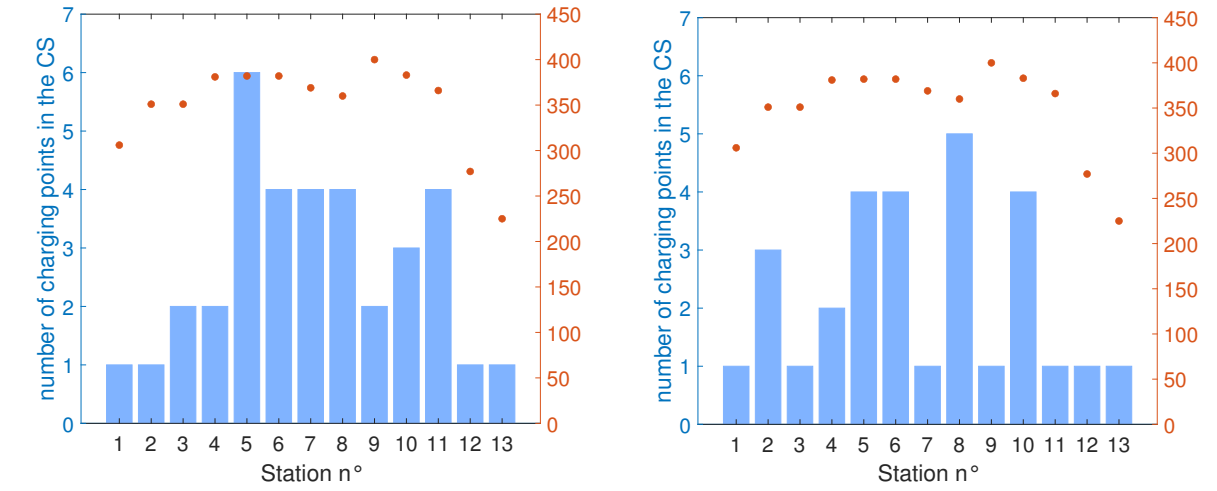

(a) with *no-communication strategy* (b) with *communication strategy*

Figure 5.7: Optimal infrastructure (left axis) and number of EVs passing in front of each station (right axis) for F_3

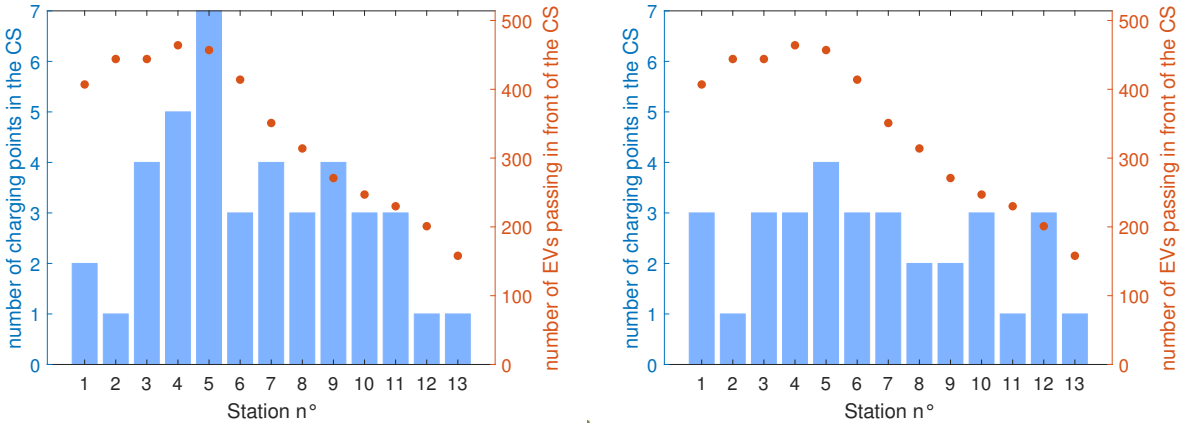

(a) with *no-communication strategy* (b) with *communication strategy*

Figure 5.8: Optimal infrastructure (left axis) and number of EVs passing in front of each station (right axis) for F_4

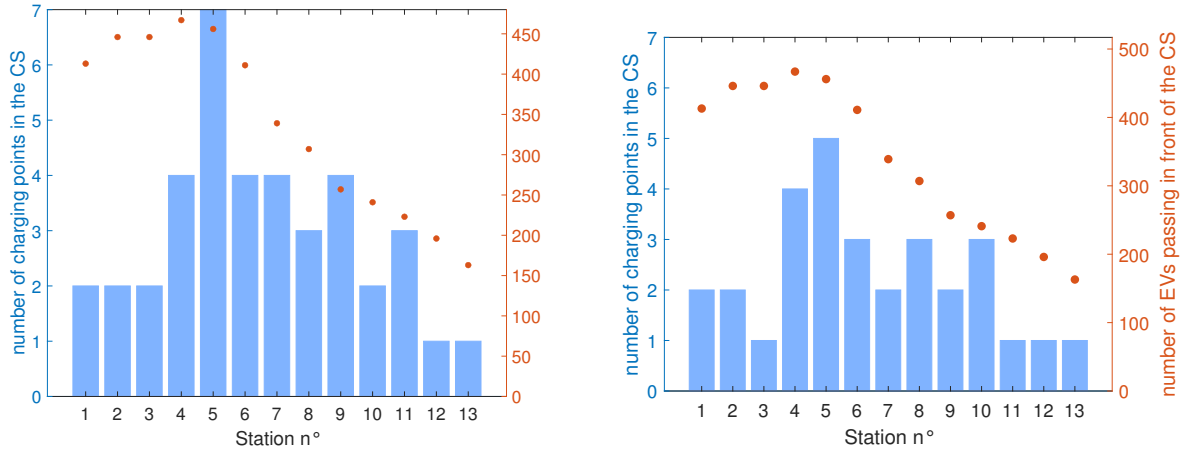

(a) with *no-communication strategy* (b) with *communication strategy*

Figure 5.9: Optimal infrastructure (left axis) and number of EVs passing in front of each station (right axis) for F_5

Figure 5.5 to Figure. 5.9). Since each fleet can represent a high-traffic situation in real life, we should compute the optimal infrastructure for all the fleets simultaneously and then compare those optimisation results for the communication and the no-communication strategies. By optimising the infrastructure for several fleets at the same time, the optimal infrastructure for the *communication strategy* should less overfit the charging infrastructure to only one specific fleet and this is what we study in next section.

5.4.2 . Optimisation 2 and 3: optimisation for all the fleets ($N_f = 5$) with one charging rate ($N_p = 1$)

For this second optimisation, we take the same fleets F_1, $F_2, \cdots$, F_5 as for Optimisation 1 but now, when we evaluate the waiting time constraint, we test the infrastructure layout on the five fleets (so $N_f = 5$ in the formulas in Section 5.2) to guarantee the waiting time maximum for all the fleets at the same time. We perform Optimisation 2 where T_{thres} = 20 minutes (Section 5.4.2.1) and then Optimisation 3 with T_{thres} = 30 (Section 5.4.2.2) minutes to assess how the waiting time threshold influences $DEAC_{FCI}$. For both thresholds, we run several times the GWO and for each run, we initialised the pack of grey wolfs with the best layout found during the previous optimisation.

5.4.2.1 . Optimisation 2: T_{thres} = 20 minutes

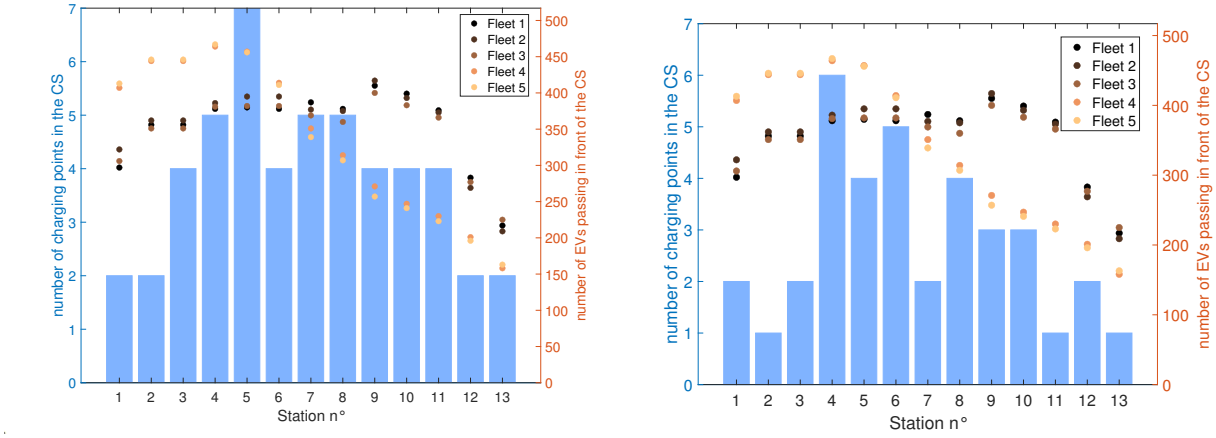

(a) with *no-communication strategy* (b) with *communication strategy*

Figure 5.10: Optimal infrastructure (left axis) and number of EVs passing in front of each station (right axis) for the five fleets ($P = \{175\}$ kW and T_{thres} = 20 min)

Table 5.9 summarises the costs $DEAC_{FCI}$ and the number of charging points obtained for each strategy. The *FCFS communication strategy* proves again its efficiency to reduce $DEAC_{FCI}$ compared with the situation of reference with even larger reduction percentages than in **Optimisation 1** (26.0 % according to Table 5.9). This improved performance is due to the fact that with the *no-communication strategy*, the EVs do not change their charging plan during their trip so the CPO is often compelled to put in a station the highest number of charging points among all the individual optimal infrastructure to guarantee for all the fleets a waiting-time maximum whereas it is not the case with the *communication strategy* (Figure 5.10b).

5.4.2.2 . Optimisation 3: T_{thres} = 30 minutes

For this optimisation, T_{thres} = 30 min. Figure 5.11 gives the optimal infrastructure computed for no-communication and communication strategies. We observe that the infrastructure for

Table 5.9: Number of charging points per station and daily equivalent annual cost $DEAC_{FCI}$ of the optimal infrastructure according to the strategy

Strategy	No-communication	Communication	Reduction (%)
Total number of CPs	45	36	20
$DEAE_{FCI}$ (€/day)	1,567	1,152	26
$DEAC_{FCI}$ (€/day)	−1,357	−2,009	26.0

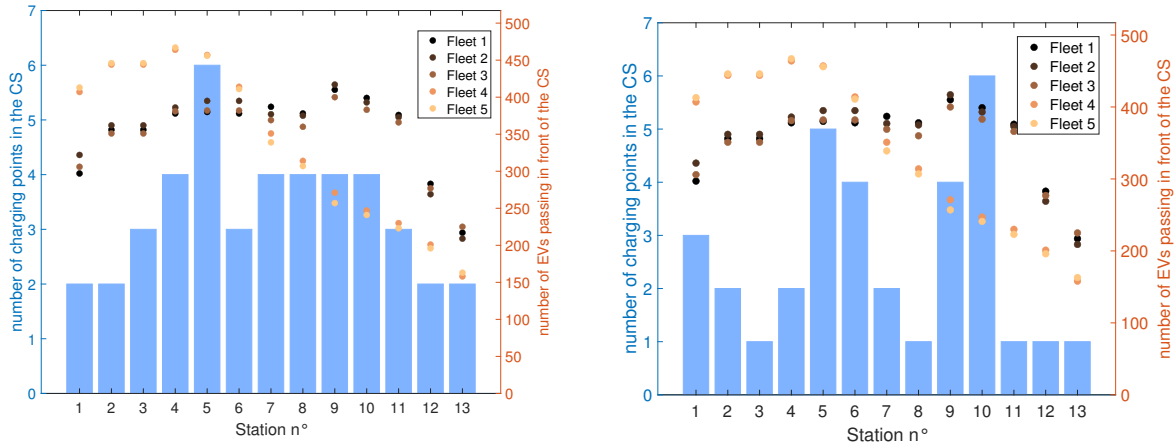

(a) with *no-communication strategy* (b) with *communication strategy*

Figure 5.11: Optimal infrastructure (left axis) and number of EVs passing in front of each station (right axis) for the five fleets ($P = \{175\}$ kW and T_{thres} = 30 min)

the *communication strategy* presents peaks of chargers in some stations while the others have only one or two chargers. Again, like in Optimisation 1, this result is due to the reduction of charger cost when the number of installed chargers in a station increases. We can wonder if the presence of those charger peaks in some stations will be a problem if we test the infrastructure with other generated fleets or if the communication strategy will help keeping the waiting time threshold under T_{thres} = 30 minutes

Table 5.10 summarises the costs $DEAC_{FCI}$ and the number of charging points obtained for each strategy when T_{thres} = 30 minutes. According to the results, the communication strategy still performs better compared with the no-communication and the increase of the waiting time threshold to 30 minutes allows to reduce the $DEAC_{FCI}$ by more than 13% in a case of no-communication and by only 4 % in a case of communication. However, that lower reduction with communication is likely due to the non convergence of the GWO and a better infrastructure layout might exist for the communication strategy when $T_{thres.}$ = 30 minutes.

5.4.3 . Optimisations 4 and 5: optimisation for all the fleets ($N_f = 5$) with multiple charging rates ($N_p > 1$)

In this section, we present the results of Optimisation 4 and 5 where the stations can propose two power levels: 50 kW and 175 kW. When multiple charging rates are considered in stations, we attribute to the drivers a vot. In Optimisation 4, this value is equal to 20 €/h and

Table 5.10: Number of charging points per station and daily equivalent annual cost $DEAC_{FCI}$ of the optimal infrastructure according to the strategy (T_{thres} = 30 minutes). The percentages in parenthesis represent the relative reduction of each result compared with the equivalent result from Optimisation 2

Strategy	No-communication	Communication	Reduction (%)
Total number of CPs	41	32	22
$DEAE_{FCI}$ (€/day)	1,3512 (-13.8%)	1,065 (-8%)	21
$DEAC_{FCI}$ (€/day)	−1,810 -(13.5%)	−2,096 (-4%)	15.8

for Optimisation 5, it is equal to 50 €/h. We remind that the possible available power levels in each station are: 50 and 175 kW. The waiting time threshold is again 20 minutes for both Optimisations.

For Optimisation 4, we first determine by iteration the optimal infrastructure for the *no-communication strategy* considering that all stations propose at least one charger per power level and then we remove the powers that were not used per station if any. We obtain the infrastructure layout presented in Figure 5.12a and notice that no 175-kW chargers are kept in the process because all EVs choose the 50-kW sockets to charge. This choice is due to the vot of the EVs (vot = 20 €/h) that favour cheaper solutions ($p_{charge}(50kW)$ = 0.35 €/kWh) even if they will take more time to charge. The $DEAC_{FCI}$ of the layout presented in Figure 5.12a is −132 €/day instead of −1,357 €/day as in Optimisation 2 (Section 5.4.2.1): the 50-kW chargers are cheaper to install compared with 175-kW chargers but the revenue they generate is not as important as for an infrastructure with only 175-kW chargers. Thus, if the CPO want to increase their revenue, they should propose only 175 kW in stations to force EVs to charge at 175 kW. In addition, the number of charging points to install with only 175-kW chargers is far less than with only 50-kW chargers (50 against 89).

However, as the 50-kW chargers are cheaper to install, it may be possible to find a layout for which the $DEAC_{FCI}$ is lower than −1,357 €/day (only 175 kW chargers) with some stations equipped only with 50-kW chargers and the others with only 175-kW sockets. We run the GWO to find those layouts for communication and no-communication strategy but the optimiser did not converge to a layout with a lower $DEAC_{FCI}$ than the ones found with Optimisation 2 ($P = \{175kW\}$).

For the Optimisation 5, the vot is now equal to 50€/h and the infrastructure layout obtained by iteration for the no-communication strategy is given in 5.12b. Now, like for the vot = 20 €/h, the drivers only select one type of chargers but this time, they choose the 175-kW level. The high value of the vot (50 €/h is considered as the vot of the drivers travelling for professional purpose) have led all the drivers to choose the highest power level to charge faster and gain time even if the charging price is highwer. Again, we have run GWO to find better layouts but the optimiser did not propose better values than Optimisation 2.

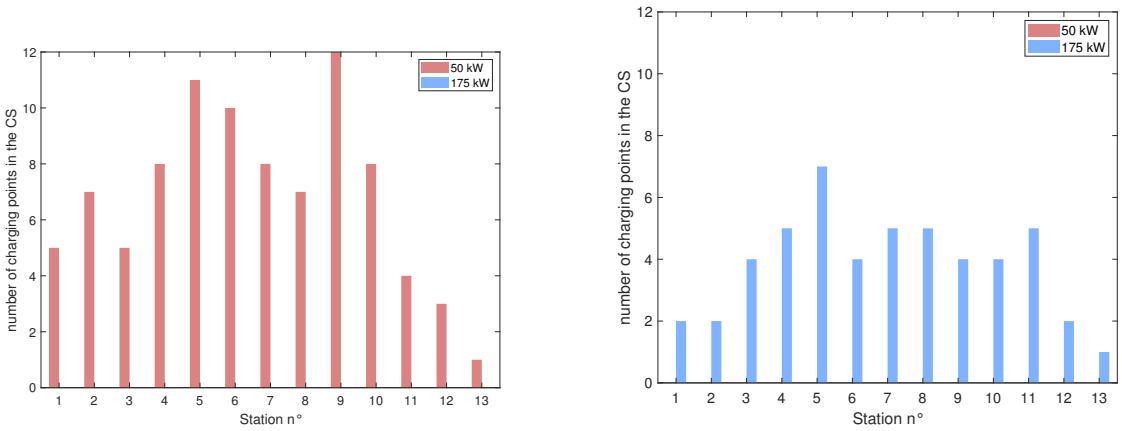

(a) with *no-communication strategy* (vot = 20 €/h) (b) with *no-communication strategy* (vot = 50 €/h)

Figure 5.12: Infrastructure layout obtained by iteration for the five fleets without communication (N_f = 5, N_p = 2)

5.5 . Conclusion

We have proved in this chapter the benefit of the communication since it helps reduce by at least 15 % (for the Optimisation with $N_f = 5$) the fast-charging infrastructure daily equivalent annual cost while guaranteeing a waiting-time maximum in stations. We compared the performance of the strategies on only five different fleets but according to the all the results, the communication always lead to an infrastructure with the lower cost compared with the no-communication strategy.

However, we use a strict threshold on the waiting time, meaning that 100% of the charging sessions should respect the constraint. Yet, we can wonder if we will still get the same level of cost reduction between the *FCFS communication strategy* and the *No-communication strategy* if we authorise the constraint to be met for the 99% percentile of the waiting-time distribution instead of 100% (like in [97]).

We also tested different value of waiting time threshold and we found that increasing the threshold from 20 minutes to 30 minutes reduces by 13% the costs for the no-communication strategy but by only 4% for the communication strategy. However, this last result should be taken carefully as we are not assured that the optimal layout found for the communication strategy is the best layout. More iterations of the GWO should be carried on.

Concerning the vot, we tested two values but for the first one, 20 €/h, all the non communicating EVs prefer charging at 50 kW and for the second value, 50 €/h, all the drivers select 175-kW chargers. In the first case with 20 €/h, the infrastructure found iteratively includes only 50 kW chargers so the profitability of the infrastructure is smaller, the number of chargers to install is much higher and the . For next studies, we should consider several class of drivers with a different vot in each class to better model the real-world strategy the EV drivers will follow and optimise the infrastructure accordingly.

For the evaluation of the infrastructure cost, as the number of EVs is growing and the infrastructure must be deployed accordingly, we should think about a way to compute the infrastructure cost dynamically according to the evolving needs and not with a constant cost as in a steady-state.

Finally, to take into account both CPOs and EV drivers' point of view, the next step is to establish the trade-off between the time spent in station T_{CS} and the cost of the charging infrastruc-

ture thanks to a multi-objective optimisation. We will detail this multi-objective optimisation in Chapter 6.

6 - Trade-off between fast-charging and infrastructure development cost

We have seen in the previous chapter the charging infrastructure optimisation with the FCFS communication strategy, where we perform a mono-objective optimisation of the charging infrastructure. The EVs in the fleet had the same charging power characteristics. In this chapter, we want to focus on another aspect the charging service, the influence of the charging power on the infrastructure to be developed independently of the *FCFS communication strategy*. EV drivers expect ultra-fast charging sessions to hasten the charging process, so they will tend to buy EV models with high charging rates. We will present in this chapter a multi-objective optimisation of the infrastructure cost and the average time spent in stations for fleets using a new strategy, the last reachable station strategy. This chapter assesses the trade-off between the benefit of increasing the proportion of high-charging-rate EVs in the fleet and the infrastructure cost. We will first present the impact of the charging power on the need for infrastructure and the influence of the battery pack characteristics on the charging rate accepted by the EV. Secondly, we will present the method used for the multi-objective optimisation before giving the results of the case studies based on the French highway A6. We will size the infrastructure according to the average annual daily traffic (AADT) on the highway instead of the traffic during crowded days.

The case studies in this chapter were established before the studies from Chapter 5, so some of the parameters taken for the scenarios in this present chapter are different and might be less representative of the situation nowadays. Still, they constitute a starting point for the reflection on the charging rate impact on the time spent in stations and on the infrastructure cost that could be adapted later to case studies with *FCFS communication strategy*.

Contents

6.1 . Fast charging challenges

As we have seen in 1, one of the levers to improve the acceptance of EVs is the reduction of the charging time for long-distance trips. The charging time reduction directly enables the reduction of the trip time $T_{trip,v}$ but, it indirectly induces the reduction of the waiting time as a lower service time (here the charging represents the service) implies a lower waiting time.Thus, it should be interesting to increase the DC charging rate of an EV to charge faster and reduce both charging time and waiting time.

6.1.1 . Increasing the charging rate and infrastructure needs

If the power increases on the EV side, adequate infrastructure should be developed to propose high charging rates (350 kW). As installing ultra-fast charging points (350 kW) generates higher costs [26, 63], we can wonder to what extent the gain of time induced by ultra-fast-charging EVs (UFC EVs) and high power infrastructure is worthwhile compared with the additional cost of the adapted infrastructure. To answer that question, we tune the share of UFC EVs travelling on the highway and, for a given percentage, we determine the pareto front that compares the cost of the charging infrastructure built and the time saved with that infrastructure layout. To evaluate the average time spent in stations, $\overline{T}_{CS}(s)$, for each infrastructure layout, we simulate fleets of 50 EVs to get a first insight into the infrastructure to be developed in case of a low AADT on the highway. We did not have time to explore the case with more EVs (in Chapter 4, we considered the AADT equals to 180 EVs). Still, this study gives some elements to evaluate the infrastructure needs if we size the infrastructure according to a low long-distance trips AADT on the highway instead of the EV volume on the highway during a crowded day (like in Chapter 5).

In this chapter, like in the previous chapter (Chapter 5), we determine the infrastructure needs thanks to the simulation of real-world long-distance trips with the simulation framework. However, we assume that the drivers follow another strategy, the **last-reachable-station strategy** (LRS strategy). Unlike the *no-communication* and *FCFS communication strategies*, the *LRS strategy* is not based on optimising the charging plan, but on the last station an EV can reach with a full charge. This strategy is supposed to report on the behaviour of EV drivers who prefer to charge the maximum energy they can (80% of the battery) before leaving the station and make the minimum number of stops.

Last-reachable station strategy

EV_v using the last-reachable station strategy charges to 80% of SoC at the furthest charging station it can reach with $SoC_{start,v}$. Then, it charges again to 80% of SoC at the last reachable station and so on until it reaches its destination d_v. As the EVs are not optimising their charging plan, they must choose a charging power level when stopping in a station with multiple charging rates. Thus, when in such a charging station, the EVs start charging at the most powerful chargers by order of arrival (FCFS) and if one level of power is saturated, the EVs charge at a lower level. When all chargers are used, the EVs wait until a charger becomes free.

The LRS strategy was chosen in [20] as a strategy of reference to prove in comparison the efficiency of the communication strategy proposed in this same paper. For the studies in this

chapter, we choose this strategy to represent the 'worst' situation where the EVs do not optimise their charging (whereas it is the case with *no-communication* and *communication strategies*) and do not communicate (contrary to the *FCFS communication strategy*).

6.1.2 . Battery architecture and battery cell c-rate

The DC charging rate of an EV depends on different characteristics of the battery pack but also on the way the BMS manages the charging. The significant characteristics impacting the charging rate are the battery architecture (400V and 800V), the c-rate of the battery cell, and the battery's capacity. The battery is in fact a battery pack of several battery cells that are organised in a certain architecture: SsPp where S gives the number of battery cells in series and P the number of battery cells in parallel. Thus, the nominal voltage of a battery pack is $V_{pack} = S \times V_{cell}$ with V_{cell} the nominal voltage of the battery cell. The battery architecture 400V or 800V indicates in which range the nominal voltage of the battery pack, V_{pack}, is: between 150 and 450V we speak of '400V architecture' and from 450V to 870V, we consider the battery has a 800V architecture [125].

We note the battery capacity E_{batt} (in kWh) and the constant current intensity the battery can deliver during one hour, C_{batt} (in Ah). The conversion from $C_{batt.}$ to E_{batt} is $E_{batt.} = C_{batt.} \times V_{pack}$.

The c-rate of the battery cell indicates how fast a battery cell can charge: the higher the c-rate is, the faster the battery cell can charge. The c-rate is equivalent to an intensity and is expressed in A and most of the time we speak of the c-rate as 1C, 2C, C/10 $\cdots$, with C the battery capacity $C_{batt.}$. If a battery cell can charge only up to 2C, it means that the totality of the battery cell capacity can be restored in minimum 30 minutes:

$$C_{batt.} = c_{rate} \times \Delta t \Rightarrow C_{batt.} = 2C_{batt.} \times \Delta t \Rightarrow \Delta t = \frac{1}{2}\text{h} \tag{6.1}$$

Now that the battery characteristics are explained, lets see the characteristics of the DC chargers. The indication of power given for each type of chargers, for instance 175 and 350 kW is incomplete since, in reality, it is often the current intensity delivered by the charger that limits the charging speed. Nowadays, the **175kW chargers** deliver a maximum of **350 A** and the 350kW chargers, 500A, but those maximum will certainly be higher in the future. Therefore, if the current intensity $I_{charger}$ is limited on the charger side, it is interesting to increase the voltage of the battery pack V_{pack} (by switching from a 400V architecture to an 800V architecture) to charge at a higher power P the battery since $P = V_{pack} \times I_{charger}$. This is why some OEMs have changed the battery architecture of their EV models to an 800V architecture to benefit from higher charging rates.

However, because of the maximum c-rate a battery cell can handle, the difference of power we can have between an 800V architecture and a 400V architecture is not as big as we can expect. For instance, lets consider two EV models, a 70kWh Hyundai Ioniq 5 with an 800V architecture and another model, identical to the Ioniq 5 but with a 400V architecture. The battery cell c-rate is set to 3C and the battery capacity to 60 Ah. If we charge those two models on a 350kW charger, the Ioniq will charge at a maximum of 240 kW and the 400V model at 220 kW (Figures 6.1a and 6.1b). For the 800V architecture, the limitation of the charging power is due to the battery c-rate maximum of 3C since the current intensity from the charger can go up to 250 A (500 / 2) in a branch but the battery cell can only handle 180 A (3 times 60 A with the c-rate = 3C). On the contrary, for the 400V architecture, the limit is on the charger side with up to 166 A per branch.

Consequently, the 800V architecture is not the only battery characteristic that differentiate the fast-charging and the ultra-fast-charging EVs, the charging speed depends on other battery

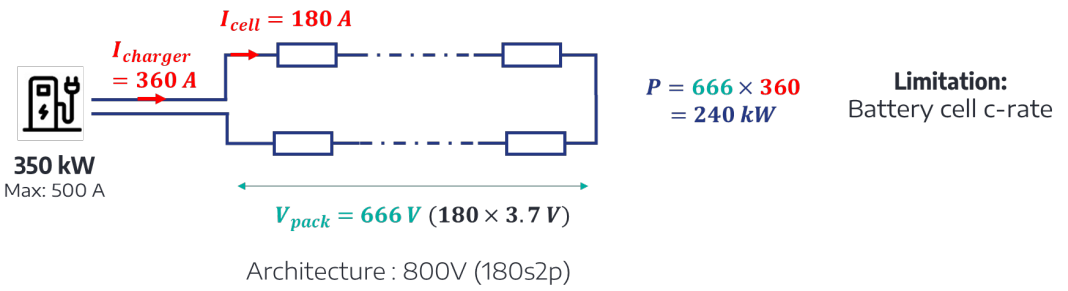

(a) Charging process of an 800V system EV (Hyundai Ioniq 5 - 72.8 kWh) on a 350 kW charger.

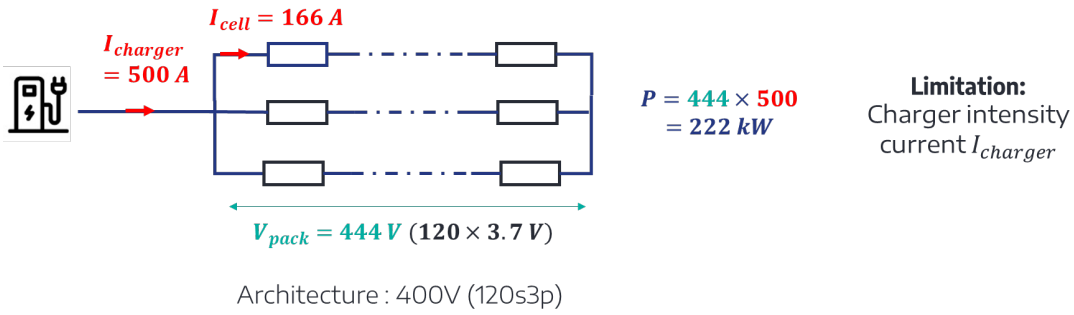

(b) Charging process of a 400V system EV (72.8 kWh) on a 350 kW charger ;

Figure 6.1: Charging process of a 70 kWh EV with $C_{batt.} = 60$ Ah and c-rate = $3C$

characteristics too and the battery management system also plays a role in accelerating the charging process. Note however that the 800V architecture is interesting for bigger battery pack (> 60 kWh) since they have more battery cells that can be put in series to increase the voltage of the pack without lowering much the number of branches and limiting this way the current maximum going in the branches.For instance, with a 96-kWh pack of 456 cells, the 800V architecture will be with 3 branches (152s3p) instead of 2 so the current will not be limited by the battery c-rate contrary to the previously studied EV with a 70-kWh battery (Figure 6.1a). In this chapter, we will not classify like we did in the article [126] the 400V-system EVs as fast-charging EVs and the 800V-system EVs as ultra-fast-charging to assess the benefit of a 800V-system EVs since we have just seen that the reality is more complex. Instead, we consider that the FC EVs charge at a maximum of 100 kW and the UFC EVs charge at 350 kW as described in Figure 6.2.

In reality, no battery pack can charge nowadays with a power of 350 kW but we hypothesise that in the future, this will be possible. Charging a 70-kWh battery pack at 350 kW means that we need battery cell with a c-rate equals to more than 4C and chargers providing at least 540 A (and not only 500 A). This is possible but we can wonder if a high c-rate will not harm the battery. Still, as we want to assess the impact of the charging speed on the infrastructure cost and the drivers' satisfaction, we consider as charging rate the highest power proposed in European ultra-fast charging stations (350 kW).

We should also mention that in reality, the charging rate is not as close to the maximum charging rate (100 or 350 kW) during the whole charge as it is in Figure 6.2 since the power normally drops from a certain SoC (quite low, between 20 to 30 %) to respect the charging profile of the battery pack and avoid overheating the battery. However, we simplify the problem and assume again that we consider the highest rate a charger can deliver to an EV according to it charging rate limitation (100 or 350 kW).

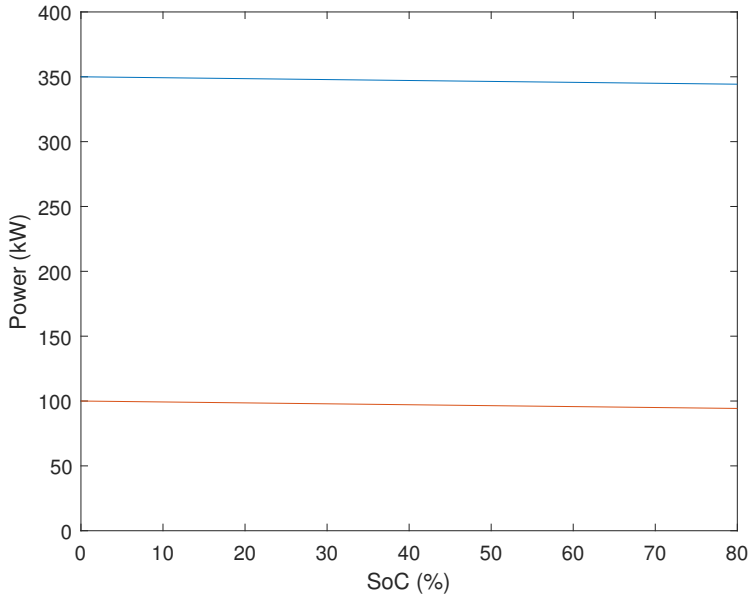

Figure 6.2: Charging curves of the 100kW and 350kW-charging EVs

6.2 . Multi-objective optimisation of the charging infrastructure

6.2.1 . Problem formulation

The problem formulation of this optimisation is similar to the one explained in Section 5.2.1 of the previous chapter, except that we perform a multi-objective optimisation: we consider the average time spent in stations, $\bar{T}_{CS}$, as an objective of the optimisation in addition to the infrastructure cost $DEAC_{FCI}$ (6.2). We test in this chapter 100 fleets of 50 EVs each ($N_f = 100$ and $N_{EV} = 50$, see Section 6.1.1) to compute the average time spent in stations $\overline{T}_{CS}$ and to check the constraint on the waiting time (6.3).

$$Objective : \min_{s} \left(DEAC_{FCI}(s),\ \overline{T}_{CS}(s) \right) \tag{6.2}$$

$$s.t.\ \forall\ EV_v,\ \forall\ CS_i \in \mathbb{CS}(s),\ t_{wait,v,i} \leq T_{thres.} \tag{6.3}$$

$$B_{ineq}.s < c_{ineq} \tag{6.4}$$

The time $\overline{T}_{CS}$ is the average time spent in stations by the EVs from the N_f fleets:

$$\overline{T}_{CS}(s) = \frac{1}{N_f \times N_{EV}} \sum_{f=1}^{N_f} \sum_{v=1}^{N_{EV}} T_{CS,f,v}(s) \tag{6.5}$$

$T_{CS,f,v}$ is the time spent in stations by EV_v from the fleet F_f when the infrastructure layout is described by s.

Concerning the constraint on the charging points, contrary to the problem depicted in Chapter 5, we accept in this chapter that the number of charging points can be null in some service areas to determine the optimal location of the charging stations. The expression (6.4) from the problem formulation gives the constraints on the charging station's location to avoid an EV from the tested fleets running out of battery. Indeed, if a service area is free of chargers, EVs will have to drive more to reach the next station, and sometimes, they will not have enough range to do so. Hence, we define a matrix B_{ineq} and a vector c_{ineq} such as: If $B_{ineq}.s < c_{ineq}$, then $\forall\ j \in [\![1,\ N_f]\!]$, $\forall\ EV_v \in F_j$ EV_v can reach d_v.

To ensure that all the EVs can reach their destination, clusters are determined according to the fleet's minimum range, to the SoC at the entrance of EVs, or to the SoC required when leaving the motorway.

6.2.2 . Charging infrastructure cost $DEAC_{FCI}$

The infrastructure cost definition is the same as in Chapter 5 and only some parameters used to compute this cost change from a chapter to the other (see Table 6.1). Note that the hardware costs are higher in this chapter than in Chapter 5 because we keep the value given in [26] without applying an annual decrease of 3% and the electricity price p_{el} for industrials is lower here since the study was done at the beginning of 2022 before the electricity price rise. The discount rate is also lower as well as the lifetime of the charger compared with Chapter 5 but the resulting coefficient, $\frac{r(1+r)^L}{((1+r)^L-1)}$, are approximately equals from a chapter to another (0.131 for the coefficient in Chapter 5 and 0.129 in this present chapter). Therefore, the only real difference between the two chapters is the hardware cost of the chargers.

Table 6.1: Values of the parameters used in this chapter

parameter	description	value %
p_{el}	electricity price per kWh for industrials	0.08 €
p_{charge}	energy price per kWh for EV drivers	0.35 € (50 kW)/ 0.59 €(150 kW)/ 0.79 € (350 kW) [1]
$C_{hard.,j}$	hardware cost per networked charger	65,000 € (150 kW)/ 120,000 € (350 kW) [2]
C_M	maintenance cost	1% of the investment
r	discount rate	5%
L	lifetime of the chargers	10 years
N_{area}	number of service areas along the highway	13
N_f	number of fleets in the sample	100

6.2.3 . Computing T_{CS} and the waiting time per session

We need the simulation framework described in Chapter 3 to check the waiting time for each charging session and determine the average time spent in stations by all the fleets ($\overline{T}_{CS}(s)$) according to the infrastructure layout s (6.5). However, contrary to the case studies in the previous chapters, we assume the EVs use another charging strategy, the *last-reachable station strategy* (see Section 6.1.1).

Like in Chapter 5, the waiting time per session is constrained by a waiting time threshold $T_{thres.}$ that we set to **15 minutes**. This threshold is lower than the ones considered in Chapter 5 ($T_{thres.} = 20$ or 30 minutes) since we accept less waiting time for a flux of EVs representing

[1] prices charged by Fastned [119] for charging at 150kW chargers and by Ionity in France [44] at 50 kW and 350kW chargers.

[2] The hardware costs come from [26].

an average traffic on the year and not a crowded day. Indeed, if we accept a high waiting time threshold $T_{thres.}$ for the average traffic, the infrastructure saturation would be unbearable during crowded days.

Figure 6.3 describes the process used in this chapter to optimise the infrastructure.

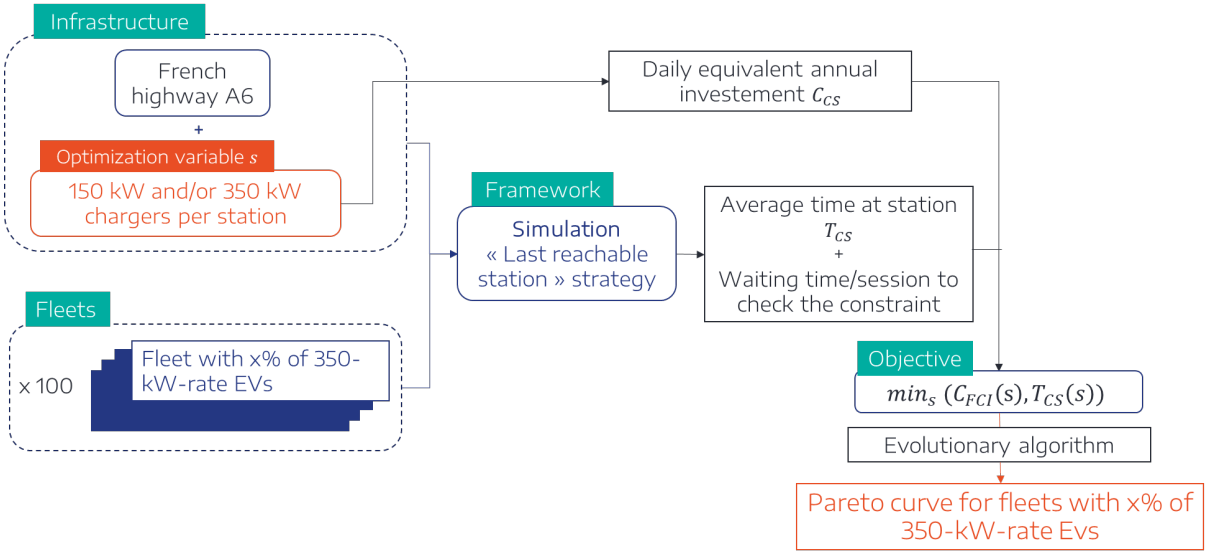

Figure 6.3: Process of the multi-objective optimisation using the simulation framework

6.2.4 . Optimisation with a differential evolution algorithm

The problem (6.2) is solved using a differential evolution algorithm to perform the mutation and the cross-over in the population of chargers distribution while the selection of the new population (the convergence) is done in the same way as in the NSGA-II algorithm [127] with a non dominated sorting of the population before selection. The parameters we use for the optimisation are given in Table 6.2.

Table 6.2: Parameters of the NSGA-II differential evolutionary algorithm for MOO

Number of genes	Population size	Number itera-tions	Precision	Mutation coeffi-cient	Crossing coeffi-cient
26 (2×13)	104 (4×26)	200	0.01	1	2

6.3 . Case studies

6.3.1 . Highway details

The parameters of the highway correspond to the ones of the French A6 highway (direction Paris - Lyon) (see Figure 6.4). Unlike the other studies in this manuscript, all the entrances/exists (51) of the highway are considered. The possible charging stations are still located in the service areas.

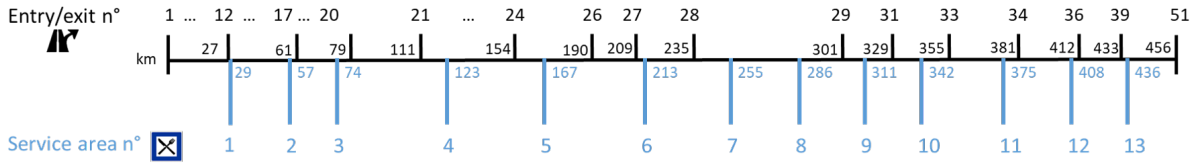

Figure 6.4: French highway A6

6.3.2 . Fleet generation

As we want to study the influence of the charging rate limit of the EVs on the service quality and the infrastructure cost, we set the same specific characteristics for all EVs in the fleet except for the level of charge (P_v).

We set the battery capacity to **70 kWh** for all the EVs in the fleet as an average of the battery capacity over all the EV models. This is the capacity chosen in the study by Enedis and RTE on the infrastructure to be developed for long-distance mobility [13]. In addition, as explained in Section 6.1.2, the maximum power an EV can handle depends on the battery's capacity. Hence, we need a relatively high battery capacity to reach high charging rates (≥ 60 kWh).

The characteristics of the EVs are given in Table 6.3.

Table 6.3: Characteristics of EV in the fleet

Capacity E_{batt_v} (kWh)	Maximum Power $P_{max,\,v}$ (kW)	Charging coeffi-cient	Speed limit (km/h)	Consumption rate (kWh/km)
70	100 or 350	500	130	0.25

The maximum power for the EVs $P_{max,\,v}$ is either 100 kW for the fast-charging EVs (like the Peugeot e-208 [128]) and 350 kW for the ultra-fast-charging EVs (see Figure 6.5). Nowadays, no EV model reaches 350 kW when charging because of the c-rate limitation of the battery cells (see Section 6.1.2), but to mark a clear distinction between the fast-charging and ultra-fast-charging EVs, we hypothesise that soon, some EV models will be able to charge close to 350 kW.

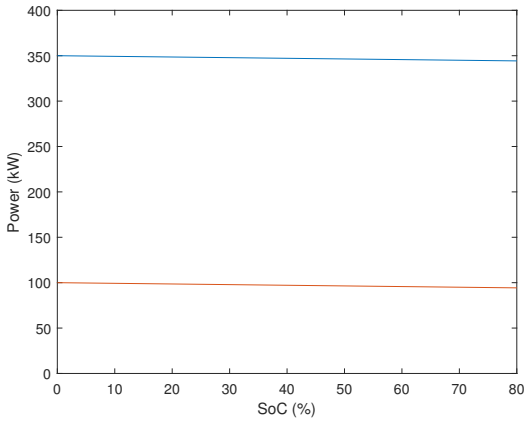

Figure 6.5: Charging curves of the 100kW and 350kW-charging EVs

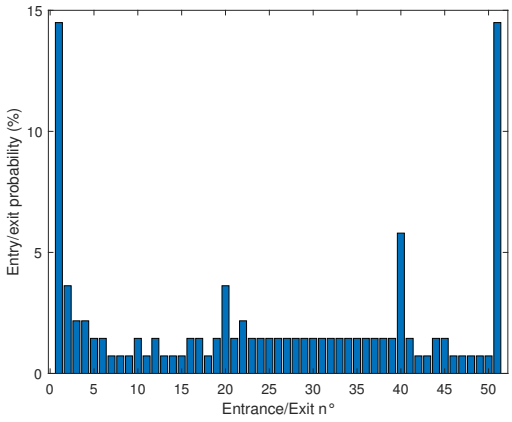

Figure 6.6: Entry and exit probabilities of each entrance/exit of the highway

We determine the pareto fronts for three different percentages x_{350} of 350kW-charging EVs in the fleets. The first test, with **1% of 350kW-charging EVs**, could represent the current situ-

ation with few electric vehicles able to charge above 250 kW DC, which is the closest value to 350 kW DC we can find on the roads nowadays. The second and the third situations, with respectively **50 and 100% of 350kW-charging EVs**, are meant to evaluate if automotive makers should develop 350kW-charging EVs or keep lower charging rates.

The SoC of each EV at the highway entrance follows a normal distribution (80%,15%) truncated at 40% and 95%. The SoC of an EV when it leaves the highway should be higher than 20%. The entrance o_v and the exit d_v of each EV_v are selected according to the probabilities given in Figure 6.6 with the condition that $o_v < d_v$.

6.4 . Pareto front results

This section presents the Pareto curves obtained after running the optimisation algorithm (see Figure 6.3) and a discussion about the results and the parameters used for the optimisation (Section 6.4.2).

6.4.1 . Trade-off between the daily equivalent annual cost and the time in stations

The Pareto fronts found for 1%, 50% and 100% of 350kW-charging EVs in the fleet are given in Figure 6.7. All the points on the different Pareto fronts have negative DEAC, which means that all those distributions of 150 and 350kW chargers are profitable for the charging operators.

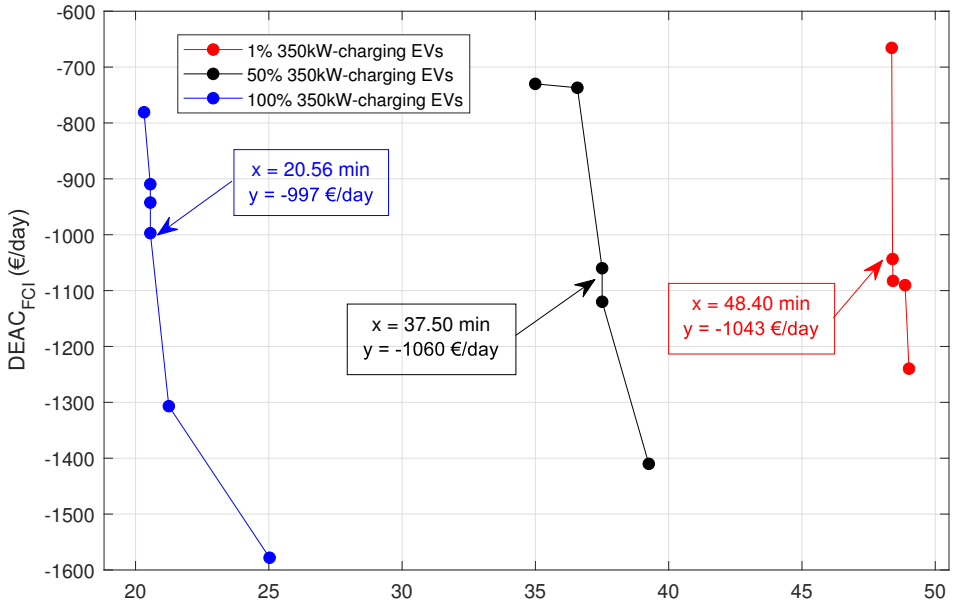

Figure 6.7: Pareto curves for 1%, 50% and 100% of 350kW-charging EVs in the fleet for MOO

We observe in Figure 6.7 that the best Pareto-front is obtained for the 100% 350-kW charging EVs share with time spent in stations running from approximately 20 minutes to 25 minutes for benefit evaluated respectively to 910 € and 1580 € per day ($-DEAC_{CI}$). This front is the best since all the points of the other Pareto-fronts are dominated by at least one point of the 100% front. More generally, it appears that the increase of the share of UFC EVs in the fleet always

decreases the average time spent in stations for optimal distributions of chargers. Indeed, if we focus on the Pareto-front of a given percentage, all the point on other Pareto-fronts corresponding to a higher share of UFC EVs are on the left of this Pareto-front. We solved another optimisation problem close to the one studied here with a genetic algorithm and found similar results: 100% shares of UFC EVs always lead to the best optimal infrastructure compared with lower UFC Evs shares.

Moreover, for the same (and sometimes even lower) cost of added infrastructure, increasing the share significantly reduce the time spent in the stations. For instance, the labelled points on Fig. 2.11 are on different Pareto-front and correspond almost to the same equivalent annual cost $DEAC_{CI}$ (approx. $-1,000e$) but the time spent in stations for fleets with 1% of UFC EVs is reduced by more than 20% in the case with 50% and divided by more than 2 in the 100% case. We even have a solution on the 100% Pareto curve (point (25 min,$-1,580$ €)) where time is reduced by 48% while guaranteeing a 27% decrease for the infrastructure DEAC compared with the optimal solution presenting the minimum EAC (and so the maximum benefit since DEAC < 0) in the situation with 1% (point (49 min, $-1,240$ €)).

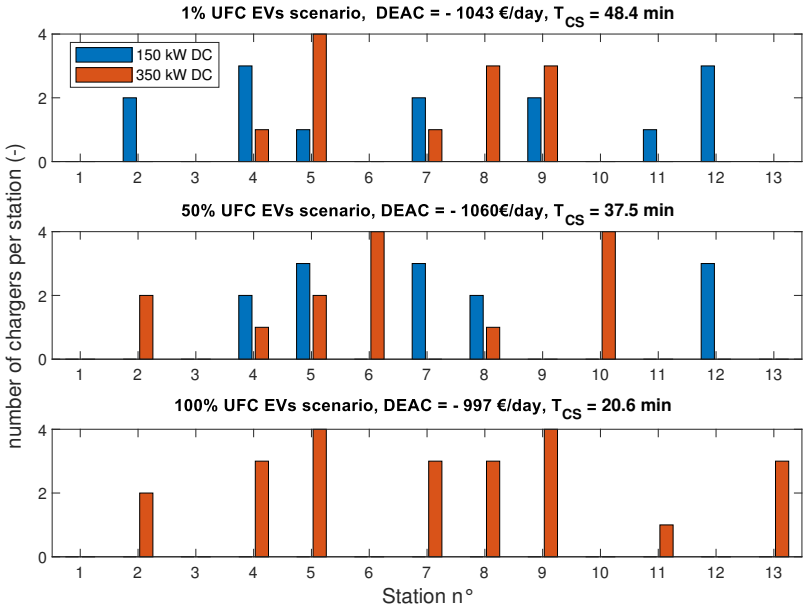

Figure 6.8: Example of 150 and 350 kW charger distribution for the labelled points in Figure 6.7.

Suppose we look at the distribution of chargers corresponding to the labelled point in Figure 6.7. In that case, we see that the power installed per station increases with the share of 350kW-charging EVs: 6300 kW installed for 1%, and respectively 6850 kW and 8050 kW for the 50% and 100% share (Figure 6.8). The power installed in the stations logically increases with the rise of the share, but the power only grows by 27% from the 1% to the 100% case, whereas the time spent in stations is reduced by more than 55%. Thus, the time spent in stations will be reduced with a manageable increase in installed power. The 8 MW of installed power for the 100% share is lower than the average installed power per station computed in the study by Enedis and RTE [13] for the scenario with the highest power demand (12 MW). The 100% distribution does not have any 150 kW charger, but it is not always the case for all optimal distributions found for the 100% share: for instance, the point (25 min, −1,580 €) with the lowest $DEAC_{FCI}$ corresponds to an infrastructure with the installation of 150 kW chargers at several service areas.

6.4.2 . Highlights and discussion on the results

We should bear in mind that we are not assured of finding the absolute best Pareto front with the evolutionary algorithms we used for the multi-objective optimisations, especially for this problem where the objective function is costly to evaluate. With 100 fleets to test for each layout s, one evaluation of the population (one iteration) by the algorithm was lasting approximately **40 minutes**. However, it is possible to find manually the lowest time we can obtain for a percentage of 350kW-charging EVs by incrementally adding 350kW chargers until the average time spent in the stations stops decreasing. Yet, we have observed that keeping some service areas with no chargers (like the area n°10 and 13) enables a better trade-off. Though, if the incremental addition of 350 kW chargers is done wisely, we can at least get the abscissa limit on the left of each Pareto front. Finding the lowest cost is more complicated. However, with the results of the evolutionary algorithms, we can find a solution we would not think of and keep searching manually in the same direction to get close to the absolute limit on the y-axis. Nevertheless, thanks to the studies lead in this chapter, we realise that the evolutionary algorithms we considered in this chapter were too long to converge and this is why we have used in Chapter 5 another algorithm, the GWO, to converge faster.

We optimised the daily equivalent annual cost of the infrastructure, so we consider the revenue generated by the charge for the CPO but we did not take into account the charging cost for the EVs in the optimisation. Consequently, for some stations where enough EV drivers stop to generate revenue that can compensate for the higher cost of one or more 350 kW chargers, the charging operators can obtain a lower $DEAC_{FCI}$ by replacing some 150 kW sockets with 350 kW chargers whereas most EV models can only charge at 100 kW and do not fully benefit from 350 kW sockets. The 100kW-charging EVs will pay more when charging at the 350 kW socket than at 150 kW sockets but will charge at the same speed as at a 150 kW socket. Therefore, this service will not benefit the EV drivers but only the charging operator. One solution would be to let the drivers choose the charging level best suited for their EV instead of always taking the highest-rate socket available, as it was implemented in this study. Then, if necessary, this solution can be combined with the consideration of the charging cost for the EV by remplacing the objective $\overline{T}_{CS}$ with the average discontent factor $\overline{DF}$ with $X \neq 0$ (see Equation (3.4)).

Another limitation concerns the hypothesis that UFC EVs with a 70-kWh battery pack are able to charge at power close to 350 kW during the whole charge whereas the current battery packs and the current intensity delivered by the chargers enables a power only up to 250 kW and for a few minutes before dropping to lower values (see Section 6.1.2). Thus, the gap between $\overline{T}_{CS}$ in the scenarios with 1% UFC EVs and the one in the scenarios with 100% might be in reality smaller than what we found in this chapter. Nevertheless, the conclusion will likely be similar if we reduce the charging power accepted by the UFC EVs to 250 kW, since the charging service will still be faster with 100% UFC EVs in the fleet than with 1%.

6.5 . Conclusions and perspectives

6.5.1 . Conclusion on the charging rate increase

We proposed in this chapter a methodology to evaluate the impact of developing 350kW-charging electric vehicle models on driver satisfaction and infrastructure cost. We performed a multi-objective optimisation using a mix of a differential evolutionary algorithm and NSGA-II. The studies aimed to find, for some chosen shares of 350kW-charging EVs, the optimal charging infrastructure layouts we should have on the French highway A6 to establish a trade-off between time spent in the station (influencing drivers' satisfaction) and infrastructure cost. To

compute the time spent in the stations, $\overline{T}_{CS}$, according to the infrastructure layout tested in the algorithm, we simulated many different EV flows on the highway based on actual traffic data and see how the EVs fan out in the charging stations. The time spent in stations T_{CS} and the average annual energy consumption used to compute the installation revenue were obtained thanks to the simulation framework described in Chapter 3.

The results showed that we could find several layouts of charging infrastructure for each percentage of 350kW-charging Evs that are profitable ($DEAC_{FCI} < 0$) and enable drivers to save as much time as possible. We can conclude that increasing the use of ultra-fast-charging EVs significantly reduces the time spent in the station for the user. At the same time, it is possible to find optimal infrastructure layouts that even lower the cost of chargers to be installed. Moreover, the installed power of the optimal infrastructure for 100% UFC EVs in the fleet is higher for the same $DEAC_{FCI}$ than for the other share of UFC EVs but the increase of the installed power is not as high as the time gain the 100% UFC EVs share brings to the fleet.

6.5.2 . Perspectives

As explained in Section 6.4.2 ,the charging price is often higher on 350kW sockets (depending on the charging operator), so, for next studies, we need to consider the charging cost for the user in the optimisation problem by setting the discontent factor as an objective of the optimisation instead of the sole time spent in stations. We should also allow the drivers to charge at the power level best suited for their EV model (100kW or 350kW-charging models). Those adaptations are needed when we have multiple powers possible per station as we did in Chapter 5 (when $N_p > 1$).

We should have more fleets in the testing sample to evaluate the time spent in the station (1000 fleets instead of 100) to get more exhaustiveness regarding traffic situations. Moreover, we have considered a fleet size of 50 EVs to reduce the evaluation cost of the objective function since we simulated 100 fleets of 50 EVs to compute the average time spent at stations and check the waiting time constraint. In reality, as seen in Chapter 5, the number of EVs going on long-distance trips can be much higher, for instance during holiday departure periods. Hence, we should evaluate how the optimal layouts evolve according to the size of the tested fleets to see if any trend emerges or if we need to apply the multi-objective method explains in this chapter for each fleet size we want to consider. In addition, if a trend is found, it would be easier to perform the infrastructure optimisation with a dynamic evolution of the number of EVs on the roads.

As for the hypothesis we have made about the drivers following the last reachable station scenario, we might introduce more random behaviour to study other possible distribution of charging events over the stations and see how the optimal planning of the charging infrastructure changes to determine the more restrictive scenario.

For instance, we can consider another strategy where the drivers stopped according to the value of their SoC. Thanks to the data retrieved from Stellantis connected vehicles, we were able to retrieve the SoC the connected EVs had when stopping to charge (see Figure 6.9) and we can use those data to elaborate a strategy of charge based on SoC.

We should aslo adapt the multi-objective optimisation presented in this chapter to a multi-objective optimisation where the *FCFS communication strategy* is used to compare its results to the one found in this chapter. An adaptation of the GWO algorithm to multi-objective optimisation exists, the Multi-Objective Grey Wolf Optimisation (MOGWO) [129], and could be run to perform this multi-objective optimisation with the *FCFS communication strategy*.

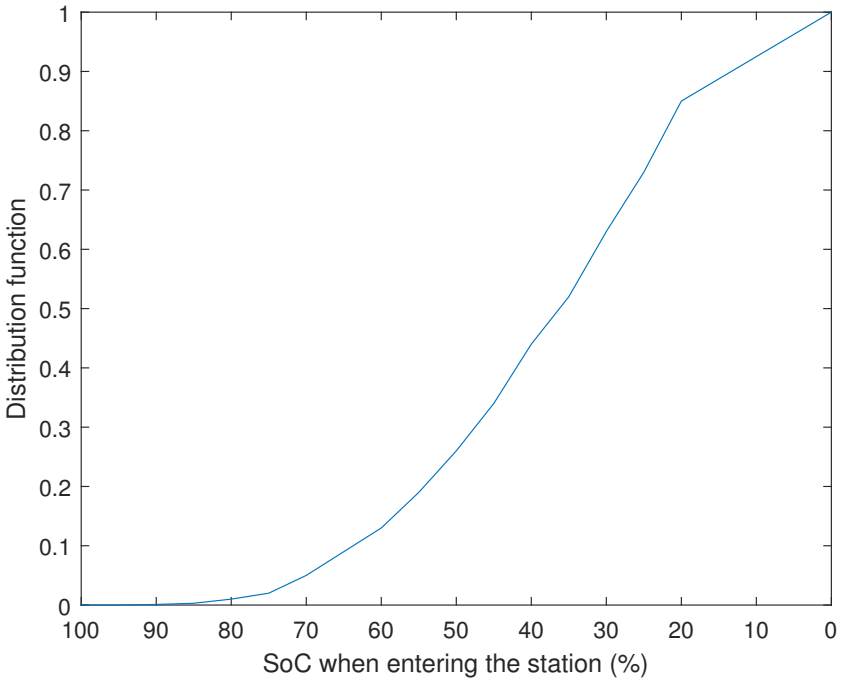

Figure 6.9: Distribution function of an EV SoC when entering a station to charge. This curve was extracted from Stellantis Connected EVs' data.

7 - Conclusion and perspectives

We have seen that the optimisation of the charging service to handle at the same time EV drivers' expectation and charging point operators' point of view is a complex problem. To answer the first objective of this thesis, we proposed to evaluate the performance of different control strategies and developed a multi-agent framework to perform the evaluation. We conclude about the control strategies in Section 7.1. Concerning the second objective, we focused on the planning of the infrastructure with and without the use of the *FCFS communication strategy* for a high traffic flow (Chapter 5) to demonstrate the benefice of the *FCFS communication strategy* in reducing the infrastructure cost with a mono-objective optimisation. Section 7.2.1 gives the conclusions about this optimisation. Then, to answer the third objective, we evaluated the impact of EVs' charging power on the trade-off between the infrastructure cost and the time spent in stations thanks to a multi-objective optimisation (Chapter 6). The communication strategy was not used in that last optimisation, and we present the highlights on that multi-objective optimisation in Section 7.2.2.

7.1 . Conclusions on the control strategies

7.1.1 . Optimising the charging plan

The optimisation of the complete charging plan to reduce trip time considering real-time waiting time and non-constant charging time is a non-trivial problem where linear programming is hardly possible. We compared in Chapter 3 three algorithms to optimise the charging plan.

The first solving algorithm is based on an **exhaustive method** where the potential charging plans are listed and the fitness of each potential solution is evaluated. This method enables charging only the energy required, thus giving lower optimal trip times. However, this method depending on the number of stops can be very time-costly to run and needs lots of data as the number of stops and of charging stations on the road increase. The second method relies on a genetic algorithm to find the amount of energy to charge per station. This method does not depend on the number of charging stops and can approach the global optimal value of the charging plan. Nevertheless, the result is not deterministic, and the genetic algorithm is the slowest method among the three studied. The third method tested is dynamic programming (DP), where the problem is divided into sub-problems associated with each charging station. We found a way to consider charging-plan-dependant waiting times in the dynamic programming whereas we did not find it in the literature [19]. Contrary to the other methods, the DP overestimates the energy to recover in stations, so the charging time is not the optimal one, but the method does not depend on the number of charging stops and does not need to list all the possible charging plans. Depending on the number of stations on the EV's way, the DP can be faster than the exhaustive method.

The DP appears to be the best method to optimise EV charging plans in real-world situations. It should be tested in the simulation framework to evaluate its performance in a dynamic traffic flow.

7.1.2 . Determining optimal charging control strategy

The introduction of communication between the EVs and the CSs to retrieve waiting time estimation according to the information shared by the EVs is the first step to better use the charging infrastructure and reduce the waiting time. Then, if in addition, the EVs minimise their

total trip time on-the-move by optimising their complete charging plan, in other words where they will charge and which amount of energy they will recover, the efficiency of the control strategy is improved. We proposed to study and improved a strategy, the *FCFS communication strategy*, that enables both the optimisation of the complete charging plan and the dynamic share of waiting time predictions. The strategy is decentralised, thus better scalable, and it is shown in [24] that the *FCFS communication strategy* performs better than the *no communication strategy*.

However, the *FCFS communication strategy* is based on a non-cooperative game even if the EVs are sharing their charging plan since each EV optimises its charging plan in a decentralised manner and chooses the plan best suited to minimise its own trip time and not the average trip time of the fleet. In addition, the priority rule in this strategy is set on a First-Come First-Served basis so EVs cannot charge on the charging slot best suited for them. Thus, we compared the *FCFS communication strategy* with a *reservation strategy* based on advance booking of charging sessions (delimited in time) to ensure that the EV will charge during the time interval that best minimise its trip time considering the bookings of other EVs. The pre-emption was not authorise for *reservation strategy* since it could deteriorate the EV drivers' experience with constant plug-in and unplug-in to let EVs with higher priority charge.

According to the results of the comparison, the *FCFS communication strategy* performs better than the *reservation strategy* since the booking of charging sessions make some EVs wait for very long time because they have to wait for higher-prioritised EVs to charge. This is due to the fact that, contrary to *FCFS communication strategy*, the first EVs to reserve do not consider the waiting time in the balance because all time slots are available. However, throughout the day, the number of charging time slots decrease and the EVs are compelled to choose charging session where they know they will wait a long time before charging. Moreover, the *reservation strategy* might be less flexible than the *FCFS communication strategy* if we take into account traffic hazards that can delay the arrival of EVs in stations and thus reduces the remaining time to charge during the booked time interval.

The comparison of both dynamic control strategies also show that even if the *FCFS communication strategy* better performs, the strategy is not sufficient to handle high saturation of the charging network so new charging points should be added in stations to improve the drivers' satisfaction by meeting the quality criteria set on the waiting time and the waiting queue length in stations.

After the comparison of both dynamic control strategies, we studied the robustness of the *FCFS communication strategy* when non-communicating EVs (following the *no communication strategy*) are introduced in the fleet. The performances of the *FCFS communication strategy* in reducing the trip time for the EVs using the strategy slowly deteriorate as the share of non-communicating EVs increases. However, this degradation of the strategy performances is gradual and with the presence of the communicating EVs, the overall average trip time for the fleet is improved compared with a situation without communication at all. This result is logical as the less the EVs are communicating, the less the stations can predict accurately the waiting time with the charging plans shared. Thus, solutions should be foreseen to improve the dynamic prediction of the waiting time and we suggest some ways of improvement in Section 7.3.1.

7.2 . Conclusions on the optimal charging infrastructure planning

Two of the objectives in this thesis are related to infrastructure planning according to different optimisation objectives and different charging strategies for the evaluation of the charging needs. We sum up the results obtained for each objective in the following sections.

7.2.1 . Optimising the infrastructure under real-time communication

We have compared in Chapter 5 the optimal infrastructure deployments in a situation where the EVs follow the *FCFS communication strategy* and another where the EVs use the *no communication strategy*. This study aims to quantify the benefit a control strategy that increases the use rate of the infrastructure (*FCFS communication strategy*) brings to a CPO. The optimisation objective is to minimise the infrastructure cost to consider the CPO's point of view and a waiting time threshold is set as a constraint. The problem is hardly differentiable since we need to run multi-agent simulations (MASs) to check the constraints under the different control strategies and the problem is similar to a combinatorial problem so we used a evolutionary-based algorithm, the Grey Wolf Optimiser to solve the problem. The Grey Wolf optimiser was chosen because it uses three best solutions to converge faster which is important regarding the running-time of MASs with the *FCFS communication strategy*.

We optimised the infrastructure for different EV fleets representing crowded days (500 EVs) and tested different waiting time thresholds (20 and 30 minutes), different values of time (20 and 50 €/h) for the drivers and different available power levels ($\{175\}$ kW or $\{50, 175\}$ kW). In all situations, the optimal infrastructure for both *communication and no communication strategies* is profitable for the CPO (the daily equivalent annual cost is negative) but it is interesting to see how the parameters affect the results. Increasing the waiting time threshold reduces by at least 13% the infrastructure cost with the no communication strategy and by only 4% with the *communication strategy* but better infrastructure layouts might exist for the *communication strategy* as we have no guarantee that the GWO gives the global optimal. Concerning the value of time and two available powers, a value of 20€/h leads all EVs following the no communication strategy to choose 50-kW chargers and the 50 €/h makes the drivers choose 175-kW. Thus, the vot has an important impact on the charging plan choices.

In any case, when we compare the optimal layouts induced by *communication and no communication strategies* for a given set of parameters (waiting time threshold, available power levels and value of time), the *communication strategy* always reduces the infrastructure cost by at least 15% and can go up to 26%.

7.2.2 . Higher power rates to reduce travelling time: impact on the infrastructure cost

In Chapter 5, we have also optimised the infrastructure layout but this time, we minimised both the trip time (time spent in stations) and the infrastructure cost according to the share of ultra-fast charging EVs (Power $\approx$ 350 kW) in the fleet. We tested 100 low-traffic fleets (50 EVs) to evaluate the average time spent in stations and the waiting time constraint (15 minutes maximum as we tested a low-traffic situation).

The ultra-fast charging EVs (UFC EVs) are randomly selected in the fleet and other EVs charge with a lower power (100 kW). The EVs do not try to minimise their trip time and follow the *last reachable station strategy*. This strategy consists in recovering the maximum of energy at the last station in range and then pursuing the trip until the next last in range stations or the destination.

The optimisation shows that the best trade-offs between the time spent in stations and the infrastructure cost are obtained for fleets with 100% of ultra-fast charging EVs. The lowest daily equivalent annual cost is found for an infrastructure layout on the Pareto-front corresponding to the 100% share of UFC EVs with an installed power per station relatively low since the faster an EV is charging, the lower the number of needed chargers to comply with the waiting time threshold. However, nowadays, no passenger cars with a 70-kWh battery pack can charge at 350 kW, but even if a share of 100% of UFC EVs on the road will unlikely be reached in the next ten years, studying this situation enables us to evaluate the maximum time we can save with a

fleet fully adapted to a 350-kW charge and to understand how the charging power of the EVs affect the cost of the infrastructure.

7.3 . Perspectives

7.3.1 . Improve the *FCFS communication strategy*

The *FCFS communication strategy* proves to be the best dynamic control strategy compared with the *reservation strategy*. Still, the strategy can be improved to predict more accurately the waiting time, especially when a part of the fleet is not communicating (see Section 4.6). To enhance the waiting time prediction, the charging stations could estimate the waiting time with all the previous charging requests they received [71] instead of only computing the waiting time based on the last charging requests. According to [18], using reinforcement learning based on previous charging requests or sessions can help anticipate the affluence in stations and could be helpful when a share of EVs is not communicating or to anticipate the potential changes other communicating EVs will do based on their previous requests. To train the reinforcement learning model, the training set can be historical data, if any are available or a generated training set with multi-agent simulation [18]. Using multi-agent simulation to generate training and testing sets might be helpful, but the trip generation should be more complex than the ones we studied in this manuscript to avoid the model being biased by the simpler probability densities we used.

Another possible improvement is the definition of EV's discontent factor. As we have seen in Section 7.2.1, the value of time represents an important parameter to be considered when optimising the infrastructure, but other parameters can affect the charging decision of an EV driver. For instance, the driver might choose a charging station based on the electricity carbon footprint the station proposes, and that can be granted, for example, by a blockchain smart contract [130].

7.3.2 . Go further in the infrastructure optimisation

We have shown the benefit of the *FCFS communication strategy* during the optimisation of the infrastructure. Still, we only aimed to minimise the charging network cost, not the EV drivers' discontent factor. Thus, we plan to perform a multi-objective optimisation of the charging infrastructure layout under a communication strategy to minimise both infrastructure cost and EV drivers' discontent factors thanks to a multi-objective GWO.

As the value of time is essential in the charging plan choice and that, in reality, contrary to what we assume in Chapter 5, all the drivers do not have the same vot, we must consider in the multi-objective optimisation different classes of drivers according to their vot and the EV model they drive.

To go further, more accurate and precise data would be helpful to determine the real-world traffic flow on a specific highway during a day (departure time, entries and exits statistics in long-distance trips, etc.) and propose a more suitable charging infrastructure for real-world case study (Section 7.3.3).

Finally, we optimise the infrastructure as if the EV flow was already stable. Still, in reality, the share of EVs on the road is rapidly growing, and we should contemplate optimising the infrastructure dynamically and not in a steady-state way. A dynamic evaluation would also be interesting to consider the evolution of EV model characteristics (, battery capacity, charging rate). However, using multi-agent simulation is time-costly, and we need to find a way to circumvent its use to plan the infrastructure according to the charging strategy followed by the EVs. When the charging strategy is not dynamic (for instance the no communication strategy or

the last in range strategy), the running time is much lower than for the communication strategy. However, it is still taking time if we want to evaluate a high number of possible days to size the infrastructure correctly. Nevertheless, to consider dynamic evolution when using the MAS, we can, for instance, consider three fleet sizes: the first for the early years of the infrastructure operation, the second for the middle of the infrastructure lifetime and the third for the last years of the infrastructure lifetime. This way, we can compute the NPV of the infrastructure with charging points added during the lifetime of the infrastructure to fit the different fleet sizes, like in [50]. Obviously, the computation time will be longer, but as we perform sizing, the running time does not represent much of a problem.

7.3.3 . EV flow accuracy

For both control strategy and infrastructure planning, we have seen that we need more accurate EV trips (departure time, entries and exit statistics in long-distance trips, etc.) to either predict the best charging behaviour or size the infrastructure on the highway according to realistic long-distance trips. We have detailed trip data from Stellantis-connected vehicles that are useful for generating long-distance trips. Still, this data is insufficient to determine real-distance trips spatially since the data come from European roads and not only from a specific highway. A potential lead for highway-specific data collection is to contact GPS navigation app owners.

A - First Appendix: definitions and proofs from Chapter 3

A.1 . Value of time

The value of time vot of a passenger corresponds to the price this passenger is willing to pay to gain time when travelling. When comparing two transportation options, the utility function of the user for solution 1 (U_1) and solution 2 (U_2) can be expressed as:

$$U_1 = w_t \cdot t_1 + w_c \cdot c_1 \tag{A.1}$$

$$U_2 = w_t \cdot t_2 + w_c \cdot c_2 \tag{A.2}$$

$$\tag{A.3}$$

With t_1 and t_2, the travelling times of solutions 1 and 2 and c_1, c_2 are the cost of solutions 1 and 2, respectively. The vo is then equal to $\frac{w_t}{w_c}$.

A.2 . Proof of waiting time computation

We corrected how the waiting time was computed in the framework for the FCFS rule, and we prove here why with a proof by recurrence on the number of persons p in a queue with a fixed number s of servers (a server is a charger in our case). It is evident that if $p \leq s$, the waiting time is null for the p^{th} person in the queue, so we will prove the computation method for cases where $p > s$.

Proof

Inductive hypothesis
For a given queue of p persons waiting for a service with s servers ($p > s$), the p^{th} person in line waits for $(p - s)$ persons to leave before being served. Note that the $(p - s)^{th}$ person to leave might not be the $(p - s)^{th}$ person in line since the service may not have the same duration for all the persons. A person leaves after being served.
Base case: $p = s + 1$
The $(s + 1)^{th}$ person in line needs to wait for only one charger to be free because the $(s + 1)^{th}$ person is the next in line to be served (there are s servers). Thus, the p^{th} (the $(s+1)^{th}$) person needs to wait for one person to leave; in other words, that $p-s = s+1-s = 1$ person leaves to be served.
Inductive step: We assume the hypothesis is true for p and we will prove it is true for $p + 1$.
The $(p + 1)^{th}$ person in line needs to wait until the p^{th} person in line starts being served to pretend for a server, so the $(p + 1)^{th}$ person needs to wait first for $p - s$ persons to leave (condition by inductive hypothesis for the p^{th} person to start being served). Then, the $(p+1)^{th}$ person has to wait for one more person to leave before being served. Thus, before being served, the $(p + 1)^{th}$ person must wait for $p - s + 1$ persons to leave the station, in other words, for $(p + 1) - s$ persons to leave, which proves the case for $p + 1$.

Therefore, the waiting time $t_{wait,p}$ for the p^{th} person in the line corresponds to the time difference between the arrival time of the p^{th} person, $t_{arr,p}$, and the departure time of the

$(p-s)^{th}$ person leaving the station (and not the p^{th} person leaving the station as it was in the inherited framework).

A.3 . Computation of charging time

A.3.1 . Constant charging power

In case the charging power $P(SoC)$ is constant on the interval $[SoC_i, SoC_{i+1}[$, the charging time t_{charge} is:

$$t_{charge} = \frac{C}{3600 \cdot P_{cst}} \cdot (SoC_{end} - SoC_{start}) \tag{A.4}$$

Proof

$dE = P.dt$ with dt in hour, $dE(t)$ is the energy charged during dt at the power $P(t)$ Case dt in second:

$$\begin{aligned} dE(t) &= 3600 \cdot P(t)dt \\ dSoC(t) &= \frac{3600}{E_{batt.}} \cdot P_{cst}dt \end{aligned} \tag{A.5}$$

So when integrating:

$$SoC_{end} - SoC_{start} = \frac{3600}{C} \cdot P_{cst} \cdot t_{charge} \tag{A.6}$$

A.3.2 . Linear decreasing charging power

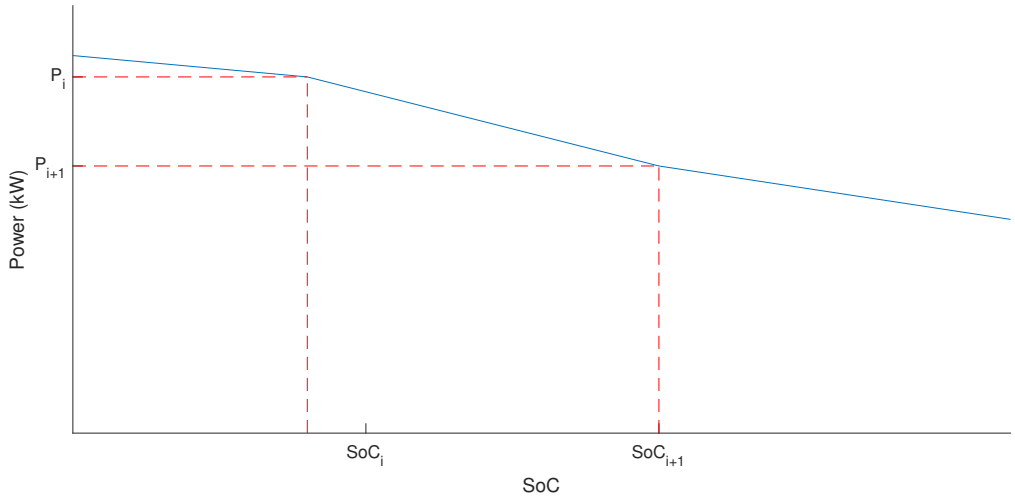

Figure A.1: Charging power linear according to the SoC on interval $[SoC_i, SoC_{i+1}[$

In this case (Figure A.1), the expression of the charging time t_{charge} is given by the equation (3.18).

$$\begin{aligned} P(SoC(t)) &= a_i(SoC(t) - SoC_i) + b_i \\ \text{with } a_i &= (P_{i+1} - P_i)/(SoC_{i+1} - SoC_i),\ P_{i+1} = P\left(SoC_{i+1}\right), \\ P_i &= P\left(SoC_i\right) \text{ and } b_i = P_i \end{aligned}$$

Proof

We have:

$$dSoC(t) = \frac{3600}{C} \cdot P(t)dt \tag{A.7}$$

So,

$$dSoC(t) = \frac{3600}{C} \cdot [a_i(SoC(t) - SoC_i) + b_i] \ dt \tag{A.8}$$

Resolution of the first order differential equation A.8.
The homogeneous solution computation is given by:

$$dSoC_H(t) = \frac{3600}{C} \cdot a_i SoC_H(t)dt \tag{A.9}$$

$$SoC_H(t) = A \cdot \exp(\frac{3600}{C} \cdot a_i \cdot t) \tag{A.10}$$

Equation (A.11) gives the particular solution computation.

$$0 = \frac{3600}{C} \cdot [a_i(SoC_P - SoC_i) + b_i] \equiv SoC_P = SoC_i - \frac{b_i}{a_i} \tag{A.11}$$

It comes:

$$\begin{aligned} SoC(t) &= A.\exp(\frac{3600}{C} a_i \ t) + SoC_i - \frac{b_i}{a_i} \\ \text{with } SoC(0) &= SoC_{start} \\ SoC\ (t) &= \left(SoC_{start} - SoC_i + \frac{b_i}{a_i}\right).\exp(\frac{3600}{C} \cdot a_i \cdot t) + SoC_i - \frac{b_i}{a_i} \end{aligned} \tag{A.12}$$

Finally, after integrating:

$$t_{charge} = \frac{C}{3600 \cdot a_i} \cdot \log\left(\left(SoC_{end} - SoC_i + \frac{b_i}{a_i}\right) / \left(SoC_{start} - SoC_i + \frac{b_i}{a_i}\right)\right) \tag{A.13}$$

B - Second Appendix: statistics analysis

B.1 . Iso-probabilistic transformation

To determine the time of entrance of the EVs, we use an iso-probabilistic transformation of the cumulative density function corresponding to the traffic flow curve (Figure B.1b).

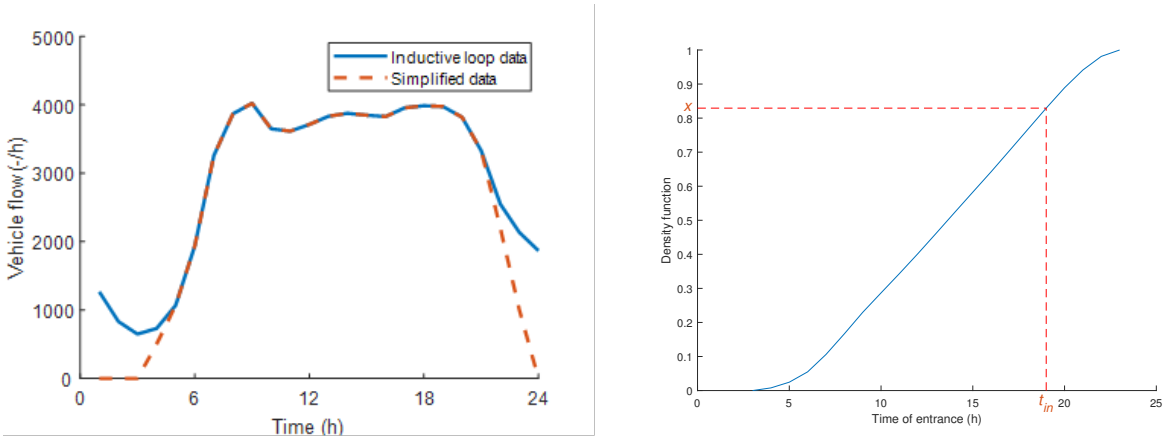

(a) (b)

Figure B.1: Figure (a): Average incoming vehicle flow per hour of the French highway A6 in Île-de-France [24]. The blue curve is the resulting average of the A6 highway sections in Île-de-France traffic flow inductive loop data counting. Figure (b):Cumulative density function $P(t_{start} \leq t)$ corresponding to the entering traffic flow per hour B.1a

With t corresponding to a time, the cumulative density function $P(t_{start} \leq t)$ corresponding to the probability for an EV to enter the highway before t is computed from the traffic flow curve. We obtain Figure B.1. Then, we select a random number x in $[0,\ 1]$ and t_{start} is the image of x by the inverse of the cumulative density function (Figure B.1).

B.2 . Work on connected vehicles data

Some clients agree to share with Stellantis data from their connected vehicles and we used the data feedback from the part of those vehicles that are electric vehicles. The raw data contains information about the EV's state (position, SoC, speed $\cdots$) at a given time. The data we want to retrieve should be linked to a long distance trip so we need first to delimit from the raw data the driving sessions. A **driving session** is delimited by the moment the EV is powered and the moment it is shut down. All the raw data that come from the same driving session share the same driving session id.

Then, the **driving sessions** should be grouped to form a **trip**. This time, the driving sessions from the same trip do not share a common id since it is not possible to identify a trip from the raw data. Therefore, we define a maximum time between two driving sessions of 2 hours. If two driving session are spaced in time by more than 2 hours, we consider the driver has started a new trip. When all the trips are identified, we sort the trips that have:

- a length higher than 100 km,
- a travelling part on the highway (speed of the EV $>$ 100 km/h),

- at least one charging pause (the SoC between two driving sessions has increased) close to the highway (average speed during 5 minutes before and after the charging session is higher than 100 km/h).

The selected trips represent the long-distance trips according to our definition (Section 1.2.1). We identified 380 EVs that made at least one long distance trip during the studied year.

From the long-distance trips data, we extract the SoC_{start}, the time of entrance on the highway t_{start} and the SoC when stopping to charge. In this manuscript we only use the SoC_{start} distribution in **Case study 2** (see Section 3.3.4) but the rest of the extracted data can be used to generate trip parameters or stopping strategies based on the SoC (see Section 6.5.2).

C - Third Appendix: Dynamic programming for charging plan optimisation

The aim of the dynamic method we propose in this thesis is to optimise the charging plan of an EV to minimise its trip time. The trip time includes the driving time t_{drive}, the charging time t_{charge} and the waiting time t_{wait}. The notations in this appendix are independent from the notations in the rest of the manuscript.

The problem is divided in subproblems with one subproblem associated with one station. Thus the subproblem k corresponds to the k^{th} station on the road. Each subproblem objective is to determine for each possible SoC_{out}^{k} (SoC the EV has when leaving the station k) the optimal energy to charge in station k to minimise the EV trip time from the beginning of the trip. The subproblem gets from the previous subproblem (subproblem $k-1$) the minimum trip time to reach each SoC_{out}^{k-1} and the associated optimal charging plan from the beginning of the trip.

We use an example to explain the process. Let's consider an EV entering the highway with $SoC_{start} = 55\,\%$ and we want to evaluate the minimum trip time to reach $SoC_{out}^{2} = 65\,\%$ in station 2. The DP algorithm will first determine the minimum trip time from the highway entrance to each SoC_{out}^{1} in station 1 (subproblem 1). This part is simple as there is only on possible path to reach each SoC_{out}^{1} with no or one possible quantity to charge in station 1 (quantity in green in Figure C.1). If no charging quantity exists, the minimum trip time for this path is set to infinite.

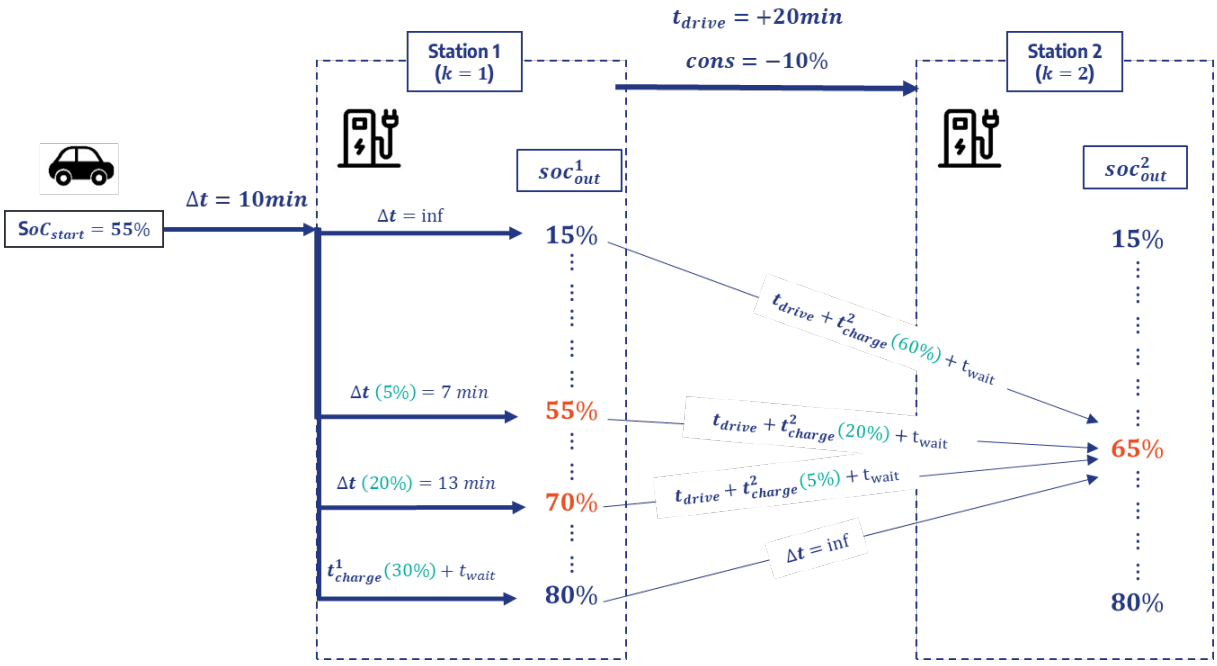

Figure C.1: Computation of minimum trip times for each possible path

Secondly, the DP computes the time for the EV to go from a given $SoC_{out,n}^{1}$ when leaving station 1 to $SoC_{out}^{2} = 65\,\%$. This time includes the driving time, the waiting time according to the arrival time in station t_{in}^{k} ($t_{in}^{k} = t_{o}^{k-1}ut + t_{drive}$) and the charging time needed to recover x_{m}^{k} % of energy. The energy to recover is:

$$x_{m}^{k} = SoC_{out}^{2} - SoC_{out}^{1} + cons_{1\to 2} \tag{C.1}$$

With $cons_{1\to 2}$ the consumption between station 1 and 2.

Thus, the minimum time to reach 65% when charging x_m^k in station 2 is the minimum time to reach $SoC_{out,n}^{k-1}$ in station 1 (computing during subproblem 1) plus the time to go from $SoC_{out,n}^1$ to $SoC_{out}^2 = 65$ %.

Once all the minimum trip times are computed for all the possible path from the beginning to reach $SoC_{out} = 65$ %, the DP deduces the path with the global minimum trip time and retrieve the charging plan of this optimal path. In our example, the charging plan with the global minimum trip time is $(x^1, x^2) = (20\%, 5\%)$ (see Figure C.2).

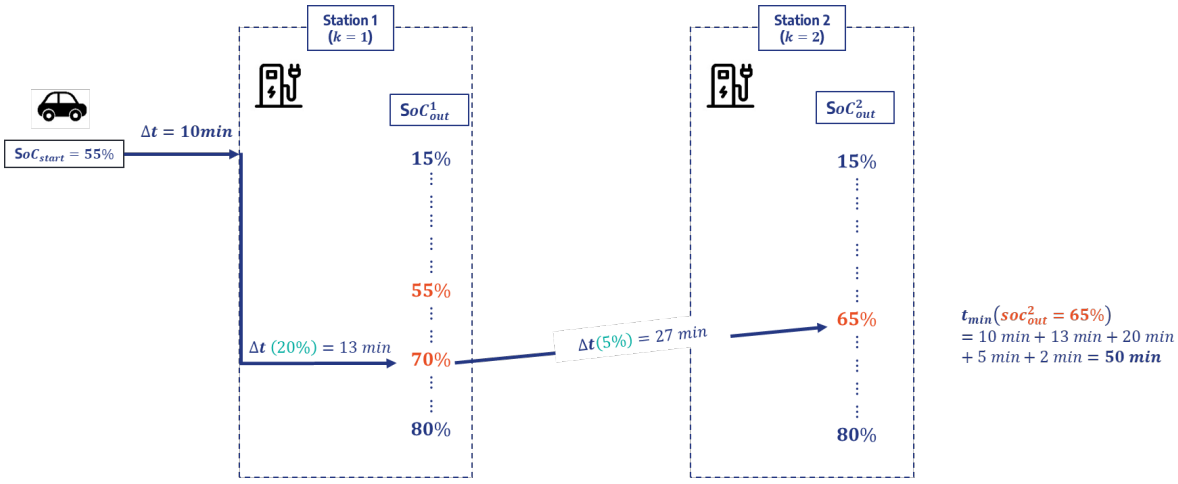

Figure C.2: Minimum trip time path finding

Then, the DP algorithm keeps in memory the global minimum trip time and the optimal charging plan to reach $SoC_{out}^2 = 65\%$ and proceed identically to compute the optimal charging plan for other values of ${}^{S}oC_{out}^2$. After those calculations, the program can go to next subproblem.

D - Fourth Appendix: Implementation adaptations and improvements

D.1 . Charging plan update correction

As the exhaustive method updates the waiting times for each listed charging plan (step 3 on Figure 3.2) and then searches the charging plan with the minimum DF at every iteration, the computing time will be high if the number of charging plans to update is not reduced to the bare minimum. J. Hassler implemented a process to remove from Ω_v charging plans that are no longer feasible (or obsolete) as the simulation goes. Those plans, $\omega_{obs.}$, are the ones for which one of the stations, CS_{i_k}, in the list of stops, was already driven past in the simulation, and one of the following conditions was not met:

- the EV did not stop at station CS_{i_k}.
- the EV stopped at station CS_{i_k} but did not charge the same amount of energy, x_{i_k}, as indicated in $\omega_{obs.}$.

For the 2nd case where the EV did not charge the same amount of energy in the station as indicated in $\omega_{obs.}$, the charging plan list reduction was removing charging plans with stop plans $(i_1, \cdots i_{N_{min,\,v}})$ still feasible because of the way the total energy to be charged was distributed among the station. For example, let's consider that, at iteration t, the best charging plan for EV is ω, which details are given in (D.1) (see (3.21 for the expression of the charging plan in the exhaustive method). The EV has already been charged at station $i_1 = 2$. At iteration $t+1$, the EV stopped at station $i_2 = 4$ and is charging.

$$\omega_v = \begin{pmatrix} i_1 & \dots & i_{N_{min,\,v}} \\ x_1 & \dots & x_{N_{min,\,v}} \end{pmatrix} = \begin{pmatrix} 2 & 4 & 6 \\ 26.3 & 25.4963 & 9.8537 \end{pmatrix} \tag{D.1}$$

Before updating its charging plan, the EV removes all the charging plans $\omega_{obs.}$ no longer feasible, either the charging plan with $i_{2,\,obs.} \neq 4$ or the charging plan with $i_{2,\,obs.} = 4$ but $x_{2,obs.} \neq x_2$. However, in the way Ω_v was built in the inherited version, even if it exists other charging plans $\omega' \in \Omega$ with $i'_1 = i_1$, $x'_1 = x_1$ and $i'_2 = i_2$, it appears that none of them verifies $x'_2 = x_2$ except for ω itself.

We give an example of ω' and ω" in Ω with $i'_1 = i"_1 = i_1$, $x'_1 = x"_1 = x_1$ and $i'_2 = i"_2 = i_2$ but, even if x'_2 and $x"_2$ are closed to x_2 they are not equal to x_2 so those charging plans are considered obsolete by the algorithm and removed from the solutions. In contrast, they could have given more flexibility to the EV's charging plan optimisation. In this situation, the EV will have at iteration $t+1$ only one charging plan remaining, ω, and will not have the possibility to change its strategy and eventually stop at station 5 as proposed by the charging plans ω' and ω" whereas the EV has enough SoC to do so.

$$\omega' = \begin{pmatrix} i'_1 & \dots & i'_{N_{min}} \\ x'_1 & \dots & x'_{N_{min}} \end{pmatrix} = \begin{pmatrix} 2 & 4 & 5 \\ 26.3 & 25.3627 & 9.9873 \end{pmatrix} \tag{D.2}$$

$$\omega" = \begin{pmatrix} i"_1 & \dots & i"_{N_{min}} \\ x"_1 & \dots & x"_{N_{min}} \end{pmatrix} = \begin{pmatrix} 2 & 4 & 5 \\ 26.3 & 25.8627 & 9.4873 \end{pmatrix} \tag{D.3}$$

To circumvent this problem, we propose another energy distribution among the station with all the charging stops having the same quantum of energy ΔE for the discretisation except for

the last stop of the charging plan, where the EV charges the remaining energy. The energy charged at the last station will not be a multiple of the ΔE except if the total energy E_{total} is a multiple of ΔE. The previous charging plans presented in this section are adapted as explained in (D.4) with a quantum of energy of $\Delta E = 0.5kWh$.

$$\omega = \begin{pmatrix} 2 & 4 & 6 \\ 26 & 25.5 & 10.15 \end{pmatrix}, \quad \omega' = \begin{pmatrix} 2 & 4 & 5 \\ 26 & 25.5 & 10.15 \end{pmatrix} \tag{D.4}$$

With this improvement, the EV can now charge at stations 2 and 4, respectively, 26 kWh and 25.5 kWh and still have the choice to charge at station 5 or station 6 the remaining 10.15 kWh.

D.2 . Adaptation of the grey wolf optimiser algorithm

We use the matlab code in [121]. However, we had to correct and improve the algorithm before using it in our simulation.

Concerning the correction, we corrected the assignment of the leading wolfs (α, β and δ) positions after sorting the positions according to the fitness value. In the original code, the positions where not sorted before the assignment.

Concerning the improvements, as the running-time of the fitness evaluation is high, we first implemented a system that keeps in program memory the previous computed fitnesses to avoid that the optimiser computes again the fitness of a position already explored. Secondly, to make the optimiser converge faster, we introduced a possible mutation that adds chargers in stations where the waiting time is above the waiting time thresholds.

Nomenclature

$DEAC_{FCI}(s)$	Daily equivalent annual cost of the infrastructure layout s
N_{area}	Number of service areas on the highway
ΔE	Energy step when listing the charging plans in the exhaustive method or in the dynamic programming method (kWh)
Δt	Simulation time step (min)
δt	Time slot: unit of time delimited by the estimated timestamp of two events that will occur in the station
$\Delta T_{CS}(F_{x,f})$	Average relative additional time spent in stations by the EVs of the fleet $F_{x,f}$
$\Delta T_{CS}(F_{x_{dist.},f,com.})$	Relative additional time spent in stations by the communicating EVs of the fleet $F_{x_{dist},f}$ compared with the FCFS communication scenario ($x = 0$)
$\Delta T_{CS}(v_{x,f})$	Relative additional time spent in stations by EV_v in the fleet $F_{x,f}$ compared with the FCFS communication scenario ($x = 0$)
$\mathbb{CS}$	Set of highway fast-charging stations
$\mathbb{E}$	Set of highway entrance/exits
$\mathbb{F}$	Fleet (set of EVs)
ω_v^*	Optimal charging plan of EV_v
ω_v	One charging plan of EV_v: energy charged per station and power level used
$\omega_{lr,v}$	Charging plan of EV_v obtained with the last-reachable strategy
$\overline{\Delta T}_{CS,x,com.}$	Average relative additional time spent in stations per communicating EV according to the percentage of disturbers x
$\overline{\Delta T}_{CS,x,no\ com.}$	Average relative additional time spent in stations per non-communicating EV according to the percentage of disturbers x
$\overline{\Delta T}_{CS,x}$	Average relative additional time spent in stations per EV according to the percentage of disturbers x
ρ_v	Consumption of EV_v (kWh/km)
τ	Time window or time interval: accumulation of adjacent time slots
$A.T.$	Estimated arrival time in a station specified in a charging request
$C.T.$	Estimated charging time in a station specified in a charging request
c_v	Charging coefficient of EV_v in the expression of the linearised charging curve P_v
$C_{charge}(\omega_v)$	Total charging cost of the EV_v associated to the charging plan ω_v (€)

$C_{FCI}(s)$	Cost of the fast charging infrastructure (€)
$C_{hard.,j}$	Hardware cost of a charger with the power level p_j (€)
$C_{install.}(s_{i,j})$	Installation cost of a charger depending on the charging rate and the number of charger installed in the station $s_{i,j}$ (€)
$C_{O\&M}$	Annual operation and maintenance cost of the infrastructure (€)
$cons._{k \to k+1}$	Consumption between station CS_k to station CS_{k+1}
CS_i	i^{th} charging station in $\mathbb{CS}$
D_v	Distance between o_v and d_v (km)
d_v	Exit number of EV_v (destination)
$data_{charge}$	Database listing all the data needed to compute T_{trip} for each possible charging plan (exhaustive method)
$DEAC_{FCI}(s)$	Daily equivalent annual cost of the infrastructure layout s
$DEAE_{FCI}(s)$	Daily equivalent annual expenditure of the infrastructure layout s
$DF_v(\omega_v)$	Discontent factor of EV_v associated to the charging plan ω_v
$E_{batt,v}$	Capacity of EV_v's battery pack (kWh)
$E_{total,v}$	Total energy needed by EV_v to complete its trip to leave the highway with at least $SoC_{tar,v}$
EV_v	v^{th} EV in fleet $\mathbb{F}$
$F_{x,f}$	f^{th} fleet tested with x percent of disturbers
K	Position of EV_v in the arrival order in a station
L	Life time of a charger (year)
N_f	Number of fleets tested during the optimisation of the infrastructure
N_p	Number of power levels in P
N_{area}	Number of service areas on the highway
N_{CS}	Number of highway fast-charging stations
$N_{limit,v}$	Number of stops a charging plan of EV_v can have
$N_{min,v}$	Minimum number of stops a charging plan of EV_v can have to make EV_v reach d_v with at least $SoC_{tar,v}$
o_v	Entrance number of EV_v (origin)
p_i	Power rate used in station CS_i to charge x_i (in a charging plan) (kW)
p_j	j^{th} power level in P

$P_v(SoC)$	Charging curve of EV_v (kW)
$p_{charge,j}$	Electricity price for a driver according to the power level p_j (€/kWh)
$P_{charge,i,j}(SoC)$	Real charging curve of an EV charging at the station CS_i on charger with level p_j (kW)
$p_{charge}(p_j)$	Electricity price for a driver according to the power level p_j (€/kWh)
p_{el}	Industrial electricity price(€/kWh)
$P_{max,v}$	Intersection between the linearised curve $P_v(SoC)$ and the axis $x = 0$ (kW)
r	Discount rate of the infrastructure investment (%)
R_i	Charging request table of station CS_i
R_{avg}	Average annual daily revenue of the infrastructure (€)
s	Vector listing the number of chargers (or sockets) per station according to their rate
$s_{i,j}$	Number of chargers with power level p_j in station CS_i
SoC	State of charge (%)
$SoC_{end,v}$	SoC of EV_v when leaving the highway
$SoC_{in,i,v}$	SoC of EV_v when entering the station CS_i
SoC_{min}	Minimum SoC
$SoC_{out,i,v}$	SoC of EV_v when leaving the station CS_i
$SoC_{start,v}$	SoC of EV_v when entering the highway
$SoC_{tar,v}$	Target SoC of EV_v when leaving the highway
$speed_v$	Speed limit of EV_v: minimum between $speed_{road}$ and $speed_{driver}$ (km/h)
$speed_{driver}$	Speed observed by the driver (driving style) (km/h)
$speed_{road}$	Speed limit on the road (km/h)
t	Simulation time (h) or iteration represented by the time interval between time $t-1$ and time t
$T_{adv.}$	Anticipation time: time before an EV enters the highway and starts the communication process
$t_{charge,i}(\omega_v)$	Charging time of EV_v in station CS_i according to the charging plan ω_v (min)
$T_{charge}(\omega_v)$	Total charging time of EV_v according to the charging plan ω_v (min)
$T_{CS}(\omega_v)$	Total time the EV_v spent or will spend in stations with the charging plan ω_v (min)
$T_{CS}(v_0)$	Time spent in stations by EV_v with the FCFS communication scenario ($x = 0$)

$T_{CS}(v_{x,f})$	Time spent in station by EV_v in the situation discribed by the fleet $F_{x,f}$
$t_{in,i}(\omega_v)$	Estimated arrival time in the station CS_i with the charging plan ω_v (h)
$t_{in,v}$	Entrance time of EV_v on the highway
$T_{other}(\omega_v)$	Total time the EV_v spent or will spend stopping and plugging with the charging plan ω_v (min)
t_{other}	Time to stop and to plug in station (5 min)
T_{thres}	Waiting time threshold during the optimisation of the infrastructure (min)
T_{travel}	Total time the EV_v spent or will spend driving (min)
$T_{trip}(\omega_v)$	Total trip time of the EV_v associated to the charging plan ω_v (min)
$t_{wait,v,i}$	Waiting time of EV_v in station CS_i (min)
$T_{wait}(\omega_v)$	Total waiting time of EV_v according to the charging plan ω_v (min)
vot	Value of time (€/h)
w_c	Cost weight in the utility function DF_v of the driver
w_t	Time weight in the utility function DF_v of the driver
X	Coefficient giving driver's preference between trip time T_{trip} and the charging cost C_{charge}
x_i	Energy charged in station CS_i (in a charging plan) (kWh)
$x_{dist.}$	Percentage of disturbers in the fleet (%)

Bibliography

[1] IRENA, "Innovation landscape brief: Electric-vehicle smart charging," International Renewable Energy Agency, brief, 2019.

[2] IPCC, "IPCC, 2023: Climate change 2023: Synthesis report. contribution of working groups i, II and III to the sixth assessment report of the intergovernmental panel on climate change [core writing team, h. lee and j. romero (eds.)]. IPCC, geneva, switzerland." edition: First. [Online]. Available: https://www.ipcc.ch/report/ar6/syr/

[3] H. Ritchie and M. Roser, "Sector by sector: where do global greenhouse gas emissions come from?" [Online]. Available: https://ourworldindata.org/ghg-emissions-by-sector

[4] Stellantis. Dare forward 2030: Care. [Online]. Available: https://www.stellantis.com/en/company/dare-forward-2030/care

[5] "Energy density," Jun. 2021, page Version ID: 1028937921. [Online]. Available: https://en.wikipedia.org/w/index.php?title=Energy_density&oldid=1028937921

[6] "AVIS de l'ADEME : Voitures électriques et bornes de recharges." [Online]. Available: https://librairie.ademe.fr/mobilite-et-transport/5877-avis-de-l-ademe-voitures-electriques-et-bornes-de-recharges.html

[7] H. Berg and M. Zackrisson, "Perspectives on environmental and cost assessment of lithium metal negative electrodes in electric vehicle traction batteries," *Journal of Power Sources*, vol. 415, pp. 83–90, Mar. 2019. [Online]. Available: https://www.sciencedirect.com/science/article/pii/S0378775319300576

[8] P. Group. Charging index 2021 – comparison of the fast charging capability of electric vehicles. [Online]. Available: https://www.p3-group.com/en/p3-charging-index-comparison-of-the-fast-charging-capability-of-various-electric-vehicles-from-a-users-perspective-update-2021/

[9] ASFA. Bornes de recharge électrique rapide - ASFA. [Online]. Available: https://www.autoroutes.fr/fr/bornes-recharge.htm

[10] W. Khan, F. Ahmad, and M. S. Alam, "Fast EV charging station integration with grid ensuring optimal and quality power exchange," *Engineering Science and Technology, an International Journal*, vol. 22, no. 1, pp. 143–152, Feb. 2019. [Online]. Available: https://www.sciencedirect.com/science/article/pii/S2215098617315057

[11] J. Serradilla, J. Wardle, P. Blythe, and J. Gibbon, "An evidence-based approach for investment in rapid-charging infrastructure," *Energy Policy*, vol. 106, pp. 514–524, Jul. 2017. [Online]. Available: https://www.sciencedirect.com/science/article/pii/S030142151730232X

[12] C. Robinson and C. Holzinger, "To 350 kW and beyond: the future of fast-charging electric vehicles," Lux Research, Tech. Rep., 2017.

[13] enedis and rte, "Etude-les-besoins-electriques-de-la-mobilite-longue-distance-sur-autoroute," study, Jul. 2021. [Online]. Available: https://www.enedis.fr/sites/default/files/

documents/pdf/enedis-etude-les-besoins-electriques-de-la-mobilite-longue-distance-sur-autoroute.pdf

[14] Q. Yang, S. Sun, S. Deng, Q. Zhao, and M. Zhou, "Optimal Sizing of PEV Fast Charging Stations With Markovian Demand Characterization," *IEEE Transactions on Smart Grid*, vol. 10, no. 4, pp. 4457–4466, Jul. 2019, conference Name: IEEE Transactions on Smart Grid.

[15] T. Oda, M. Aziz, T. Mitani, Y. Watanabe, and T. Kashiwagi, "Mitigation of congestion related to quick charging of electric vehicles based on waiting time and cost–benefit analyses: A japanese case study," *Sustainable Cities and Society*, vol. 36, pp. 99–106, Jan. 2018. [Online]. Available: https://www.sciencedirect.com/science/article/pii/S2210670717307230

[16] A. Amin, W. U. K. Tareen, M. Usman, H. Ali, I. Bari, B. Horan, S. Mekhilef, M. Asif, S. Ahmed, and A. Mahmood, "A Review of Optimal Charging Strategy for Electric Vehicles under Dynamic Pricing Schemes in the Distribution Charging Network," *Sustainability*, vol. 12, no. 23, p. 10160, Jan. 2020, number: 23 Publisher: Multidisciplinary Digital Publishing Institute. [Online]. Available: https://www.mdpi.com/2071-1050/12/23/10160

[17] C. Liu, M. Chai, X. Zhang, and Y. Chen, "Peer-to-peer electricity trading system: smart contracts based proof-of-benefit consensus protocol," *Wireless Networks*, Feb. 2019.

[18] A. Viziteu, D. Furtună, A. Robu, S. Senocico, P. Cioată, M. Remus Baltariu, C. Filote, and M. S. Răboacă, "Smart Scheduling of Electric Vehicles Based on Reinforcement Learning," *Sensors*, vol. 22, no. 10, p. 3718, Jan. 2022, number: 10 Publisher: Multidisciplinary Digital Publishing Institute. [Online]. Available: https://www.mdpi.com/1424-8220/22/10/3718

[19] S. Souley, K. Gillet, G. Colin, A. Simon, C. Nouillant, and Y. Chamaillard, "Optimization of the travel time of an electric vehicle with consideration of the recharging terminals," *IFAC-PapersOnLine*, vol. 54, no. 2, pp. 121–126, Jan. 2021. [Online]. Available: https://www.sciencedirect.com/science/article/pii/S240589632100447X

[20] V. del Razo and H.-A. Jacobsen, "Smart Charging Schedules for Highway Travel With Electric Vehicles," *IEEE Transactions on Transportation Electrification*, vol. 2, no. 2, pp. 160–173, Jun. 2016, conference Name: IEEE Transactions on Transportation Electrification.

[21] J. Hassler, Z. Dimitrova, M. Petit, and P. Dessante, "Service for optimization of charging stations selection for electric vehicles users during long distances drives: time-cost tradeoff," *IOP Conference Series: Materials Science and Engineering*, vol. 1002, p. 012029, Dec. 2020, publisher: IOP Publishing. [Online]. Available: https://doi.org/10.1088/1757-899x/1002/1/012029

[22] Y. He, K. M. Kockelman, and K. A. Perrine, "Optimal locations of U.S. fast charging stations for long-distance trip completion by battery electric vehicles," *Journal of Cleaner Production*, vol. 214, pp. 452–461, Mar. 2019. [Online]. Available: https://www.sciencedirect.com/science/article/pii/S0959652618339040

[23] A. Propre. (2022) Recharge renault megane électrique : le guide complet. [Online]. Available: https://www.automobile-propre.com/voitures/renault-megane-electrique/recharge/

[24] J. Hassler, Z. Dimitrova, M. Petit, and P. Dessante, "Optimization and Coordination of Electric Vehicle Charging Process for Long-Distance Trips," *Energies*, vol. 14, no. 13, p. 4054, Jan. 2021, number: 13 Publisher: Multidisciplinary Digital Publishing Institute. [Online]. Available: https://www.mdpi.com/1996-1073/14/13/4054

[25] A. M. Mowry and D. S. Mallapragada, “Grid impacts of highway electric vehicle charging and role for mitigation via energy storage,” *Energy Policy*, vol. 157, p. 112508, Oct. 2021. [Online]. Available: https://linkinghub.elsevier.com/retrieve/pii/S0301421521003785

[26] M. Nicholas, “Estimating electric vehicle charging infrastructure costs across major U.S. metropolitan areas,” International Council on Clean Transportation, Working Paper, Aug. 2019. [Online]. Available: https://theicct.org/sites/default/files/publications/ICCT_EV_Charging_Cost_20190813.pdf

[27] C. général au développement durable, “La mobilité à longue distance des français en 2014,” no. 693, 2015.

[28] IEA, “Global EV Outlook 2021 – Analysis.” [Online]. Available: https://www.iea.org/reports/global-ev-outlook-2021

[29] L2C2, “[Baromètre] Juillet 2021 : un marché automobile en repli ; les véhicules électriques et hybrides rechargeables endiguent la chute.” [Online]. Available: http://www.avere-france.org/Site/Article/?article_id=8024

[30] L’argus. Bornes de recharge rapide. l’État va débloquer 100 millions d’euros. [Online]. Available: https://www.largus.fr/actualite-automobile/bornes-de-recharge-rapide-letat-va-debloquer-100-millions-deuros-10542404.html

[31] CO emission performance standards for cars and vans. [Online]. Available: https://climate.ec.europa.eu/eu-action/transport/road-transport-reducing-co2-emissions-vehicles/co2-emission-performance-standards-cars-and-vans_en

[32] S. Bobba, S. Carrara, J. Huisman, F. Mathieux, and C. Pavel, *Critical Raw Materials for Strategic Technologies and Sectors in the EU - A Foresight Study*.

[33] M. de la transition écologique et de la cohésion des territoires. Résultats détaillés de l’enquête mobilité des personnes 2019. [Online]. Available: https://www.statistiques.developpement-durable.gouv.fr/resultats-detailles-de-lenquete-mobilite-des-personnes-de-2019

[34] M. W. Verbrugge and C. W. Wampler, “On the optimal sizing of batteries for electric vehicles and the influence of fast charge,” *Journal of Power Sources*, vol. 384, pp. 312–317, Apr. 2018. [Online]. Available: https://www.sciencedirect.com/science/article/pii/S037877531830185X

[35] J.-Y. Hwang, S.-J. Park, C. S. Yoon, and Y.-K. Sun, “Customizing a Li–metal battery that survives practical operating conditions for electric vehicle applications,” *Energy & Environmental Science*, vol. 12, no. 7, pp. 2174–2184, Jul. 2019, publisher: The Royal Society of Chemistry. [Online]. Available: https://pubs.rsc.org/en/content/articlelanding/2019/ee/c9ee00716d

[36] S. Shokrzadeh and E. Bibeau, “Sustainable integration of intermittent renewable energy and electrified light-duty transportation through repurposing batteries of plug-in electric vehicles,” *Energy*, vol. 106, pp. 701–711, Jul. 2016. [Online]. Available: https://www.sciencedirect.com/science/article/pii/S0360544216302602

[37] “Introduction to charging technologies: Conductive charging: AC or DC?” [Online]. Available: https://www.mobility-academy.eu/mod/book/view.php?id=80&chapterid=437

[38] M. Nicholas and D. Hall, “Lessons learned on early electric vehicle fast-charging deployments,” International Council on Clean Transportation, White paper, Jul. 2018.

[39] K. technologies, “Scienlab Charging Discovery System – Verification of Interoperability of all EV and EVSE Charging Interfaces,” 2021, section: Article Section. [Online]. Available: https://www.keysight.com/fr/en/assets/7120-1049/application-notes/5992-4424.pdf

[40] V. Salapić, M. Gržanić, and T. Capuder, “Optimal sizing of battery storage units integrated into fast charging EV stations,” in *2018 IEEE International Energy Conference (ENERGYCON)*, Jun. 2018, pp. 1–6.

[41] A. Tomaszewska, Z. Chu, X. Feng, S. O’Kane, X. Liu, J. Chen, C. Ji, E. Endler, R. Li, L. Liu, Y. Li, S. Zheng, S. Vetterlein, M. Gao, J. Du, M. Parkes, M. Ouyang, M. Marinescu, G. Offer, and B. Wu, “Lithium-ion battery fast charging: A review,” *eTransportation*, vol. 1, p. 100011, Aug. 2019. [Online]. Available: https://www.sciencedirect.com/science/article/pii/S2590116819300116

[42] Z. Guo, B. Y. Liaw, X. Qiu, L. Gao, and C. Zhang, “Optimal charging method for lithium ion batteries using a universal voltage protocol accommodating aging,” vol. 274, pp. 957–964. [Online]. Available: https://www.sciencedirect.com/science/article/pii/S0378775314018047

[43] Virta. EMSP and CPO: the two sides of EV charging network operators. [Online]. Available: https://www.virta.global/blog/emsp-cpo-ev-charging-roles-responsibilities

[44] How much does it cost to charge at IONITY? [Online]. Available: https://support.ionity.eu/en/payment-billing/how-much-does-it-cost-to-charge-at-ionity

[45] W. Kong, Y. Luo, G. Feng, K. Li, and H. Peng, “Optimal location planning method of fast charging station for electric vehicles considering operators, drivers, vehicles, traffic flow and power grid,” *Energy*, vol. 186, p. 115826, Nov. 2019. [Online]. Available: https://www.sciencedirect.com/science/article/pii/S0360544219314987

[46] W. Yin, Z. Ming, and T. Wen, “Scheduling strategy of electric vehicle charging considering different requirements of grid and users,” *Energy*, vol. 232, p. 121118, Oct. 2021. [Online]. Available: https://linkinghub.elsevier.com/retrieve/pii/S0360544221013669

[47] Y.-C. Yeh and M.-S. Tsai, “Development of a Genetic Algorithm based electric vehicle charging coordination on distribution networks,” in *2015 IEEE Congress on Evolutionary Computation (CEC)*, May 2015, pp. 283–290, iSSN: 1941-0026.

[48] E. Xydas, C. Marmaras, and L. M. Cipcigan, “A multi-agent based scheduling algorithm for adaptive electric vehicles charging,” *Applied Energy*, vol. 177, pp. 354–365, Sep. 2016. [Online]. Available: https://linkinghub.elsevier.com/retrieve/pii/S0306261916306286

[49] R. Rana, S. Bhattacharjee, and S. Mishra, “A Two Layer Cooperative Game theoretic Approach for Optimal Operation of Fast Charging Stations,” *IFAC-PapersOnLine*, vol. 52, no. 4, pp. 282–287, Jan. 2019. [Online]. Available: https://www.sciencedirect.com/science/article/pii/S240589631930549X

[50] E. Suomalainen and F. Colet, “A Corridor-Based Approach to Estimating the Costs of Electric Vehicle Charging Infrastructure on Highways,” *World Electric Vehicle Journal*, vol. 10, no. 4, p. 68, Dec. 2019, number: 4 Publisher: Multidisciplinary Digital Publishing Institute. [Online]. Available: https://www.mdpi.com/2032-6653/10/4/68

[51] "ADVENIR Le programme," Feb. 2016. [Online]. Available: https://advenir.mobi/le-programme/

[52] I. T. D. M. F. Fauzan, "A review on challenges and opportunities of electric vehicles (EVS)," vol. 42, pp. 127–134.

[53] G. Napoli, A. Polimeni, S. Micari, G. Dispenza, and V. Antonucci, "Optimal allocation of electric vehicle charging stations in a highway network: Part 2. the italian case study," vol. 26, p. 101015. [Online]. Available: https://www.sciencedirect.com/science/article/pii/S2352152X19302889

[54] T. Franke, I. Neumann, F. Bühler, P. Cocron, and J. F. Krems, "Experiencing Range in an Electric Vehicle: Understanding Psychological Barriers," *Applied Psychology: An International Review*, vol. 61, no. 3, pp. 368–391, Jul. 2012, publisher: Wiley-Blackwell. [Online]. Available: https://search.ebscohost.com/login.aspx?direct=true&db=bsu&AN=74713001&lang=fr&site=ehost-live

[55] S. Funke, P. Plötz, and M. Wietschel, "Invest in fast-charging infrastructure or in longer battery ranges? A cost-efficiency comparison for Germany," *Applied Energy*, vol. 235, pp. 888–899, Feb. 2019. [Online]. Available: https://www.sciencedirect.com/science/article/pii/S0306261918317021

[56] A. France, "Etude prospective pour le déploiement de stations de recharge," 2020. [Online]. Available: https://cloud.acoze.org/index.php/s/0uVkHOjLPsGoutz

[57] E. Figenbaum, "Battery Electric Vehicle Fast Charging–Evidence from the Norwegian Market," *World Electric Vehicle Journal*, vol. 11, p. 38, May 2020.

[58] S. Jawad and J. Liu, "Electrical Vehicle Charging Services Planning and Operation with Interdependent Power Networks and Transportation Networks: A Review of the Current Scenario and Future Trends," *Energies*, vol. 13, no. 13, p. 3371, Jan. 2020, number: 13 Publisher: Multidisciplinary Digital Publishing Institute. [Online]. Available: https://www.mdpi.com/1996-1073/13/13/3371

[59] G. Wager, J. Whale, and T. Braunl, "Driving electric vehicles at highway speeds: The effect of higher driving speeds on energy consumption and driving range for electric vehicles in Australia," *Renewable and Sustainable Energy Reviews*, vol. 63, pp. 158–165, Sep. 2016. [Online]. Available: https://www.sciencedirect.com/science/article/pii/S1364032116301721

[60] R. Shabbar, A. Kasasbeh, and M. M. Ahmed, "Charging Station Allocation for Electric Vehicle Network Using Stochastic Modeling and Grey Wolf Optimization," *Sustainability*, vol. 13, no. 6, p. 3314, Jan. 2021, number: 6 Publisher: Multidisciplinary Digital Publishing Institute. [Online]. Available: https://www.mdpi.com/2071-1050/13/6/3314

[61] J. Liu, J. Peper, G. Lin, Y. Zhou, S. Awasthi, Y. Li, and C. Rehtanz, "A planning strategy considering multiple factors for electric vehicle charging stations along german motorways," vol. 124, p. 106379. [Online]. Available: https://www.sciencedirect.com/science/article/pii/S0142061520310346

[62] N. S. Pearre, L. G. Swan, E. Burbidge, S. Balloch, L. Horrocks, B. Piper, and J. Anctil, "Regional electric vehicle fast charging network design using common public data," vol. 13, no. 11, p. 212, number: 11 Publisher: Multidisciplinary Digital Publishing Institute. [Online]. Available: https://www.mdpi.com/2032-6653/13/11/212

[63] T. Bräunl, D. Harries, M. McHenry, and G. Wager, "Determining the optimal electric vehicle DC-charging infrastructure for Western Australia," *Transportation Research Part D: Transport and Environment*, vol. 84, p. 102250, Jul. 2020. [Online]. Available: https://www.sciencedirect.com/science/article/pii/S1361920919308740

[64] H. Basset, E. Suomalainen, and J.-B. Segard, "Charging infrastructures modelling, using a long-distance trip database."

[65] E. Suomalainen, J. Berrada, and S. Coeugnet-Chevrier, "Modèle économique de la route électrique," VEDECOM, Tech. Rep., Dec. 2020.

[66] I. García-Magariño, G. Palacios-Navarro, R. Lacuesta, and J. Lloret, "ABSCEV: An agent-based simulation framework about smart transportation for reducing waiting times in charging electric vehicles," vol. 138, pp. 119–135. [Online]. Available: https://www.sciencedirect.com/science/article/pii/S1389128618301282

[67] A. Gusrialdi, Z. Qu, and M. A. Simaan, "Distributed Scheduling and Cooperative Control for Charging of Electric Vehicles at Highway Service Stations," *IEEE Transactions on Intelligent Transportation Systems*, vol. 18, no. 10, pp. 2713–2727, Oct. 2017. [Online]. Available: http://ieeexplore.ieee.org/document/7862908/

[68] Y. Wang, J. Shi, R. Wang, Z. Liu, and L. Wang, "Siting and sizing of fast charging stations in highway network with budget constraint," vol. 228, pp. 1255–1271. [Online]. Available: https://www.sciencedirect.com/science/article/pii/S0306261918310535

[69] Enedis, "Utilisation et recharge: enquete comportementale aupres des possesseurs de vehicules electriques." [Online]. Available: https://www.enedis.fr/sites/default/files/documents/pdf/utilisation-et-recharge-enquete-comportementale-aupres-des-possesseurs-de-vehicules-electriques-octobre-2022.pdf

[70] A. Pan, T. Zhao, H. Yu, and Y. Zhang, "Deploying public charging stations for electric taxis: A charging demand simulation embedded approach," vol. 7, pp. 17 412–17 424, conference Name: IEEE Access.

[71] H. Qin and W. Zhang, *Charging scheduling with minimal waiting in a network of electric vehicles and charging stations*, Sep. 2011, journal Abbreviation: Proc. 8th ACM VANET Pages: 60 Publication Title: Proc. 8th ACM VANET.

[72] J. Tan and L. Wang, "Real-Time Charging Navigation of Electric Vehicles to Fast Charging Stations: A Hierarchical Game Approach," *IEEE Transactions on Smart Grid*, vol. 8, no. 2, pp. 846–856, Mar. 2017, conference Name: IEEE Transactions on Smart Grid.

[73] J. Rezgui, S. Cherkaoui, and D. Said, "A two-way communication scheme for vehicles charging control in the smart grid," in *2012 8th International Wireless Communications and Mobile Computing Conference (IWCMC)*, Aug. 2012, pp. 883–888, iSSN: 2376-6506.

[74] A. Cortés and S. Martínez, "Optimal plug-in electric vehicle charging with schedule constraints," in *2013 51st Annual Allerton Conference on Communication, Control, and Computing (Allerton)*, Oct. 2013, pp. 262–266.

[75] F. L. D. Silva, C. E. H. Nishida, D. M. Roijers, and A. H. R. Costa, "Coordination of Electric Vehicle Charging Through Multiagent Reinforcement Learning," *IEEE Transactions on Smart Grid*, vol. 11, no. 3, pp. 2347–2356, May 2020, conference Name: IEEE Transactions on Smart Grid.

[76] R. Bernal, D. Olivares, M. Negrete-Pincetic, and Lorca, "Management of EV charging stations under advance reservations schemes in electricity markets," *Sustainable Energy, Grids and Networks*, vol. 24, p. 100388, Dec. 2020. [Online]. Available: https://www.sciencedirect.com/science/article/pii/S2352467720303192

[77] S.-N. Yang, W.-S. Cheng, Y.-C. Hsu, C.-H. Gan, and Y.-B. Lin, "Charge scheduling of electric vehicles in highways," *Mathematical and Computer Modelling*, vol. 57, no. 11, pp. 2873–2882, Jun. 2013. [Online]. Available: https://www.sciencedirect.com/science/article/pii/S0895717711007394

[78] J. Rezgui and S. Cherkaoui, "Smart charge scheduling for EVs based on two-way communication," in *2017 IEEE International Conference on Communications (ICC)*, pp. 1–6, ISSN: 1938-1883. [Online]. Available: https://ieeexplore.ieee.org/document/7996983

[79] E. Yudovina and G. Michailidis, "Socially Optimal Charging Strategies for Electric Vehicles," *IEEE Transactions on Automatic Control*, vol. 60, no. 3, pp. 837–842, Mar. 2015. [Online]. Available: https://ieeexplore.ieee.org/document/6873288

[80] Y. Luo, T. Zhu, S. Wan, S. Zhang, and K. Li, "Optimal charging scheduling for large-scale EV (electric vehicle) deployment based on the interaction of the smart-grid and intelligent-transport systems," *Energy*, vol. 97, pp. 359–368, Feb. 2016. [Online]. Available: https://linkinghub.elsevier.com/retrieve/pii/S0360544216000098

[81] Y. Wang, J. Bi, W. Guan, and X. Zhao, "Optimising route choices for the travelling and charging of battery electric vehicles by considering multiple objectives," *Transportation Research Part D: Transport and Environment*, vol. 64, pp. 246–261, Oct. 2018. [Online]. Available: https://linkinghub.elsevier.com/retrieve/pii/S1361920916307106

[82] S. Pourazarm, C. G. Cassandras, and A. Malikopoulos, "Optimal routing of electric vehicles in networks with charging nodes: A dynamic programming approach," in *2014 IEEE International Electric Vehicle Conference (IEVC)*, Dec. 2014, pp. 1–7.

[83] Y. Wang, J. Bi, W. Guan, C. Lu, and D. Xie, "Optimal charging strategy for intercity travels of battery electric vehicles," *Transportation Research Part D: Transport and Environment*, vol. 96, p. 102870, Jul. 2021. [Online]. Available: https://www.sciencedirect.com/science/article/pii/S1361920921001711

[84] F. He, Y. Yin, and S. Lawphongpanich, "Network equilibrium models with battery electric vehicles," *Transportation Research Part B: Methodological*, vol. 67, pp. 306–319, Sep. 2014. [Online]. Available: https://www.sciencedirect.com/science/article/pii/S0191261514000915

[85] J. Chamberlain, E. Simhon, and D. Starobinski, "Preemptible queues with advance reservations: Strategic behavior and revenue management," vol. 293, no. 2, pp. 561–578. [Online]. Available: https://www.sciencedirect.com/science/article/pii/S0377221720310900

[86] Y. Cao, S. Liu, Z. He, X. Dai, X. Xie, R. Wang, and S. Yu, "Electric vehicle charging reservation under preemptive service," in *2019 1st International Conference on Industrial Artificial Intelligence (IAI)*, pp. 1–6.

[87] R. Flocea, A. Hîncu, A. Robu, S. Senocico, A. Traciu, B. M. Remus, M. S. Răboacă, and C. Filote, "Electric Vehicle Smart Charging Reservation Algorithm," *Sensors*, vol. 22, no. 8, p. 2834, Jan. 2022, number: 8 Publisher: Multidisciplinary Digital Publishing Institute. [Online]. Available: https://www.mdpi.com/1424-8220/22/8/2834

[88] R. Basmadjian, B. Kirpes, J. Mrkos, M. Cuchý, and S. Rastegar, "An Interoperable Reservation System for Public Electric Vehicle Charging Stations: A Case Study in Germany," in *Proceedings of the 1st ACM International Workshop on Technology Enablers and Innovative Applications for Smart Cities and Communities*, ser. TESCA'19. New York, NY, USA: Association for Computing Machinery, Nov. 2019, pp. 22–29. [Online]. Available: http://doi.org/10.1145/3364544.3364825

[89] B. Vaidya and H. T. Mouftah, "Smart electric vehicle charging management for smart cities," *IET Smart Cities*, vol. 2, no. 1, pp. 4–13, Mar. 2020. [Online]. Available: https://onlinelibrary.wiley.com/doi/10.1049/iet-smc.2019.0076

[90] M. Kuby and S. Lim, "The flow-refueling location problem for alternative-fuel vehicles," *Socio-Economic Planning Sciences*, vol. 39, no. 2, pp. 125–145, Jun. 2005. [Online]. Available: https://www.sciencedirect.com/science/article/pii/S0038012104000175

[91] H. Gao, K. Liu, X. Peng, and C. Li, "Optimal Location of Fast Charging Stations for Mixed Traffic of Electric Vehicles and Gasoline Vehicles Subject to Elastic Demands," *Energies*, vol. 13, no. 8, p. 1964, Jan. 2020, number: 8 Publisher: Multidisciplinary Digital Publishing Institute. [Online]. Available: https://www.mdpi.com/1996-1073/13/8/1964

[92] G. Napoli, A. Polimeni, S. Micari, L. Andaloro, and V. Antonucci, "Optimal allocation of electric vehicle charging stations in a highway network: Part 1. methodology and test application," vol. 27, p. 101102. [Online]. Available: https://www.sciencedirect.com/science/article/pii/S2352152X19302828

[93] S. Mirjalili, S. M. Mirjalili, and A. Lewis, "Grey Wolf Optimizer," *Advances in Engineering Software*, vol. 69, pp. 46–61, Mar. 2014. [Online]. Available: https://www.sciencedirect.com/science/article/pii/S0965997813001853

[94] A. Saldarini, S. M. Miraftabzadeh, M. Brenna, and M. Longo, "Strategic approach for electric vehicle charging infrastructure for efficient mobility along highways: A real case study in spain," vol. 5, no. 3, pp. 761–779, number: 3 Publisher: Multidisciplinary Digital Publishing Institute. [Online]. Available: https://www.mdpi.com/2624-8921/5/3/42

[95] Q. Liu, J. Liu, W. Le, Z. Guo, and Z. He, "Data-driven intelligent location of public charging stations for electric vehicles," *Journal of Cleaner Production*, vol. 232, pp. 531–541, Sep. 2019. [Online]. Available: https://www.sciencedirect.com/science/article/pii/S0959652619319304

[96] C. A. Vandet and J. Rich, "Optimal placement and sizing of charging infrastructure for EVs under information-sharing," *Technological Forecasting and Social Change*, vol. 187, p. 122205, Feb. 2023. [Online]. Available: https://www.sciencedirect.com/science/article/pii/S0040162522007260

[97] J. Rich, C. A. Vandet, and N. Pilegaard, "Cost–benefit of a state-road charging system: The case of Denmark," *Transportation Research Part D: Transport and Environment*, vol. 109, p. 103330, Aug. 2022. [Online]. Available: https://linkinghub.elsevier.com/retrieve/pii/S1361920922001584

[98] J. Hassler, "Long distance trips with electric vehicles: which benefit of a communication between vehicles to coordinate charging?" Dec. 2022.

[99] S. Hess, M. Bierlaire, and J. W. Polak, "Estimation of value of travel-time savings using mixed logit models," vol. 39, no. 2, pp. 221–236. [Online]. Available: https://www.sciencedirect.com/science/article/pii/S0965856404001028

[100] A. S. Mussa, M. Klett, M. Behm, G. Lindbergh, and R. W. Lindström, "Fast-charging to a partial state of charge in lithium-ion batteries: A comparative ageing study," vol. 13, pp. 325–333. [Online]. Available: https://www.sciencedirect.com/science/article/pii/S2352152X17301913

[101] ABRP, "A better route planner," 2023. [Online]. Available: https://abetterrouteplanner.com/

[102] Fastned. Renault. [Online]. Available: https://support.fastned.nl/hc/en-gb/articles/360035723373-Renault

[103] InsideEVs. Peugeot e-208 DC charging test: Peak rate is close to 100 kW. [Online]. Available: https://insideevs.com/news/463106/peugeot-e208-dc-charging-test/

[104] V. Prasad, B. V.H, and T. A. Koka, "Mathematical analysis of single queue multi server and multi queue multi server queuing models: comparison study," *Global Journal of Mathematical Analysis*, vol. 3, no. 3, p. 97, Jun. 2015. [Online]. Available: http://www.sciencepubco.com/index.php/GJMA/article/view/4689

[105] M. de la transition écologique et de la cohésion des territoires. Enquête nationale transports et déplacements (entd) 2008. [Online]. Available: https://www.statistiques.developpement-durable.gouv.fr/enquete-nationale-transports-et-deplacements-entd-2008

[106] M. de la transition ecologique. Trafic moyen journalier annuel sur le réseau routier national - data.gouv.fr. [Online]. Available: https://www.data.gouv.fr/en/datasets/trafic-moyen-journalier-annuel-sur-le-reseau-routier-national/

[107] D. E. Goldberg and J. H. Holland, "Genetic algorithms and machine learning," vol. 3, no. 2, pp. 95–99. [Online]. Available: https://doi.org/10.1023/A:1022602019183

[108] MATLAB. Find minimum of function using genetic algorithm - MATLAB ga - MathWorks france. [Online]. Available: https://fr.mathworks.com/help/gads/ga.html

[109] R. Bellman, R. Bellman, and R. Corporation, *Dynamic Programming*, ser. Rand Corporation research study. Princeton University Press, 1957. [Online]. Available: https://books.google.fr/books?id=rZW4ugAACAAJ

[110] A. Popiolek, Z. Dimitrova, J. Hassler, M. Petit, and P. Dessante, "Comparison of decentralised fast-charging strategies for long-distance trips with electric vehicles," *Transportation Research Part D: Transport and Environment*, vol. 124, p. 103953, Nov. 2023. [Online]. Available: https://www.sciencedirect.com/science/article/pii/S1361920923003504

[111] Matmut, "Pourquoi et quand prendre des pauses lors des longs trajets en voiture - Matmut," Mar. 2019. [Online]. Available: https://www.matmut.fr/assurance/auto/conseils/pause-longs-trajets-voiture

[112] Argus, "A quoi ressemble le parc automobile français en 2020 ?" 2020. [Online]. Available: https://www.largus.fr/actualite-automobile/a-quoi-ressemble-le-parc-automobile-francais-en-2020-10582413.html

[113] AVERE, “Baromètre, janvier 2021 - Des immatriculations de véhicules électriques particuliers en repli, comme le marché automobile français dans sa globalité,” 2021. [Online]. Available: https://www.avere-france.org/publication/barometre-janvier-2021-des-immatriculations-de-vehicules-electriques-particuliers-en-repli-comme-le-marche-automobile-francais-dans-sa-globalite/

[114] ASFA, “Key figures ASFA 2018,” 2018. [Online]. Available: https://www.autoroutes.fr/FCKeditor/UserFiles/File/ASFA_Chiffres_Cles18(2).pdf

[115] mathworks, “Find outliers in data - MATLAB isoutlier - MathWorks France,” 2023. [Online]. Available: https://fr.mathworks.com/help/matlab/ref/isoutlier.html

[116] C. Stratégies, “ANALYSES-Electric vehicle charging infrastructure,” July 2019, Tech. Rep., 2019. [Online]. Available: https://www.ecologie.gouv.fr/sites/default/files/2019-07-Synth%C3%A8se-IRVE-English.pdf

[117] A. Popiolek, P. Dessante, M. Petit, Z. Dimitrova, and M. Waraq, “Highway charging infrastructure costs reduction for limited-range electric vehicles with real-time communication,” in *2023 IEEE Transportation Electrification Conference & Expo (ITEC)*, pp. 1–8, ISSN: 2473-7631.

[118] Setra, “Fonctions temps-débit sur les autoroutes interurbaines,” Rapport technique. [Online]. Available: http://www.cerema.fr/fr/centre-ressources/boutique/fonctions-temps-debit-autoroutes-interurbaines

[119] Prices. [Online]. Available: http://fastnedcharging.com/en/ev-charging-price

[120] H. Singh, M. Kavianipour, M. Ghamami, and A. Zockaie, “Adoption of autonomous and electric vehicles in private and shared mobility systems,” *Transportation Research Part D: Transport and Environment*, vol. 115, p. 103561, Feb. 2023. [Online]. Available: https://www.sciencedirect.com/science/article/pii/S136192092200387X

[121] Grey wolf optimizer (GWO). [Online]. Available: https://fr.mathworks.com/matlabcentral/fileexchange/44974-grey-wolf-optimizer-gwo

[122] adrien.ayffre. Départs en vacances : 99 % des aires de service des autoroutes concédées sont équipées en recharge rapide. [Online]. Available: https://www.avere-france.org/departs-en-vacances-99-des-aires-de-service-des-autoroutes-concedees-equipees-en-recharge-rapide/

[123] Bjørn Nyland. Nissan ariya 63 & 87 kWh charging battle vs volvo c40 and VW ID5. [Online]. Available: https://www.youtube.com/watch?v=-2-_NrXTtOg

[124] A. Popiolek, “Optimised fast-charging service to allow long-distance trips with electric vehicles.” online, 2021, place: Paris.

[125] C. Jung, “Power Up with 800-V Systems: The benefits of upgrading voltage power for battery-electric passenger vehicles,” *IEEE Electrification Magazine*, vol. 5, no. 1, pp. 53–58, Mar. 2017, conference Name: IEEE Electrification Magazine.

[126] A. Popiolek, P. Dessante, M. Petit, and Z. Dimitrova, “Enabling ultra-fast charging with 800v-battery architecture: balance between time spent at stations and charging infrastructure profitability.”

[127] K. Deb, A. Pratap, S. Agarwal, and T. Meyarivan, "A fast and elitist multiobjective genetic algorithm: NSGA-II," *IEEE Transactions on Evolutionary Computation*, vol. 6, no. 2, pp. 182–197, Apr. 2002, conference Name: IEEE Transactions on Evolutionary Computation.

[128] Fastned. Fastned peugeot e-208. [Online]. Available: https://support.fastned.nl/hc/en-gb/articles/360012789898-Peugeot

[129] S. Mirjalili, S. Saremi, S. M. Mirjalili, and L. d. S. Coelho, "Multi-objective grey wolf optimizer: A novel algorithm for multi-criterion optimization," *Expert Systems with Applications*, vol. 47, pp. 106–119, Apr. 2016. [Online]. Available: https://www.sciencedirect.com/science/article/pii/S0957417415007435

[130] Engie. TEO (the energy origin) garantit l'origine de l'énergie verte avec la blockchain. [Online]. Available: https://innovation.engie.com/fr/news/medias/nouvelles-energies/teo-the-energy-origin-garantie-origine-energie-verte-blockchain/13243